

gmif

D6-41115

RESEARCH STUDY ON ANTISKID BRAKING
SYSTEMS FOR THE SPACE SHUTTLE

by

J. A. Auselmi, L. W. Weinberg, R. F. Yurczyk, W. G. Nelson

The Boeing Company

Boeing Commercial Airplane Company

(NASA-CR-124349) RESEARCH STUDY ON
ANTIISKID BRAKING SYSTEMS FOR THE SPACE
SHUTTLE (Boeing Commercial Airplane Co.,
Seattle) 226 p HC \$13.50 CSCL 22B

N73-28449

G3/ ^{3/}~~10~~

Unclas
17436

Prepared for

NATIONAL AERONAUTICS AND SPACE ADMINISTRATION

George C. Marshall Space Flight Center

Marshall Space Flight Center, Alabama 35812

Contract NAS 8-27864

D6-41115

RESEARCH STUDY ON ANTISKID BRAKING
SYSTEMS FOR THE SPACE SHUTTLE

by

J. A. Anselmi, L. W. Weinberg, R. F. Yurczyk, W. G. Nelson

The Boeing Company

Boeing Commercial Airplane Company

Prepared for

NATIONAL AERONAUTICS AND SPACE ADMINISTRATION

George C. Marshall Space Flight Center

Marshall Space Flight Center, Alabama 35812

Contract NAS 8-27864

FEB 1973

CONTENTS

| | Page |
|--|------|
| I SUMMARY | 1 |
| II INTRODUCTION | 6 |
| III TRADE STUDIES OF EXISTING INDUSTRY ANTISKID SYSTEMS | 8 |
| Description of the Goodyear (Lockheed L-1011) Skid Control System | 8 |
| Description of the Hydro-Aire (Boeing 747) Skid Control System | 16 |
| Description of the Hydro-Aire (Boeing 737) Skid Control System | 24 |
| Description of the Bendix (Boeing 2707-300) Skid Control System | 28 |
| Description of the SPAD (Concorde) Skid Control System | 36 |
| Summary of Trade Studies | 44 |
| System Ratings | 47 |
| Wheel Speed Transducer | 48 |
| Power Line Noise | 49 |
| Power Supply | 50 |
| IV TRADE STUDIES OF NEW BRAKE CONTROL CONCEPTS | 53 |
| Discussion of Brake Torque as a Means of Antiskid Control | 53 |
| Description of the Boeing Closed Loop Antiskid System | 66 |
| V REDUNDANCY REQUIREMENTS TRADE STUDY | 75 |
| Redundancy Requirements Assumptions | 75 |
| Advanced 737 Brake System Fault Tree Analysis | 76 |
| Summary of Results | 95 |
| Alternative Configurations | 96 |
| Conclusions | 101 |

CONTENTS-Continued

| | Page |
|---|---------|
| VI LABORATORY EVALUATION OF ANTISKID SYSTEMS | 114 |
| Description of Antiskid Simulation | 114 |
| Analog Computer Simulation | 114 |
| Hydraulic Simulation | 116 |
| Description of Laboratory Screening Test | 120 |
| Stability Studies | 120 |
| Performance-Adaptability Studies | 121 |
| Operational Studies | 122 |
| Data Recorded During Tests | 125 |
| Evaluation of Laboratory Results | 126 |
| Discussion of Pen Chart Recordings | 127 |
| Discussion of Tabulated Test Data | 151 |
| Discussion of Grading | 171 |
| Grading Criteria | 171 |
| VII SPACE SHUTTLE HARDWARE CRITERIA | 176 |
| Antiskid Valve | 177 |
| Brake Dynamics | 184 |
| Hydraulic System | 190 |
| Wheel Speed Transducer | 192 |
| VIII CONCLUSIONS | 195 |
| IX RECOMMENDATIONS | 196 |
| APPENDIX I 747 Brake System Fault Tree Analysis | 197 |
| APPENDIX II Space Shuttle Parameters for Skid Control | 209 |
| Simulation | |
| APPENDIX III Space Shuttle Screening Data | 211 |

TABLES

| NO. | | PAGE |
|-----|---|------|
| I | Estimated System Weight | 102 |
| II | Summary-Probability of Brake Loss Due to Hydro-Mechanical Failure | 105 |
| III | Summary-Probability of Brake Loss Due to Skid Control Failure | 106 |
| IV | Space Shuttle Parameters for Skid Control Simulation | 209 |
| V | Shuttle Lab Screening Tabulated Data | 211 |
| VI | Comparison of System Strut Damping Ratios | 173 |
| VII | Space Shuttle System Grading | 175 |

FIGURES

| NO. | | PAGE |
|-----|--|------|
| 1 | Goodyear Antiskid System Schematic (Lockheed L-1011) | 10 |
| 2 | Goodyear Antiskid Wheel Speed Transducer (Lockheed L-1011) | 14 |
| 3 | Goodyear Antiskid Servo Valve (Lockheed L-1011) | 15 |
| 4 | Hydro-Aire Mark III Antiskid System Schematic (Boeing 747) | 18 |
| 5 | Hydro-Aire Mark III Antiskid Servo Valve (Boeing 747) | 22 |
| 6 | Hydro-Aire Mark III Antiskid Wheel Speed Transducer (Boeing 747) | 23 |
| 7 | Hydro-Aire Mark III Antiskid System Schematic (Boeing 737) | 25 |
| 8 | Hydro-Aire Mark III Antiskid Servo Valve (Boeing 737) | 27 |

FIGURES-Continued

| NO. | | PAGE |
|-------|--|-------|
| 9 | Hydro-Aire Mark III Antiskid Wheel Speed Transducer (Boeing 737) | 29 |
| 10 | Bendix Antiskid System Schematic (Boeing 2707-300) | 31 |
| 11 | Bendix Antiskid Wheel Speed Transducer (Boeing 2707-300) | 34 |
| 12 | Bendix Antiskid Servo Valve (Boeing 2707-300) | 35 |
| 13 | S.P.A.D. Antiskid System Schematic (Concorde) | 39 |
| 14 | S.P.A.D. Antiskid Servo Valve (Concorde) | 42 |
| 15 | S.P.A.D. Antiskid Wheel Speed Transducer | 43 |
| 16 | Typical Braked Aircraft Tire Mu-Slip Curve | 45 |
| 17 | Free Body Diagram of a Braked Wheel | 56 |
| 18 | S.P.A.D. Ground Torque Relationship | 59 |
| 19 | Basic S.P.A.D. System | 60 |
| 20 | Ground Torque Determination | 61 |
| 21 | Space Shuttle Hydraulic Frequency Response | 63 |
| 22 | Brake Torque Frequency Response | 64 |
| 23 | Proposed Optimizer Using Measure Brake Torque | 65 |
| 24 | Proposed Maximum Detector and Variable Integrator Gain | 67 |
| 25 | Boeing Closed Loop Antiskid System | 69 |
| 26 | Closed Loop Modulator | 70 |
| 27 | Closed Loop Modulator Characteristic | 71 |
| 28 | Second Order Lead Characteristics | 73 |
| 29-40 | Advanced 737 Brake System Fault Tree Analysis | 79-90 |
| 41 | Ground Rule 1 | 92 |
| 42 | Ground Rule 2 | 93 |
| 43 | Ground Rule 3 | 94 |
| 44 | Boeing 737 (Baseline Brake Control System) Left Side Shown | 107 |

FIGURES-Continued

| NO. | | PAGE |
|-----|---|------|
| 45 | Configuration A, Ground Rule 3 - 1 Brake Plus Skid Control Each Side | 108 |
| 46 | Alternate Configuration A - Left Side Shown | 109 |
| 47 | Configuration B - Ground Rule 2 Typical Wheel | 110 |
| 48 | Alternate Configuration B - Typical Wheel | 111 |
| 49 | Configuration C - Ground Rule 1 - Typical Wheel | 112 |
| 50 | Alternate Configuration C - Typical Wheel | 113 |
| 51 | Simulator Block Diagram | 115 |
| 52 | Hydraulic Skid Control Simulation | 117 |
| 53 | Picture of Analog Lab | 118 |
| 54 | Picture of Hydraulic Simulation | 119 |
| 55 | Wet Runway Curves | 123 |
| 56 | .5 MU With 4.5 Hz Strut-Bendix System | 132 |
| 57 | .5 MU With 11.5 Hz Strut-Bendix System | 133 |
| 58 | MU Steps With 7.5 Hz Strut-Bendix System | 134 |
| 59 | Wet Runway Curve 1 With 7.5 Hz Strut-Bendix System | 135 |
| 60 | .5 MU With 4.5 Hz Strut-Boeing Closed Loop System | 140 |
| 61 | .5 MU With 11.5 Hz Strut-Boeing Closed Loop System | 141 |
| 62 | MU Steps With 7.5 Hz Strut-Boeing Closed Loop System | 142 |
| 63 | Wet Runway Curve 1 With 7.5 Hz Strut-Boeing Closed Loop System | 143 |
| 64 | .5 MU With 4.5 Hz Strut-Hydro-Aire Mark III System | 147 |
| 65 | .5 MU With 11.5 Hz Strut-Hydro-Aire Mark III System | 148 |

FIGURES-Continued

| NO. | | PAGE |
|-----|---|------|
| 66 | MU Steps With 7.5 Hz Strut - Hydro-Aire Mark III System | 149 |
| 67 | Wet Runway Curve 1 With 7.5 Hz Strut - Hydro-Aire Mark III System | 150 |
| 68 | Performance-Adaptability Test 1, .5 MU, 4.5 Hz Strut | 153 |
| 69 | Performance-Adaptability Test 1, .2 MU, 4.5 Hz Strut | 154 |
| 70 | Performance-Adaptability Test 1, Curve 1, 4.5 Hz Strut | 155 |
| 71 | Performance-Adaptability Test 1, .5 MU, 11.5 Hz Strut | 156 |
| 72 | Performance-Adaptability Test 1, .2 MU, 11.5 Hz Strut | 157 |
| 73 | Performance-Adaptability Test 1, Curve 1, 11.5 Hz Strut | 158 |
| 74 | Performance-Adaptability Test 1, .5 MU, 7.5 Hz Strut | 159 |
| 75 | Performance-Adaptability Test 1, .4 MU, 7.5 Hz Strut | 160 |
| 76 | Performance-Adaptability Test 1, .3 MU, 7.5 Hz Strut | 161 |
| 77 | Performance-Adaptability Test 1, .2 MU, 7.5 Hz Strut | 162 |
| 78 | Performance-Adaptability Test 1, .1 MU, 7.5 Hz Strut | 163 |
| 79 | Performance-Adaptability Test 1, .075 MU, 7.5 Hz Strut | 164 |
| 80 | Performance-Adaptability Test 2, .5 MU, 7.5 Hz Strut | 165 |
| 81 | Performance-Adaptability Test 3, 7.5 Hz Strut | 166 |
| 82 | Operational Studies Test 1, Curve 1, 7.5 Hz Strut | 168 |

FIGURES - Continued

| NO. | | PAGE |
|-------------|--|---------|
| 83 | Operational Studies Test 1, Curve 2, 7.5 Hz Strut | 169 |
| 84 | Efficiency Comparison Stabilized Landings | 170 |
| 85 | Space Shuttle 3-Way Valve SN 211 | 179 |
| 86 | Space Shuttle Goodyear 737 Valve | 181 |
| 87 | Space Shuttle Hydraulic Frequency Response with Goodyear 737 Valve SN 99 | 182 |
| 88 | .5 MU Closed Loop System Sensitivity Study | 183 |
| 89 | .2 MU Closed Loop System Sensitivity Study | 185 |
| 90 | Wet Runway (Curve 1) Closed Loop Sensitivity Study | 186 |
| 91 | Space Shuttle - 737 and 747 Brake | 187 |
| 92 | Brake Pressure Step Down Response Tests | 188 |
| 93 | Brake Pressure Step Up Response Tests | 189 |
| 94 | Space Shuttle Brake Torque Frequency Response Simulation | 191 |
| 95 | Space Shuttle Hydraulic Frequency Response with Short Brake Line | 193 |
| 96 - 106 | 747 Brake System Fault Tree Analysis | 198-208 |

I. SUMMARY

The brake control system is critically linked to total Space Shuttle vehicle performance in that it has a direct effect on the economics and safety of operation of the vehicle. Payload factors can be governed by the vehicle stopping ability. The payload capability can be drastically reduced by excess weight in the overall landing gear system or specifically, in one of its subsystems such as the braking system.

To serve as an introduction and background on commercially available modern antiskid systems, the first task exercise explained and described these systems. System operational details and system control philosophies were presented for each system as well as a modern aircraft application for each system. Antiskid systems on the Concorde (SPAD System), Boeing 747 and Advanced 737 (Hydro-Aire Mark III System), Boeing SST (Bendix Ship Command System), and Lockheed L-1011 (Goodyear System) were described. In addition to the basic aircraft braking optimization, the antiskid system descriptions also presented such functions as locked wheel protection and touchdown protection.

Once the four systems were described the basic antiskid systems were applied to the Space Shuttle vehicle and graded on their applicability. It was found that all four systems could successfully be implemented on the Shuttle, but that some would lend themselves to this application more easily than others. Based on such items as relative complexity, susceptibility to noise vibration, and difficulty in implementation the four systems were rated in this order of preference: Hydro-Aire Mark III System, Goodyear L-1011 System, Bendix SST System and SPAD Concorde System. This rating is strictly based on descriptive information made available by the manufacturers. Some of the information was not too detailed so an accurate evaluation could not be made. Actual hardware systems from some of these manufacturers were evaluated in the laboratory on a brake control simulator in Section VI of this program. This is a far more accurate evaluation of the

systems. Unfortunately, all suppliers did not participate in the laboratory screening so the descriptive evaluation is the only available information on these systems.

The systems were not assessed from a cost standpoint. Since none of these systems are rated for space craft use, their cost for Space Shuttle use would not be accurately determined at this time. From another standpoint the top two contenders have had extensive use and experience in commercial and military aircraft and have shown themselves to be relatively trouble free.

In the second task of this contract several studies were made of new brake control system concepts. A braking concept based on antiskid system control by utilizing measured brake torque and its properties is presented in detail. To maximize braking, developed ground force must be kept at a maximum. In an optimal control system the ground force must be known. Since it is not practical to measure ground force directly, several methods are shown how this variable can be constructed using measured brake torque. A system is presented detailing how this concept might be implemented. It is shown that a system already uses a form of this concept in its operation, SPAD.

Another skid control system concept is presented which deals with wheel deceleration control. This system concept is embodied in the Boeing developed Boeing Closed Loop System. This experimental antiskid system is presented in detail for system description and analysis. Details of the system design and operation are presented in this section and later on in the lab screening section results of the Closed Loop lab tests are presented and discussed. The results show the system to be competent although

both industry systems which were tested, Hydro-Aire and Bendix, demonstrate better performance. In concept and design the Closed Loop system is relatively simple and therefore has an advantage over more complex systems requiring more circuitry.

The third task dealt with redundancy considerations which were based on the Boeing Advanced 737. Three ground rules were defined based on assumptions made about the mission requirements of the Space Shuttle. These ground rules were used to analyze what implementation was required to provide for an antiskid control system with electronic Fail Operational/Fail Operational/Fail Safe capability and hydromechanical Fail Operational/Fail Safe capability. To aid in this redundancy study, Fault Tree Analysis was used. Both the Advanced 737 and 747 brake control system were analyzed and their fault trees are presented for study.

The three ground rules that were defined each required a different level of redundancy. Ground rule 3 only required one operating brake on each side of the shuttle vehicle. Ground rule 2 required that any three brakes be operational. Ground rule 1 required that all four brakes be operational. To meet the electronic as well as hydromechanical operational requirements obviously dictate a much greater degree of redundancy for ground rule 1 than 3. Tables were prepared that show the expected probabilities for each system for given ground rules. An expected system weight is also included to indicate what each level of redundancy requires in terms of weight penalty.

In addition to the detailed system implementations alternates were suggested which although do not have the strict degree of redundancy required per given ground rule, do have an extremely

remote probability of failure. These alternatives do achieve nearly the same probabilities of failure while simplifying the implementation in terms of cost and weight.

The fourth task involved establishing an analog-hydraulic computer simulation of the Space Shuttle which was then used to screen the participating vendor systems. A complete set of tests were established especially for the Space Shuttle vehicle and each system was subjected to these tests. Of the four antiskid system manufacturers invited only Hydro-Aire and Bendix agreed to participate. To add completeness to the second task description of the Boeing Closed Loop system it was screened along with the other two systems in this fourth section. Ample data reduction and description are presented for a representative set of tests each system was subjected to, so that along with the preliminary descriptions presented in Section III, the Hydro-Aire and Bendix systems are thoroughly analyzed for performance. Goodyear and S.P.A.D. system performance rating was not possible because of their absence from the screening tests.

The three systems that were tested were given a weighted point total with the result that the Hydro-Aire and Bendix system scored virtually the same grade. In stopping distance performance the Hydro-Aire system had the edge, while in stability the Bendix system was first. Both systems were found to be qualified for Space Shuttle use from a stopping performance standpoint. Other factors such as manufacturing techniques and how applicable they are to space flight use were not judged. However, there appears to be no impediment in this respect for either system.

The final task presented criteria for hardware used for the antiskid system on the Space Shuttle. Tests were run using the

Boeing Closed Loop system that established trends that are helpful during design stages of the system. Design considerations such as brake line length, brake actuator hydraulic volume, brake torque dynamics, and antiskid valve design were analyzed. Using the results of these tests show that the proper choice of valve, and the proper combination of brake volume, brake line length can result in a better responding hydraulic system. Since any reduction in hydraulic phase lag is beneficial, this approach is certainly worth careful analysis and design. Brake torque response is shown to be critical in the system performance. The less phase lag from the brake the better the system's performance and stability will be. In general, the antiskid system implementation must be looked at from a total system standpoint in that all aspects of the design are important to the performance and stability of the braking system.

II. INTRODUCTION

This document describes the work completed in the five specific tasks undertaken under Contract NAS 8-27864. The nature of work conducted under this contract is a research study on a brake control system for use on the Space Shuttle vehicle. This work involved five tasks each designated to provide information on the design requirements and the utility of existing brake control systems on Space Shuttle. The following will serve to briefly introduce each task:

In Section III, the first task, trade studies were conducted of existing antiskid braking systems with respect to applicability and compatibility to the Space Shuttle. Included in these investigations were the systems similar to those used on the Concorde (SPAD), Boeing 747 and Advanced 737 (Hydro-Aire Mark III), Boeing SST (Bendix), and Lockheed L-1011 (Goodyear). A technical evaluation of these systems was conducted on their applicability and compatibility to the Space Shuttle in terms of complexity, cost and maintenance.

In Section IV, the second task, trade studies of new brake control system concepts were undertaken so that design risks could be identified for implementing on the Space Shuttle. Also an alternate antiskid system was presented and tested. This system derives its control from wheel deceleration.

In Section V, the third task, techniques for implementing a system with electronic Fo/Fo/Fs and hydromechanical Fo/Fs capability was investigated. Tradeoff and alternate designs were also looked at to assess the advantages of reducing redundancy requirements from a cost and weight standpoint.

In Section VI, the fourth task, extensive computer, hardware simulation investigations were performed which included the principle Space Shuttle landing gear characteristics and vehicle parameters provided by NASA/MSFC. Early utilization of a antiskid simulation in

the Space Shuttle design stages can be extremely cost effective. This ensures that the braking system can perform to its maximum and also identify potential problems early in the design to ensure a cost effective development and flight test program. In this study, each participating vendor antiskid system was subjected to laboratory screening tests and the results of each were graded according to a designated point system to give some insight into the applicability and compatibility of these systems to Space Shuttle operation.

In Section VII, the fifth task, preliminary hardware characteristics were established for Space Shuttle skid control system hardware. Subjects covered were antiskid valve, wheel speed transducer, brake torque characteristics, etc. The intent is to specify criteria for the brake control system as well as related systems so that optimum total system performance can be identified in the early design.

III. TRADE STUDIES OF EXISTING INDUSTRY ANTISKID SYSTEMS

Trade studies of existing state-of-the-art antiskid systems have been conducted. Each system is described with the help of block diagrams and illustrations as to its implementation on the subject aircraft. Included in this study are the systems used on the Lockheed L-1011 (Goodyear System), Boeing 747 and Advanced 737 (Hydro-Aire Mark III System), Boeing 2707-300 (Bendix System), and Concorde (SPAD System). Each antiskid system is then rated as to its applicability and compatibility to a Space Shuttle vehicle.

DESCRIPTION OF THE GOODYEAR (LOCKHEED L-1011) SKID CONTROL SYSTEM

The Lockheed L-1011 skid control system is the latest Goodyear system developed for a large jet transport aircraft. It is a representative Goodyear state-of-the-art antiskid system and was, therefore, chosen for study in the program. A description of this system follows.

The eight main wheels of the L-1011 aircraft are each provided with skid protection by the Goodyear Skid Control System. Each wheel has its own wheel speed sensor, control circuit and electro-hydraulic servo valve. An electrically operated valve allows the pilot to select either the normal or alternate hydraulic system. These systems share a common skid control circuit but each has its separate valve driver. Hydraulically the two systems are completely separated, having their own power supply, metering valve, and antiskid valve. The two hydraulic systems tie into each brake through a single line via a shuttle valve.

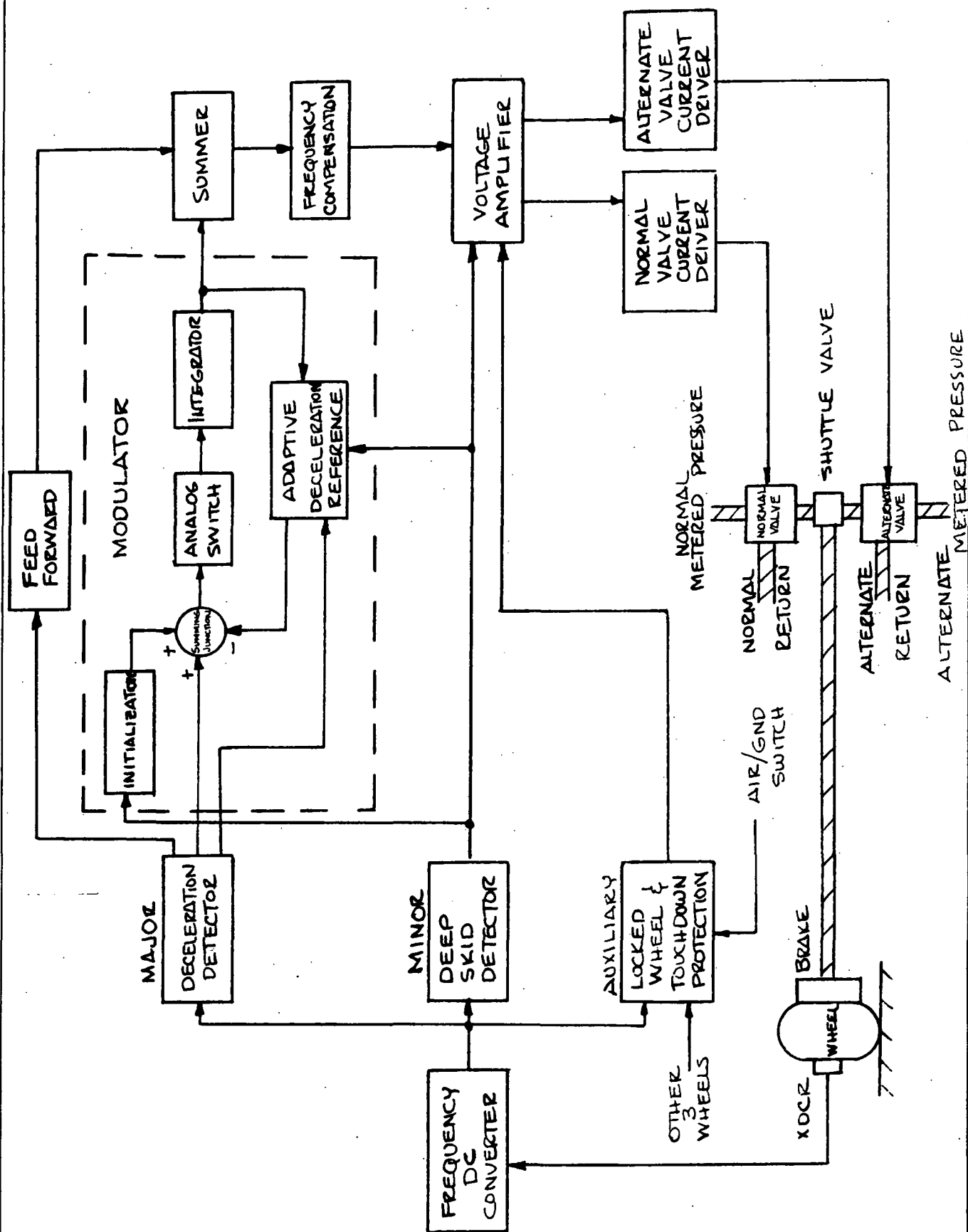
In addition to normal skid protection, locked wheel protection is provided for each of the eight main wheels as a backup control. There are two locked wheel arming circuits associated with the eight main wheels, one grouping the inboard wheels, the other the outboard. When the four wheel speeds are above the locked wheel arming point, locked wheel protection is applied to all four associated wheels. If any of these four wheels drops below a preset speed value, the locked wheel circuit will fully release the brake pressure to that wheel. At

very low taxi speeds the locked wheel protection drops out to permit normal braking during taxiing. Each locked wheel arming circuit has a memory to provide protection for a length of time even if all four wheels lock up simultaneously.

In addition to providing skid control during normal braking, the system protects each braked wheel upon touchdown such that no metered pressure can be applied to the brake until the airplane is sensed to be on the ground. On the L-1011 airplane this is accomplished by a squat switch on each main gear. Full brake release signals are applied to each brake until the wheels have spun up to a level to override this signal or the squat switch signal is removed by compression of the shock struts. Thereafter brake pressure can be applied and the anti-skid system can operate normally.

The L-1011 Goodyear Skid Control System is represented by the block diagram in Figure 1. Each braked wheel has its own transducer which produces an AC signal with frequency proportional to wheel speed. This signal is received by the frequency DC converter where it is changed to an analog DC voltage proportional to wheel speed. The signal is a continuous monitor of wheel speed and is applied to three control loops of the skid control system. These three control loops are responsible for all ranges of brake control operation. One loop, called the auxiliary loop, is responsible for both locked wheel and touchdown protection and has already been described. The remaining two, the major and minor loops, are responsible for the main skid control function. The minor loop will be described first as it serves as an initialization to the major loop.

The minor control loop consists mainly of the deep skid detector which contains both memory and skid threshold circuitry. Its operation also involves elements common to the other loops. These include the frequency converter, voltage amplifier, current driver and anti-skid valve. The wheel speed signal is continually monitored in the



minor control loop. When a wheel speed departure from synchronous speed exceeds the deep skid detector threshold level, input signals are provided to both the voltage amplifier and modulator. The voltage amplifier signal immediately sends a full release signal to the valve current driver causing full brake pressure release. The deep skid signal input to the modulator serves as the first step or initialization procedure in the major control loop which is described later.

Throughout the antiskid operation the deep skid detector monitors the wheel speed so that no skids in excess of the threshold departure level will go undetected and uncontrolled. Upon recovering of the wheel velocity the minor loop control is removed and subsequent braking control, within the threshold departure is handled by the major control loop.

The major control loop is the dominant control in the system and as such involves the most complexity. Compared to the minor loop which is an on-off discontinuous control, the major loop provides continuous brake modulation and consequently smoother braking control. Elements associated with this loop are as follows: deceleration detector, feed forward circuit, modulator, summer and frequency compensator. The modulator consists of an initialization circuit, an analog switch and integrator, and an adaptive deceleration reference. Basically the major loop provides control by providing brake pressure modulation which is proportional to wheel speed deceleration.

Wheel speed is continually monitored by the deceleration detector. Since the following description applies to the major control loop, assume that the previous skid required control correction from the minor loop and that once the wheel recovered the remaining control involved only the major loop. Thus the deceleration detector will only be seeing skids of less than the minor loop threshold velocity departure. During this time while the minor loop is controlling, the deep skid detector provides a signal to the initialization circuit

which is proportional to the time duration of the skid. The error signal generated at the summing junction results from initialization, deceleration detector, and Adaptive Deceleration Reference (ADR) inputs. This error is integrated by the integrator circuit and its magnitude is determined by size of error signal. Other factors affecting integrator signal magnitude include time and integrator gain.

The deceleration error generated at the summing junction (See Figure 1) is established by referencing the deceleration detector and initialization signal from the deep skid detector to the level from the ADR. To adapt to varying runway conditions, the ADR circuit requires several extra inputs. These are feedback from the integrator and inputs from both deep skid and deceleration detectors. When a deep skid is encountered (change in wheel velocity greater than the minor loop threshold) the ADR level is lowered from its normal value, but returns again to a higher reference level during skid recovery. During this time the braked wheel has turned around from the skid deceleration and begins spinning back up to synchronous wheel speed. When the wheel has completely spun up the deceleration detector level drops to zero so that the summing junction produces a deceleration error due to the presence of an ADR signal. The error signal is integrated resulting in a gradual increase of brake pressure which eventually precipitates another skid. This has the effect of reversing the deceleration error signal since now the signal from the deceleration error is something greater than zero. Summing this up with the ADR signal produces an error signal with an opposite sign. This has the immediate effect of reversing the direction of the integrator causing brake pressure decrease. Assuming this control action has sufficient authority to correct the wheel skid, the skidding wheel will regain synchronous speed, deceleration detector signal will drop to zero again and the entire process repeats.

Inputs from the deceleration detector and integrator are used

to enable the ADR to conform to the varying decelerations such that system efficiency is kept high. Thus the ADR level is continually changing due to varying runway conditions. Other components in the major loop include a lead circuit to anticipate and quicken the system response. Its input comes from the deceleration detector and output is fed to the summer. The summer combines signals from both the feed forward and the integrator. The summation of these signals is then input to the frequency compensation circuit. This circuit is designed to compensate dynamically for the signal attenuation in the hydraulics at higher frequencies. It also has the effect of extending system response to a higher frequency range. This serves to help stabilize the tendency to excite fore and aft gear oscillations.

The Goodyear L-1011 wheel speed transducer shown in Figure 2 is unique in that it contains no moving parts. Essentially the transducer contains two basic elements, the sensor mounted in the axle and exciter ring mounted in the hub cap. The sensor consists of a permanent magnet core and four equally spaced poles on its periphery. Forty-eight equally spaced soft iron teeth inside the exciter ring rotate about the sensor which produces a fluctuation in the magnetic field proportional to wheel speed.

A Goodyear antiskid valve is shown in Figure 3. It is a two-stage valve with flapper nozzle first stage and spool, sleeve second stage. In the first stage the torque motor consisting of a permanent magnet and flapper armature operates as part of a hydraulic bridge. Two orifices in the bridge are fixed and the two associated with the flapper are variable. With no valve signal the first stage is relaxed with the flapper centered between the two nozzles and flow through them is equal. As shown in Figure 3, with no valve signal present the second stage spool position allows full pilot's metered pressure to the brake. Applying a valve signal deflects the flapper, unbalances the hydraulic bridge which moves the spool in the second stage and

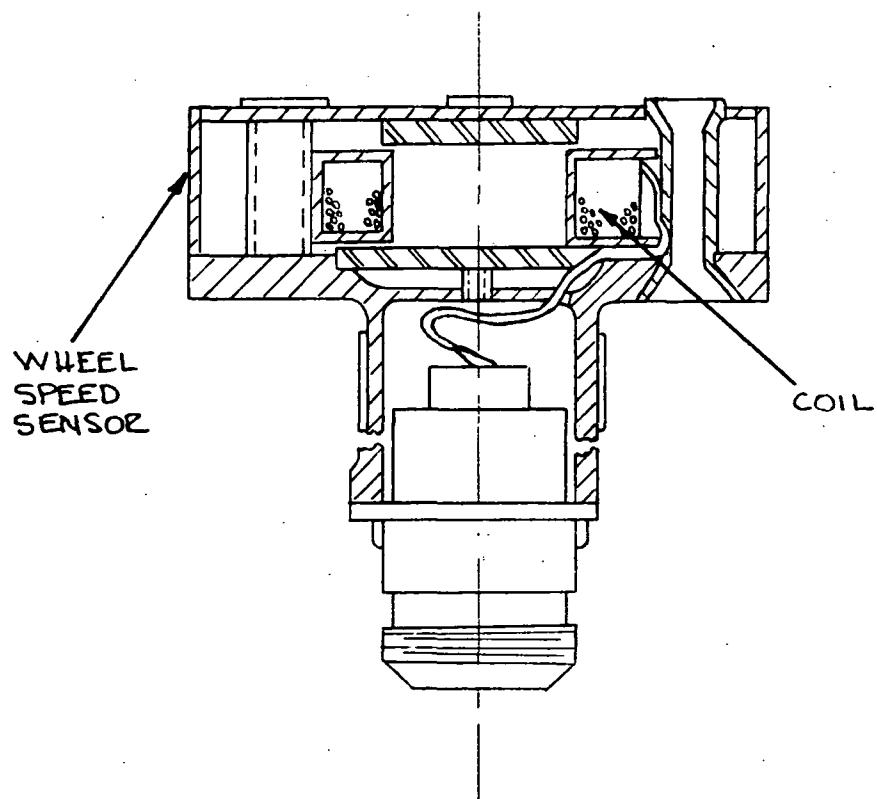
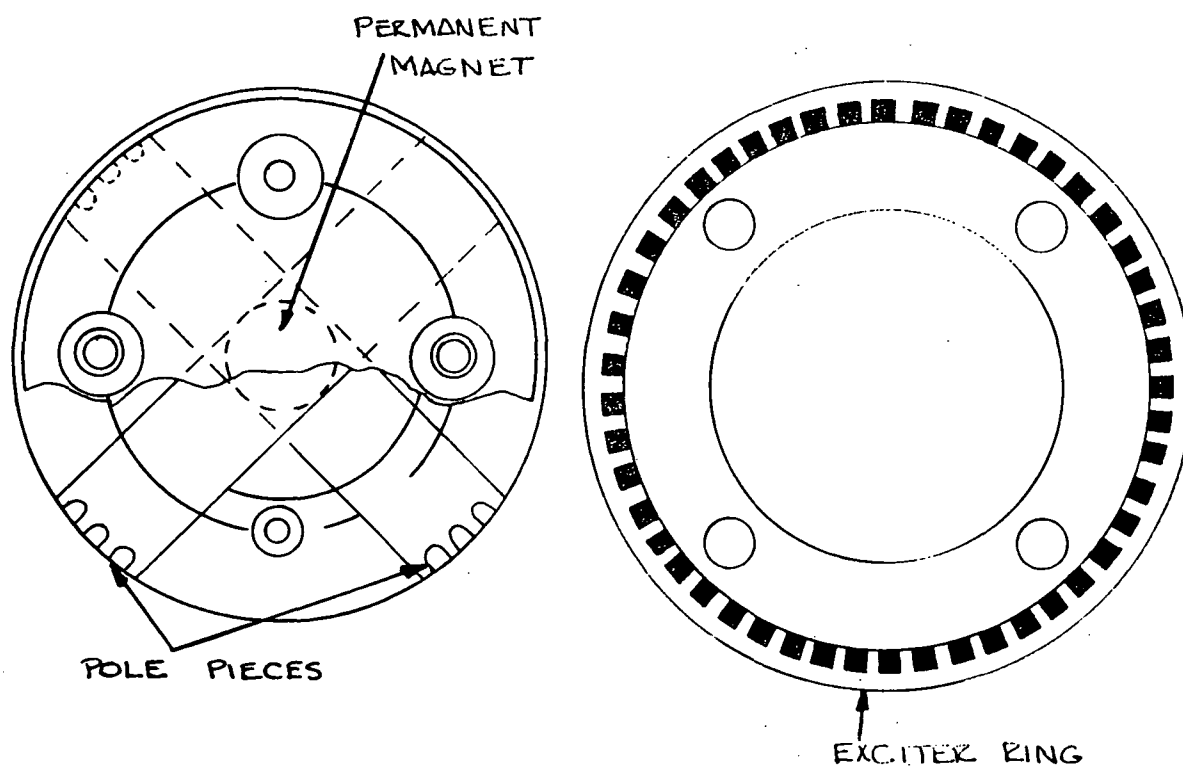


Figure 2. GOODYEAR ANTISKID WHEEL SPEED TRANSDUCER (LOCKHEED L-1011)

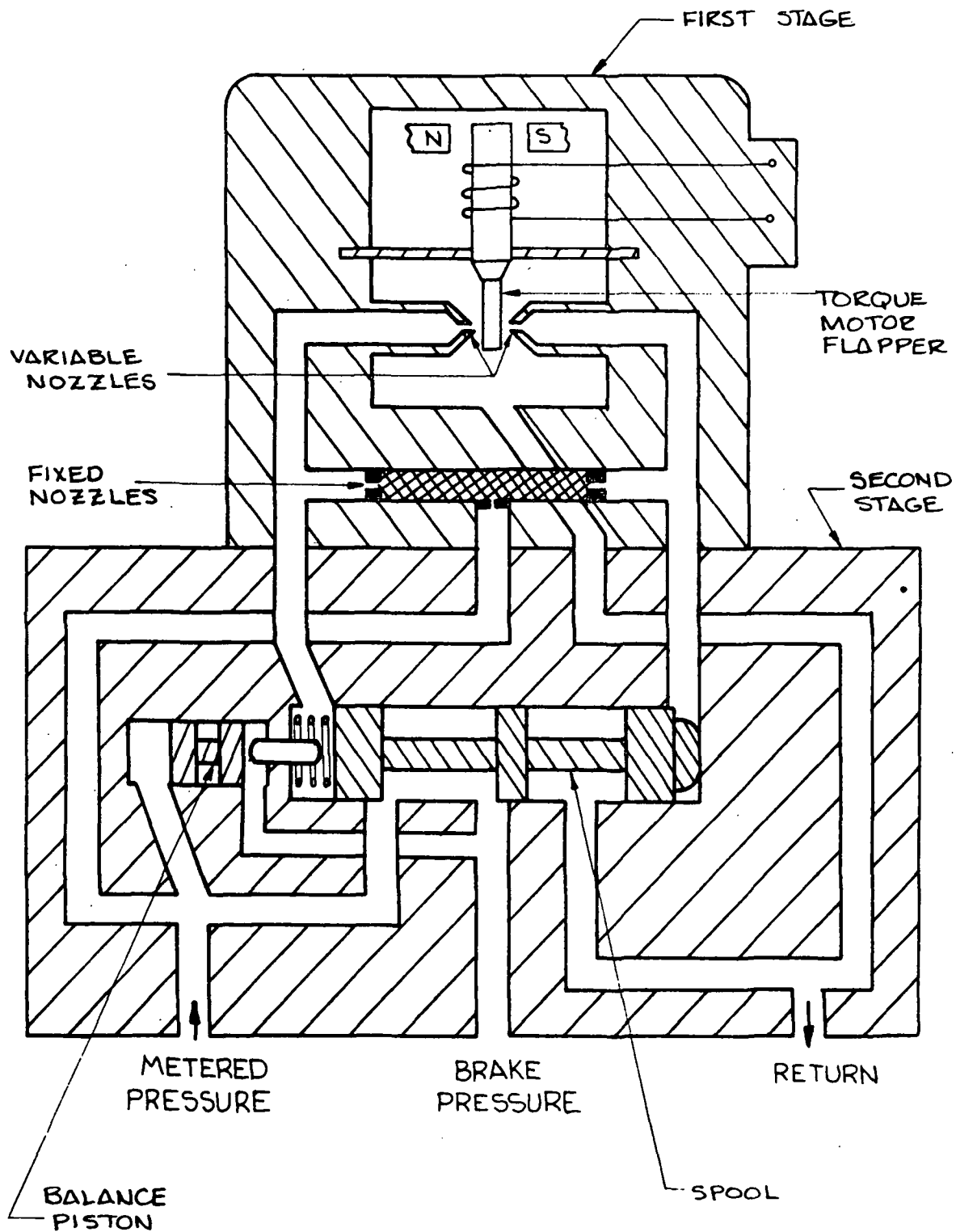


Figure 3. GOODYEAR ANTISKID SERVO VALVE (LOCKHEED L-1011)

now acts as a metering device to reduce pressure to the brake. The spring in the second stage acts to keep the spool in the fully opened position. During valve operation forces from the spring, balance piston and hydraulics position the spool until an equilibrium is reached.

DESCRIPTION OF THE HYDRO-AIRE (BOEING 747) SKID CONTROL SYSTEM

The Boeing 747 skid control system is one of the latest adaptations of the Hydro-Aire Mark III antiskid system. This system is representative of Hydro-Aire's latest development and was, therefore, chosen for this study. A description of this system follows.

The Hydro-Aire Mark III antiskid system provides individual skid protection for the sixteen main wheels of the Boeing 747 airplane. In the normal braking system, each wheel has its own speed sensor, antiskid control circuit and electro-hydraulic servo valve. A motor driven interconnect valve controlled by the pilot allows selection of the Number 4 (primary) or Number 1 (secondary) hydraulic system to power this brake system. (The 747 has four hydraulic systems).

In addition to the normal system, there is a reserve system which can be selected by the pilot. This system uses paired wheel control, i.e., a dual pair of wheels on a truck is controlled by only one antiskid valve. The valve signal is composed of the highest control signal from each pair of control circuits so that the wheel with the lowest runway friction will dictate control to the other wheel. Both normal and reserve systems have separate pilot metering valves which are slaved together for pilot input force. Inadvertent use of both systems together causes no operating difficulties except the possible reduction of antiskid efficiency. Also the pilot must exert some additional force to actuate both normal and reserve metering valves together.

Touchdown protection on the 747 is provided through the use

of the landing gear logic system. Proximity switches (two per truck) sense when the airplane is on the ground by having any two trucks out of tilt across the airplane. This condition provides a signal from both the primary and secondary landing gear logic systems grounding the brake release bias voltage to the antiskid system velocity comparator, (See Figure 4). This allows normal antiskid operation when the pilot meters sufficient pressure to cause tire skidding. Wheel spinup will override the touchdown protection signal permitting normal braking if the air/ground switches are not activated upon touchdown.

Locked wheel protection is provided for each wheel having antiskid protection. Four sets of four wheel groups are used. Both front and rear left outboard wing gear wheels are paired together with the right front and rear inboard body gear wheels. This same sequence is used to combine the remaining three locked wheel groups. In each four-wheel group each wheel control circuit has three other velocity references besides its own to provide locked wheel protection reference. A memory circuit for each wheel provides locked wheel protection even if all four wheels in a group are locked simultaneously.

The Mark III skid control system is represented by Figure 4 in a simplified, but functional form. A transducer is used in each braked wheel to provide instantaneous wheel speed information. The wheel speed transducer is a frequency modulating device which produces an AC signal with frequency proportional to wheel speed. This signal passes through a squaring network in the control circuit, then is fed into a demodulator, which is called the frequency converter in the block diagram. The signal emerging from the converter is a DC analog voltage that directly varies with wheel speed.

The aircraft velocity and deceleration reference is provided by the reference deceleration and reference velocity functions shown in the block diagram. At wheel spinup the velocity comparator develops an error signal which forces the velocity reference to increase until the error signal ceases. In this manner the simulated reference

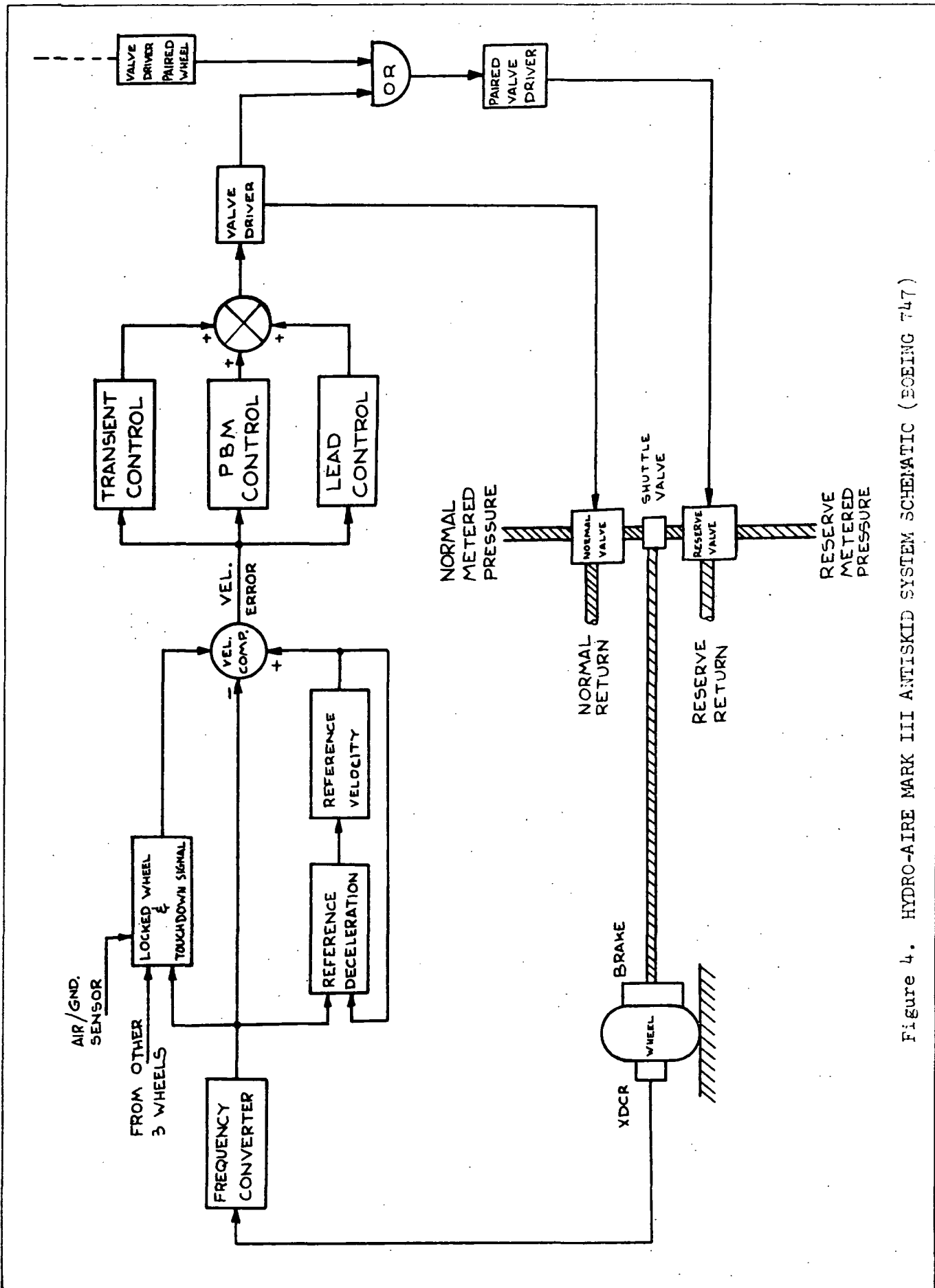


Figure 4. HYDRO-AIRE MARK III ANTISKID SYSTEM SCHEMATIC (BOEING 747)

airplane is initialized at touchdown for the braking condition to follow.

The reference deceleration function provides an output which is the derivative of the gradually changing component of the wheel velocity, and thus is proportional to aircraft deceleration. During the interval when the aircraft is braking or decelerating, the reference deceleration serves as the input driving function for the reference velocity function. Thus the reference velocity function provides an equivalent aircraft velocity.

Wheel speed information coming from the velocity to DC converter and the reference velocity are summed at the input to the velocity comparator becoming the differential input to the comparator. The output of the comparator is the velocity error signal for that wheel and it provides the input driving function for the PBM, (Pressure Bias Modulation), transient control function and lead circuit. These three functions are responsible for the normal control of the system, each having a separate control function.

The PBM control is the time integral of the velocity error and in comparison to the transient control is slower to respond to error signals. It controls the rate at which pressure is brought on when the brake pressure is lower than skid pressure. As an integrator it has the characteristic of serving as a memory device, not allowing brake pressure to be reapplied at a higher level than that which previously caused a skid. This also serves to help the system adapt to varying runway conditions.

The transient control is characterized by a fixed gain and threshold. Its input is the velocity error coming from the velocity comparator and thus is a proportional control once the appropriate threshold is exceeded.

The remaining control element, lead, is in the form of a velocity

error rate, and is coupled into the summing amplifier. Since it represents the rate of velocity change, a differentiation, it provides a dynamic lead function which anticipates and initiates the brake pressure modulation to help control skids. The transient control provides the main recovery from skids, while the lead control is used to quicken the system response thus improving efficiency. Appropriate use of lead control can also improve overall system strut damping by way of dynamic compensation.

The remaining system components include the summing amplifier and valve driver. Signals from the PBM, transient and lead controls are summed together by the summing amplifier and this output is the driving function for the valve driver. Essentially the valve driver provides current for the servo valve for a given voltage input from the summing amplifier.

To summarize the description of the Mark III system, a typical skid cycle will be described. As braking is initiated, PBM will always attempt to bring on more brake pressure so that eventually the braked wheel will begin to develop a slip and then go into an actual skid. This condition will develop an error signal in the velocity comparator since the reference velocity and wheel speed signal will begin to disagree. The responses to this skid condition are described in the order of normal occurrence. Any change in the wheel speed signal such as a skid will develop a signal from the reference deceleration function. This will tend to drive down the value of the reference velocity and also provide a signal to the summing amplifier. Since the reference deceleration signal is a derivative of the wheel speed, it tends to anticipate or lead the correction signal to the summing amplifier. After the velocity error exceeds a certain threshold, the transient control responds and continues skid pressure correction proportional to the magnitude of the velocity error. To insure that the same brake pressure is not reapplied after a skid, the velocity error drives down the value

of the PBM so that it has a lower value than that previous to this skid. As soon as the velocity error signal is decreased by virtue of the wheel spinning up again, the transient and lead functions disappear, leaving the PBM to regain control, re-apply brake pressure and increase brake pressure until the entire cycle is repeated again.

The Hydro-Aire Mark III valve is shown in Figure 5. It is a two-stage valve with a flapper, nozzle type first stage and spool, sleeve second stage. The permanent magnet torque motor in the first stage operates the flapper. The hydraulic bridge built around the flapper consists of two fixed and two variable nozzles. Movement of the flapper unbalances the bridge with a resultant pressure differential applied to the second stage spool. Movement of this spool from the relaxed position serves to reduce pilot's metered pressure to the brake. The forces on the spool work to position it until an equilibrium position is reached. The value is shown in its relaxed position, i.e., no current to the first stage.

The wheel speed transducer used in the Mark III system is shown in Figure 6. This device is self-contained and is mounted in the axle. The bearing mounted rotor is driven by a bellows mounted in the hub cap and has the advantage of eliminating any undesirable effects from misalignment. Both the rotor and the stator are made of ferrous material and have 200 teeth. A magnetic field is established by supplying current to the stator coil from the antiskid circuit. As the rotor turns, the alternating alignment and misalignment of the teeth in the rotor and the stator vary the reluctance in the magnetic circuit. This results in an alternating current in the supply current which generates an AC frequency proportional to wheel speed.

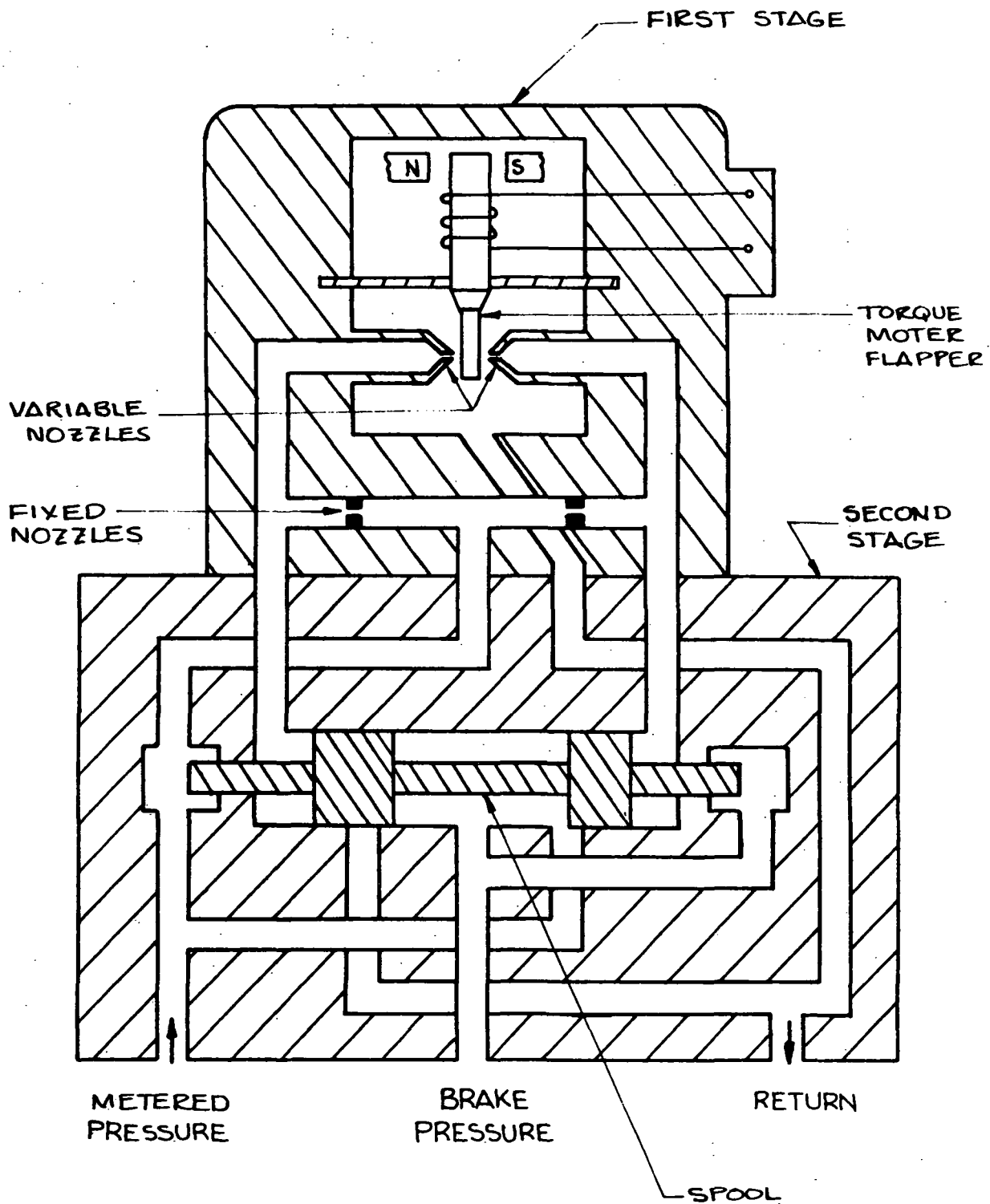


Figure 5. HYDRO-AIRE MARK III ANTISKID SERVO VALVE (BOEING 747)

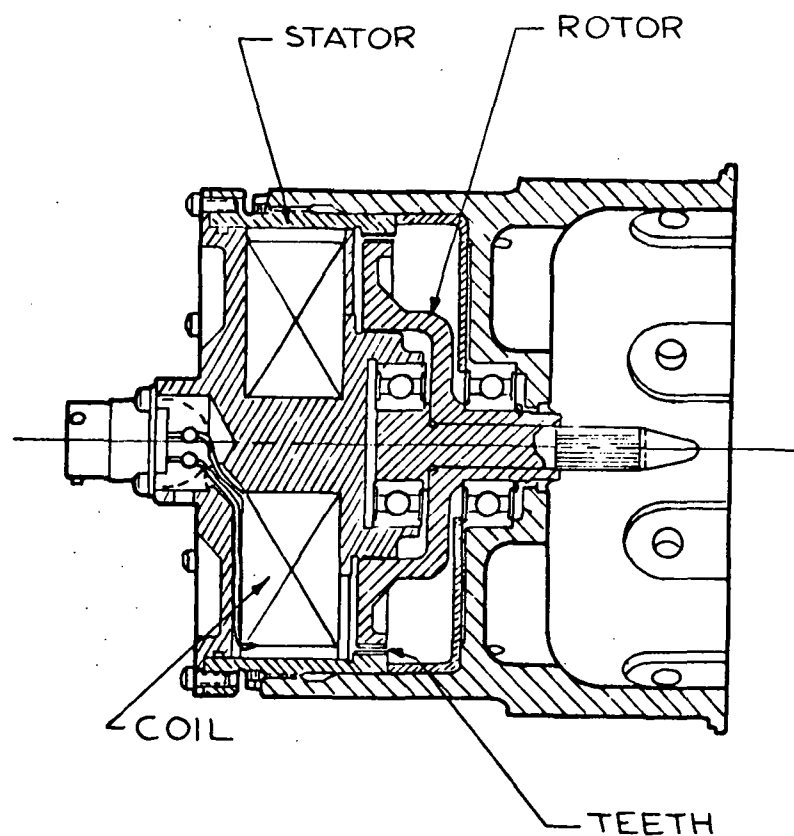


Figure 6. HYDRO-AIRE MARK III ANTISKID WHEEL SPEED TRANSDUCER (BOEING 747)

DESCRIPTION OF THE HYDRO-AIRE (BOEING 737) SKID CONTROL SYSTEM

The Boeing Advanced 737 skid control system is included in this study because it represents a good comparison case for the space shuttle redundancy requirements study. The control circuitry is very similar to the already described 747 system and the reader is referred to that description. The greatest difference in design between the 737 and 747 systems is largely that due to the difference in number of braked wheels. With only four wheels, the 737 system had to be laid out with far greater emphasis on symmetrical failure modes to meet safety requirements. For this reason the two inboard wheels are powered by one hydraulic system while the two outboard are powered by a separate system. Pilot's control of flow to the brakes is accomplished through two dual metering valves. Each dual valve controls flow to the brakes on one side of the airplane.

Touchdown protection is provided to only inboard wheels on this airplane. With only one air to ground squat switch, a single failure in the air mode would mean that at low airplane velocity all four main brakes would be fully released if all four had touchdown protection. Thus the reason why only two wheels are protected. If brakes are inadvertently applied prior to touchdown, two protected wheels will adequately meet safety requirements. Figure 7 represents a simplified Mark III diagram for the Advanced 737. The basic control components are functionally the same as found on the 747 (See Figure 4) differing mainly in their tuning values. These minor differences come about because of differences in the wheel speed transducers, wheel size, hydraulic systems and landing gear configurations that exist on these two airplanes. The description given for the 747 basic control system will therefore adequately describe the 737 system. The redundancy requirements of the 737 system are met by the two separate hydraulic systems so there is no need for a reserve or backup braking system like the paired wheel control system on the 747. Each main wheel has only one control card, transducer and control valve.

NOTE: TOUCHDOWN PROTECTION
ON INBOARD WHEELS ONLY

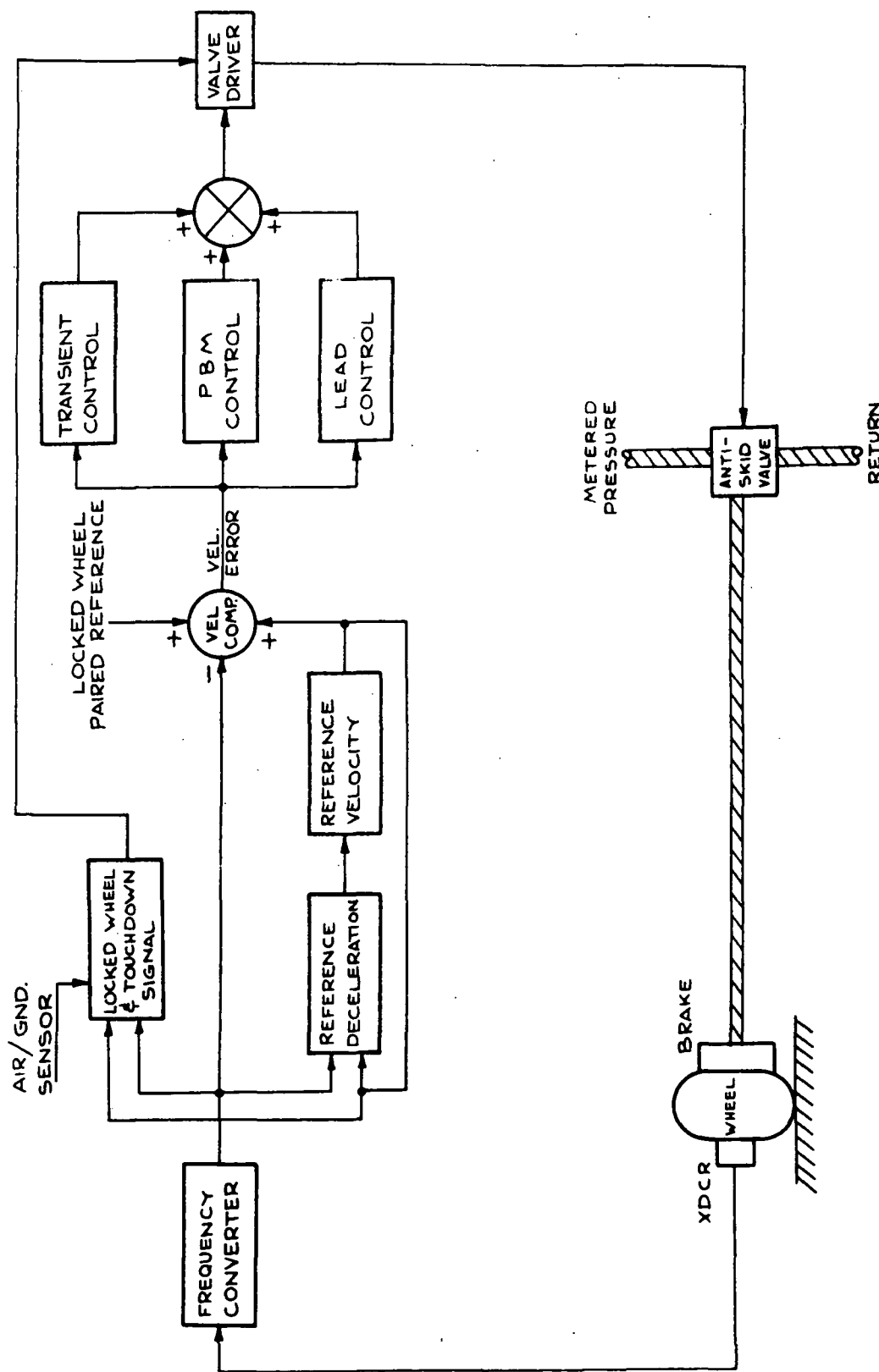


Figure 7. HYDRO-AIRE MARK III ANTISKID SYSTEM SCHEMATIC (BCEING 737)

Both touchdown and locked wheel protection on the Advanced 737 provide a valve signal that is 125 percent of the normal full transient signal. This signal will ensure that the brake pressure is fully released. Touchdown protection will be present when the wheels are not spinning and the squat switch is in the air mode. If either the squat switch ground signal or the wheels spinup conditions occur, the release signal will disappear and the pilot can meter brake pressure. During a normal braking stop, if one wheel of a locked wheel pair drops 75 percent below the other, a locked wheel signal will be present at the valve driver of the locked up wheel. Locked wheels are paired inboard-inboard and outboard-outboard. If for some reason the squat switch does not switch to the ground mode after landing, the wheel speed signal will override as long as the velocity is above a very low level. At this point the locked wheel signal will reappear preventing any more braking on those wheels that have this protection.

The servo valve used in the 737 system is shown in Figure 8. Compared to the 747 valve, it is less complicated to manufacture because it does away with several close tolerance requirements. Referring to Figure 5 the 747 second stage spool has two additional forces applied to the spool. These are eliminated with the 737 type valve by rearranging the flow in the second stage. This also requires a change in the operation of the first stage hydraulic flapper-nozzle.

In the 747 valve, the neutral flapper position (center position) produces a balanced hydraulic bridge and forces on the second stage spool permit full pilot's metered pressure to the brake. In the 737 valve, the neutral position of the flapper is hard over against the return side nozzle. To get zero brake pressure in the 737 type valve the flapper must be biased hard over against the metered pressure nozzle so that first stage nozzle flow is completely cut off. The second stage spool is spring biased to insure full braking capability with no current input signal to the valve.

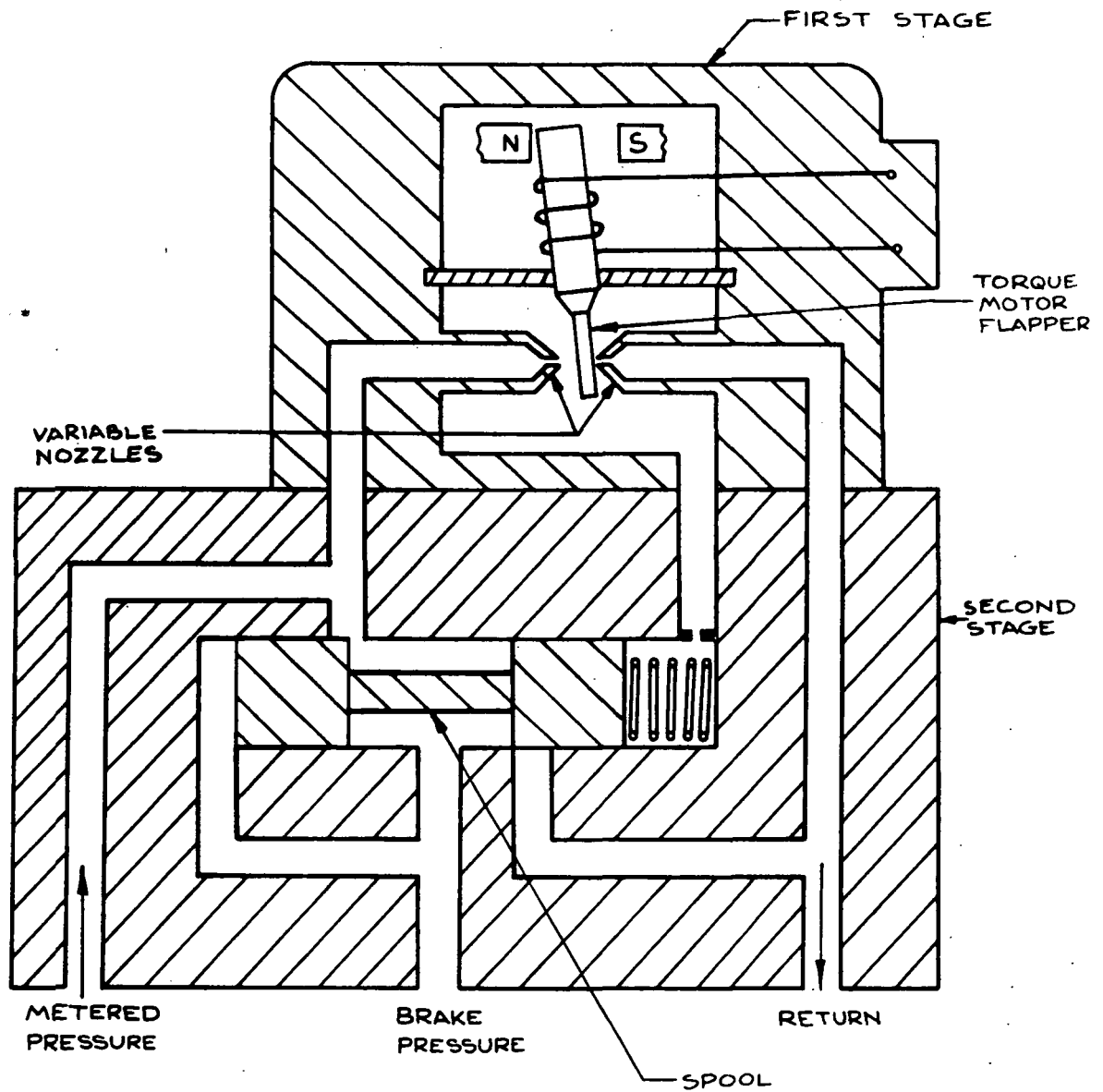


Figure 8. HYDRO-AIRE MARK III ANTISKID SERVO VALVE (BOEING 737)

The 737 transducer shown in Figure 9 is functionally similar to the 747 transducer (see Figure 6). In the 737 unit, the rotor is mounted in a dual roller bearing and axial thrust is absorbed through a ball at the end of the shaft. This is a slightly different arrangement than the 747 transducer as Figure 6 will show. The 737 transducer only has 150 teeth compared to 200 teeth in the improved 747 unit. (Most of the early 747 airplanes use 50 teeth transducer along with a different filter in the skid control module).

DESCRIPTION OF THE BENDIX (BOEING 2707-300) SKID CONTROL SYSTEM

The Bendix, Boeing 2707 (USA-SST) skid control system represents the latest Bendix development in antiskid systems and therefore was chosen for this study. Its description follows.

The twelve pairs of co-rotating main wheels of the Boeing 2707 (USA-SST) are each provided with individual antiskid protection. Each wheel pair has its own wheel speed sensor, brake, control circuit, and electro-hydraulic servo valve. This, the normal system, is powered hydraulically by the "B" aircraft hydraulic system. The vehicle also has a standby control system which has its own set of six paired wheel control circuits, separate hydraulic system and paired antiskid servo valves. The wheels are paired across the truck.

If the "B" hydraulic system fails, the system automatically switches to the standby system. In the event the normal systems fails other than hydraulically, the pilot can also manually switch to the standby system. Once in the standby mode and failure of its hydraulic system occurs (the "D" system on the aircraft), the standby system can be powered by an auxiliary pump. This pump is connected into the "D" system plumbing downstream of the normal "D" system pump and thus serves as a backup power source.

Locked wheel protection is provided in addition to the normal

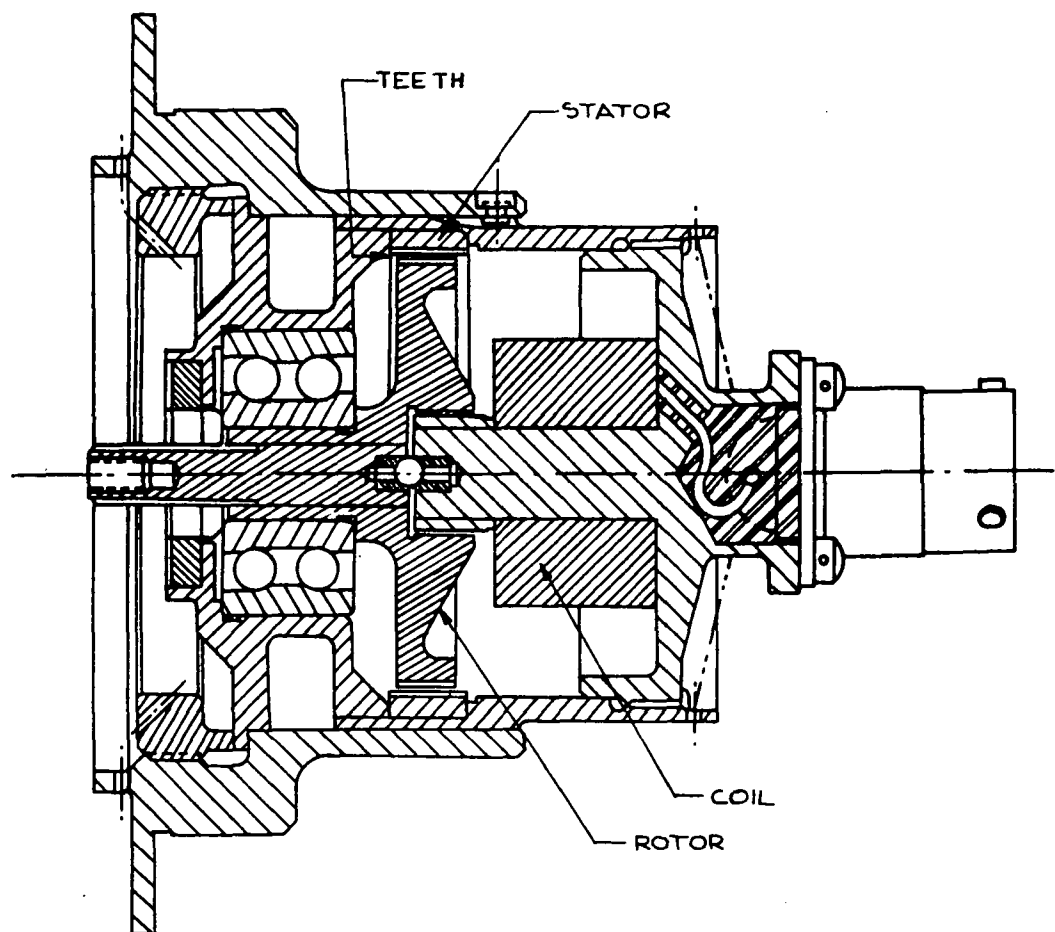


Figure 9. HYDRO-AIRE MARK III ANTISKID WHEEL SPEED TRANSDUCER
(BOEING 737)

antiskid control. The reference velocities of two wheels are paired together to provide locked wheel reference for each other. The pairing scheme is equidistant across the airplane with the left forward outboard wheel paired to the right forward inboard wheel. This scheme is continued through the remaining five pairs of wheels. If and when a locked wheel occurs during normal antiskid control, the locked wheel circuit will provide a full release signal to that individual wheel. This signal is maintained until the wheel speed recovers to near synchronous speed when normal antiskid control resumes.

Touchdown protection is also provided in addition to the normal antiskid protection. There are two air to ground sensors used, one in the nose and one in the main gear. Prior to landing, when the two sensors are in the air mode, the touchdown circuit provides a full brake release signal to all wheels. When the airplane lands, a 5.5 second timer is started either by main gear wheel spinup or the main gear squat switches to the ground mode. Brake release signals to all main wheels then continues until the nose gear squat switches to ground mode or the 5.5 second interval elapses. At that time normal braking and antiskid control is possible. This time delay is necessary to prevent brake application before nose gear touchdown to assure pilot comfort and structural integrity.

The Bendix antiskid system can be represented in block diagram form as seen in Figure 10. In the diagram just prior to the valve driver, the summing junction shows an input called pilot brake application signal. In this airplane an electrical system takes the place of normal cable rigging and metering valve. The pilot's pedals are connected to multiple rotary LVDT transducers which convey brake application signals to the antiskid control system. Then the correct signal is chosen (mid value logic scheme) and is processed and then sent to the summing junction.

From this point on, the system performs conventionally, i.e., as

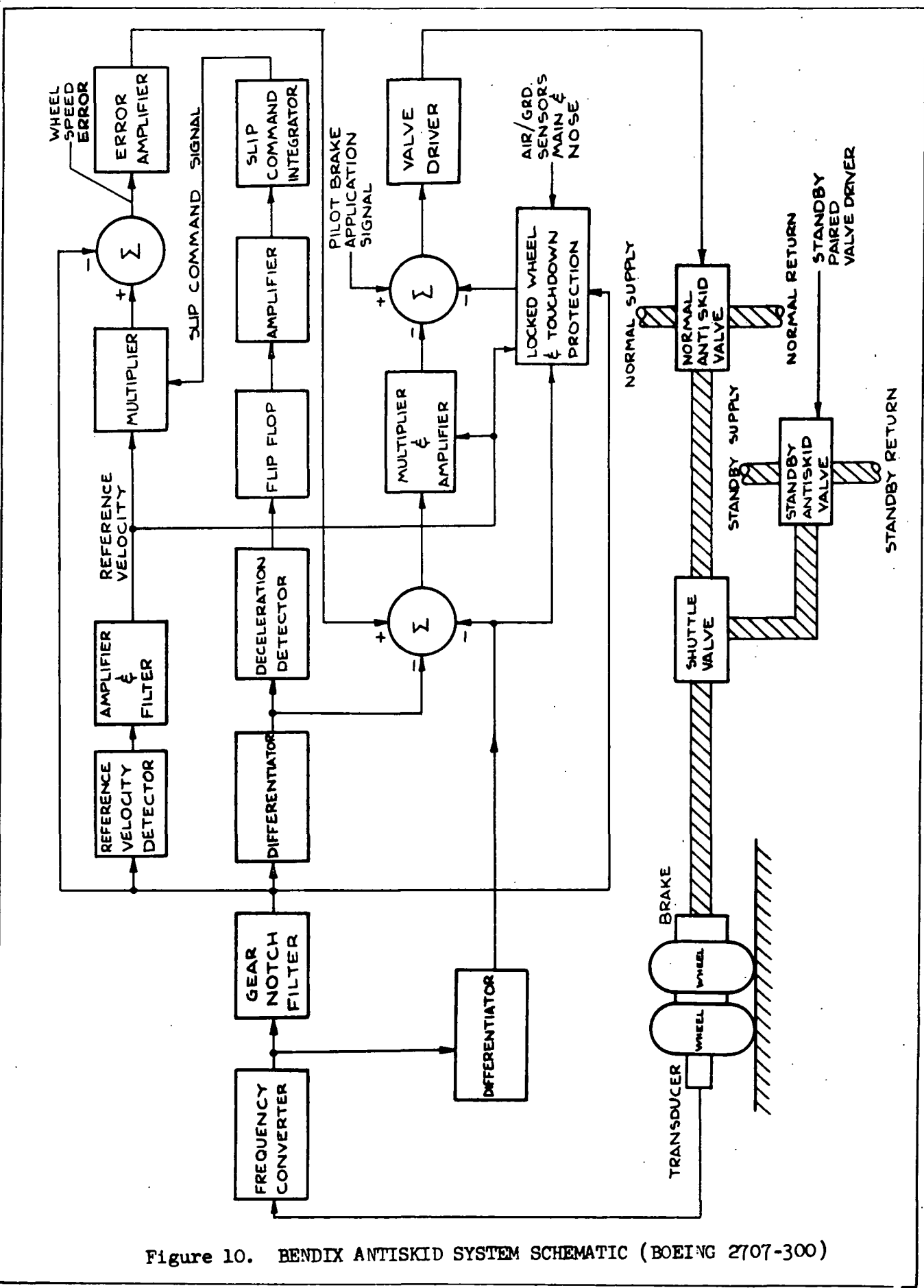


Figure 10. BENDIX ANTISKID SYSTEM SCHEMATIC (BOEING 2707-300)

any system with a pilot's brake metering valve, since if the pilot commands more brake pressure than the tire can handle without skidding, the skid control system provides a signal which modulates the brake pressure and provides efficient brake control. Each brake co-rotating pair of wheels has its own wheel speed transducer. This is an ac signal with frequency proportional to wheel speed. The frequency converter in the control card doubles frequency, amplifies and squares it, pulse shapes the squared signal, then demodulates and filters it to provide a dc signal proportional to wheel speed. This output is sent to a notch filter which is tuned to the landing gear natural frequency and acts to dampen landing gear oscillations. Wheel speed signals from the converter and notch filter are applied as input signals to the rest of the control circuitry. In the reference velocity circuit the wheel speed signal is filtered such that if the speed is suddenly lowered, the velocity reference input to the error summing junction, when compared to the wheel speed will develop an error signal. The reference velocity signal is also multiplied by the slip command signal which provides a commanded wheel speed.

The slip command channel consists of a differentiator, detector, monostable flip-flop, amplifier and integrator. These components are in a straight line in the middle of the diagram. The function of the slip command circuit is to provide an incremental reduction of slip which serves to reduce brake torque. When a sufficient deceleration is detected the flip-flop changes state and after a fixed increment reverts back to its original state. The result is a pulse signal of fixed height and width which is amplified and integrated becoming the slip command signal. This signal is supplied to a multiplier and is multiplied by the reference velocity signal. The threshold in the deceleration detector is varied as a function of wheel speed which acts to provide consistent dynamic response regardless of wheel speed.

In addition to the gear notch filter a deceleration signal is

fed into the wheel speed error circuit to provide additional damping of landing gear oscillations.

The wheel speed error signal is generated by summing the two wheel speed derivative signals and the output from the error amplifier. This error amplifier signal comes from the summation of the wheel speed signal from the notch filter and the product signal of slip command and reference velocity circuit. This summing point signal is then fed to a multiplier along with the reference velocity signal producing a function which serves to change the gain of the system as a function of reference velocity. Finally the multiplier output is fed to the valve driver to modulate the pilot's commanded brake pressure to produce efficient braking control.

Basically the Bendix system operates on the principle of commanding a fixed slip to the braked wheel. If and when the peak slip is exceeded the slip command channel produces a pulse signal which drives the wheel slip back to the stable front side of the tire friction relationship by reducing brake torque. After the slip command signal vanishes, the fixed slip command signal will begin increasing brake torque again such that the system will again search for the peak friction point.

The Bendix wheel speed transducer is shown in Figure 11. It is an inductor type alternator which provides a sinusoidal output signal. The transducer incorporates a 50-tooth permanent magnet rotor supported by two ball bearings. The eight pole stator with 48 tooth spacing and the rotor are housed in an aluminum case. The output of the transducer is 50 Hz per wheel revolution.

The Bendix antiskid valve is shown schematically in Figure 12. It is a two-stage, jet pipe first stage and spool type second stage valve. The jet pipe first stage drives the second stage in proportion to the input signal. With no input current the flow is directed equally to both receiver inlets since the jet pipe is positioned

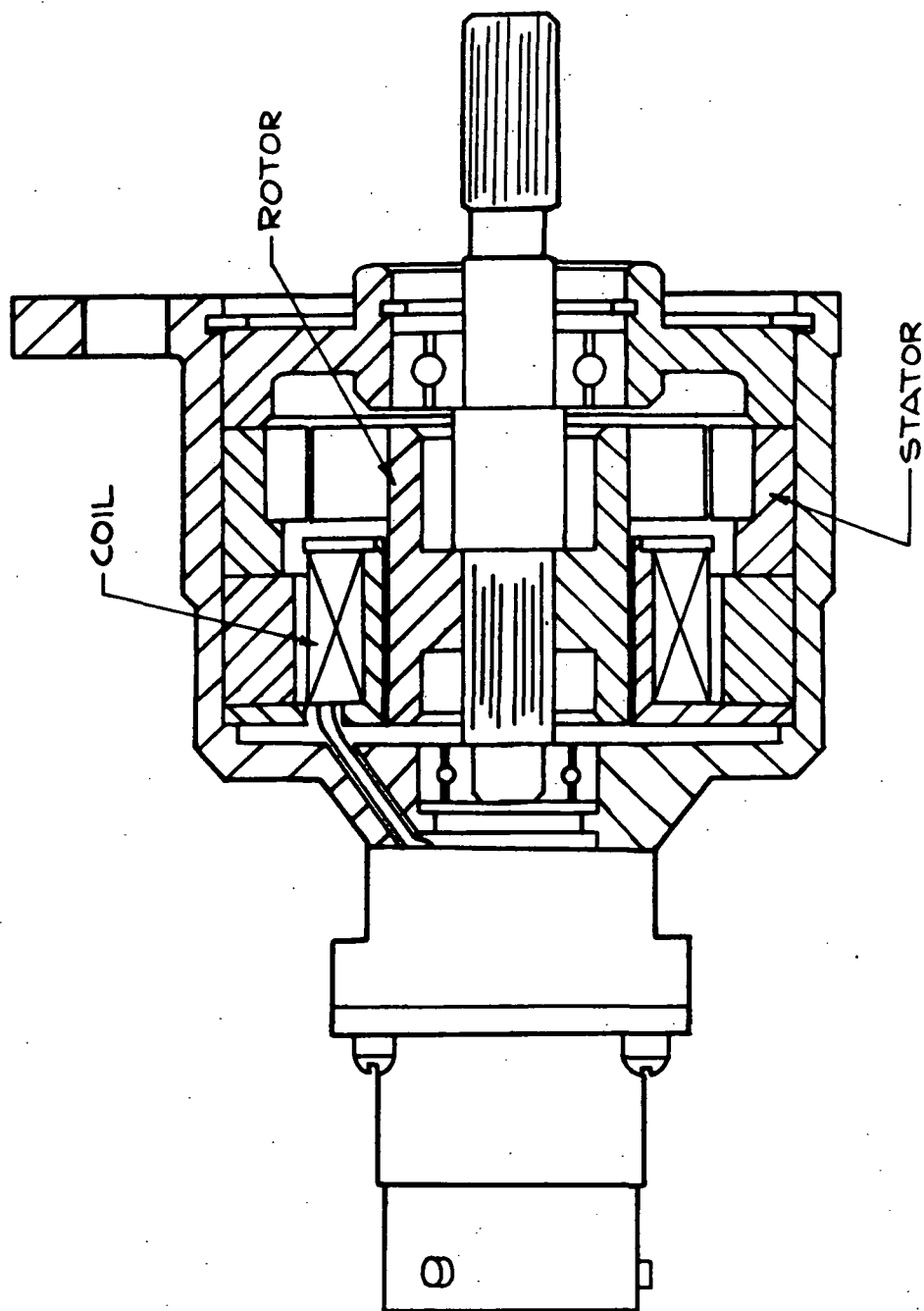


FIGURE 11. BENDIX ANTISKID WHEEL SPEED TRANSDUCER (BOEING 2707-300)

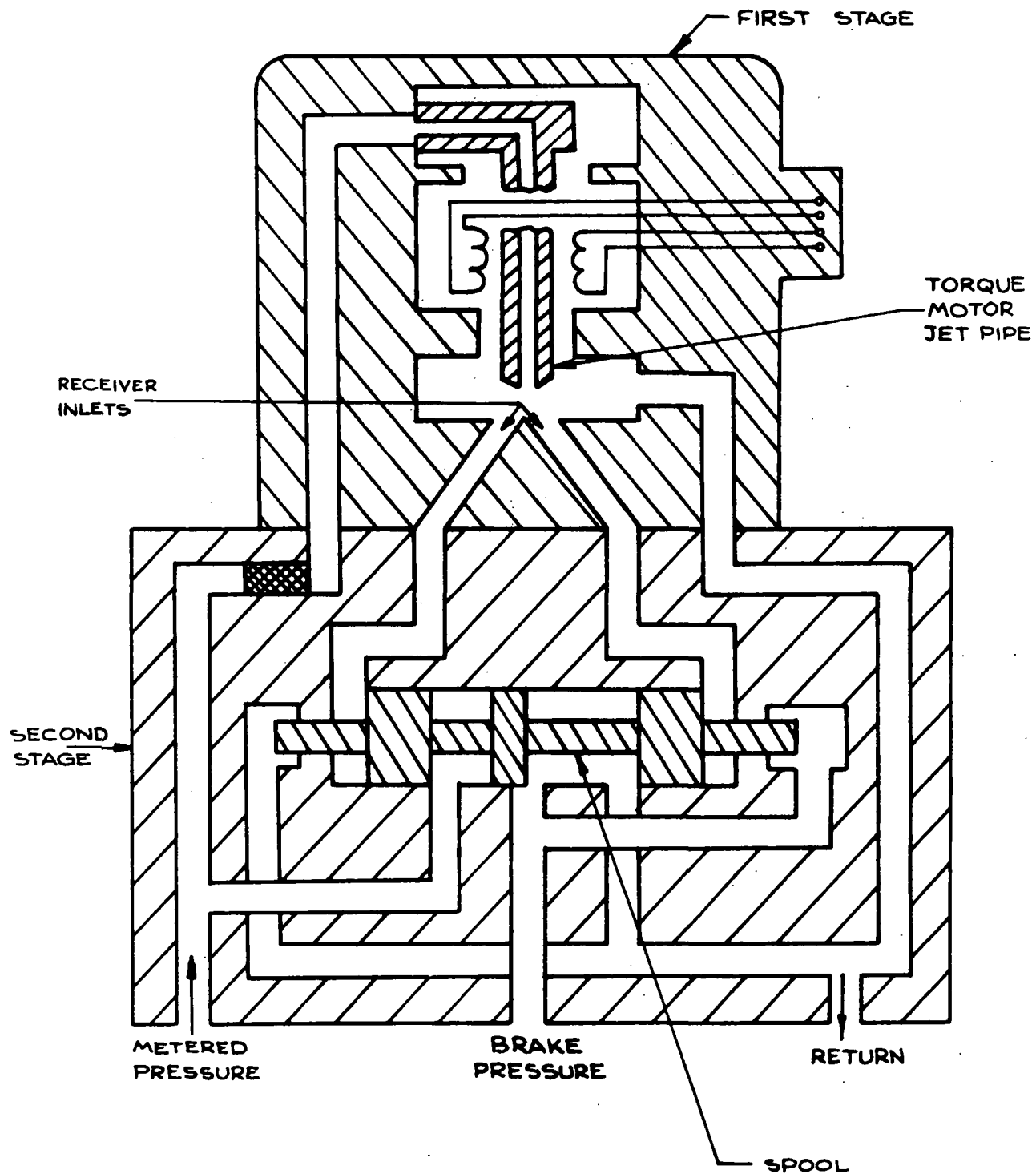


Figure 12. BENDIX ANTISKID SERVO VALVE (BOEING 2707-300)

directly over them. An input signal deflects the jet torque motor nozzle to either side, unbalances the flow through the receiver inlets and drives the second stage spool in the direction of the unbalanced force. Brake pressure at one end and return pressure at the opposite end also act to position the spool. Pressure control to the brake is produced by this adjustment of forces on the spool. When the commanded brake pressure is reached, the return pressure and brake pressure serve to balance spool forces.

DESCRIPTION OF THE SPAD (CONCORDE) SKID CONTROL SYSTEM

The SPAD (Manufactured by Hispano - Suiza Division of LaSneema) skid control system as it is implemented on the Concorde, represents the latest SPAD development. It was therefore chosen for this study. Its description follows.

The eight main gear wheels of the Concorde aircraft are provided with antiskid protection in the normal brake control system. Each main gear wheel has its own wheel speed transducer skid control circuit and electro-hydraulic servo valve. There are also two wheel speed transducers on the unbraked nose wheels which generate reference aircraft velocity for the system. The system is comprised of four separate antiskid control boxes each controlling a dual pair of wheels on a truck. The electronic control circuit for the normal brake control system provides for no antiskid system backup. There is only one valve, one control card and one wheel speed transducer per main gear wheel.

There are two separate aircraft hydraulic systems available to power the normal brake control system. The "green" system is the primary hydraulic power source for the normal brake control system, but if failure in this "green" system occurs, the "yellow" hydraulic system is substituted by an automatic change over valve. Further, the pilot has the option of selecting the normal brake control system or an emergency system. If the emergency system is

selected, the normal brake control system will be shut down and the emergency system will be powered by the "yellow" hydraulic system. This emergency system is without antiskid protection, and the pilot pedal input is by direct hydraulic metering valves, one for each side of the airplane, instead of the electronic pedal transducer system used in the normal control system. All eight main wheel brakes have a separate provision for emergency brake actuation so that the normal and emergency systems are completely distinct. As a further precaution the "yellow" hydraulic system has a separate electric pump to maintain an accumulator charge in the event of "yellow" hydraulic pump failure.

In addition to normal antiskid control during braking, there is a touchdown protection provided such that the main gear wheels have antiskid protection even before the wheels spin up. This protection comes about naturally from an initial reference condition built in to provide reference aircraft velocity before the nose wheels spin up. There are main gear and nose gear air to ground sensors which provide signals to furnish the antiskid system with the initial reference velocity at main gear touchdown. The value of the initial reference velocity is such that it closely resembles the actual touchdown velocity. Upon nose gear touchdown the nose wheel transducers provide the actual aircraft velocity.

Locked wheel protection is provided for each main gear wheel. If any braked wheel velocity drops below a fixed speed the locked wheel circuit sends a maximum current signal to the servo valve which fully dumps the brake pressure to that wheel. Since both nose wheels provide reference aircraft velocity for all eight main wheel circuits, there is no main wheel pairing for locked wheel reference in this system. This is unlike the other antiskid systems which have an electronic "reference wheel" and require velocity pairing as an additional safety precaution.

The SPAD antiskid control system is represented by the simplified diagram in Figure 13. Wheel speed transducers, which are D.C. tachometers, provide direct velocity signals to the control circuit. The nose gear tachometer signals provide a continuous aircraft reference velocity during the landing roll while each main gear tachometer signal provides direct instantaneous braked wheel speed information. Assuming the normal antiskid system is in operation, the pilot's pedal command are electrical signals sent directly to all eight main anti-skid valves. This eliminates the need for separate brake metering valves which are in the 747 and L-1011 systems discussed earlier. However, the rest of the SPAD antiskid system is like these other systems, with the control circuit maximizing the braking effort whenever sufficient brake pressure is metered to cause skidding.

The skid control system has a basic control loop which collects its main and nose wheel speed inputs at the first summing junction ($\Sigma 1$) on the diagram of Figure 13. (Assume that there is no optimizer signal present for this preliminary discussion. The optimizer function will be described later). The nose wheel speed signal is multiplied by a gain value "K" which produces a velocity reference speed reduced by an amount equal to the desired slip velocity. The desired slip is at the peak of the ground friction force-slip curve. These inputs summed at the summing junction provide an error signal which will drive the amplifier to produce a valve signal so that brake pressure will increase until the braked wheel slows to the desired sliding velocity. This is an unstable condition so the wheel will eventually go deeper into the skid. With no signal from the optimizer, its rapidly reducing velocity triggers a limit "safety stop" in the locked wheel protection circuit. This sends a maximum valve signal through summing junction ($\Sigma 2$) to fully release brake pressure. As the wheel velocity recovers, the locked wheel signal releases the servo valve, allowing normal system operation to resume.

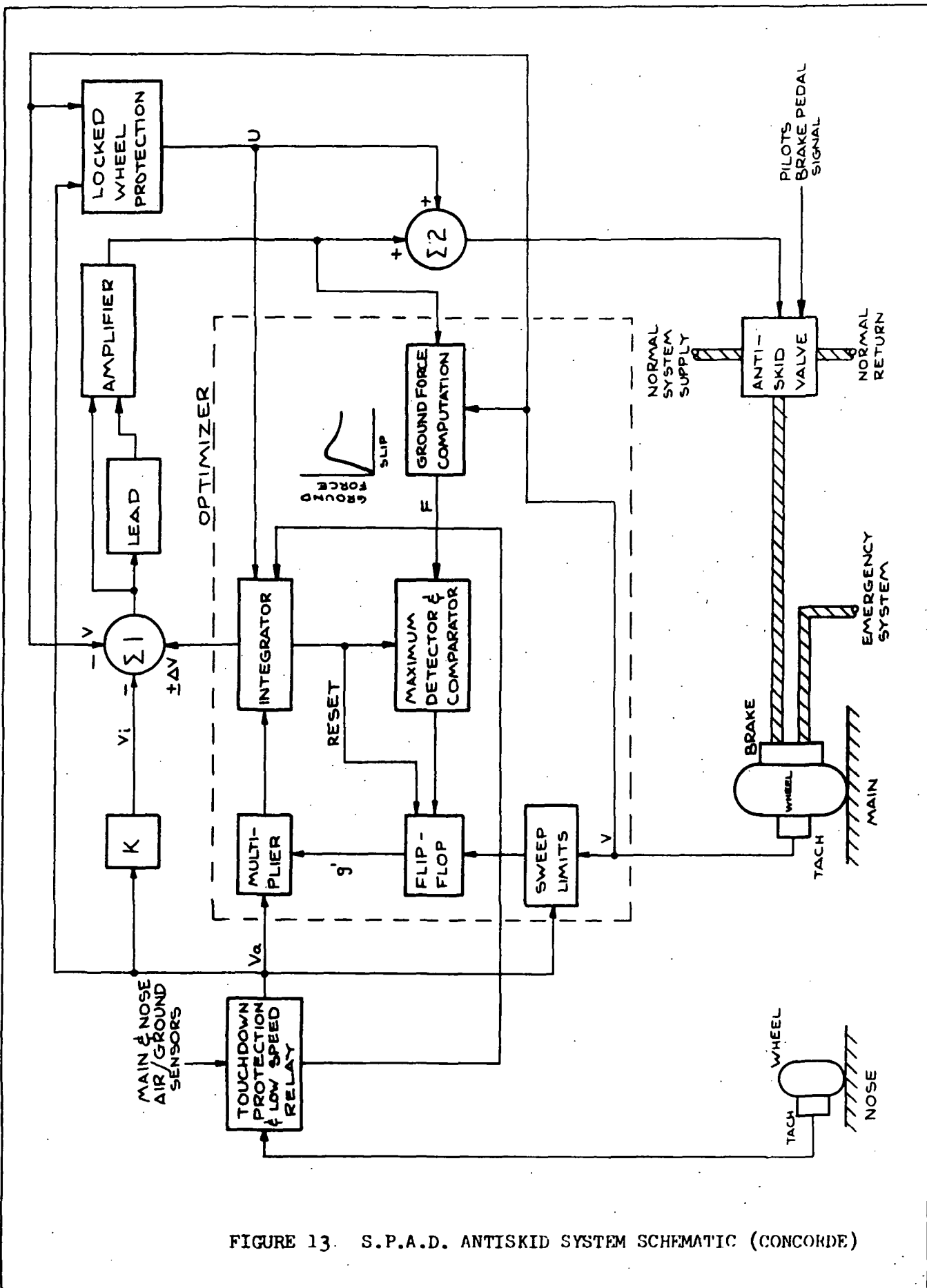


FIGURE 13. S.P.A.D. ANTISKID SYSTEM SCHEMATIC (CONCORDE)

Now assume the optimizer is in the control loop. At the resumption of antiskid operation, the integrator (see Figure 13) within the optimizer is at an initial condition (flip-flop in its initial state) and it begins to integrate its input signals such that the brake pressure steadily increases. As the tire slip is in effect moving up the front side of the ground friction curve toward the peak friction force, the "ground force computation" circuit tracks the pseudo ground force parameter "F". As this value increases the "maximum detector" will sense the peak force value and compare the continuing ground force signal to the peak value. The delta force value generated as the tire slip continues past the peak will grow until a threshold is exceeded, thus triggering the flip-flop to its opposite state. The input of the flip-flop "g'" and aircraft velocity "Va" are multiplied and integrated and the resultant signal ΔV becomes the new optimizer signal. Changing the state of the flip-flop reverses the direction of the integrator thus allowing the system to sweep back and forth across the peak of the ground force-tire slip curve.

If for some reason the flip-flop does not get a command from the "maximum detector," the "sweep limits" circuit acts to reverse the state of the "flip-flop" so that the operating point of the system will still sweep back and forth across the ground force peak. The sweep limits serve chiefly to enable the optimizer to function efficiently even though there might not be a detectable ground force peak.

Although the system can operate efficiently by sweeping between the wider pre-set sweep limits, the optimizer relies heavily on detecting the ground force peak for minimum sweep and thus maximum efficiency. Ground force is not available directly so the valve current and wheel speed are filtered in the "ground force computation" circuit to produce a pseudo ground force. The multiplier is used in the optimizer to keep a constant integrator sweep rate throughout the range of aircraft velocity.

Any time the braked wheel velocity drops below the safety stop value which acts as a backup to the "sweep limits," the locked wheel circuit interrupts braking and re-initializes the integrator, maximum detector and flip-flop. Once wheel velocity recovers, the locked wheel circuit releases control of the optimizer and allows it to resume its peak sweeping function.

The touchdown protection circuit also incorporates a low speed relay which reverts the optimizer integrator to its initial conditions when the aircraft speed drops below 10% of its touchdown velocity. This imposes a constant slippage of the braked wheel at low velocity.

The SPAD antiskid servo valve, shown in Figure 14, is a two-stage valve. It has a flapper nozzle first stage and a spool type second stage. In this valve the torque motor has two separate windings, one controlled by pilot signals and the other by the skid control system. The first stage flapper creates variable nozzles which control the two hydraulic signals leading to the second stage. These hydraulic signals act upon either end of the spool and with the spring force position the spool in the direction of unbalanced forces. As pressure is metered to the brake, this force acting on the differential spool area acts as the sole feedback to halt the motion of the spool and achieve balance. When there is no first stage signals, the spring in the second stage ensures that the spool will not prevent full system pressure from reaching the brake. Thus the pilot pedal transducer signal must provide a full brake release signal when the pedals are not depressed.

The SPAD wheel speed transducers (Figure 15) are DC tachometers. The two nose wheel transducers are gear driven at two times wheel speed. The eight transducers on the main gear wheels are driven directly and thus rotate at the instantaneous wheel velocity. These DC tachometers produce a voltage signal which is proportional to wheel speed. The rotor is composed of seven grooves, and has a

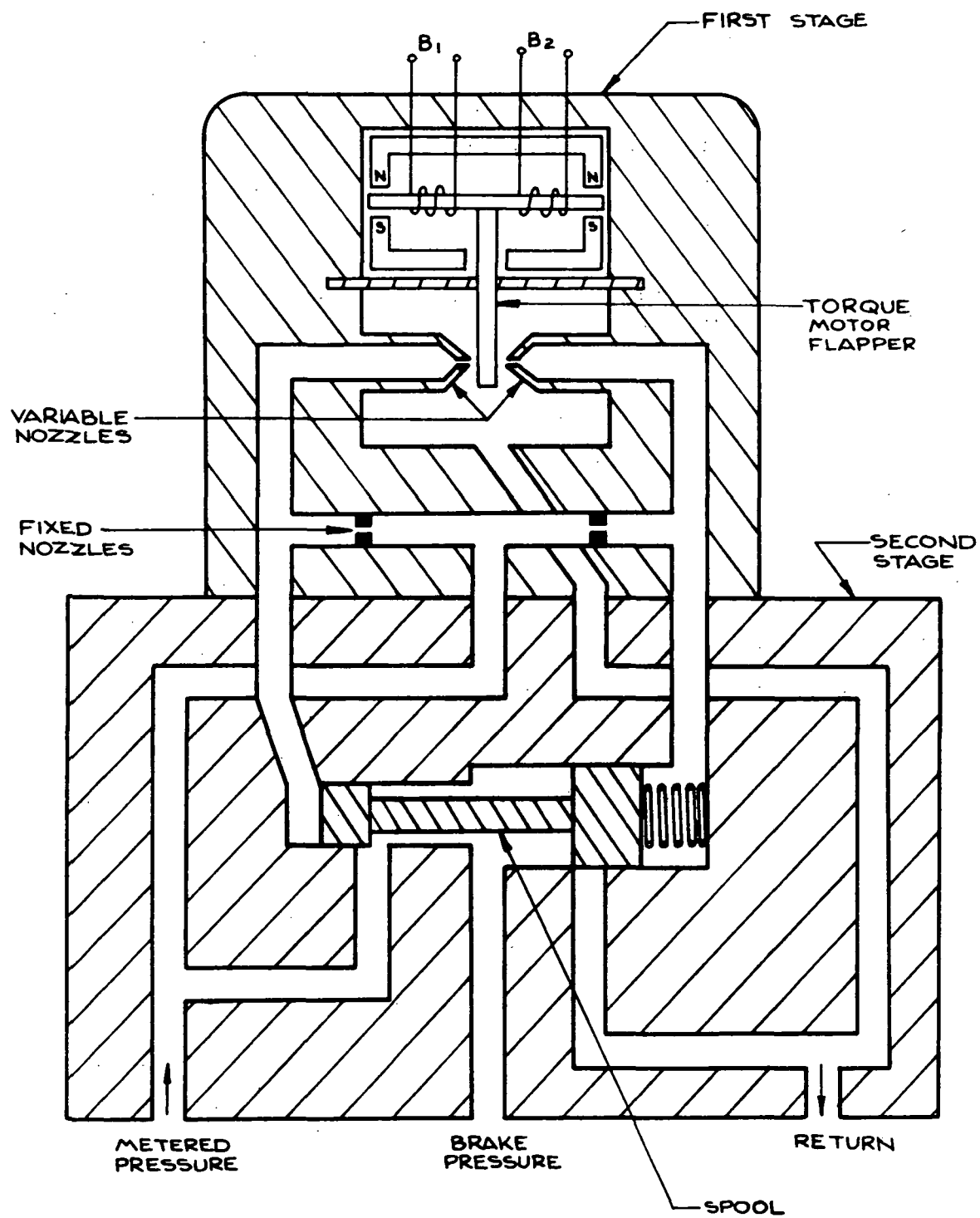


FIGURE 14. S.P.A.D. ANTISKID SERVO VALVE (CONCORDE)

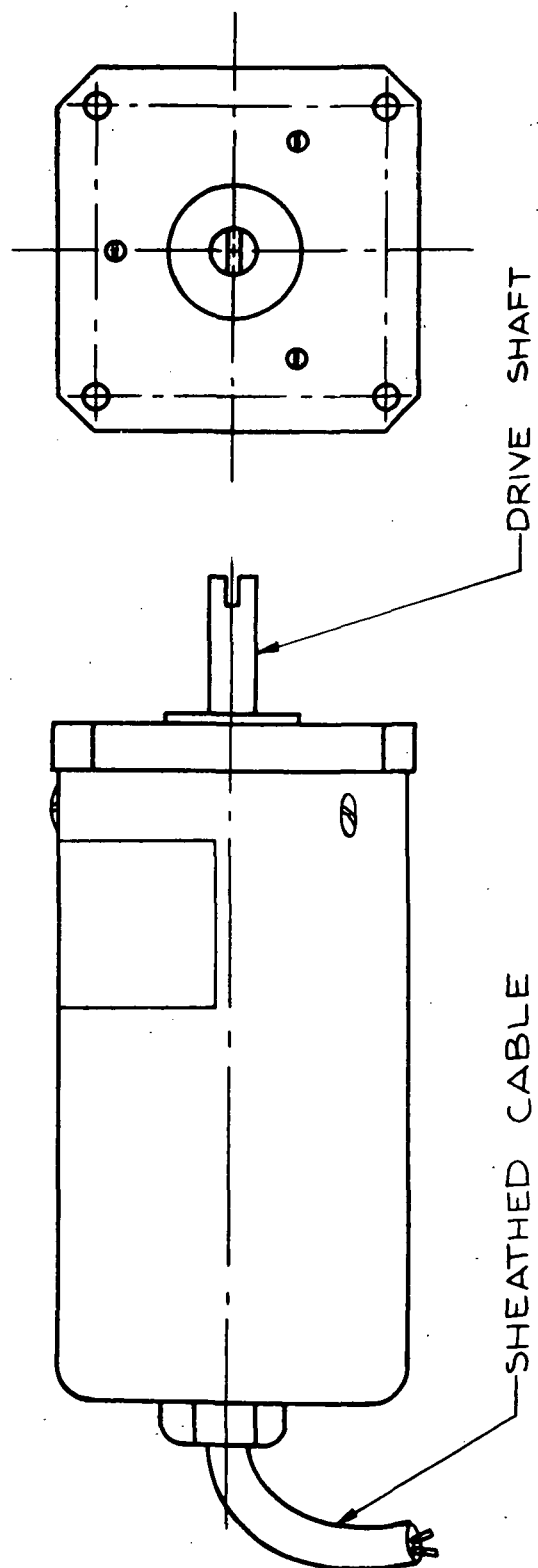


FIGURE 15. S.P.A.D. ANTISKID WHEEL SPEED TRANSDUCER

seven blade commutator. Two carbon brushes are spring loaded against the commutator. The armature shaft is supported by two lubricated sealed bearings. The permanent magnet core used in the tachometer is flux stable over the expected range of temperatures.

SUMMARY OF TRADE STUDIES

Historically, antiskid systems on aircraft were designed to prevent damaging tire lockups during braking. The sole function of the antiskid system was to detect skids, release brake pressure, allow the skidding wheel to spin back up, then re-apply brake pressure. This type of control did indeed prevent tire blowouts, but offered little in the way of efficient braking.

Antiskid systems have since evolved into what can be called brake control systems. Modern systems still provide blowout protection, but their real importance involves providing highly efficient stopping performance. To do this, the braked wheel must be slowed below its synchronous speed until the maximum braking force is reached, i.e., the peak of the mu-slip curve, Figure 16, which is usually about 90 percent of synchronous speed. However, maintaining the precise wheel speed is difficult because this is an unstable condition where the tire has a tendency to suddenly go into a much deeper skid. The ability of a skid control system to maintain control near the peak of the mu-slip curve is a measure of its efficiency.

The four modern skid control systems chosen for this study all provide braking control of an efficient nature, while also providing blowout protection. Since the only information that these skid control systems have available is wheel speed, the type of control these systems rely on deals with the wheel speed deceleration, sliding velocity and percent slip. Each system uses the wheel velocity signal differently to effect desirable brake control efficiency. A short summary of the salient features of each system follows.

The Goodyear L-1011 antiskid system produces an electronic

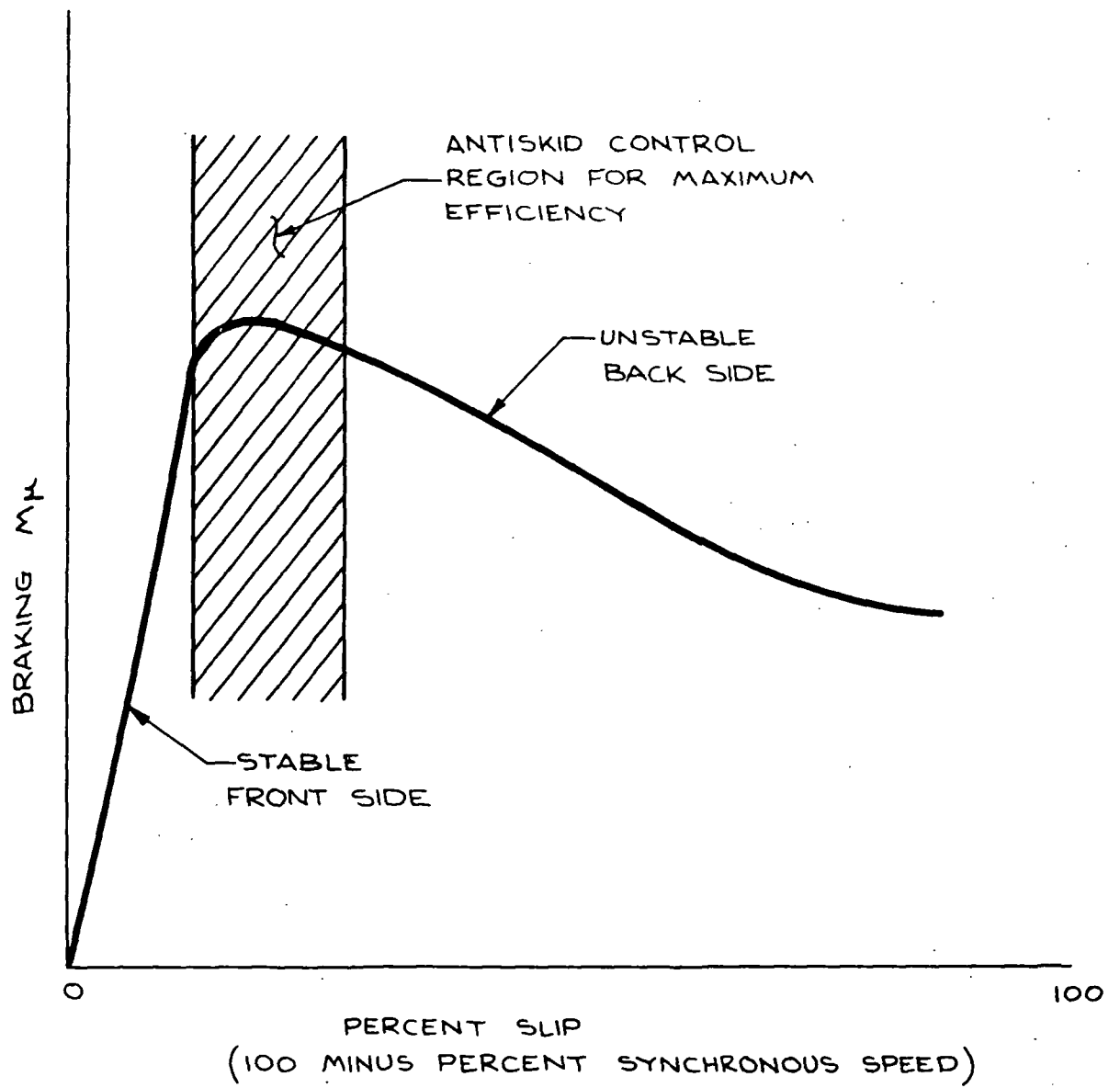


FIGURE 16. TYPICAL BRAKED AIRCRAFT TIRE μ -SLIP CURVE

reference airplane velocity and from this generates the deceleration error of the braked wheel. Whenever the braked wheel velocity exceeds a certain deceleration limit corrective brake pressure modulation takes place. An adaptable deceleration reference is used in this system to ensure high efficiency over a wide range of operating conditions.

The Hydro-Aire Mark III 747 and 737 systems use an electronic reference airplane velocity to compare to the braked wheel velocity. The difference in velocity or delta velocity is used to correct the brake pressure in proportion to the velocity error signal. This system is thus able to maintain a high efficiency over a wide range of operating conditions.

The Bendix 270/-300 (American SST) antiskid system generates an electronic reference velocity which when compared to the braked wheel velocity determines an error signal. This signal is used to provide a commanded fixed slip so that high braking efficiency can be maintained. If and when the fixed slip is exceeded a pulse signal from the slip command modulator reduces brake pressure so that the proper slip velocity can be re-established.

The SPAD skid control system used on the Concorde airplane generates its reference airplane velocity from nose wheel tachometers. This reference is compared to the braked wheel velocity to provide an error signal which is used to establish a certain sliding velocity. To find the best velocity an optimizer circuit sweeps the braked wheel velocity back and forth over a narrow band about the peak ground friction value.

All four antiskid systems use integral control as a memory device to keep the system operating at the peak ground force. Each system also uses dynamic lead compensation to help in quickening the response to wheel skids and thus improving performance.

SYSTEM RATINGS

The four major vendor's systems have been described as they were implemented for a specific application, i.e., Hydro-Aire on the 747 and 737, Goodyear on the L-1011, Bendix on the 2707 (SST) and SPAD on the Concorde. Each of these systems would require some configuration changes for space shuttle vehicle application. However, the basic antiskid functions would not be altered and can be assumed to apply as described.

Each system offers certain advantages over the others and all are capable of efficiently performing their intended function. This is evident from the fact that each was selected for use on aircraft designated for commercial and/or military use. However, some differences do exist which can influence the applicability to space shuttle. The differences are relative complexity, susceptibility to noise vibration, difficulty in implementation and system cost. These systems have been rated under four categories for this study, each having a maximum of 25 points.

Under the first item, complexity, the four systems were rated as follows:

| | |
|------------|----|
| Hydro-Aire | 24 |
| Goodyear | 22 |
| SPAD | 19 |
| Bendix | 19 |

Both the Hydro-Aire and Goodyear systems were given high ratings since both systems achieve the intended functions with relative simplicity of design. The SPAD system is slightly more complicated because of its wheel speed transducers. The most complex is the Bendix system which has a much greater number of control circuitry components.

Rating under the second item, susceptibility to noise and vibration, is as follows:

| | |
|------------|----|
| Hydro-Aire | 23 |
| Bendix | 21 |
| Goodyear | 19 |
| SPAD | 18 |

Discussion of the above rating will be dealt with under two categories: wheel speed transducer and power line noise.

Wheel Speed Transducer

o L-1011, Goodyear

The L-1011 transducer is an exciter ring-sensor device. Two types of non-concentric errors can exist with this type of transducer. The first type forms a constant gap offset and does not modulate the transducer output signal. A fixed offset gap is caused by mounting the exciter ring off center with the sensor centered with respect to the axle. The second concentric error is caused when the sensor is off center. This forms a traveling gap causing an amplitude modulation of the transducer output signal. Vibration or installation error can cause either or both types of concentric errors.

A variable reluctance sensor of this type has an output of about 0.5 volts rms, producing 42 pulses per revolution. Such a low pulse count requires considerable filtering at the converter output to smooth the dc analog voltage which incorporates a time delay. The low output signal, being just slightly over the noise level, would be the minimum acceptable.

o Wheel Speed Transducer, 2707-300 Bendix

The 2707-300 transducer is an inductor type alternator producing 50 pulses per revolution at about 0.7 volts rms. This type of a transducer has its stator and rotor mounted in a housing where the spacing is provided by its own bearings. This system is still susceptible to fixed and variable gap errors but to

a lesser degree than the L-1011 system. A third error with this type of transducer would be a non-concentric drive where the drive path would be elliptical rather than circular. This error produces frequency modulation of the transducer output. It is minimized by a long drive arm. The voltage output and frequency is approximately the same as that of the L-1011 transducer.

o Wheel Speed Transducer, Concorde, SPAD, Hispano Suiza

The SPAD transducer is a tachometer generator type supplying seven pulses per revolution at an open circuit voltage of about 6 volts. The low frequency could imply that quite heavy filtering is required for operation at low speed. Increased maintenance may be encountered with a carbon brush system. The high signal output insures an adequate signal to noise ratio.

o Wheel Speed Transducer, 747-737, Hydro-Aire

The 747 wheel speed transducer is an inductor alternator transducer similar in design to Bendix. It is current excited to produce about a 5-volt output insuring an adequate signal to noise ratio. The early 747 transducers produced 50 pulses per revolution, which was changed to 200 pulses per revolution on later airplanes. The Advanced 737 transducer produces 150 pulses per revolution. The high frequency requires very little filtering and thus a minimum time delay.

Power Line Noise

Antiskid control units can be powered directly from an aircraft supply if some means is provided to protect the control circuitry from such a noisy environment. Such a means takes the form of a buffer supply, pre-regulator, regulator and filters, used singularly or combinations thereof as requirements dictate.

It is practical to limit the load to one supply to an antiskid pair of wheels (left inboard - right inboard, etc.) so that any power

failure cannot cause a total loss of braking and so that any loss that does occur will not unbalance the braking action, endangering steering control.

In the case where a number of different level outputs are required, the voltage buildup and decay at turn-on or turn-off should have the same time constant. A poor design would be a case where the negative power to an operational amplifier circuit built up much slower than the positive power to provide unwanted outputs due to control power excursions.

Power Supply

- o L-1011, Goodyear

The L-1011 is dependent upon one supply for all braked wheels. In this case, a single failure in the power supply could cause loss of all antiskid protection. Transformers are used to isolate the regulated power from voltage fluctuations. The plus and minus supplies are regulated and filtered. Current limiters provide protection against overloads and shorts. Detailed circuits are not available at this time for analysis.

- o 2707-300, Bendix

Dual power supplies are used in both normal and standby system. Each supply contains a current limiter, voltage regulator, filtering and a dc to dc converter. Physical and electrical isolation is maintained for both power supplies and their sources. A high degree of noise rejection isolates the aircraft noise from the control circuitry. Supply redundancy prevents a single failure from causing loss of antiskid protection.

- o Concorde, SPAD

An ac power supply is provided common to a braked pair of wheels. Each wheel control card has its own filtering and regulator. A single failure cannot cause loss of all antiskid control. Such

a system satisfactorily isolates the aircraft power line noise from the antiskid control circuitry. Detailed circuitry for analysis was not provided at this time.

o 747-737, Hydro-Aire

Each 747 wheel card has its own filtering and regulator. The regulators are powered off of aircraft dc power. The Advanced 737 has an ac supply for each braked pair of wheels then an individual regulator and filters for each wheel card. Each system provides good isolation from transients and power line noise.

Under the third category, Implementation, the four systems were rated as follows:

| | |
|------------|----|
| Goodyear | 23 |
| Hydro-Aire | 23 |
| Bendix | 20 |
| SPAD | 17 |

Both the Goodyear and Hydro-Aire systems were rated high since there was nothing notably deficient in their ability to be implemented on a Space Shuttle vehicle. Bendix was downrated somewhat because their complicated circuitry would require somewhat more weight, space and power. The SPAD system was given the lowest rating since its use of geared nose wheel transducers for reference speed signal complicates the installation of this system.

The fourth rating category involves cost. This can be divided into two sub-categories, initial and maintenance cost. Assuming initial cost information was available for these systems, it would represent the implementation of those systems on the related aircraft chosen for this study. Thus these prices would not reflect the implementation on the proposed space shuttle and, therefore, would not be representative. Another factor that must be considered is the quality

control requirements for the skid control system in the Space Shuttle application.

Conventional aircraft rated skid control hardware would not qualify for space. For these reasons initial cost information is not available at this time.

A measure of the anticipated maintenance costs would be reflected in the degree of complexity of the system and in the service experience of the equipment. In that respect, the Hydro-Aire and Goodyear systems, which are the least complex and comprise 99 percent of the free world's skid control systems now in operation, have been relatively trouble free.

Based on the foregoing evaluation the main contenders for a space shuttle role are Hydro-Aire Mark III and Goodyear L-1011 system. In view of the pending hardware screening efforts the relative position of all four systems is not considered firmly established. The final standing of these current systems will be summarized in Section VI, Laboratory Evaluation of Antiskid Systems.

IV. TRADE STUDIES OF NEW BRAKE CONTROL CONCEPTS

In Section III four antiskid systems are described as they presently exist on current aircraft (except Bendix-SST system which was to be on the B2707-300). This description indicated how conventional systems produce braking system control. What will be undertaken in this present section is a description and discussion of several alternate system approaches. First the concept of using measured brake torque as a control parameter will be analyzed as well as a proposed system incorporating this approach. Next the Boeing Closed Loop antiskid system will be described. This is a completely functioning system that has been actually flight tested some years ago. This system was also tested in the laboratory along with the other vendor systems and the results will be presented in Section VI.

DISCUSSION OF BRAKE TORQUE AS A MEANS OF ANTISKID CONTROL

Brake torque has been proposed as a parameter to be utilized in a brake control system. In any given conventional brake control system, brake torque is being controlled indirectly by the action of the system through modulation of the antiskid valve. Because of inherent system lags and unknown gain values, it would appear logical to investigate the use of brake torque feedback in a more active way.

Before brake torque can be used it first must lend itself to measurement. For a truck type main gear braking system, the equalizer rod force can provide a measure of brake torque through the use of a strain gauge. Except for the brake bearing forces which can be neglected, the equalizer rod reacts brake torque to the strut inner cylinder. For brake systems having only two wheels per strut, the measurement of brake torque becomes more difficult. Again strain gauges can be used to measure axle strain, but unfortunately the resultant signal would reflect more than just the desired brake torque. The problem arises from additional axle torsional loads caused by conditions other than

just the desired brake torque. Other means might be used to detect brake torque on a dual wheel configuration such as the use of load cells, but not without a weight penalty.

Assuming that by some means brake torque could be measured, it is not unlikely that the condition of the signal would be unacceptable. The environment of the brake, both heat and vibration levels would cause extreme reliability problems in service. Next the noise content of the brake torque signal might easily "swamp" out the torque information. Squeal and chatter oscillations would cause an excessively noisy signal, for instance. However, supposing these problems could be solved, the next step is to decide how to utilize the brake torque signal so that it could be a meaningful control function.

Three means for incorporating brake torque into the skid control system will be discussed: a system that uses brake torque alone for its control; a system that uses wheel speed and a brake torque simulation for its control; a system that uses wheel speed plus the measured brake torque for its control.

The reliance on brake torque solely to control the braked wheel would have at least two obstacles to overcome. First the brake torque information would not be sufficient to determine the velocity, i.e., slip condition of the wheel. Except for some extraneous signals (this would apply only to two-brake struts where the axle is instrumented to measure torque) the only means to create torque is to apply some brake pressure to determine if a wheel is turning. Yet if the wheel is locked up, the application of brake pressure would certainly rule out the wheel spinning up. This locked wheel condition could happen during hydroplaning or at the low velocity portion of a braking run.

Secondly, the installed torque for any given brake is too dependent on brake usage history and maintenance to establish a meaningful analog of brake torque, i.e., the relationship between torque and

brake pressure is not necessarily a fixed parameter. Scaling one brake for a certain brake torque signal level would not hold for another brake or for the same brake at a different point in the wear history of the same brake. The scatter in brake torque gain from one brake to another would rule out any simple use of the brake torque signal for a continuous control signal. The skid control system would be designed for a specific brake torque gain level, yet from one brake to the next there would be no consistency. The result would be a system that would perform inefficiently with one brake and maybe not at all with another. Performance results would certainly be unpredictable. Therefore brake torque alone is not sufficient as a control parameter.

The next two systems use brake torque feedback along with the more conventional use of the brake wheel velocity. Neither system uses brake torque directly but instead creates a ground force signal from the brake torque and wheel speed signal. To better appreciate the reason why ground force is utilized, some analysis of the typical wheel dynamics of a braked wheel are necessary. The simplified diagram of such a system appears in Figure 17. The simplified equation of the wheel dynamics will be presented,

$$\text{GROUND TORQUE} - \text{BRAKE TORQUE} = I\alpha$$

where I represents all the rotational inertias in the wheel, tire and brake. These are assumed constant over a given braking run. The term α represents the deceleration-acceleration of the tire, wheel, and rotating brake parts. This expression is deliberately simplified for ease of description by ignoring other higher order effects such as tire footprint displacement and other strut dynamics due to other braked wheels sharing the same strut.

For a given brake torque level, the ground torque will tend to counteract until no wheel deceleration is present. As long as the wheel operates on the front side of the ground force curve (see

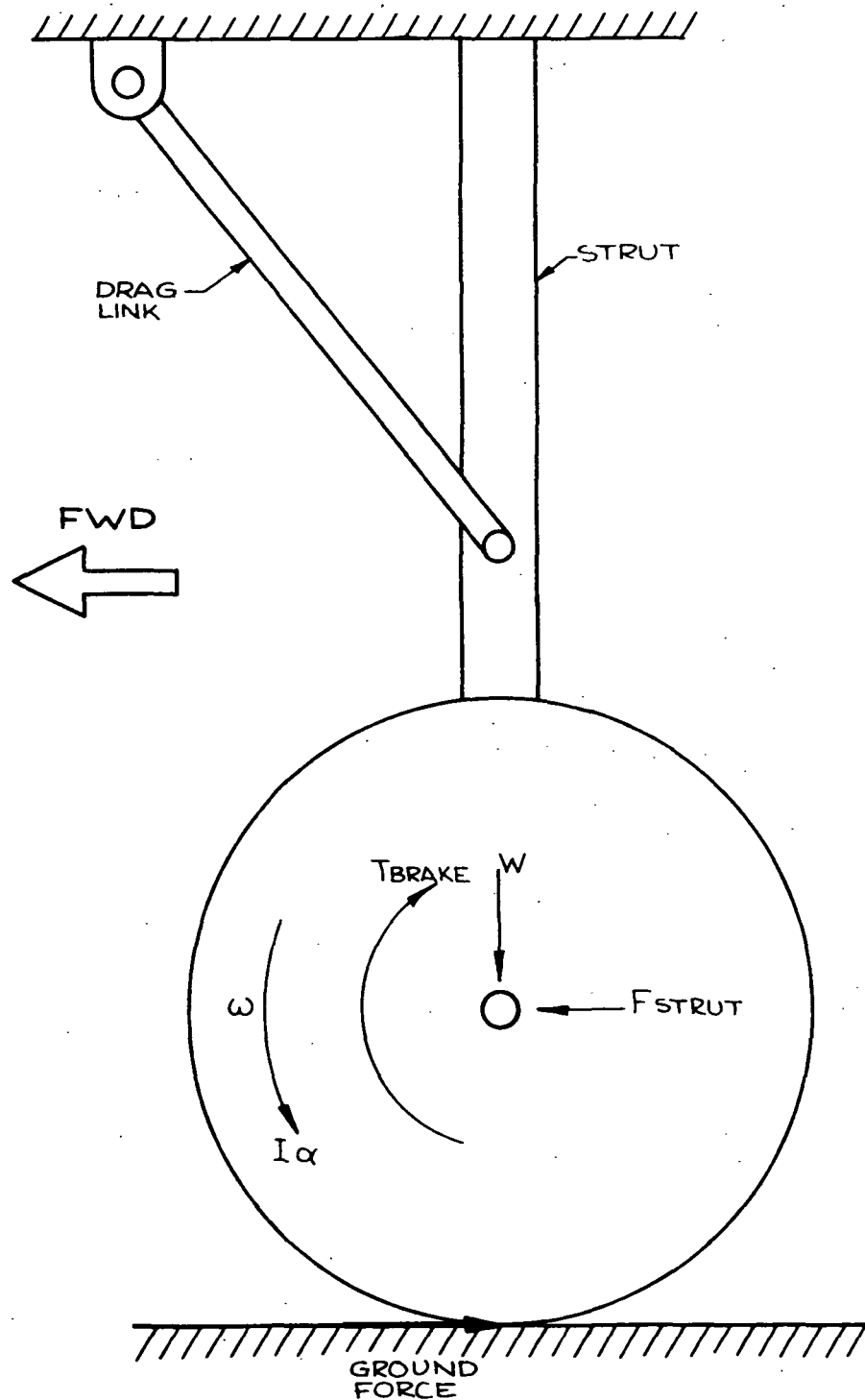


FIG. 17 FREE BODY DIAGRAM OF A BRAKED WHEEL

Figure 16) the ground torque will be forced to react sufficient torque to balance the applied brake torque, i.e., ground torque equals brake torque. However, by either forcing the brake torque higher, or encountering a sudden decrease in the ground torque would cause the wheel velocity to slide beyond the stable region and cause deceleration of the wheel in proportion to the torque unbalance. The ground torque would drop as the wheel approaches lockup and the inertia of the wheel would for an instant maintain the brake torque until lockup occurs. Once the wheel is fully locked the ground torque would again equal the brake torque ignoring strut dynamics which would cause oscillations in both the ground torque and brake torque in this lockup case. Inherent in this wheel lockup case is the fact that brake torque, while being what the skid control system controls, may not be the driving function in the wheel dynamics equation. For example, the action as the decelerating wheel passes the unstable ground force peak is precipitated by the change in ground force. That is, the ground force leads the brake torque at this time. Its value along with the higher order inertial effects, dictates what the brake torque will be. Brake torque, to have any value, must be reacted by ground force. With the airplane stopped, braked wheel locked, applying any amount of brake pressure will not produce any discernable brake torque. If brake torque is highly dependent upon ground torque, then the parameter that must be controlled is ground torque.

The expression governing this relationship can be easily obtained from the wheel dynamics equation by simply solving for ground torque,

$$\text{GROUND TORQUE} = I\alpha + \text{BRAKE TORQUE}$$

Assuming that I is the known wheel, tire and rotating brake inertia, and assuming I is constant, the two necessary variables that must be available is brake torque, and wheel deceleration. Wheel deceleration presents no problem because the wheel velocity is already available and can be readily differentiated. Accurate brake torque

information, however, is more difficult to obtain.

The SPAD system, discussed in Section III, approaches a brake torque feedback system by creating a pseudo brake torque signal. This signal is generated by filtering the servo-valve signal (See Figure 18). The assumptions made here are that the valve to brake pressure and brake pressure to brake torque relationships are known and can be predicted. As the system is implemented there is another assumption made which is that the wheel velocity term is adequate, thus eliminating the necessity of obtaining wheel deceleration.

The SPAD system represents an implemented system which incorporates the analytical conclusion that the optimal system will always maximize the available ground force (See Reference NAS 8-28250 "Optimal Braking Studies," August 1972). To facilitate this analysis, the basic control circuit utilized in the SPAD system is presented in Figure 19 in simplified form (See Figure 13 for details). This discussion will concentrate on the optimizer circuit. The manner in which the optimizer is implemented and functions has already been presented in detail. The proposed system dealing with the use of brake torque will only involve certain aspects of the optimizer.

The SPAD system does not require the value of the ground force but just an indication of its peak value. This is done by sampling the ground force and holding the peak value whenever it is reached. Once the peak value is detected an error is developed which acts to reverse the pressure sweep direction. In this manner the peak value acts only as a trigger to sense when the maximum ground force has been exceeded.

Another approach which may be taken to more accurately simulate ground torque is shown schematically in Figure 20. Notice that the derivative of the wheel speed is not the true derivative but is attenuated by a simple lag filter. This is necessary to keep electrical noise to an acceptable level. Also the first and second

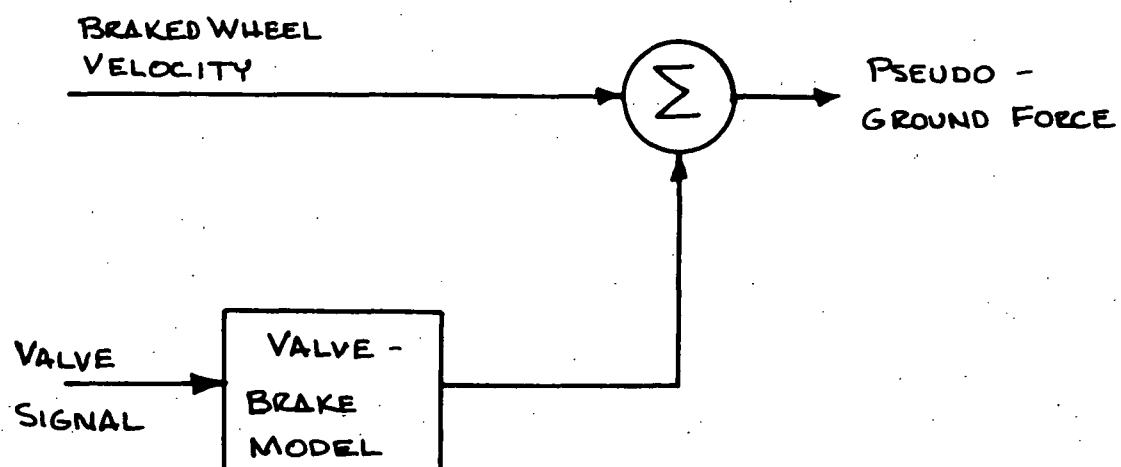


FIGURE 18. SPAD GROUND TORQUE RELATIONSHIP

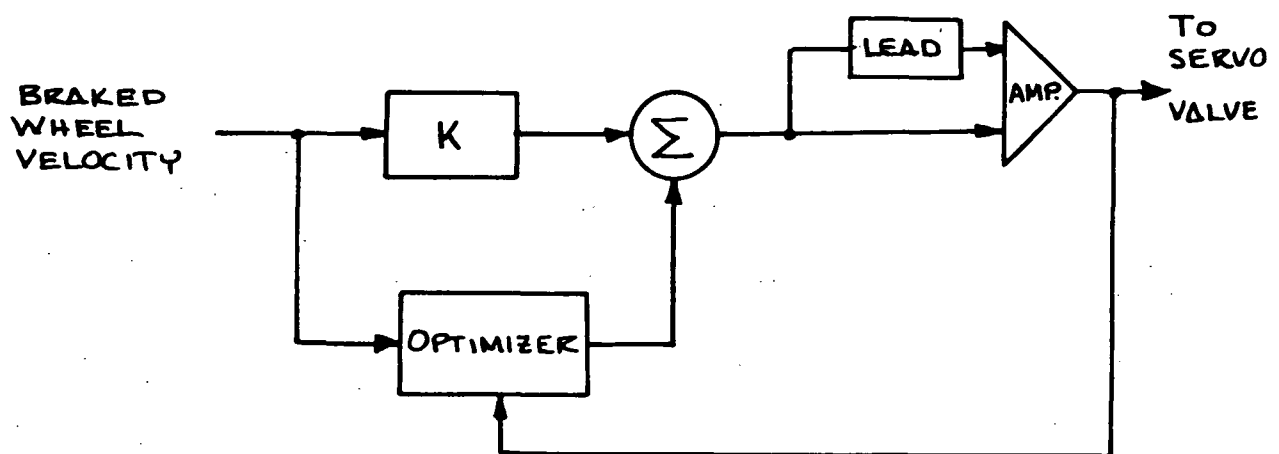
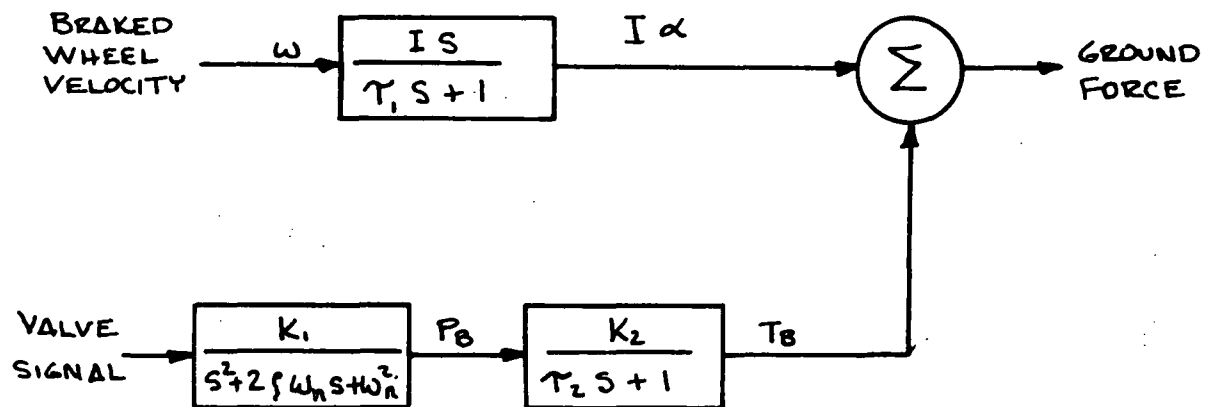


FIGURE 19. BASIC SPAD SYSTEM



SYMBOLS

| | |
|------------------|-------------------|
| α | Deceleration |
| I | Inertia |
| K_1, K_2 | Gain values |
| τ_1, τ_2 | Time constants |
| ζ | Damping ratio |
| ω_n | Natural frequency |
| s | Laplace operator |
| P_B | Brake pressure |
| T_B | Brake Torque |

FIGURE 20.

GROUND TORQUE DETERMINATION

order filters used to generate the brake pressure and brake torque are linear approximations to the real dynamic relationship. Although this is a more faithful simulation of ground torque than utilized by the SPAD system, it is still just an approximation.

A look at Figure 21 shows what the actual frequency response of the Space Shuttle hydraulic simulation may be. To simulate this would require at least a third order system to generate up to 270 degrees of phase lag. But an additional problem requires simulating the proper attenuation or gain response such that it coordinates both the magnitude and phase plot. Of course, the more nonlinear the actual dynamics to be simulated the more difficult becomes the implementation of that simulation. Figure 22 represents brake torque frequency response actually measured on a dynamometer. The task of simulating this becomes quite difficult again because of the complexity and nonlinearity of the dynamic response. The point that must be made is that the simulation shown in Figure 19 is just an approximate simulation, more complete than SPAD, but still not complete. This leads to the desirability of having the actual measured brake torque for purposes of simulating ground torque.

With brake torque available, simulating ground torque only requires the wheel deceleration signal. As pointed out before in this discussion, there might be some undesirable aspects to this brake torque signal, but basically the resultant ground torque simulation would be more accurate. The proposed antiskid system will closely approximate the existing SPAD system, but the more accurate ground force simulation using measured brake torque will be incorporated.

The proposed system that utilizes brake torque can be seen in Figure 23. The ground force simulation is made up of wheel deceleration and brake torque. This ground force signal is not used to indicate any absolute magnitude, but rather the peak value is important. To detect the peak ground force it is proposed that the signal be differentiated. This would have the feature of not only detecting the

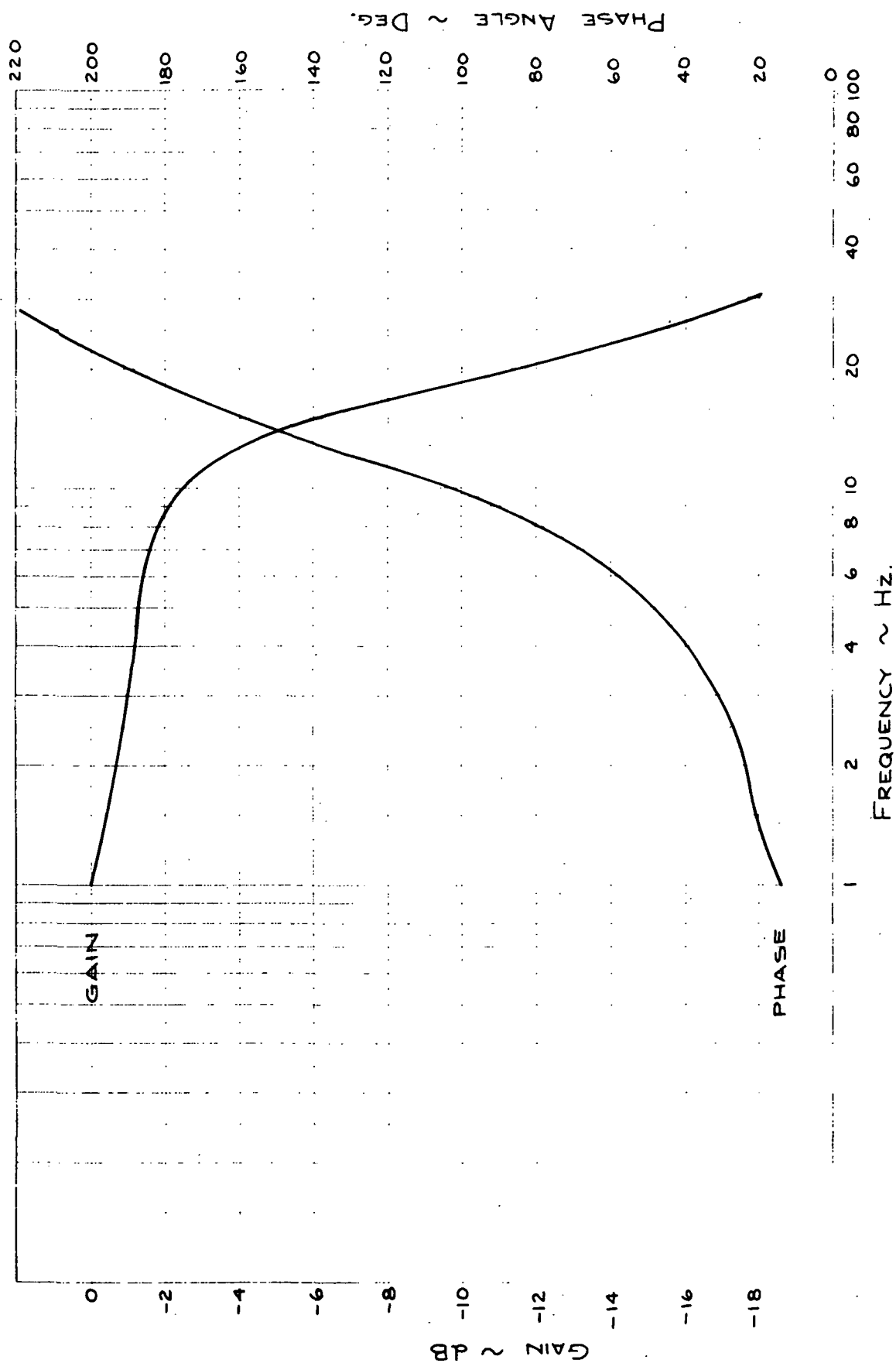


FIG. 21 SPACE SHUTTLE HYDRAULIC FREQUENCY RESPONSE
WITH 3-WAY VALVE

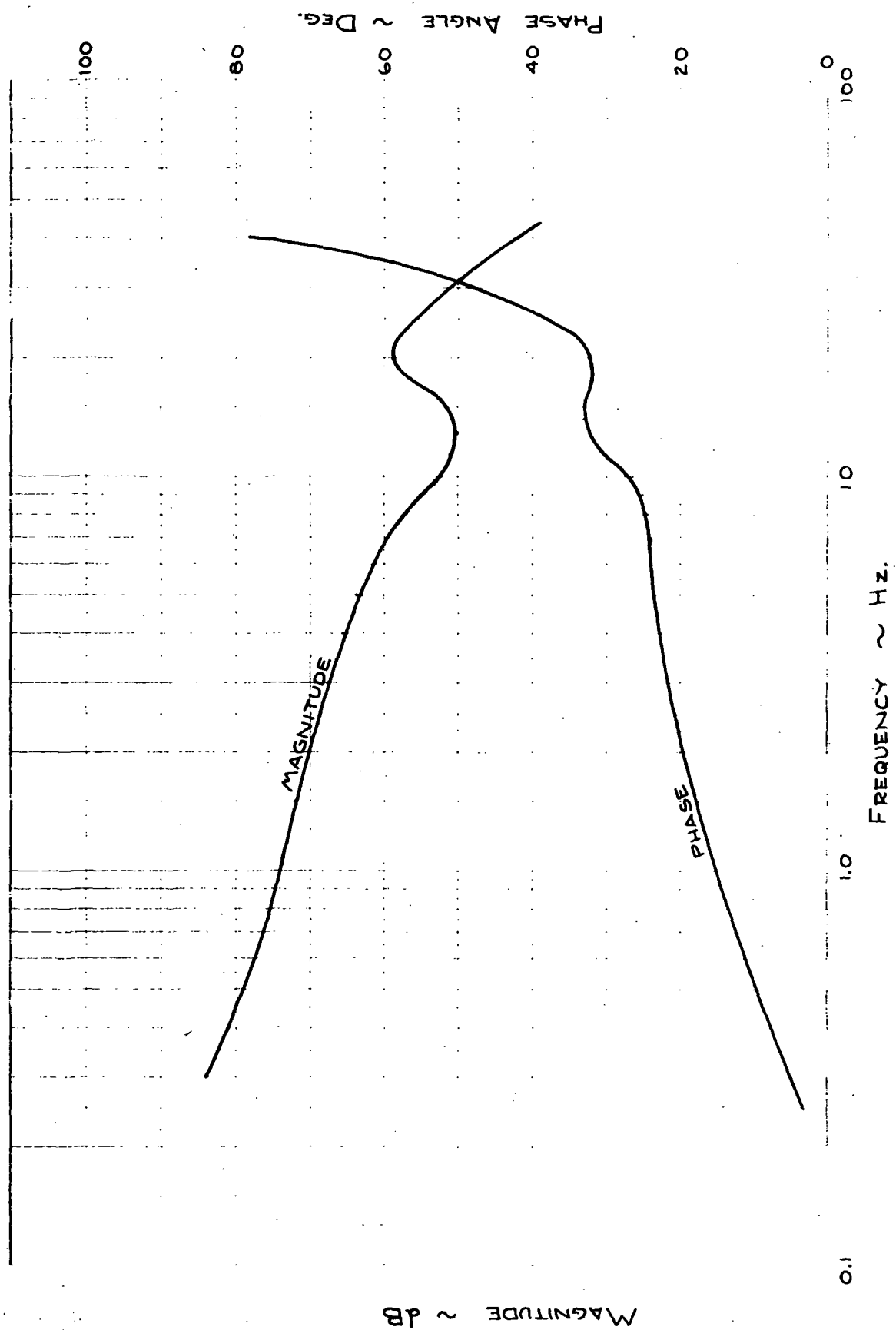


FIG. 22 BRAKE TORQUE FREQUENCY RESPONSE

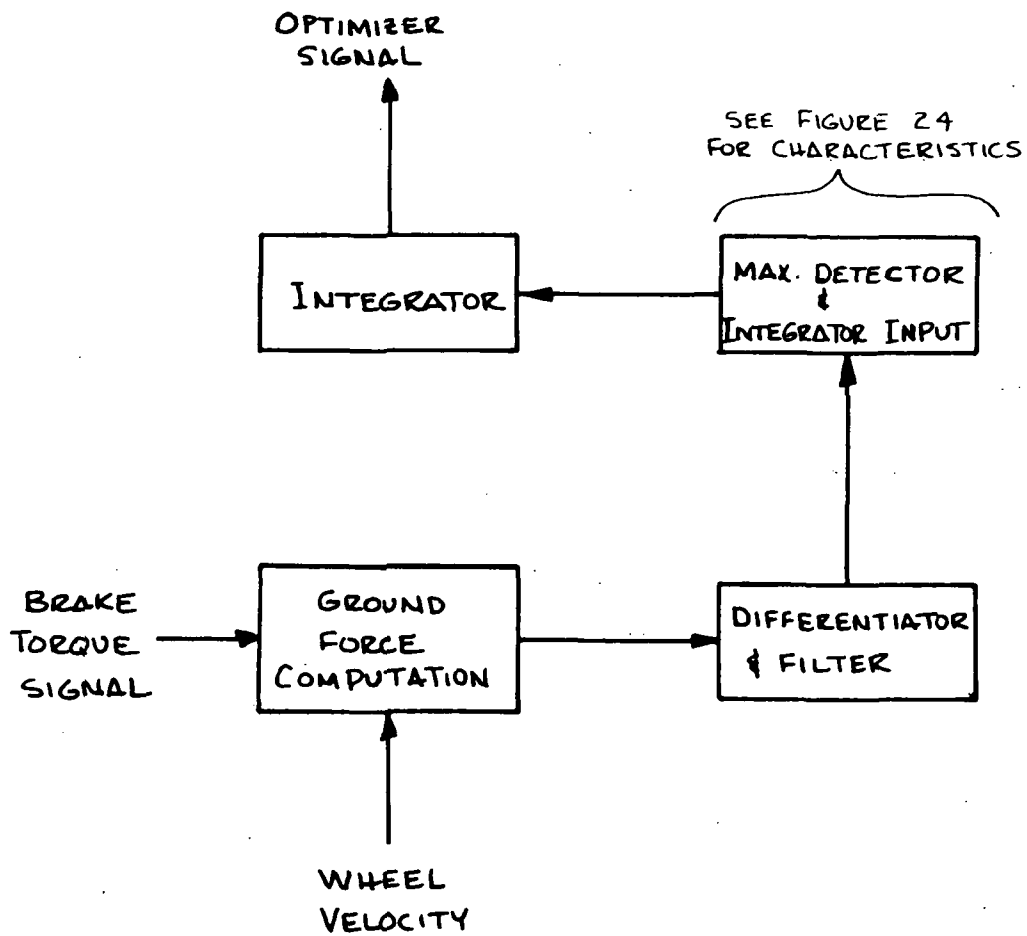


FIGURE 23. PROPOSED OPTIMIZER USING MEASURED BRAKE TORQUE

peak value but also using the inherent inflection point surrounding this maxima. The maximum detector shown in Figure 23 would have a proposed characteristic shown in Figure 24. When the inflection point of the ground force is neared and reached, the value of the derivative would diminish, becoming zero when the peak ground force is reached. Using this ground force derivative to control the maximum detector would enable it to provide a variable input to the sweep integrator. This provides two operational changes to the optimizer. First, the ground force signal is continuously monitored instead of the sample-hold method. Secondly, the integrator sweep rate is variable with the rate of change of ground force. Note the deadband about the origin in Figure 24. This is to help eliminate the "nervousness" of the derivative signal in the presence of noise. Overall the optimizer circuit would exhibit a signal more continuous in nature than the basic SPAD system approach.

Practical details such as necessary noise filtration, width of the deadband in the maximum detector and slopes or gains on the integrator inputs would have to be worked out and refined during the development of this proposed system. Obtaining the necessary stability margins may be difficult with this system. These matters are beyond the scope of this discussion, however.

DESCRIPTION OF THE BOEING CLOSED LOOP ANTISKID SYSTEM

The Boeing Closed Loop System evolved several years back as an improvement of the Goodyear antiskid system used on the early 737's. This Closed Loop system was developed by Boeing and also is under a Boeing patent. It was extensively flight tested on the 737 "Short Field" demonstrator but never evolved into a certified system and therefore has not been used on a production Boeing airplane. Nevertheless, the system recently has undergone some improvements to reflect experience gained from past brake control system development programs.

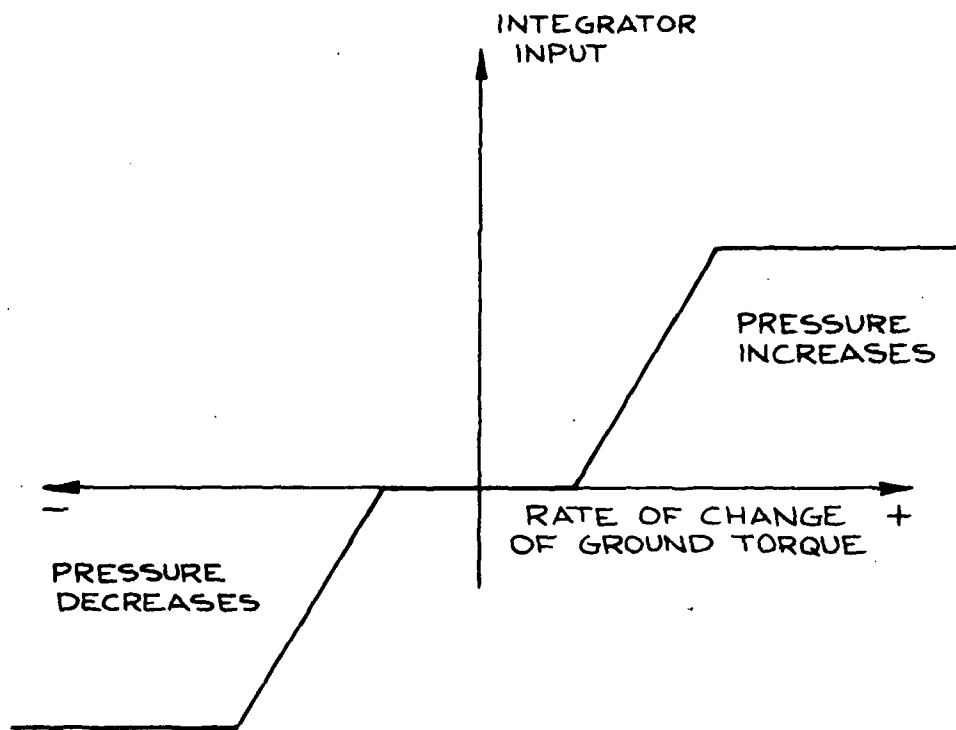


FIG. 24 PROPOSED MAXIMUM DETECTOR AND VARIABLE INTEGRATOR GAIN

A block diagram of the system is shown in Figure 25. There are three control loops that constitute the basic functions of this system; the skid detector loop provides full brake release to control deep skids. It also serves as an initialization of the closed loop modulator. The closed loop modulator provides the major control. It adjusts the working level of the brake pressure to adapt to the varying runway friction conditions. The second order lead loop provides dynamic compensation for inherent lags in the systems; thus it acts to improve overall system performance.

The skid detector provides a fixed amplitude signal whenever its dual threshold is exceeded. This signal provides a full brake release signal to the valve amplifier which releases all brake torque. This signal also provides the initialization signal to the modulator via the overtorque circuit. The skid detector dual threshold requires that the wheel deceleration must exceed a fixed rate and at the same time the change in velocity must exceed a fixed value. When these conditions occur the skid detector releases the brake pressure and initializes the modulator. The nature of this skid detector control is mainly that of a backup control. Whenever wheel deceleration exceeds the authority of the modulator, the skid detector provides for rapid brake torque release and lets the wheel recover to its synchronous velocity. Thus the skid detector is assigned a minor backup role.

The major control element in this system is the modulator (see Figure 26). It functions by comparing the wheel deceleration to that of a fixed deceleration reference and integrates the resultant deceleration error. The output characteristics of the modulator can be seen in Figure 27. When no wheel deceleration is present (at initial brake application or during spinup after a skid) the modulator calls for its maximum rate of increasing brake pressure. Pressure increase will continue at a declining rate as wheel deceleration increases until the deceleration detector senses a value equal to the level

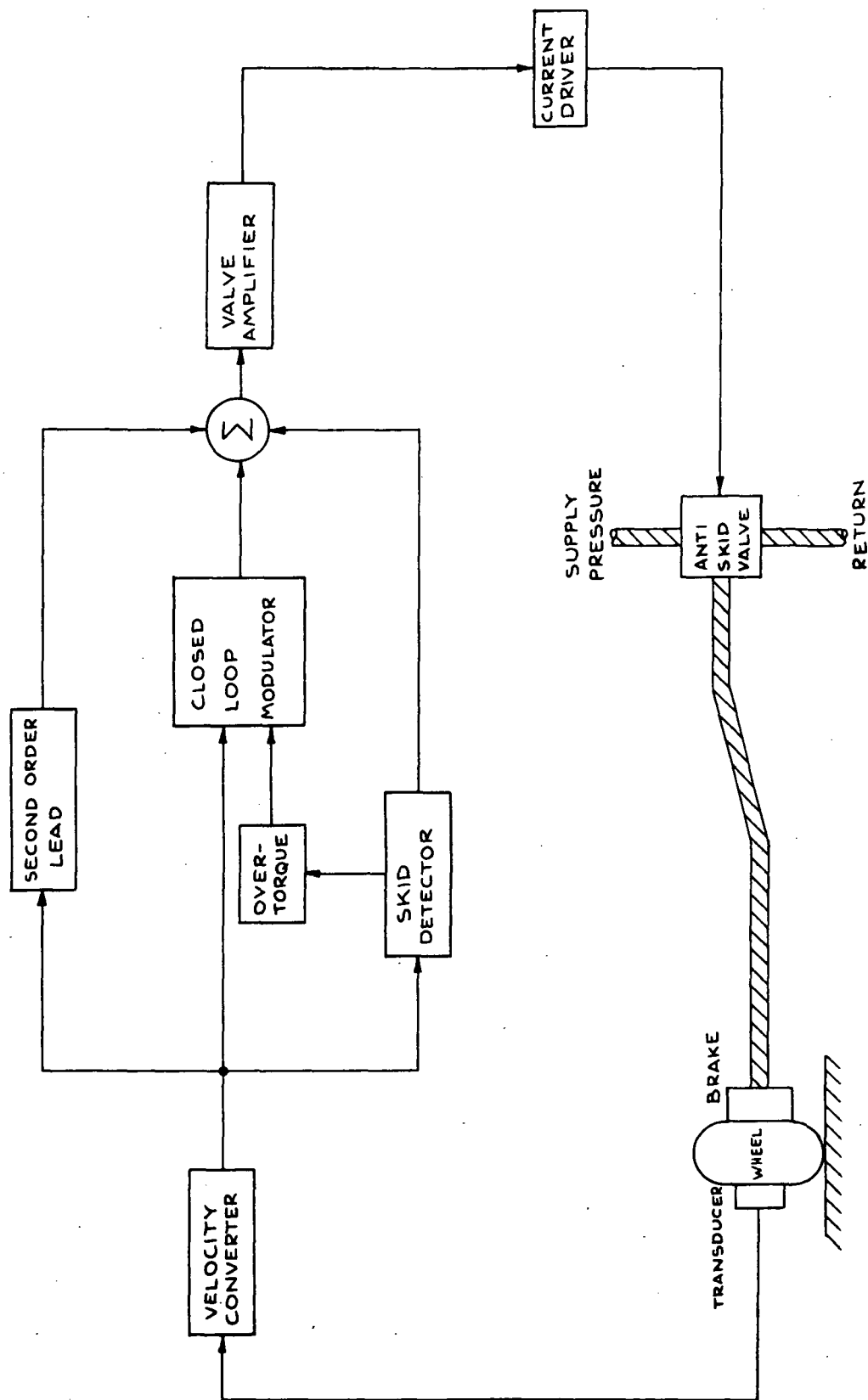


FIGURE 25. BOEING CLOSED LOOP ANTISKID SYSTEM

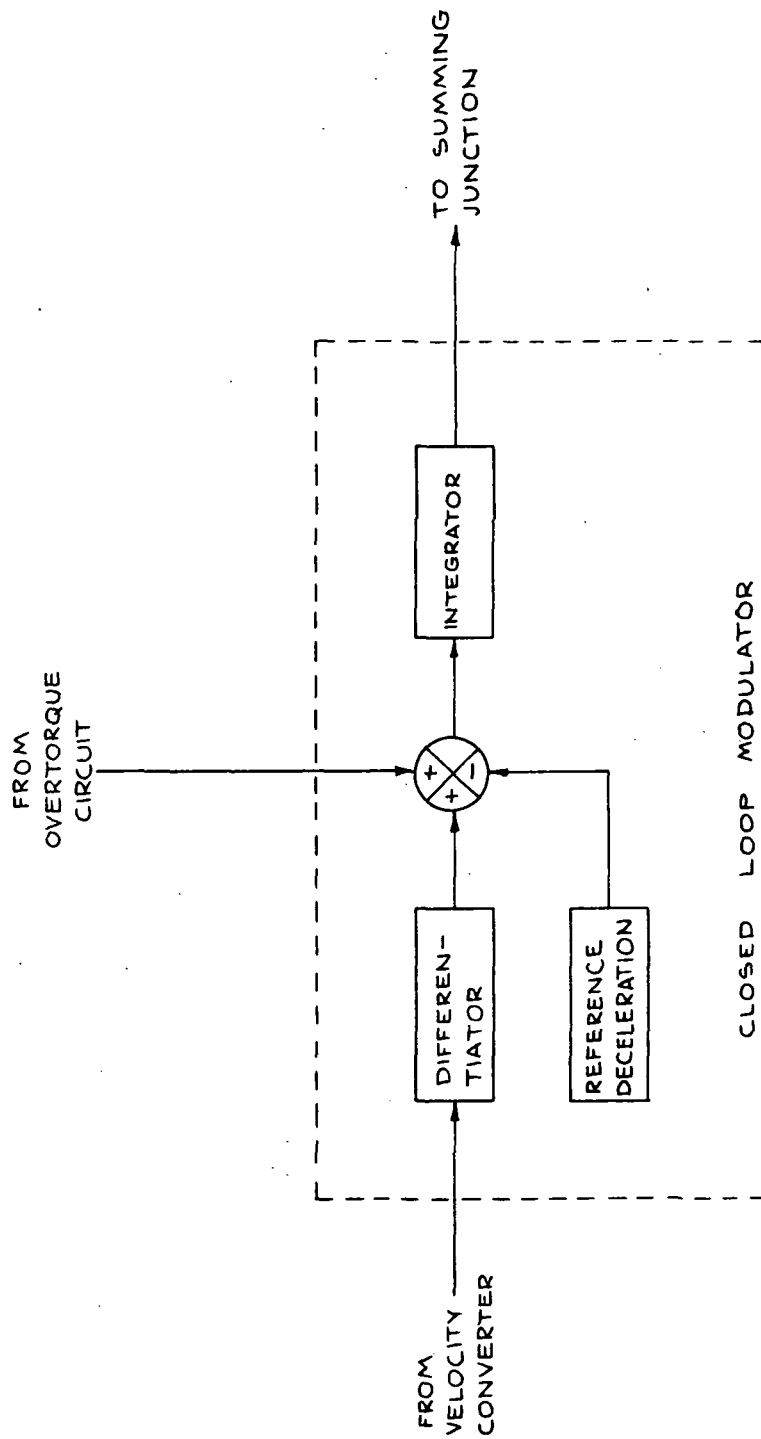


FIGURE 26. CLOSED LOOP MODULATOR

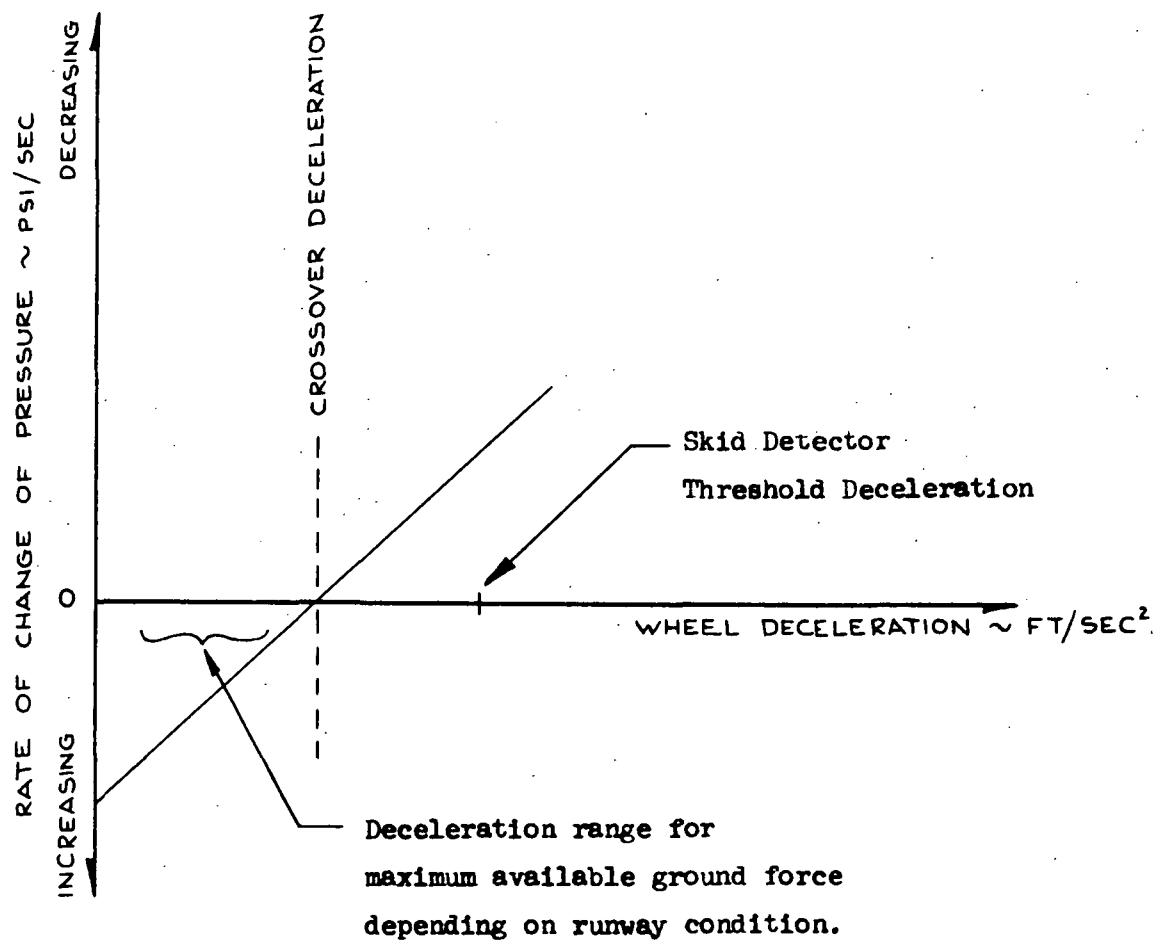


FIGURE 27. CLOSED LOOP MODULATOR CHARACTERISTIC

called the crossover deceleration (See Figure 27). This allows the brake torque to ease the wheel into more and more slip until the friction peak is momentarily met and then exceeded. The crossover value is above the deceleration level that can be sustained by the available tire-to-ground force so that the maximum permissible braking force (torque) level is reached as the brake pressure is easing upward. Once the peak available ground force is exceeded the wheel deceleration will increase thus passing the crossover level. Once the wheel exceeds the fixed deceleration crossover, the modulator calls for a decrease in brake pressure, the rate dependent on wheel deceleration.

Assuming the ground friction characteristics are not changing drastically, the modulator can and will smoothly regulate the brake pressure, keeping the braked wheel right at the ground friction peak. If, however, the rate of wheel deceleration and change in velocity exceed the skid detector threshold, the modulator is overridden by the detector momentarily to release brake pressure and permit wheel speed recovery. It is the function of the overtorque circuit to then re-establish the modulator control after the skid detector again becomes inactive.

Greatly assisting both the skid detector and modulator loops is the second order lead control. The name second order refers to the fact that it ideally takes the second derivative of any wheel velocity variation and inputs this to the valve amplifier. Of course, the amount of phase lead is a function of frequency and since a filter must be added to control electrical noise, the phase lead drops precipitously at frequencies above 15 Hz (See Figure 28). Even so, between 1 and 12 Hz the lead provided by this control aids the system in two very important ways. First, it compensates for built-in inherent phase lags in the system. Lags that occur in the velocity converter, lags that are always present in the servo valve and brake hydraulics. This results in substantially improving the phase margin and thus the stability threshold of the system. Secondly, the lead compensation by its very

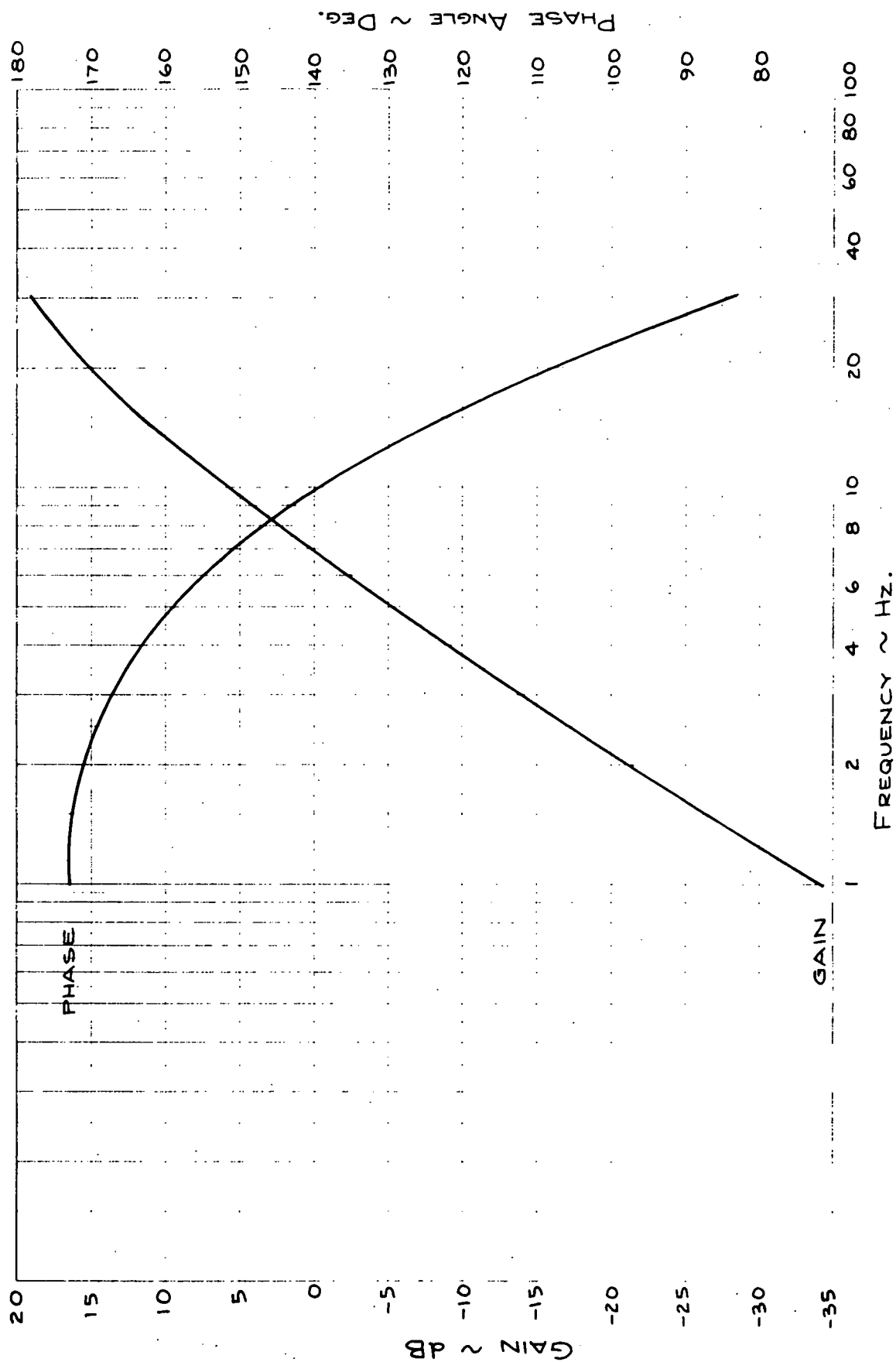


FIG. 28 SECOND ORDER LEAD CHARACTERISTICS

derivative function leads or anticipates brake pressure correction to begin corrective modulation before the regulator modulator can respond. This results in an overall better performing system.

The remaining elements of this system are the summing amplifier and the valve amplifier. The summing amplifier continuously adds the signals from the three control loops and sends this signal to the valve amplifier. Here it is amplified and converted into current to drive the servo valve.

Such functions as touchdown protection and locked wheel protection are not included in the system since it is only a developmental laboratory model. The servo valve used with this closed loop system is like that shown and described in Section III, Figure 8. There is no actual transducer proposed with this system. It was run in the lab using a transducer simulation and was operated on the airplane with a Goodyear transducer similar to that described for the L-1011 system. (See Figure 2).

V. REDUNDANCY REQUIREMENTS TRADE STUDY

The first effort in this trade study was an evaluation of the 747 brake system to establish a baseline. Basic analysis of the 747 system was done by using Fault Tree techniques. This is a failure mode and effect analysis method that offers a graphic evaluation of multiple failures. The completed Fault Tree Analysis was used as the basic reference for assessing component failures required to give resultant critical system failures. An evaluation of the 747 service performance was completed to give a baseline safety requirement for the proposed Space Shuttle braking system. The baseline safety requirement for the Space Shuttle system will be evaluated against the proposed ground rules to establish the redundancy requirements to meet the baseline for each condition.

After evaluation of the 747 it quickly became obvious that this system was not a good baseline for Space Shuttle evaluation. The large difference in number of braked wheels between the 747 and the Space Shuttle makes direct comparison difficult.

The Advanced 737 system, having four braked wheels and the same type antiskid system as the 747, represents a better choice. Therefore the Advanced 737 system was analyzed. It, rather than the 747 system, was used to give a baseline safety requirement for the Space Shuttle braking system. The 747 system Fault Tree Analysis will be submitted for comparison purposes only (see Appendix).

REDUNDANCY REQUIREMENTS ASSUMPTIONS

Due to a lack of detailed information concerning the Space Shuttle brake system requirements, the following assumptions were made for purposes of assessing redundancy requirements:

I. MISSIONS WHERE BRAKING SYSTEM IS REQUIRED.

- o Return from space landing
- o Ferry flight refused takeoff (RTO)
- o Ferry flight landing
- o Pre and post ferry flight taxi

II. VEHICLE BRAKING CONFIGURATION

- o Four main gear braked wheels (2 per strut)
- o Split rudder for speed brake
- o No spoilers to dump lift
- o Drag chutes
- o No engines for return from Space landing

These assumptions were then used to develop the appropriate ground rules for analyzing an antiskid system from a failure analysis standpoint.

ADVANCED 737 BRAKE SYSTEM FAULT TREE ANALYSIS

Fault Tree Analysis is a failure mode analysis that graphically depicts the progressive paths that, upon occurrence, result in an undesired event. In this study the undesired event is inadequate braking when associated with the selected ground rules. Since the objective of this analysis is to establish redundancy requirements, the analysis is simplified by not considering human inputs and the electrical circuitry involved with testing and status monitoring.

Two basic logic gates are used in constructing a Fault Tree: the AND gate, where all conditions leading to the gate must be met for occurrence of the event and the OR gate where any of conditions are sufficient for the event to occur. The AND gate can be visualized as a series of switches which must all be on for current to flow while the OR gate would be a set of parallel switches, any one of which will complete a circuit. One

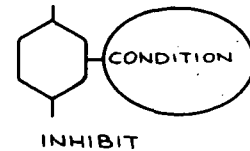


AND

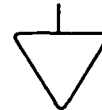
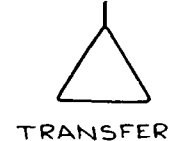


OR

other logic gate appears in the analysis and this is the inhibit gate. In this analysis it is used to represent systems with On-Off switching and represents the status of the system. Specifically it is associated with the auto brake and skid control systems which the crew would have an option regarding their use.



One other symbol is used extensively in the analysis and this is the transfer symbol, represented by a triangle. The triangle with the apex up represents an identical input, either to permit continuance of the analysis on a subsequent page or more significantly to represent an identical event as an input to more than one branch of the Fault Tree. The transfer symbol with the apex down signifies a similar input with the same type, but physically different components. The transfer symbol with the horizontal input line represents the events to which the other transfer symbols refer.



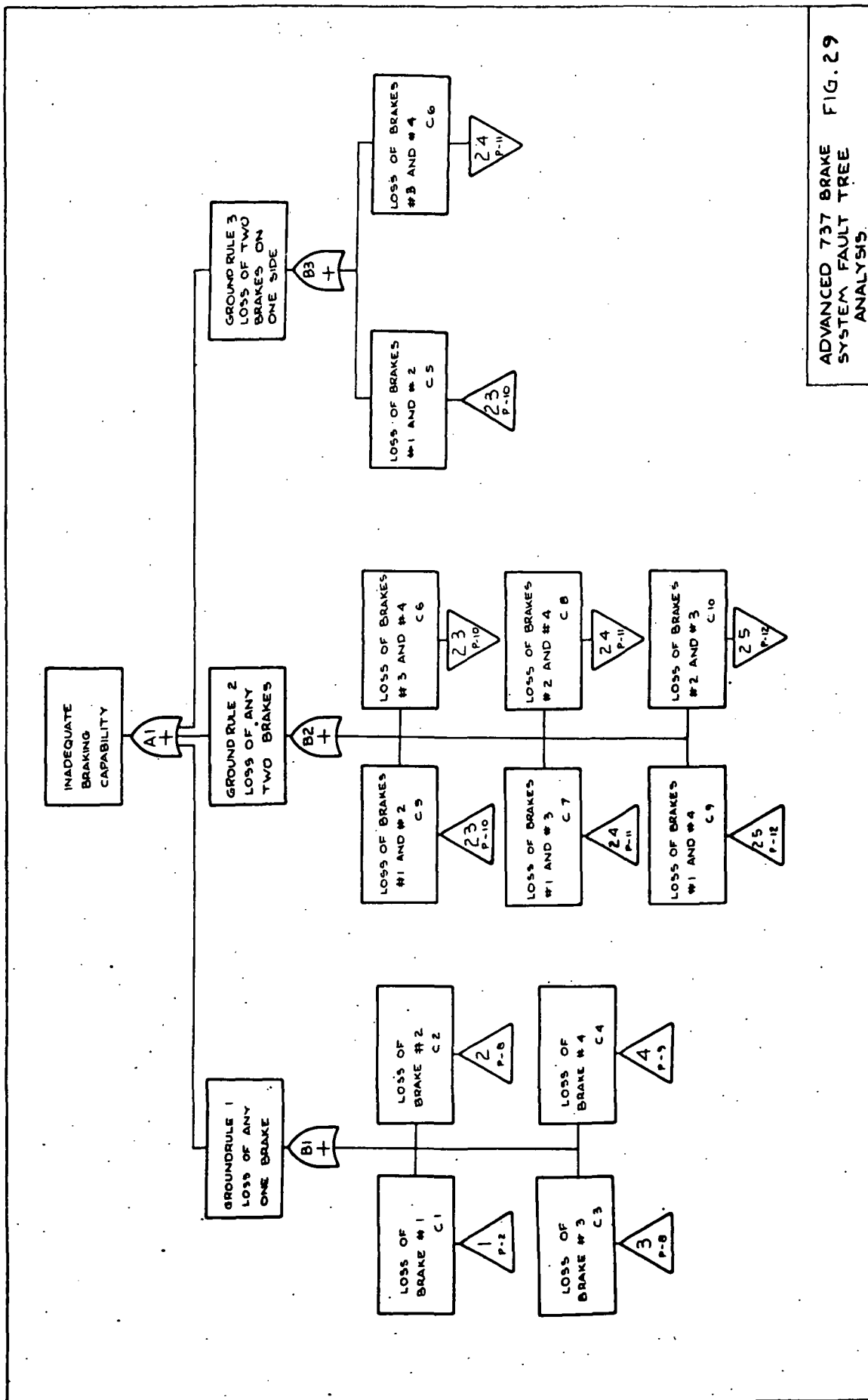
The Fault Tree analysis is read from the top with each branch depicting the events that are necessary and sufficient to cause the undesired event. This is continued until the component level or at least an independent, easily defined, event level is reached. The component failures are shown in the fault tree as circles. The independent events, such as loss of a hydraulic system are shown as diamonds. The use of the diamond generally signifies an event that could be further analyzed. For this application of establishing redundancy requirements, items such as the hydraulic sources and support structure failures can be considered as single events

without further analysis.

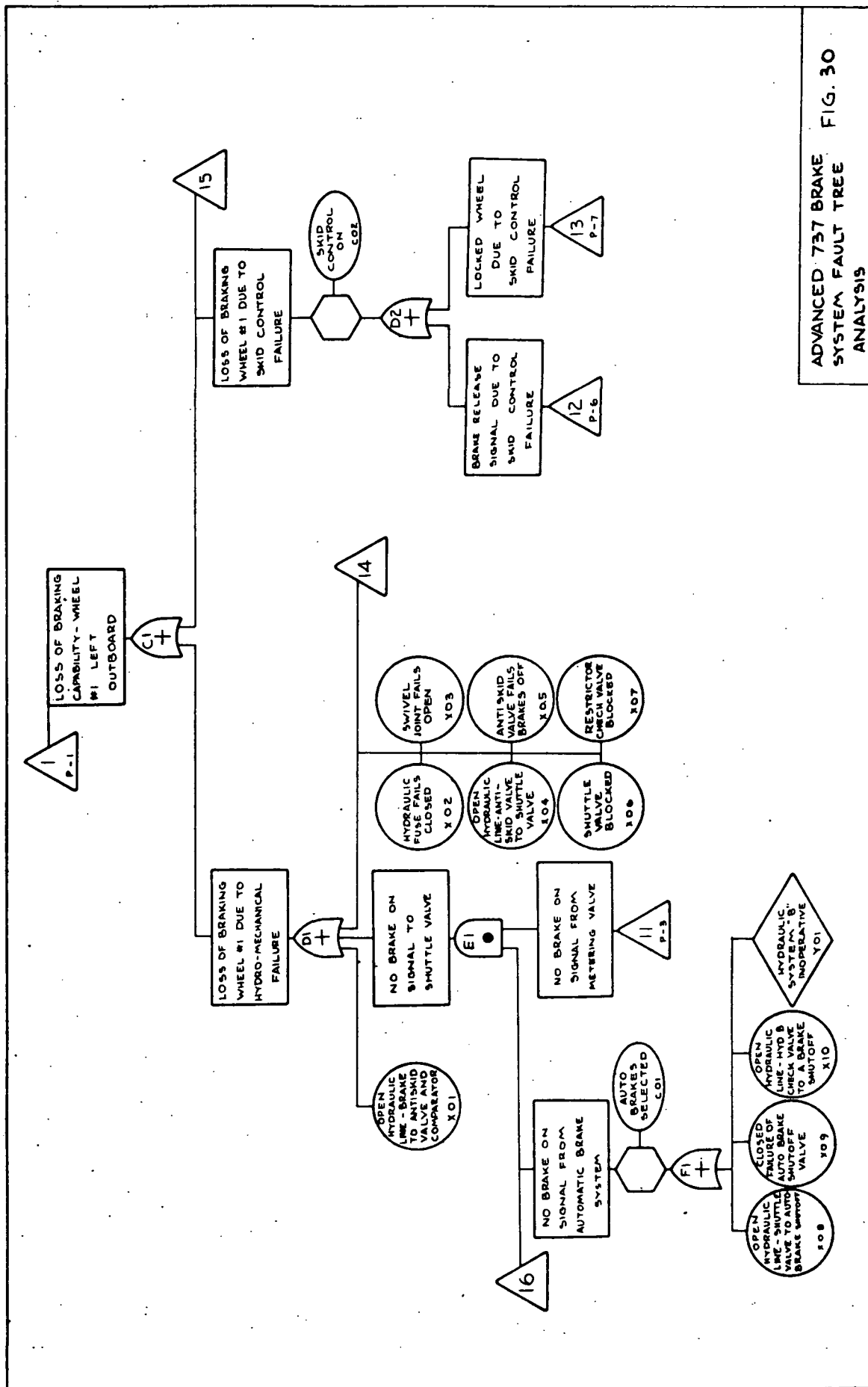
The concepts of necessary and sufficient merit further definition. There are often features in a system which have no significance to a particular analysis. In this study for example, the locked wheel protection system gives brake release signals when a wheel slows up more than a certain reference value. If the locked wheel is due to normal braking variations, this constitutes normal operation of the brake system and not a failure. If the locked wheel is due to a failure in the system this does appear in the Fault Tree as flag notes 2 and 3 in the brake release Fault Tree. There are several failures that can result in loss of braking efficiency, either mechanical or electrical. This analysis is done on an all on or all off basis so that these failures are not included.

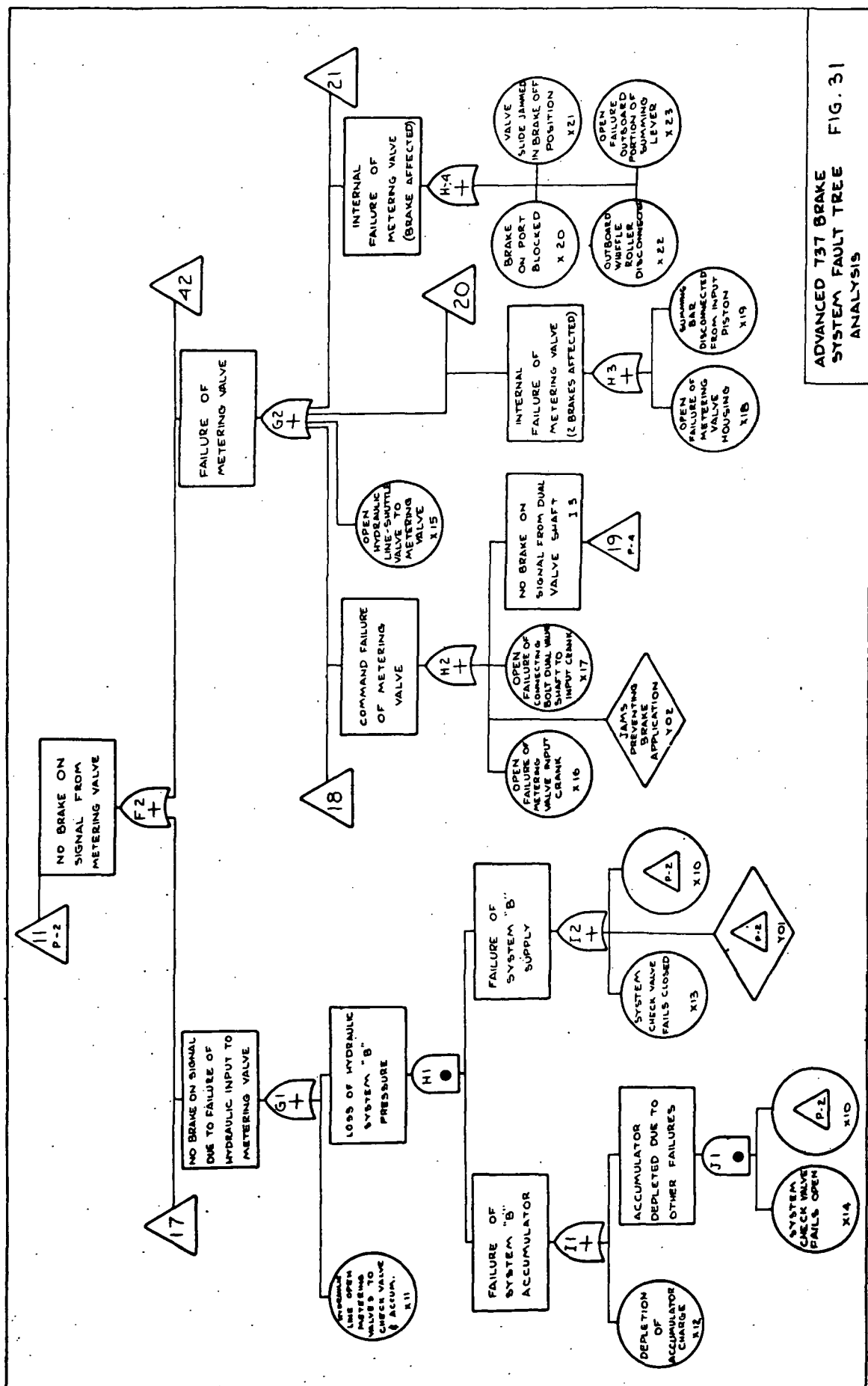
Since the objective of the study is to recommend redundancy requirements for the Space Shuttle in relation to specified ground rules, the baseline analysis of the 737 will be used in concept only. Figures 29 through 40 represent the Fault Tree Analysis of the advanced 737 brake system with the top events selected from the Space Shuttle ground rules. Certain deviations are made from standard Fault Tree techniques to enhance the readability of the presentation. For example, Figures 38, 39 and 40 which show combinations of wheel pair failures can actually be inferred in evaluation of single wheel failures.

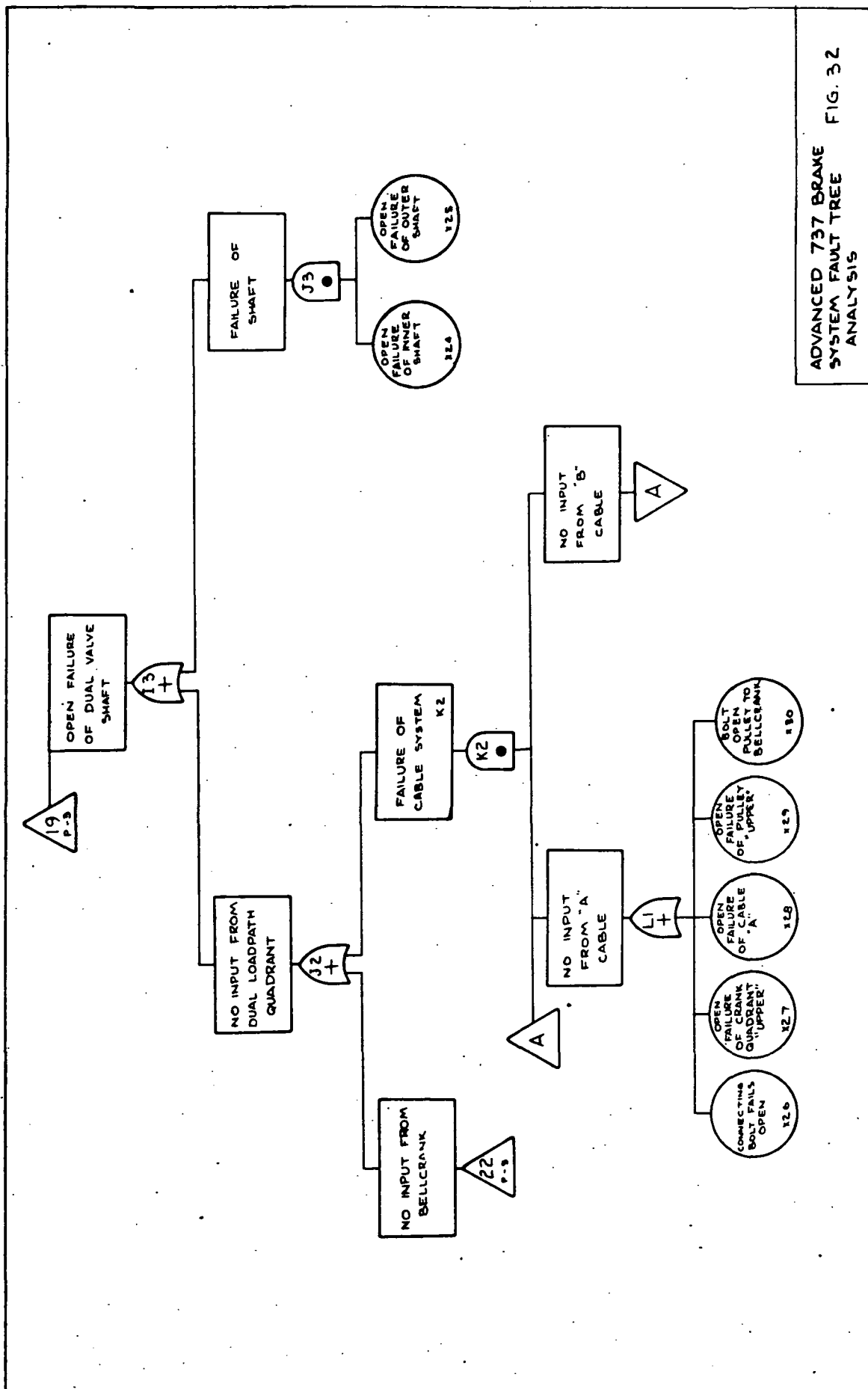
Task III of this contract calls for investigation of techniques for implementing a skid control system with electronic Fail Operational/Fail Operational/Fail Safe, (FO/FO/FS), and hydromechanical Fail Operational/Fail Safe, (FO/FS) capability. Fail Operational is defined as retention of full required braking capability, including skid control after a failure when evaluated against the following conditions or groundrules:



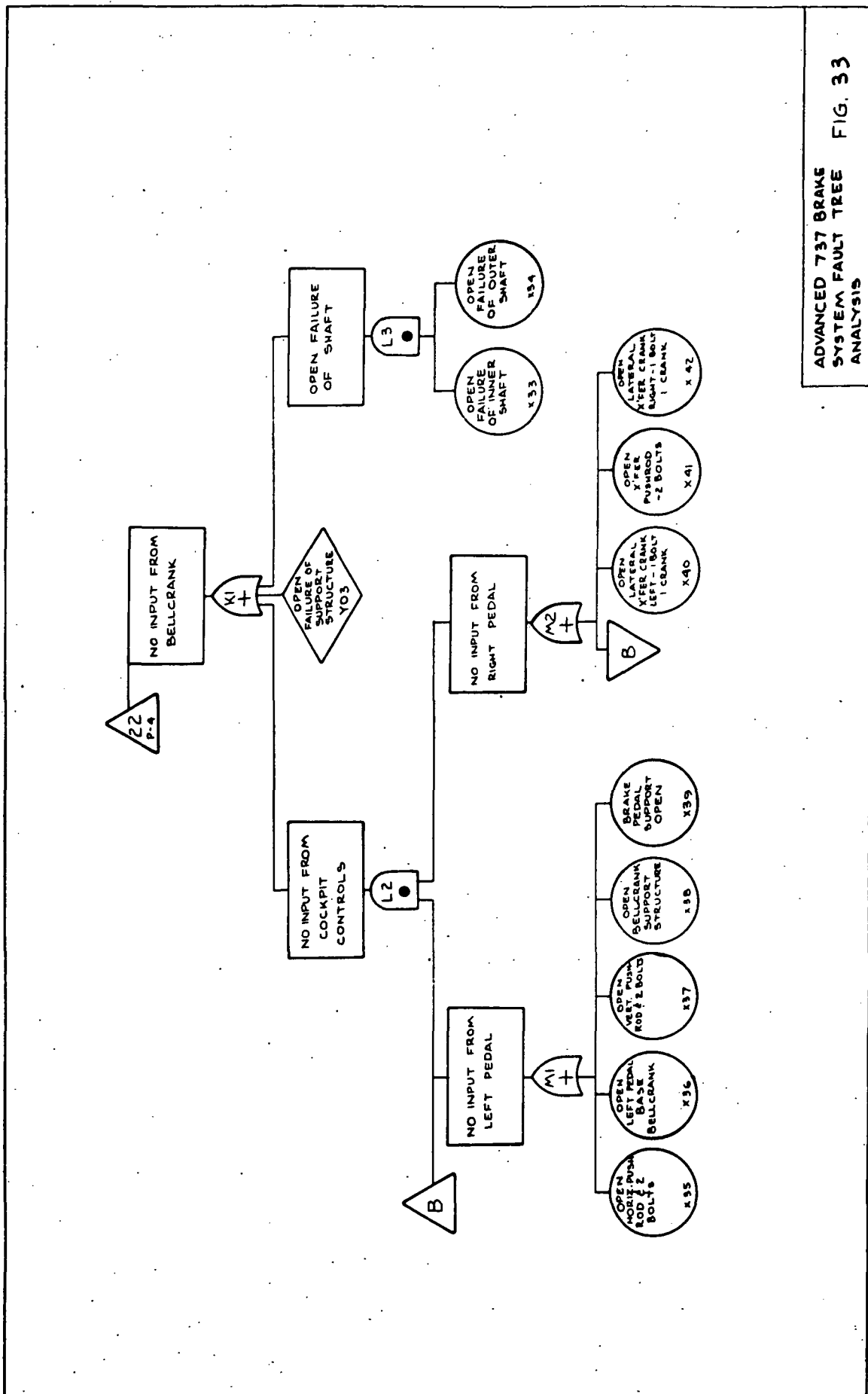
ADVANCED 737 BRAKE SYSTEM FAULT TREE ANALYSIS FIG. 29



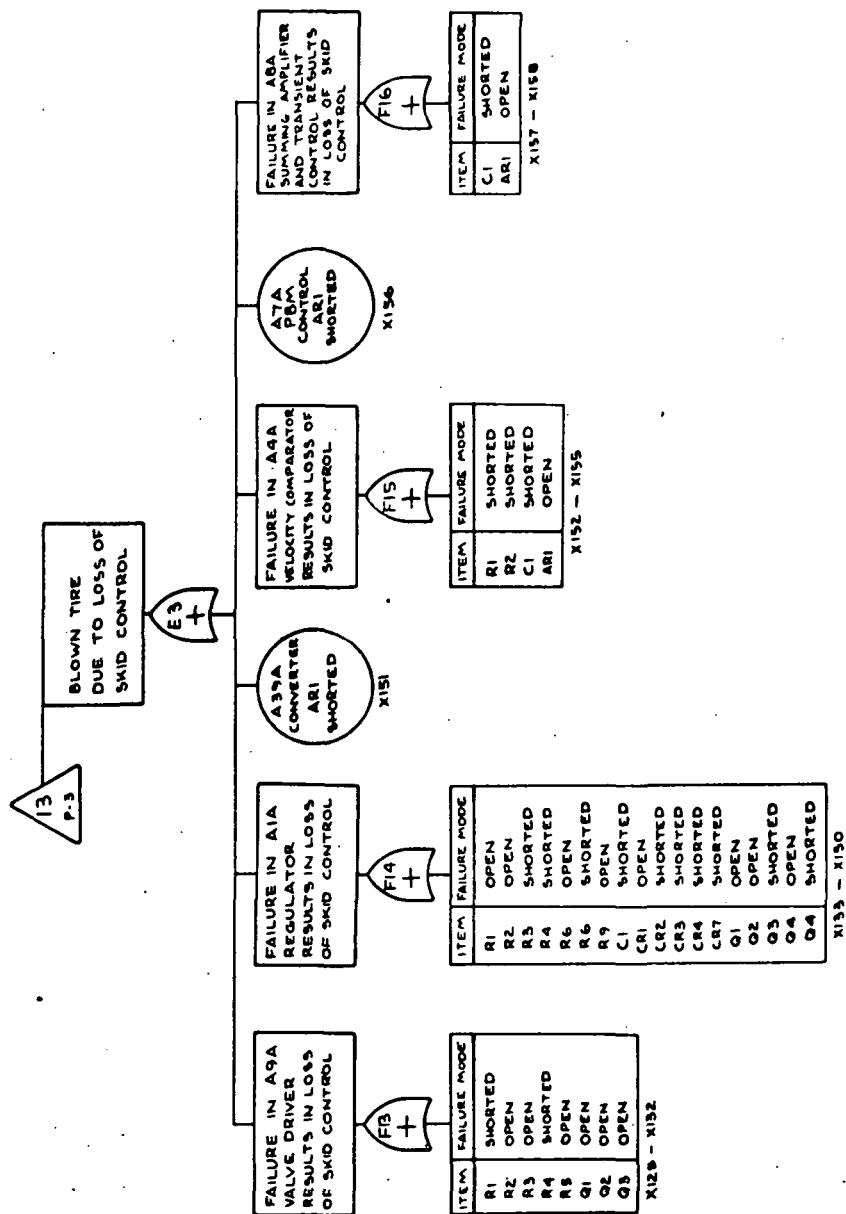




ADVANCED 737 BRAKE
SYSTEM FAULT TREE
ANALYSIS

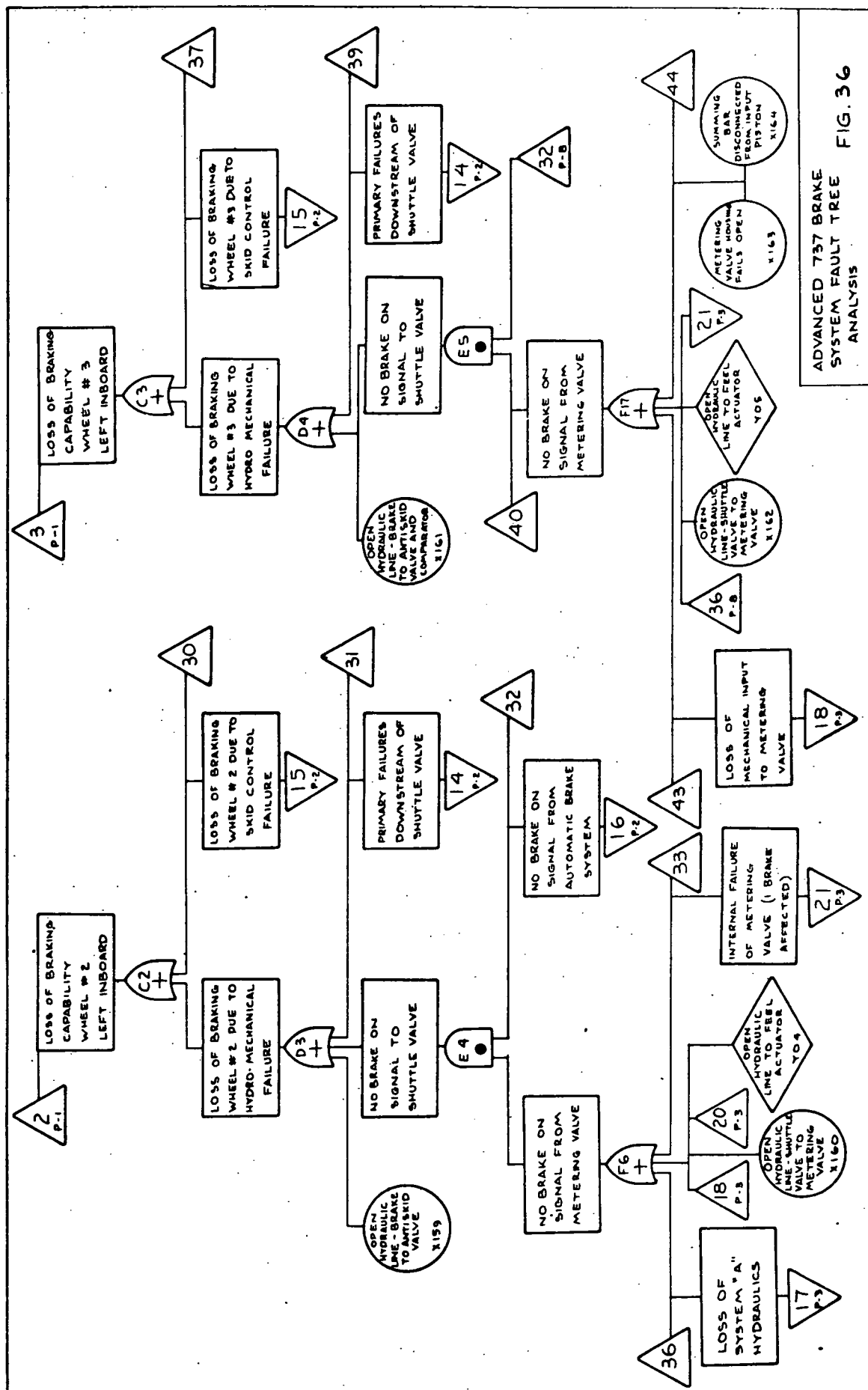


ADVANCED 737 BRAKE
SYSTEM FAULT TREE ANALYSIS FIG. 33



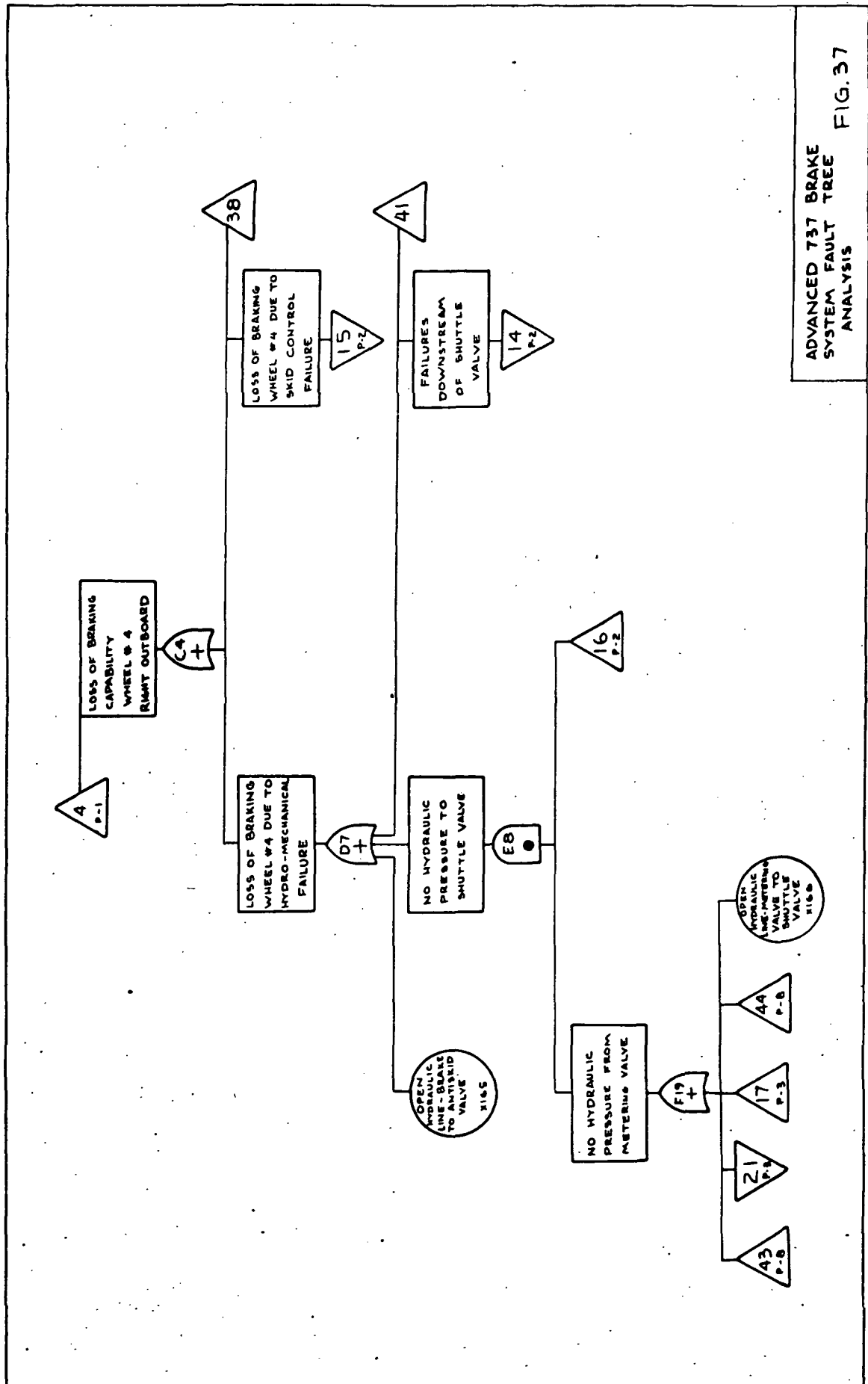
ADVANCED 737 BRAKE
SYSTEM FAULT TREE
ANALYSIS

FIG. 35

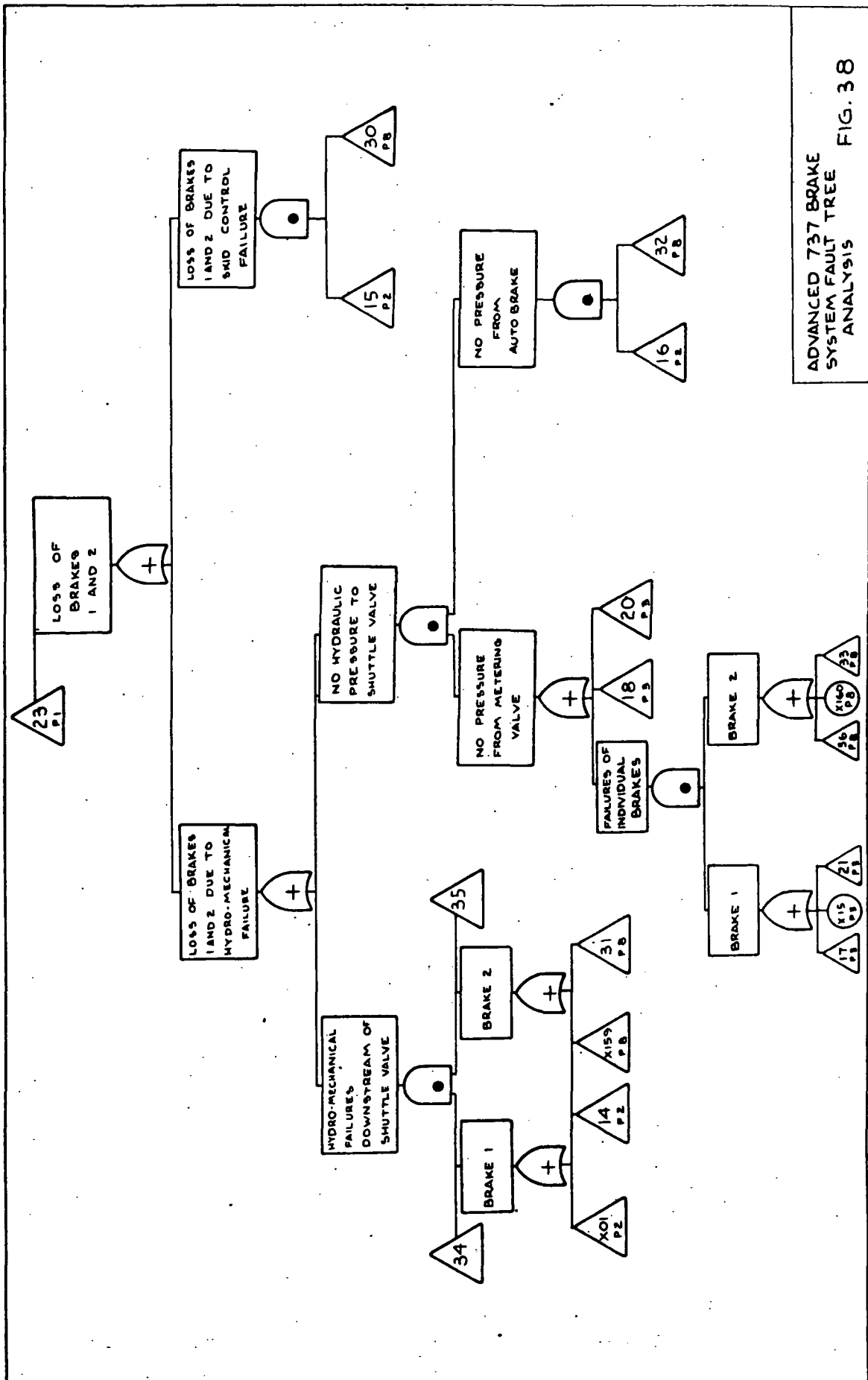


ADVANCED 737 BRAKE
SYSTEM FAULT TREE
ANALYSIS

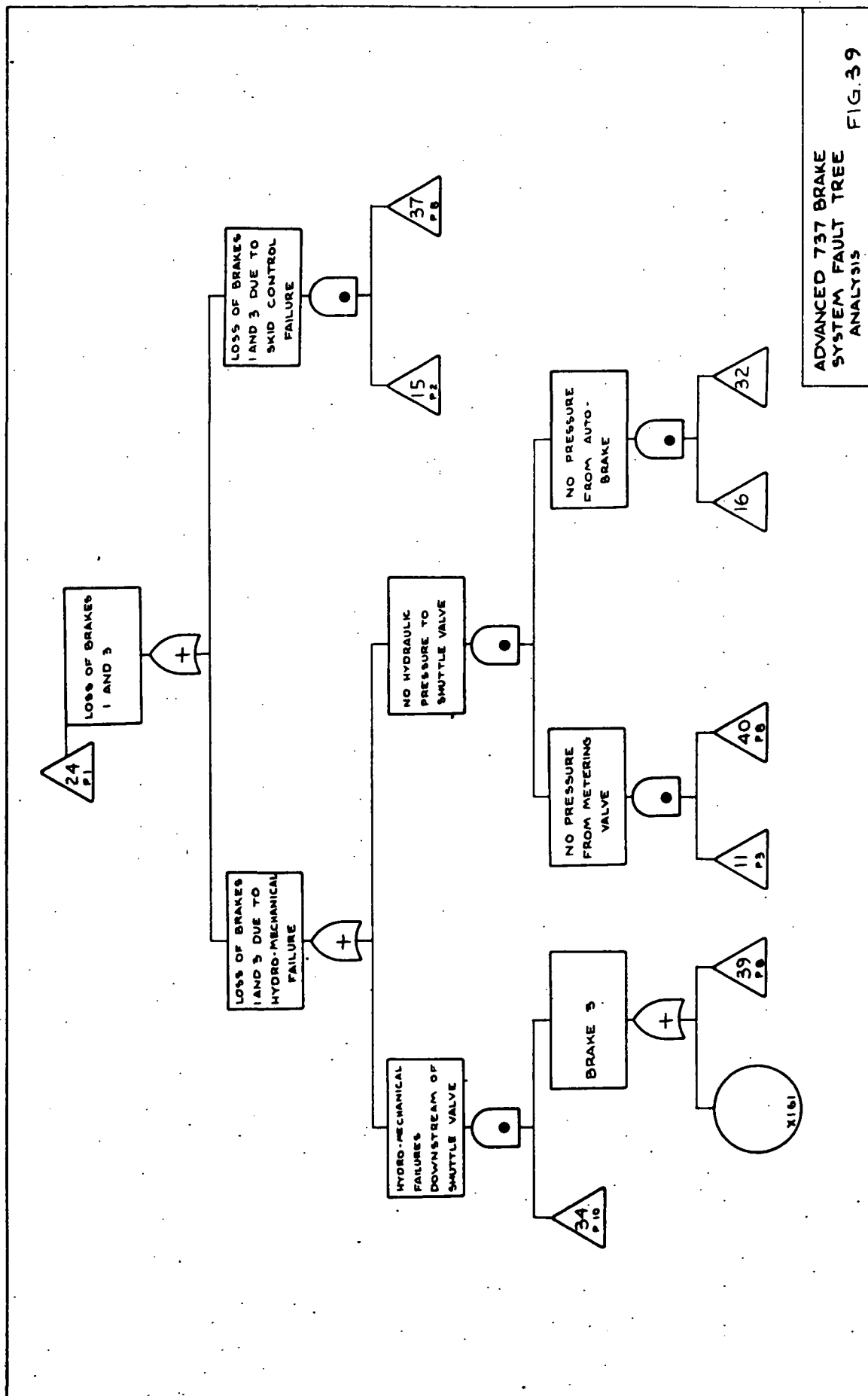
FIG. 36



ADVANCED 737 BRAKE
SYSTEM FAULT TREE
ANALYSIS
FIG. 37

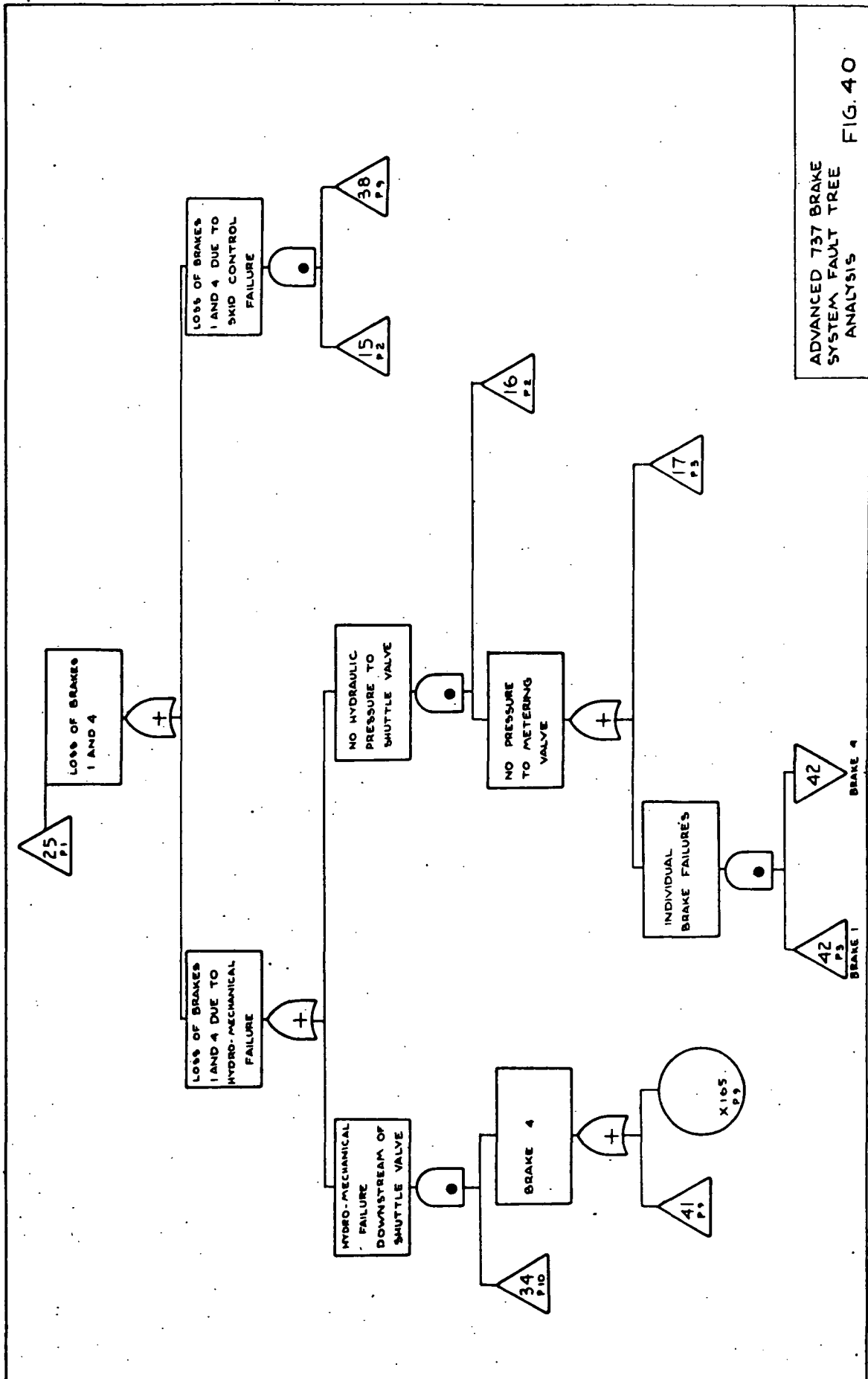


ADVANCED 737 BRAKE
SYSTEM FAULT TREE
ANALYSIS
FIG. 38



ADVANCED 737 BRAKE
SYSTEM FAULT TREE
ANALYSIS

FIG.39

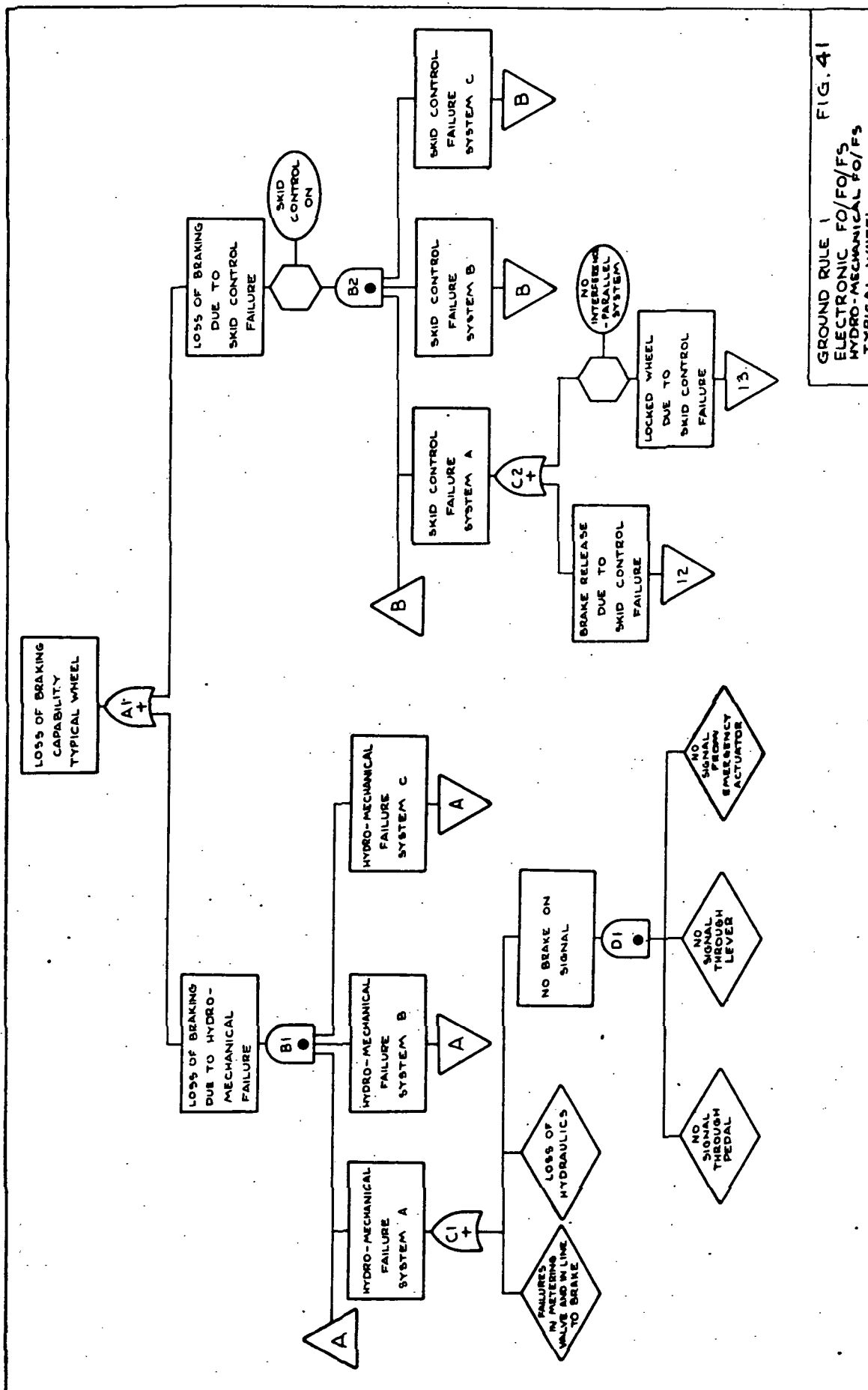


ADVANCED 737 BRAKE
SYSTEM FAULT TREE
ANALYSIS FIG. 40

- (1) Assume all brakes and skid control must be operative (see Figure 41 for Fault Tree).
 - (a) Brake energy capability of all brakes is required, or
 - (b) Stopping performance requires all four brakes to meet field length requirements, or
 - (c) Three brakes required to meet (a) and (b) above but asymmetric control problem exists with one brake inoperative.
- (2) Assume three brakes and skid control must be operative (see Figure 42 for Fault Tree).
 - (a) Brake energy requirement is met with one brake operative.
 - (b) Field length requirement is met with one brake inoperative.
 - (c) No control problem exists with one brake inoperative.
- (3) Assume two brakes (one each side) and skid control must be operative (see Figure 43 for Fault Tree).
 - (a) Brake energy requirement is met with two brakes inoperative.
 - (b) Field length requirement is met with two brakes inoperative.

Fail safe is defined as retention of capability to stop the vehicle after failure, however, precise manual control may be required. This analysis only considers those components upstream of the brake assembly. Fault Tree Analysis was the basic tool used in establishing the critical modes of failure for the subject braking systems.

The Hydro-Aire Mark III system was selected as the baseline skid control system for comparison purposes. This system is used in several airplanes including the 747 and advanced 737. The complete brake systems for the 747 and 737 were analyzed by the Fault Tree technique. The 737 system was selected as the overall baseline system since it is a 4-wheel configuration which is more comparable to the proposed Space Shuttle than the 16 wheel 747. It should be emphasized that the analysis of the 737 included in this document is in reference to groundrules specified for the Space Shuttle and should not be



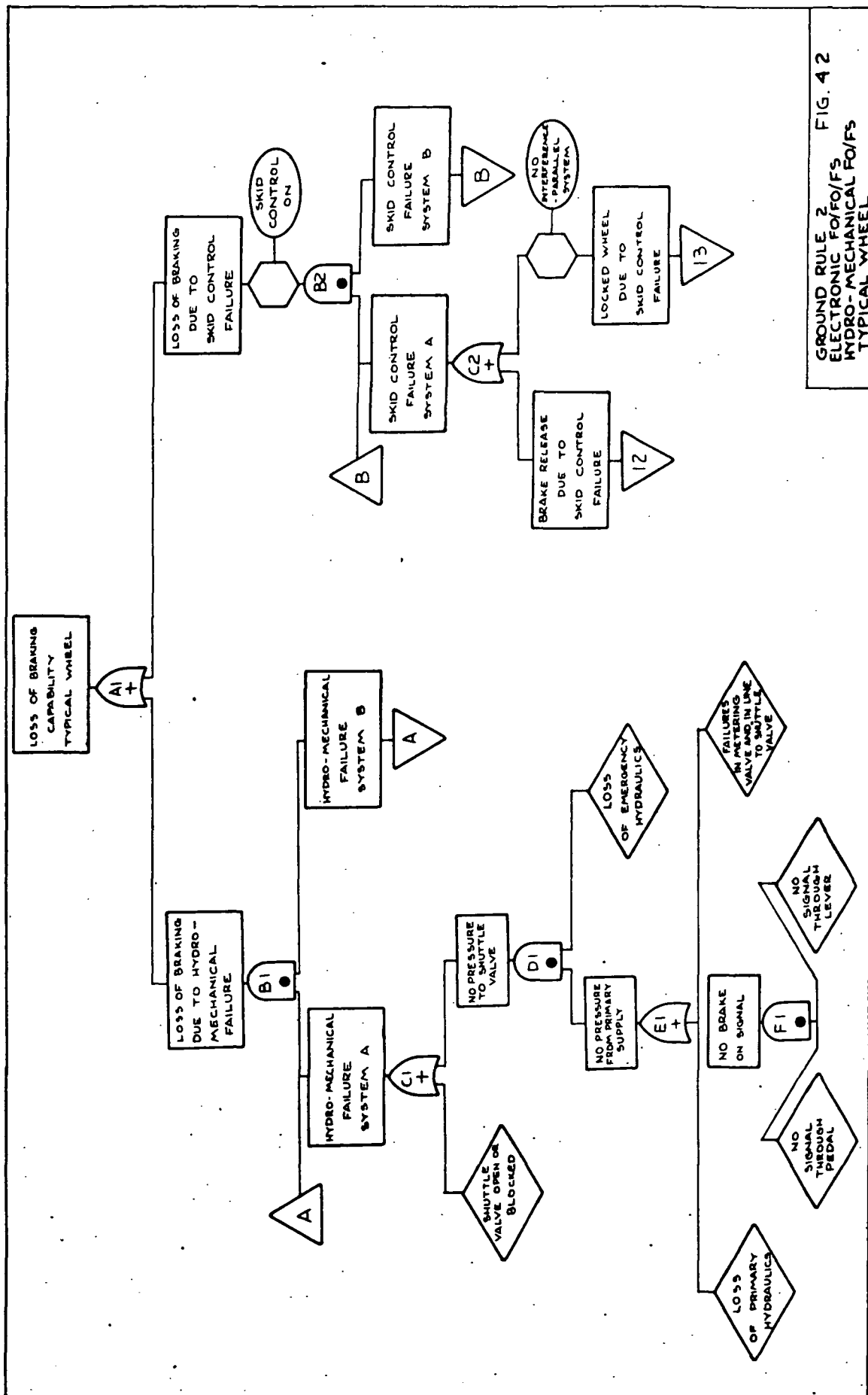
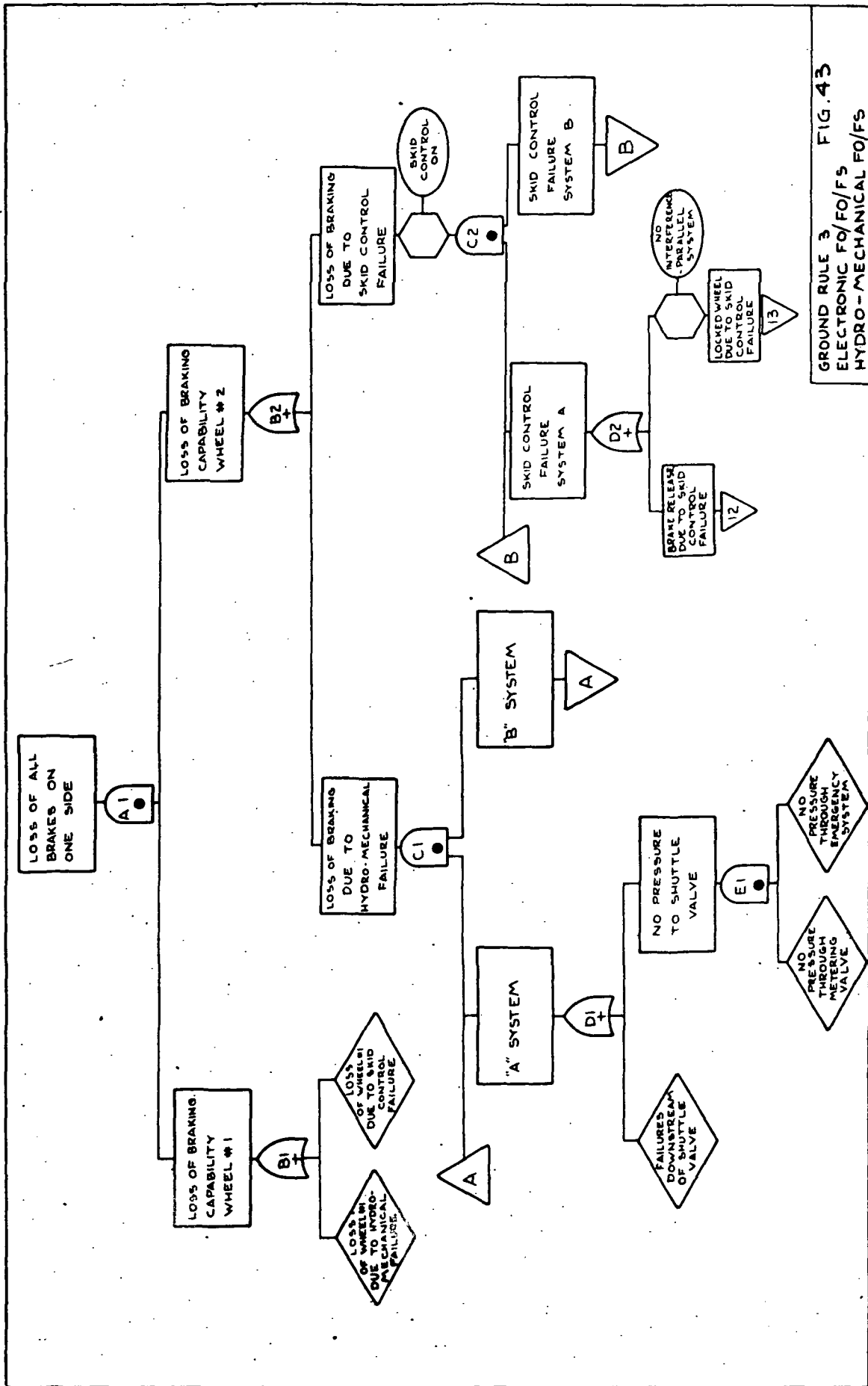


FIG. 4.2
GROUND RULE 2
ELECTRONIC FO/FO/FS
HYDRO-MECHANICAL FO/FS
TYPICAL WHEEL



GROUND RULE 3 FIG. 43
ELECTRONIC FO/FO/FS
HYDRO-MECHANICAL FO/FS

construed as an analysis of its capability in commercial service.

SUMMARY OF RESULTS

The Hydro-Mechanical System

It is the objective of this exercise to specify redundancy requirements in order to achieve a hydro-mechanical Fail Operational (FO), Fail Safe (FS) capability for the Space Shuttle brake system. The results of the analysis of the Advanced 737 brake (baseline) system and the redundancy required to meet the Space Shuttle objective are summarized as follows:

- o Ground Rule 3 - One brake on each side required. Single failures in the baseline system (Figure 44) can result in the loss of braking capability of one wheel. This would be acceptable under ground rule 3 for fail operational but a second failure affecting the wheel on the same side would not meet the requirement, therefore, the system cannot be considered FO/FS under this ground rule.

To achieve FO/FS under this ground rule, two failures must be required to lose a single brake at least for the inboard or outboard pair of wheels. See Figure 45.

- o Ground Rule 2 - 3 brakes required.
The baseline configuration also would be fail operational under this ground rule although the probability of the second failure state would be greater since any other wheel failure would constitute system failure.

To achieve FO/FS under this ground rule two failures must be required to lose any brake. See Figure 47.

- o Ground Rule 1. All brakes required.
Single failures that result in loss of a single brake leave

insufficient braking capability by definition, therefore under ground rule 1 the baseline system is not fail safe after any failure. Implementation of an FO/FS capability would require three separate inputs to each brake. See Figure 49.

The Skid Control System

The objective for the skid control system is FO/FO/FS. This means that after two failures the system must be still fully operational with the capability for reversion to manual brakes should further failure occur. There are two failure modes in the skid control circuit that can result in loss of braking, i.e., brake release signals and locked brake signals. The redundancy requirements for the antiskid system to meet the three ground rules are similar to the hydro-mechanical system with one additional requirement, to be able to turn the systems off and revert to manual brakes. Therefore, the skid control system must have similar alternatives to those discussed in the hydro-mechanical summary.

GROUND RULE 3 - Dual inputs to inboard or outboard pair (Fig. 45)

GROUND RULE 2 - Dual inputs to all wheels (Fig. 47)

GROUND RULE 1 - Triple inputs to all wheels (Fig. 49)

ALTERNATIVE CONFIGURATIONS

For each configuration developed to meet the electronic FO/FO/FS and hydro-mechanical FO/FS, an alternative configuration was developed which may not meet the full redundancy objectives for the space shuttle but does retain an extremely remote probability of failure. The resulting six configurations are presented in a matrix with the relative probabilities of failure under each groundrule shown for each configuration.

The Fault Tree Analysis has been used to establish critical failure modes and the results will be used as the reference for discussion of Space Shuttle redundancy requirements. It is again noted

that referral to the baseline aircraft is under groundrules defined for use on the Space Shuttle and does not constitute evaluation under commercial service requirements. All numerical predictions are based on standard reference data and are presented to show relative probabilities only.

The recommended concepts for achieving electronic FO/FO/FS and hydro-mechanical FO/FS are based on independent failure paths. Alternate configurations were developed which compromise the independent failure objective but retain extremely remote failure probabilities.

Groundrule 3 - 1 Brake Plus Skid Control Each Side

- o Electronic FO/FO/FS - Examination of the Advanced 737 brake system shows no redundancy in the skid control input to each brake. Therefore any skid control failures lead directly to failure of the brake. Under groundrule three, loss of skid control to one wheel is still acceptable for adequate braking capability or FO. To achieve FO/FO no additional single failure can result in less than one wheel per side available. This is not true for the baseline configuration since the second failure could be the brake on the same side. The system is still considered fail safe since antiskid can be turned off and an emergency stop made with manual brakes. Additions to the baseline system necessary to achieve FO/FO would be a redundant skid control system to either the inboard or outboard pair of wheels. With this addition the only second failure that could fail a wheel would be on the opposite side of the aircraft thereby meeting the groundrule. A refinement is required in the skid control logic to the wheel pair with dual antiskid so that failures leading to locked brake signals are detected and the affected system deactivated so that the alternate system can continue to control the wheel. This failure detection and switching logic system is shown in Figure 45. An alternative approach

would be a failure detection system consisting of a sensing light and pilot controlled transfer switch with transfer valve at the hydraulic supply.

- o Hydro-Mechanical FO/FS - The critical mode failures using the Fault Tree Analysis of the baseline system shows single failures which result in loss of braking on one wheel. As in the case of the electronic input this is acceptable under groundrule 3 as FO. If the additional failure affects the wheel on the same side the system is unacceptable since no brakes on one side cannot be compensated by steering and rudder to achieve an emergency stop. Therefore a redundant input to one opposite wheel pair is also required to achieve hydro-mechanical FO/FS.

The examination of the hydro-mechanical system must be continued to insure that the redundant brake inputs are sufficiently independent upstream of the brake assembly so that there are no failures in hydraulic and mechanical sources which can occur and negate the apparently adequate redundancy.

There are single point failures which result in loss of one hydraulic system and the associated accumulator and consequent loss of control of the inboard or outboard pair of brakes. Even for failures where accumulator volume is still available for emergency manual stop, skid control is not available so that the brakes can be considered not operational.

Dual failures can result in loss of all hydraulics. A third hydraulic system is, therefore, recommended to supply the input to the selected opposite wheel pair to achieve FO/FS capability.

There are failures in the metering valve and in the mechanical linkage to the valve which can affect both brakes on one side. The metering valve failure modes can be eliminated by use of

a separate metering valve for each of the above recommended brake actuation paths or a total of three valves. The separate valves eliminate the possibility of failures in the single loadpath between the cockpit input dual valve shaft and the individual metering valve pistons.

The mechanical linkage to the dual valve shaft has no single open failure that results in less than fully operational brakes. The possibility of a jam does exist. Careful design can reduce this risk to an acceptable level. A second open failure in the linkage could fail both brakes so that an alternate fail-safe mechanical brake on device must be provided to achieve FO/FS. A triple loadpath linkage to the cockpit is a possibility but a simpler method could be a hydraulic input similar to the Advanced 737 automatic brake system, but designed for emergency stop conditions rather than its present intent of passenger comfort. If the Space Shuttle is to be operated by a single crewmember, a second mechanical input is required to replace the second pilot. This could be accomplished by either a dual structure pedal arrangement or a hand lever.

- o Proposed System - Figure 45 is a schematic brake system which suggests the type of arrangement that would be required to achieve the desired redundancy under groundrule 3. This system will be designated as Configuration A.

The predominant failure path in both the baseline and this proposed Space Shuttle system is the hardware between the metering valve and the brake assembly. Reasonable trade offs in hardware upstream of the metering valve would not have great effect on the overall system failure probability. Alternate configuration A is therefore presented as shown in Figure 46. The emergency braking system and the third hydraulic system are eliminated.

Groundrule 2 - 3 Brakes Plus Skid Control

- o Electronic FO/FO/FS - The recommendations made under groundrule 3 would not be sufficient to provide FO/FO/FS under groundrule 2 since two failures could deactivate the single input wheel pair and result in inadequate skid control. Therefore it is recommended that dual skid control inputs be provided for each wheel. The dual inputs must include logic to prevent locked wheel signals from affecting both inputs. See Figure 47.
- o Hydro-Mechanical FO/FS - Dual hydro-mechanical inputs to each brake assembly will be necessary to achieve FO/FS under groundrule 2. With dual inputs, there are no double failure combinations downstream of the metering valves which can result in the loss of more than the allowed one brake. As discussed previously, there are dual failures that can result in loss of all brakes or both brakes on one side. To achieve FO/FS under groundrule 2 it is recommended that an emergency brake control be added using a third hydraulic system to provide a fail safe capability.
- o Proposed System - Figure 47 is a schematic brake system which suggests an arrangement that would provide the desired redundancy. The system will be designated as configuration B.

Reasonable tradeoffs under Groundrule 2 would be elimination of the emergency brake actuation system and the third hydraulic system. This would have negligible effect on the probability of a single wheel loss and would still give a probability of dual wheel loss equivalent to the loss of both primary hydraulic systems. Figure 48 presents a configuration incorporating these tradeoffs and is designated as configuration B alternate.

Groundrule 1 - All Brakes and Skid Control





- o Electronic FO/FO/FS - Since all brakes and skid control are required under groundrule 1 each wheel must be FO/FO/FS. This indicates a requirement for three independent skid control inputs with proper failure detection and switching logic.
- o Hydro-Mechanical FO/FS - Three independent hydro-mechanical inputs to each brake are also required to achieve the desired redundancy. Three brake actuation paths are also required.
- o Proposed System - Figure 49 suggests a hardware system that would represent implementation of the independent fault path requirements. The system is designated as Configuration C. The emergency actuator could be any device such as a solenoid or pneumatic actuator which moves the metering valve to a brake on position.


The emergency actuator could be deleted from this proposed configuration with negligible effect on the overall failure probability. The most likely failure path would then be in the linkage from the metering valves to the cockpit. This system will be designated as Configuration C alternate. See Figure 50.


CONCLUSIONS

Groundrules 1, 2, and 3 are representative of the tradeoffs to be made in final selection of a brake system for the Space Shuttle vehicle. Table 1 shows an estimate of the weight, broken down by subsystem, for each proposed configuration. The brake assembly weight is included because it represents a tradeoff item due to the different energy requirements under the three different groundrules. Under groundrule 1, where all brakes are required, the brake weight is minimum since they are sized to meet minimum energy requirements. However, the cost of the electrical and mechanical hardware required


TABLE 1
ESTIMATED SYSTEM WEIGHT

| CONFIGURATION | BRAKE  | ANTISKID SYSTEM  | MECHANICAL ACTUATION  | HYDRAULIC  | TOTAL |
|--|---|--|--|---|-------|
| Baseline System 737 Type System Applied to Space Shuttle | 760 | 30 | 30 | 90 | 910 |
| A (Figure 2) | 1000 | 50 | 35 | 160 | 1245 |
| A Alternate (Fig. 3) | 1000 | 50 | 33 | 130 | 1213 |
| B (Figure 4) | 800 | 70 | 38 | 220 | 1128 |
| B Alternate (Fig. 5) | 800 | 70 | 35 | 180 | 1085 |
| C (Figure 6) | 760 | 100 | 45 | 270 | 1175 |
| C Alternate (Fig. 7) | 760 | 100 | 40 | 270 | 1170 |

 Assumes structural carbon brake with sufficient heat sink capability to meet the energy requirements under the ground rules specified for each configuration.

 Antiskid system includes the control box, transducers, valves, failure monitoring, and transfer logic circuits, wiring and support brackets.

 Mechanical actuation includes all equipment and support brackets from the pedals to the brake metering valves. Also includes emergency actuation equipment.

 Hydraulics include all hydraulic equipment from the accumulator to the brake. Also includes tubing, support brackets and hydraulic fluid.

to provide the desired redundancy would be maximum. Conversely, the groundrule 3 design provides part of the required redundancy in excess brake energy capability which increases the system weight but reduces control system complexity and cost.

The space (wheel cavity volume) required to accommodate the brake under ground rule 3 would make that configuration rather difficult to implement. Also, field length requirements may be a factor prohibiting this configuration.

The system designated configuration C required for electrical FO/FO/FS and mechanical FO/FS would be very difficult to implement because of the three wheel speed transducer requirement and the triple brake actuation system requirement. Therefore, from a cost, weight, and complexity trade standpoint, configuration B, or some variation on it is optimum for the imposed conditions.

System and component weights shown in Table 1 are based on typical present day aircraft design practices. This procedure for assessing weight was used because space shuttle vehicle design details were not available when this study was done. Some space shuttle vehicle braking system component weights will be lower than those estimated where new technology is applied in the design, e.g., titanium tubing in the hydraulic system and integrated circuits in the antiskid electronic system.

Also, the brake control system (pilot's pedals to the brake metering valve) is assumed to be mechanical as in present day operational jet aircraft. With an electrical control system, pilots command could go directly to the antiskid valves and the metering valve would be deleted. The weight of an electrical system would be less than a mechanical system if special cable tension devices are required due to temperature extremes. Also, space constraints may dictate use of an electrical system.

Tables 2 and 3 are presented to summarize the relative probabilities of failure to meet the adequate braking groundrules for the six configurations developed in this study. No attempt is made to select the optimum brake system by failure probability only, but the information contained in Tables 2 and 3 in conjunction with brake weight estimates presented in Table 1 should provide the necessary decision information.

TABLE 2

| SUMMARY - PROBABILITY OF BRAKE LOSS DUE TO HYDRO-MECHANICAL FAILURE | | | | |
|---|---------------------|-------------------------|--------------------------|------------------------------------|
| CONFIGURATION | BRAKING REQUIREMENT | FOUR BRAKES REQUIRED | THREE BRAKES REQUIRED | TWO BRAKES (Each Side) REQUIRED |
| BASELINE | | 7.2×10^{-5} | 3.9×10^{-9} | 1.3×10^{-9} |
| A | | 3.6×10^{-5} | 6.4×10^{-10} | 2×10^{-12} |
| A ALTERNATE | | 4.3×10^{-5} | 9×10^{-10} | 2×10^{-12} |
| B | | 3.6×10^{-11} | 2.7×10^{-18} | 2×10^{-12} |
| B ALTERNATE | | 10.2×10^{-12} | 1.96×10^{-12} | 2×10^{-12} |
| C | | 13.2×10^{-18} | 2.7×10^{-18} | 2.7×10^{-18} |
| C ALTERNATE | | 1×10^{-12} | 1×10^{-12} | 1×10^{-12} |

TABLE 3

| SUMMARY - PROBABILITY OF BRAKE LOSS DUE TO SKID CONTROL FAILURE | | | | |
|---|---------------------|---|--|--|
| CONFIGURATION | BRAKING REQUIREMENT | FOUR BRAKES WITH SKID CONTROL REQUIRED | THREE BRAKES WITH SKID CONTROL REQUIRED | TWO BRAKES(Each Side) WITH SKID CONTROL REQUIRED |
| BASELINE | | 6×10^{-5} | 2.7×10^{-9} | 9×10^{-10} |
| A | | 3×10^{-5} | 4.5×10^{-10} | 6.8×10^{-15} |
| B | | 9×10^{-10} | 6×10^{-19} | 2×10^{-19} |
| C | | 1.4×10^{-14} | 2×10^{-28} | 2.8×10^{-42} |

LEFT SIDE

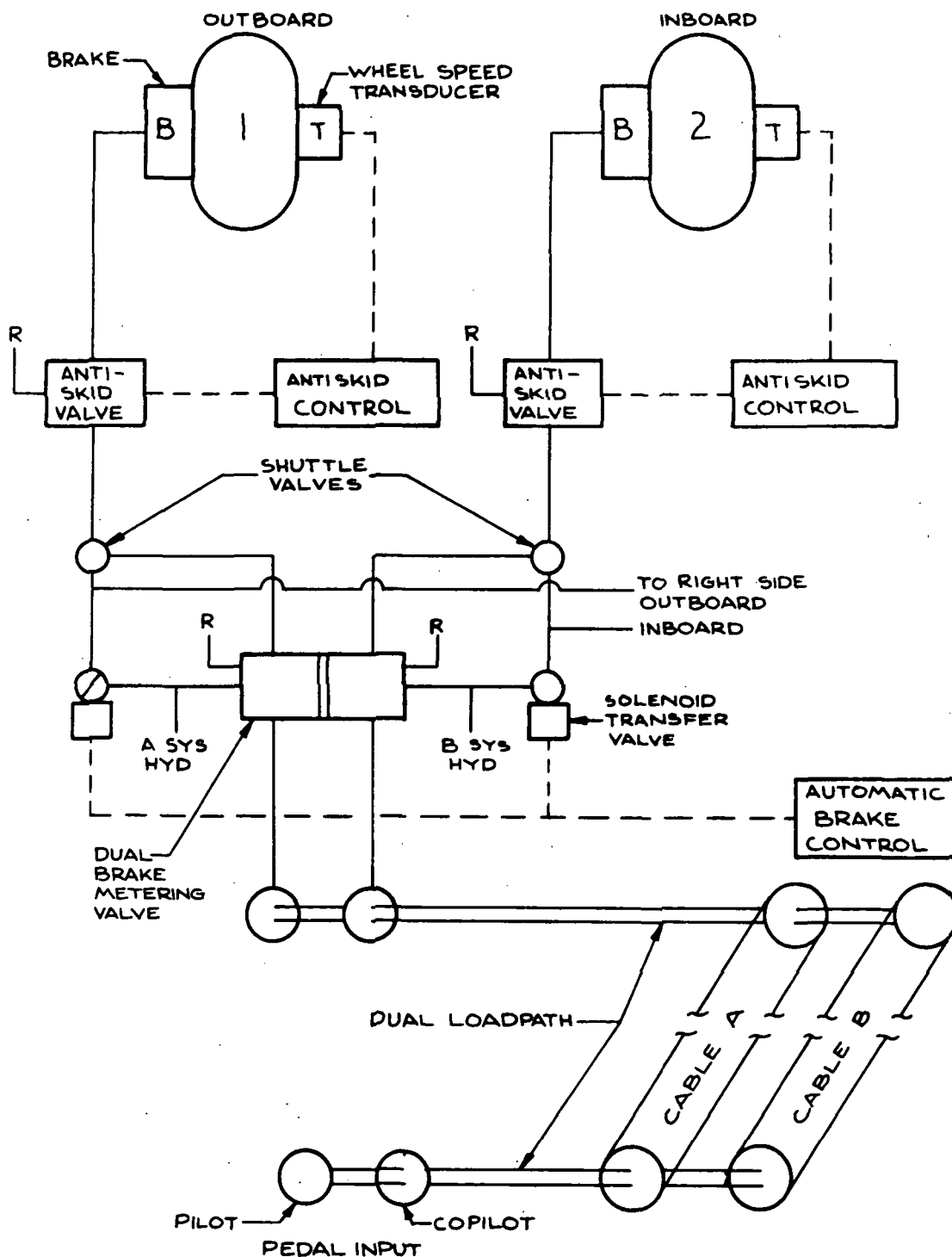


FIGURE 44. BOEING 737 (BASELINE BRAKE CONTROL SYSTEM) LEFT SIDE SHOWN
RIGHT SIDE SIMILAR

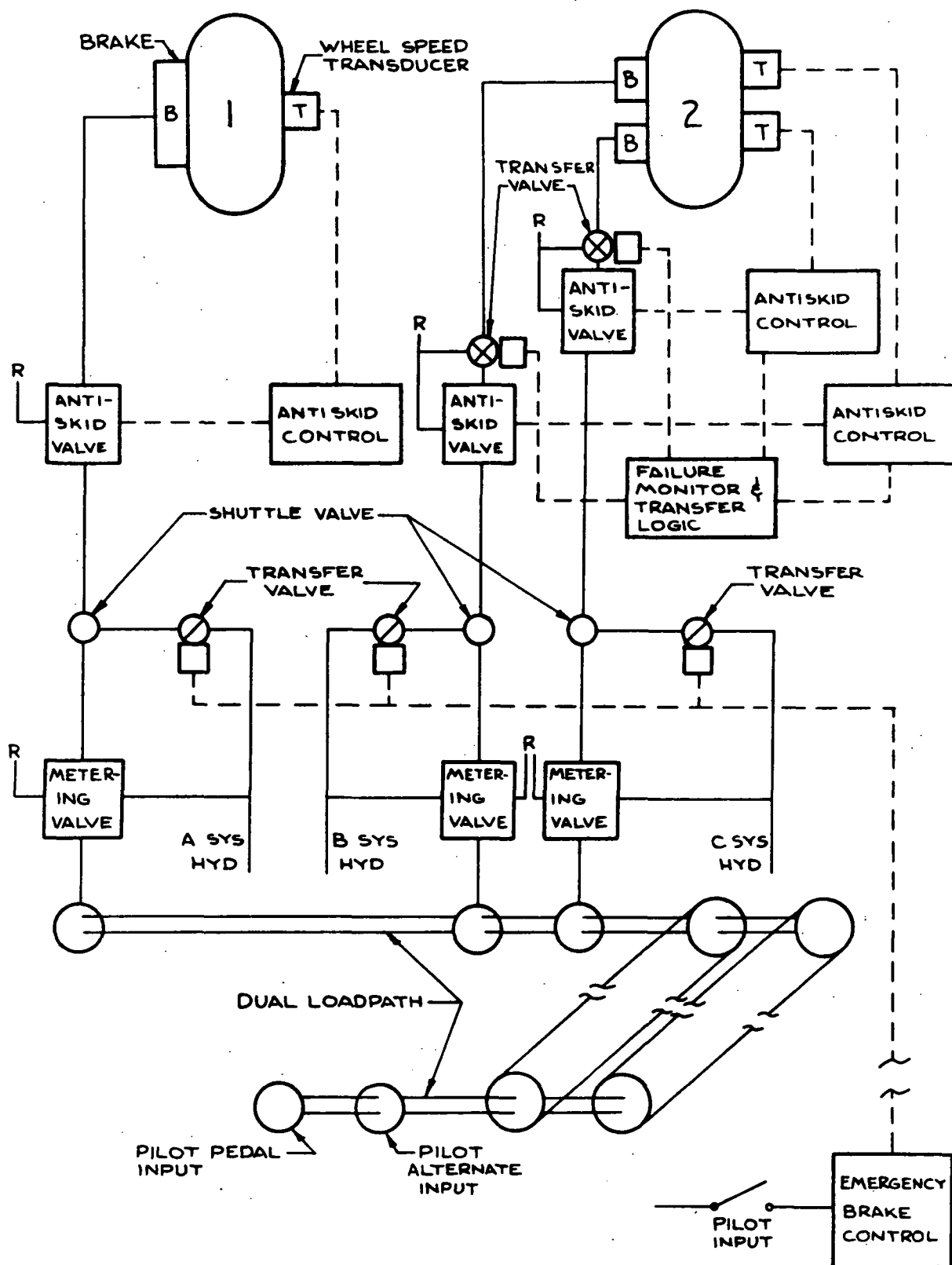


FIGURE 45. CONFIGURATION A, GROUNDRULE 3 - 1 BRAKE PLUS SKID CONTROL EACH SIDE - LEFT SIDE SHOWN, RIGHT SIMILAR

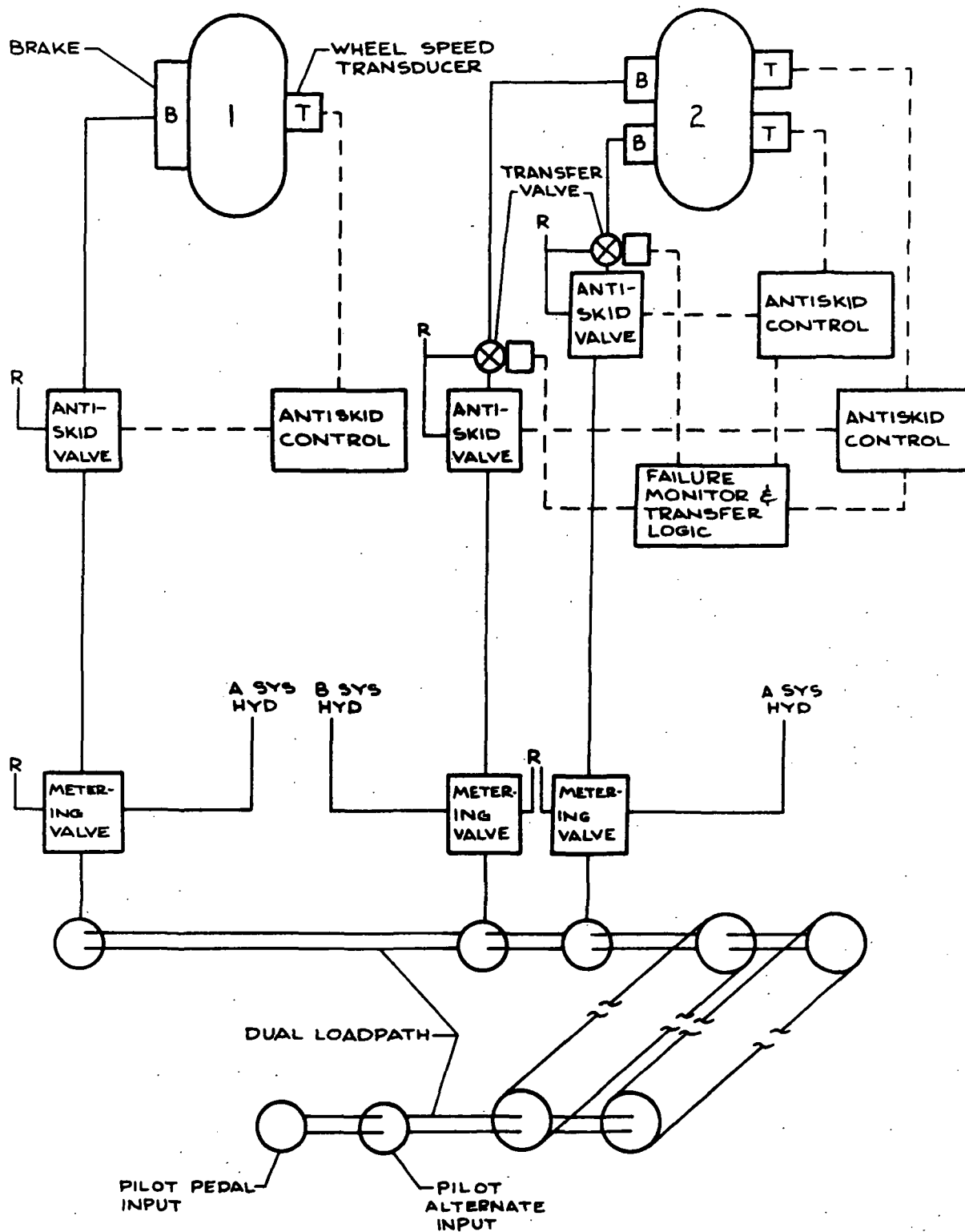


FIGURE 46- ALTERNATE CONFIGURATION A - LEFT SIDE SHOWN, RIGHT SIDE SIMILAR

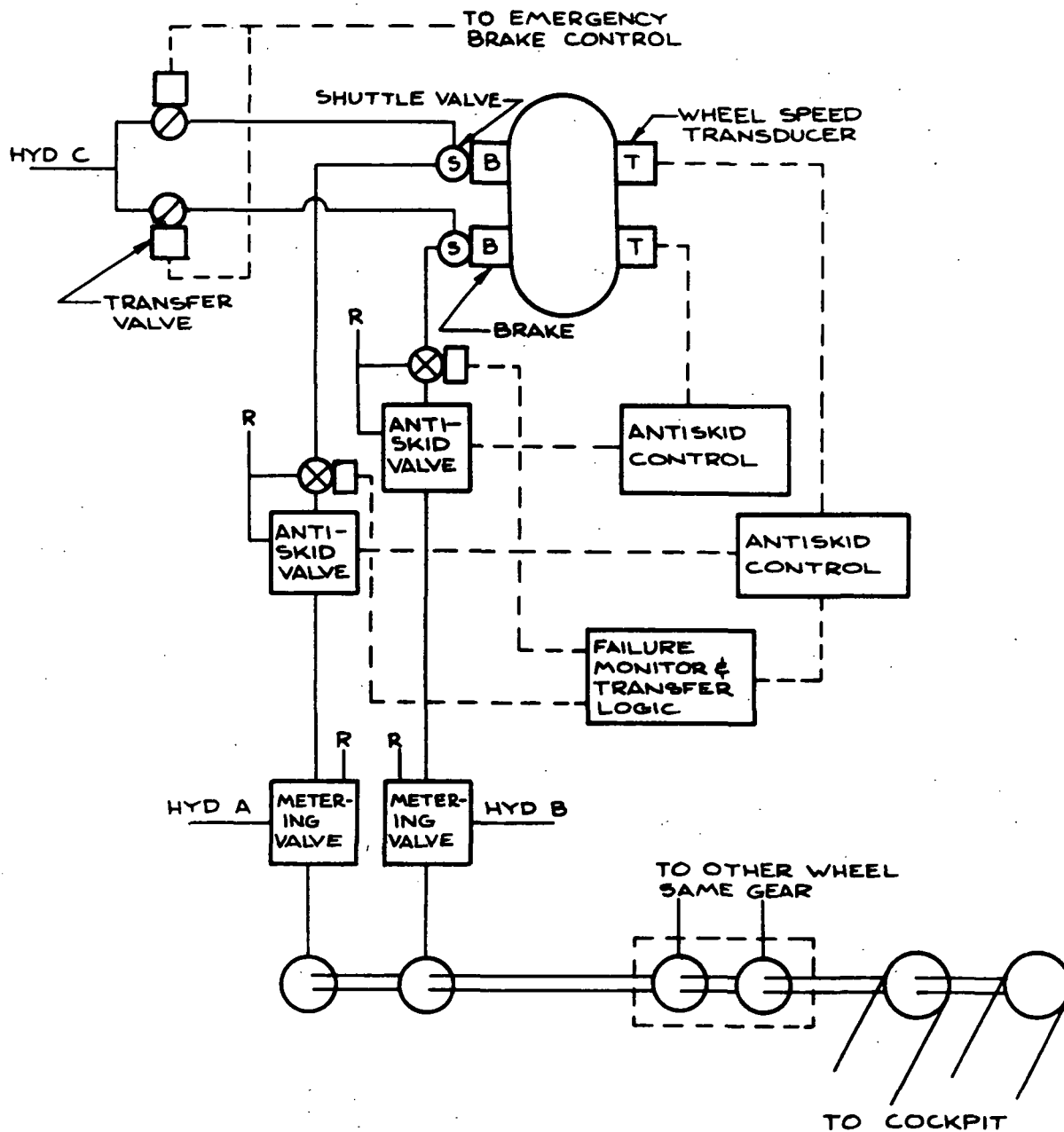


FIGURE 47 - CONFIGURATION B - GROUNDRULE 2 TYPICAL WHEEL

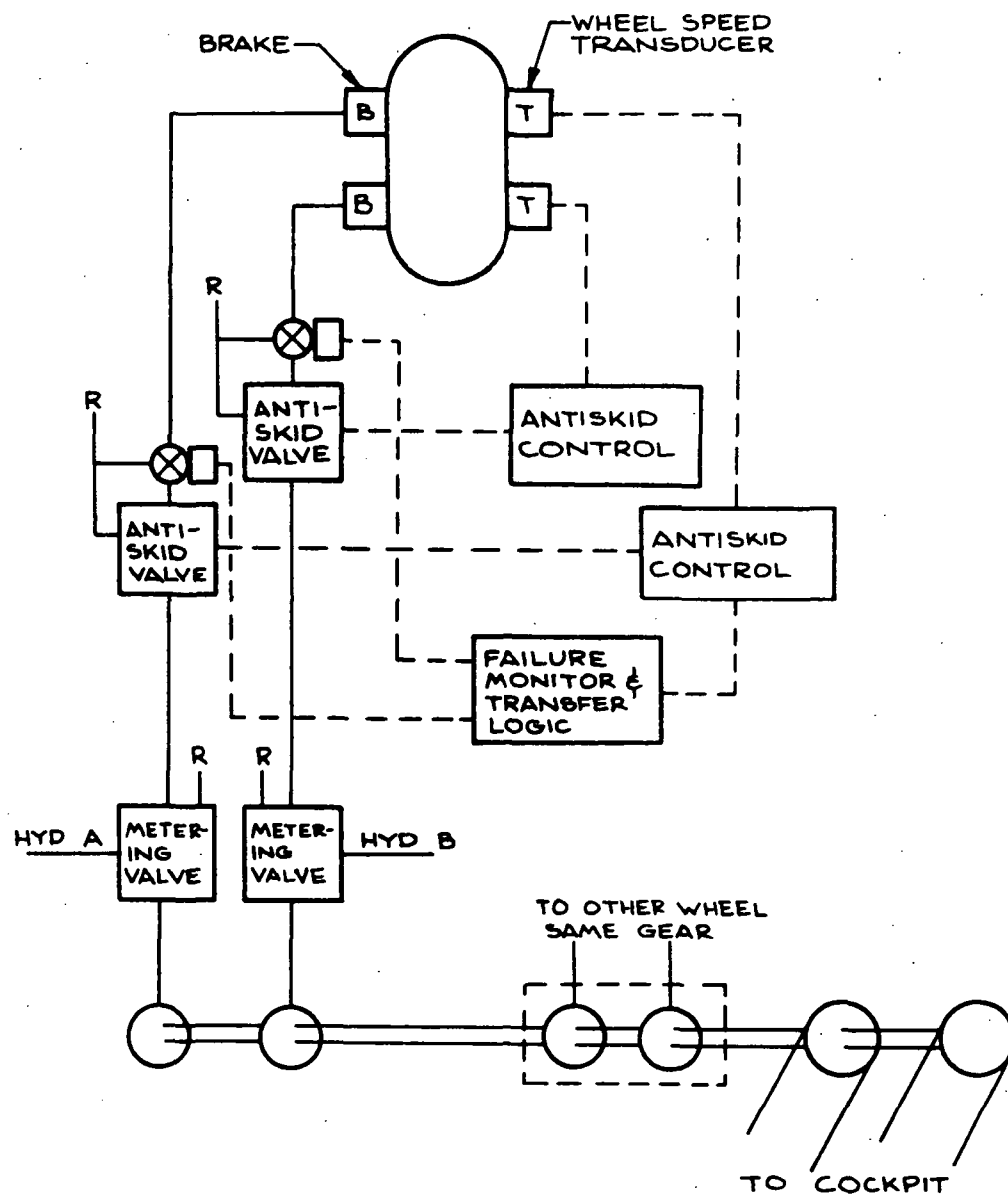


FIGURE 48- ALTERNATE CONFIGURATION B - TYPICAL WHEEL

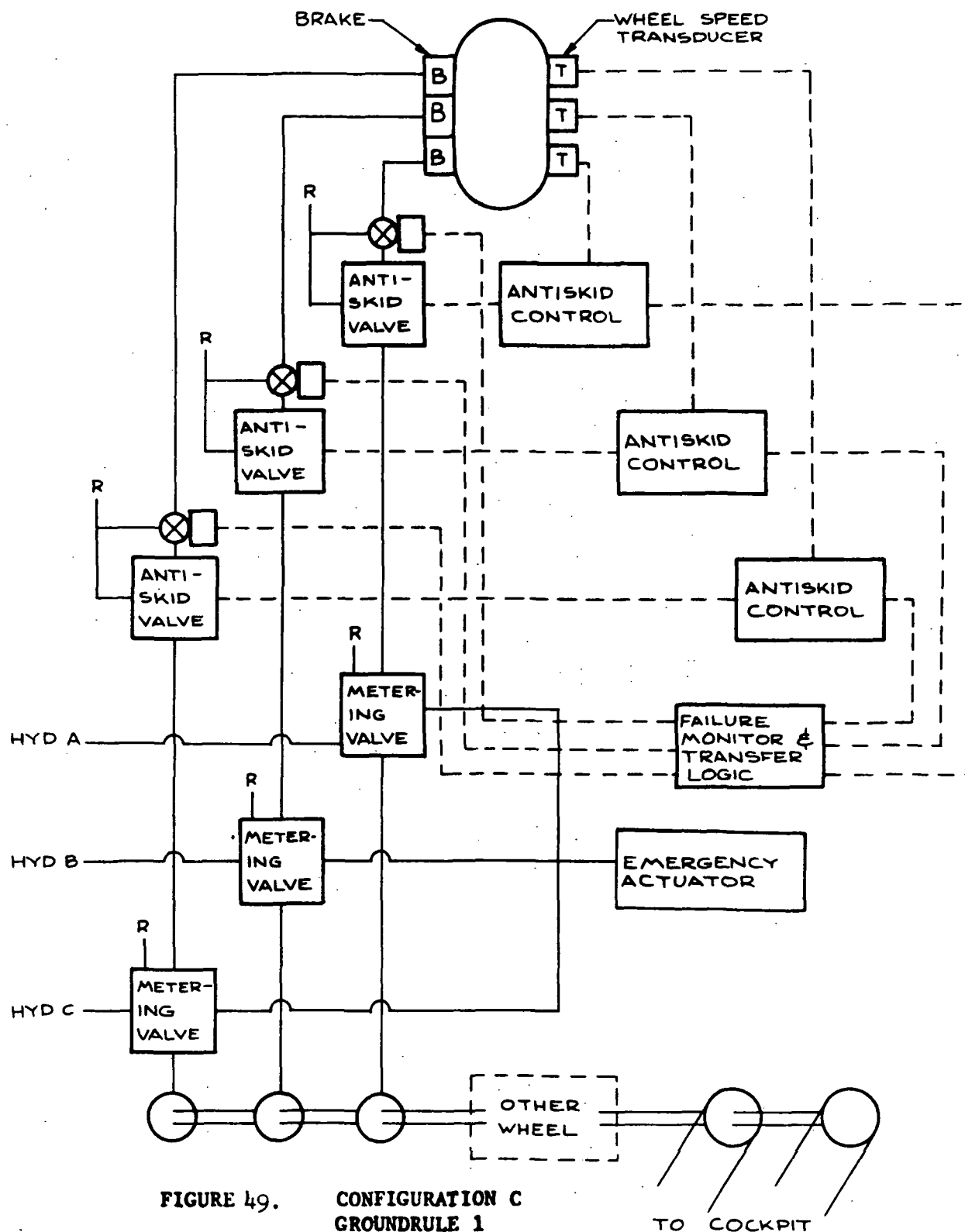


FIGURE 49. CONFIGURATION C
GROUNDRULE 1
TYPICAL WHEEL

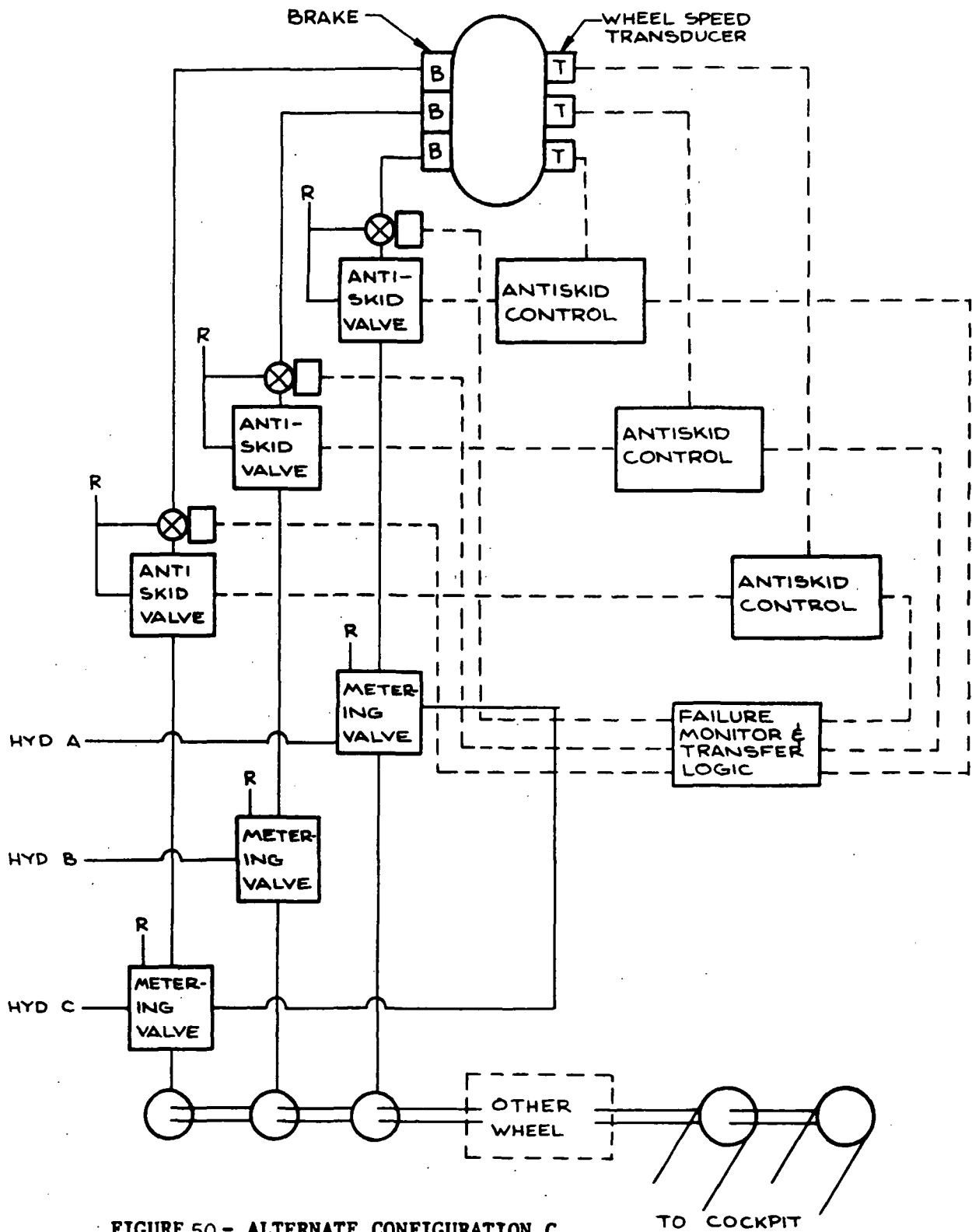


FIGURE 50 - ALTERNATE CONFIGURATION C
TYPICAL WHEEL

VI. LABORATORY EVALUATION OF ANTISKID SYSTEMS

DESCRIPTION OF ANTISKID SIMULATIONS

The Boeing antiskid simulation used for this study consisted of one of the available general purpose skid control simulations. The complete simulation consists of an analog computer programmed to simulate aircraft related dynamics while the braking system related hydraulics is actually used directly in the simulation. Since the entire simulation operates in real time, an actual aircraft antiskid system can be tested directly. Both the computer simulation and hydraulic implementation will be described. See Figure 51.

Analog Computer Simulation

A general Boeing commercial aircraft type antiskid simulation was used but rescaled and modified to reflect the dynamics of the Space Shuttle. But the NASA specified Shuttle parameters (see Table 4) were incorporated with no major change to existing simulation models.

Several aspects of the Space Shuttle configuration and operating envelope differ considerably from a typical jet transport aircraft. These influences were accounted for. The simulation consists of all essential vehicle and landing gear system parameters which include the following:

- o Vehicle static and dynamic characteristics

- Touchdown dynamics
- Pitching dynamics
- Aerodynamics
- Center of gravity and gear position

- o Landing Gear Dynamics

- Shock strut (vertical motion)
- Shock strut (horizontal motion)
- Tire and wheel

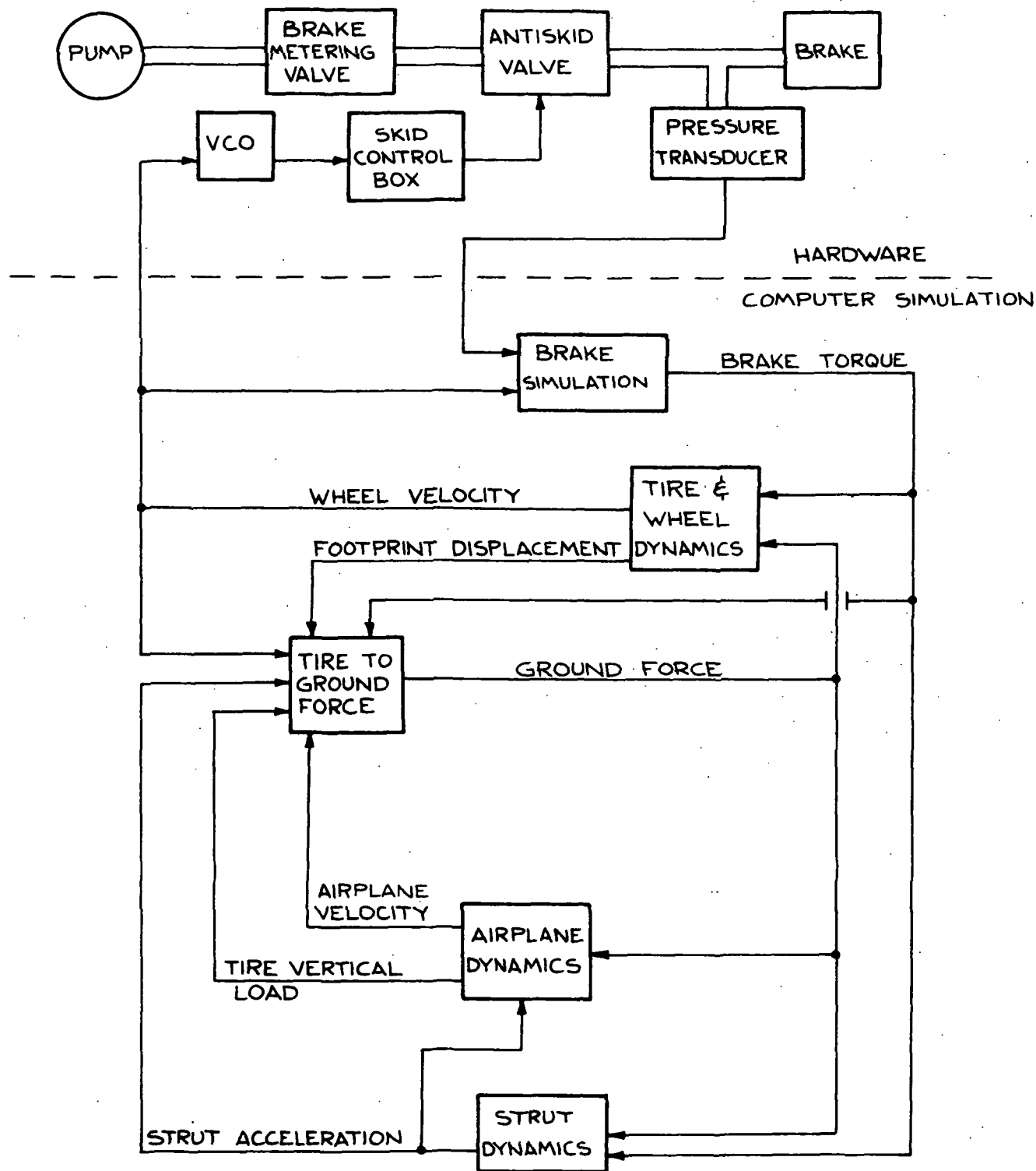


FIG. 51 SIMULATOR BLOCK DIAGRAM

- o Brake Torque Characteristics

- Response
- Peaking
- Fade

- o Tire-Ground Interface Characteristics

- Thermodynamics
- Tire mechanical properties
- Tire dynamics

Hydraulic Simulation

The hydraulic related aspects of the antiskid simulation are actually real hydraulic components. Line lengths and diameters are implemented as they were judged to be on the Space Shuttle (See Fig. 52). From energy requirements and wheel size the 747A brake was chosen for the simulation. The Space Shuttle was judged to have a brake-by-wire actuation system so no metering valve was incorporated. Pilot's brake pedal input was simulated by an antiskid valve signal which held off all brake pressure until the computer run was initiated and then ramped up to 211 kg/cm^2 (3000 lbs/in^2) in 300 milliseconds. As shown in Figure 52 the following components were used to generate the proper hydraulic system response:

- Tubing
- Brake
- Accumulator

Both the analog and hydraulic simulation facilities used in this study can be seen in Figures 53 and 54.

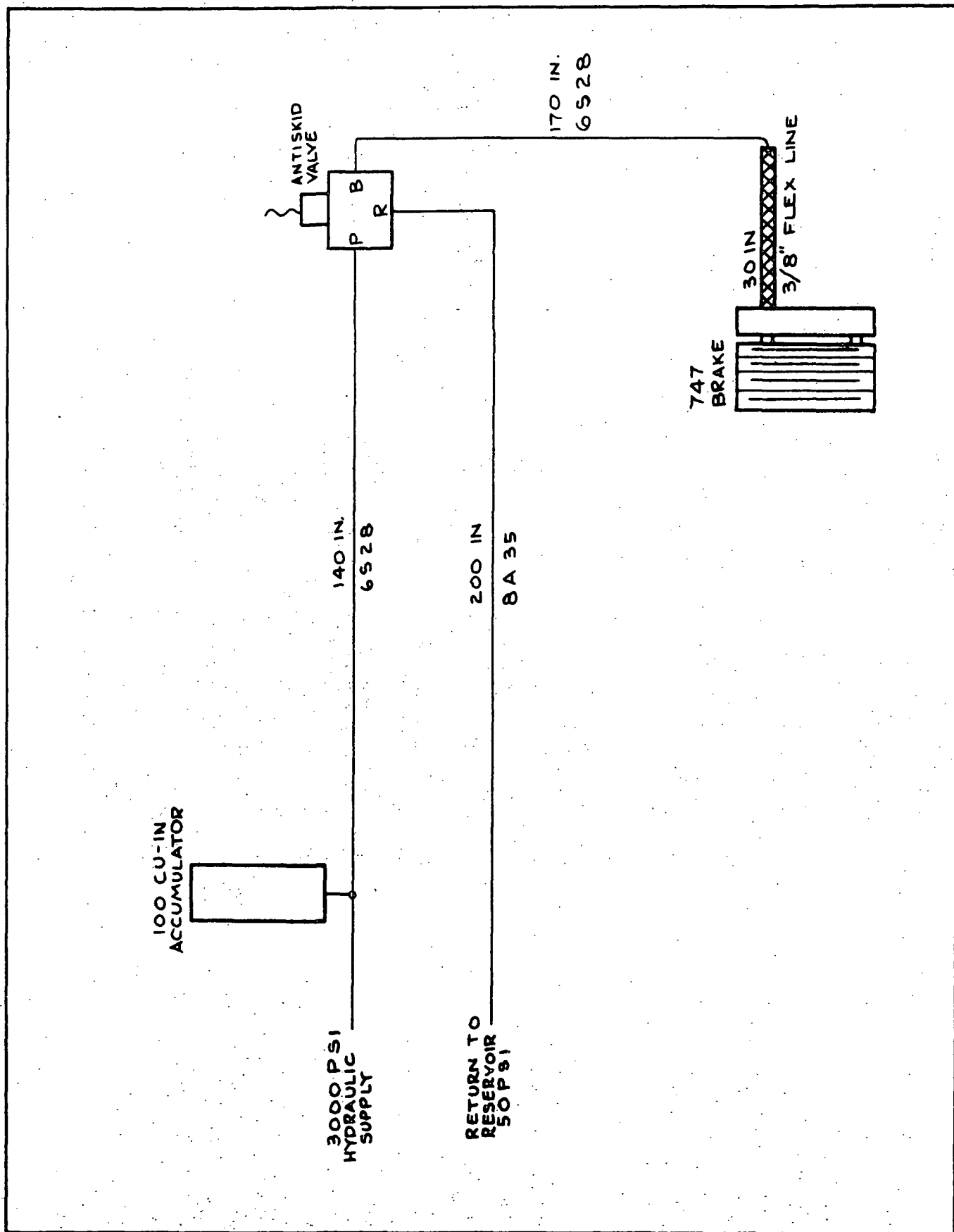


FIGURE 52. HYDRAULIC SKID CONTROL SIMULATION



FIG. 53 ANTISKID COMPUTER FACILITY

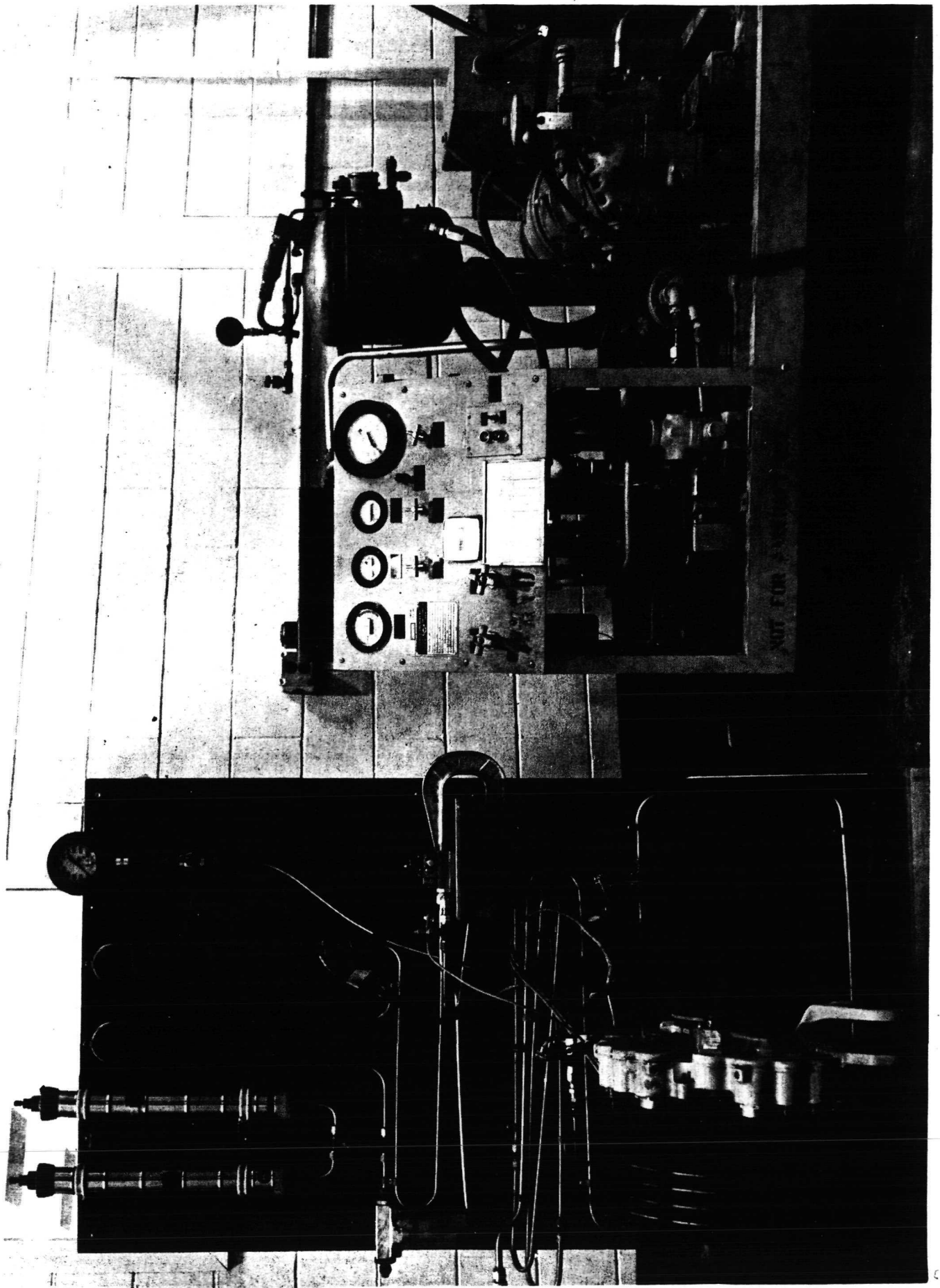


FIG. 54 ANTISKID HYDRAULIC SIMULATION

DESCRIPTION OF LABORATORY SCREENING TESTS

The tests can be divided into three major categories:

- o Stability Studies
- o Performance - Adaptability Studies
- o Operational Studies

Stability Studies

Freedom from gear walk is an important safety consideration. Hence, the tendency of a skid control system to contribute to the stability of the gear must be evaluated. The systems will be judged on their ability to provide damping to the strut motion or conversely their tendency to couple into the oscillation thereby causing divergence. The resultant strut vibration amplitudes produced by skid control system operation will also be evaluated. The systems will be tested at three different strut frequencies (4.5 Hz., 7.5 Hz., and 11.5 Hz., 7.5 Hz. nominal) representing the change in natural frequency due to different vehicle gross weights. Also this covers the expected range of frequencies the eventual nominal strut frequency will be on the Space Shuttle.

Test 1. Gear Walk

Purpose:

To determine the contribution of the skid control system to landing gear oscillations (gear walk).

Procedure

During this run, the brake torque will be made to peak from its programmed value to 1.5 times its value at critical times during a stop. One example of a critical time is when the tire slip is on the backside or unstable side of the friction curve. The strut displacement will be monitored to determine the influence of the control system on the strut stability. A range of both gear frequencies and strut damping ratios will be tested.

Performance - Adaptability Studies

The skid control systems will be evaluated under three categories, stabilized landings, touchdown profile, and notch mu steps. These tests were chosen to provide a measure of their performance and adaptability capabilities.

Test 1. Stabilized Landings

Purpose:

To measure skid control system performance under a stabilized braking condition.

Procedure:

During these tests the Shuttle vehicle was braked at a pre-selected brake application velocity of 334 km/hr (180 knots). Maximum effort braking continued until the vehicle was brought to a low velocity of 37 km/hr (20 knots) at which point the braking run was considered stopped. During these tests the available maximum mu was held at a constant value throughout an entire run. Values used for each run varied. For runs where the strut frequency was nominally 7.5 Hz the mu's were: .5, .4, .3, .2, .1, .075. For both the 4.5 and 11.5 Hz. strut frequency runs the mu's were: .5, .2 and wet runway curve 1. See Figure 55 for the wet runway profiles used in the computer simulation.

Test 2. Landing Touchdown Profile

Purpose:

To determine antiskid system transient response to changing load profile on the braked wheels due to shuttle vehicle bounce upon touchdown.

Procedure:

During this test the normal main gear wheel load is taken from zero to maximum (this upper value is, of course, modulated by

the airplane pitching model depending on the amount of vertical and rotational momentum transfer from main gear to nose gear) in approximately 250 milliseconds. Then after another 100 milliseconds the load drops to zero and stays there for 200 milliseconds, then ramps back up to maximum in 400 milliseconds. (Note, this profile is a much simplified load profile but the test is intended to approximate a touchdown bounce and thereby test the antiskid system's adaptability). Touchdown test was only conducted at a μ value of .5.

Test 3. Mu Step Changes

Purpose:

To determine system adaptability to sudden changes in μ simulating a series of wet spots or tar strips on an otherwise dry runway.

Procedure:

The computer run starts at a μ value of .54 and maintains this level for approximately six seconds. Abruptly μ drops to a level of .16, stays at this low value for 600 milliseconds then just as abruptly changes back up to .54 μ . This sequence of events repeats every seven seconds throughout the braking run. On the average five μ steps occurred during the actual tests. The more inefficient system would be subjected to more steps since they are a function of time.

Operational Studies

Tests in this group simulate conditions that are normally encountered in aircraft service. The Shuttle vehicle could also reasonably be expected to encounter these conditions in use. They include:

Test 1 Wet Runway

Two typical velocity dependent wet runway profiles were used to simulate wet and flooded runway conditions. See Figure 55.

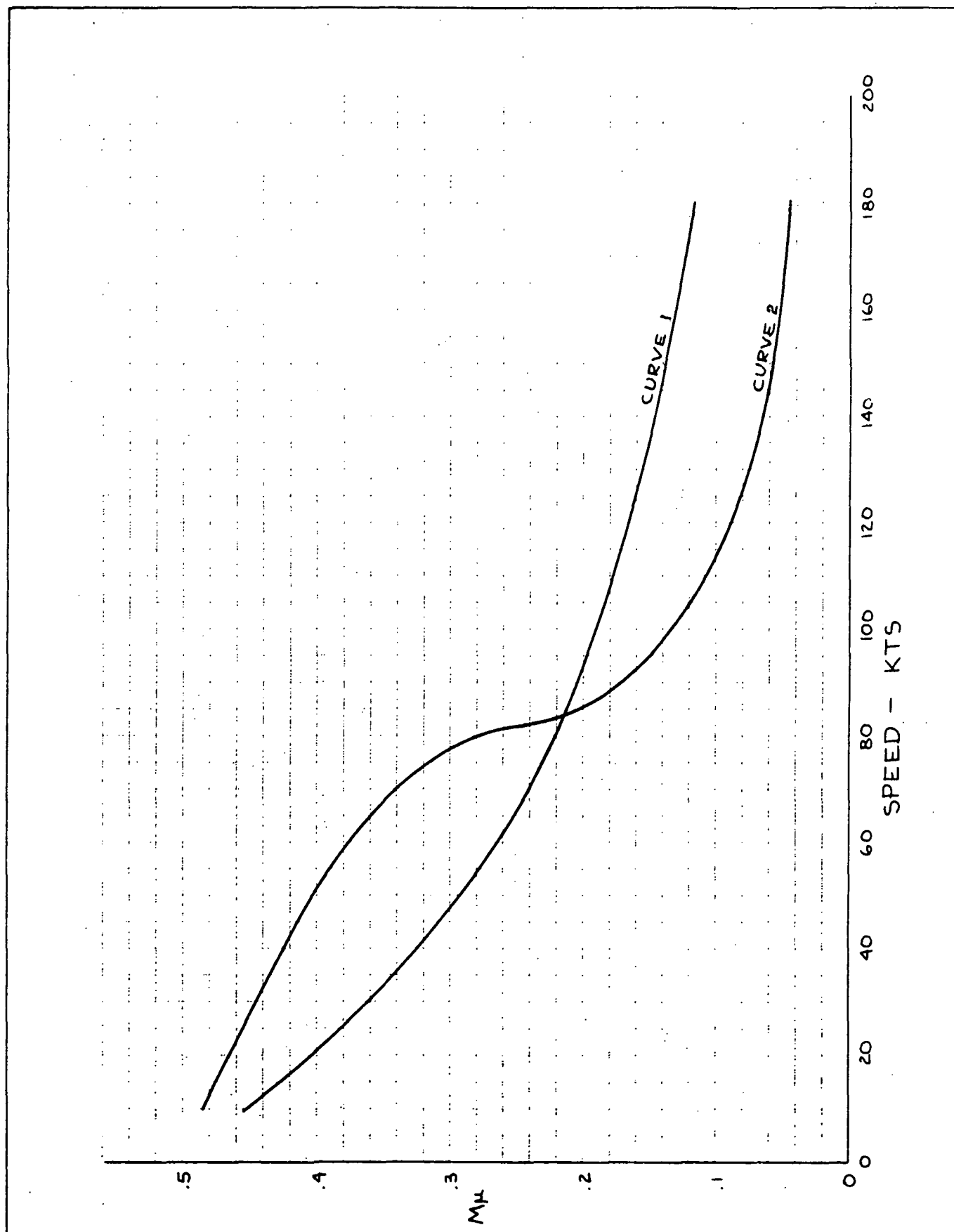


FIGURE 55. WET RUNWAY MU VERSUS SPEED - SPACE
SHUTTLE VEHICLE SKID CONTROL SIMULATION

Test 2 Landing Weight Variation

An upper and lower shuttle vehicle landing weight and brake application velocity were tested. The upper was 100,000 kg (220,000 lbs) and the brake application velocity was 352 km/hr (190 knots). The lower range was 81,820 kg (180,000 lbs) and a brake application velocity was 315 km/hr (170 knots). These two weight and velocity ranges were tested to expose the antiskid system to the expected operating range of the Shuttle vehicle.

Test 3 Wheel Inertia Variation

An upper and lower wheel inertia were tested since a range of rotating inertias could be expected depending on wheel and tire size, material used and the composition and size of the brake. The upper inertia tested was 14.75 n-m-sec^2 (20 ft-lb-sec^2) and the lower inertia was 8.85 n-m-sec^2 (12 ft-lb-sec^2). Nominally the inertia was 11.1 n-m-sec^2 (15 ft-lb-sec^2) used throughout the rest of the tests.

Test 4 Brake Torque Peaking

Low wheel speed braking can produce an increased braking sensitivity commonly called torque peaking. The antiskid systems were subjected to this test to see how well they adapted their performance to this condition. If a system does not handle this condition properly the gear stability can become critical.

Test 5 Tire Heating

The projected load that each main tire is expected to support will put the tire into a region of potential efficiency loss during braking. The inflation pressure in the tire is expected to be much higher than conventional commercial jet transports. To account for this efficiency loss a tire thermal effect must be added that will reduce tire-ground available μ whenever the tire is slid beyond 10% slip. What the simulation accomplishes is a reduced μ value momentarily after any prolonged skids. Each system is tested to see how well it can adapt to this situation.

Test 6 Drag Chute

The Shuttle vehicle will deploy drag chutes upon touchdown. Each antiskid system was tested with a simulated deployed drag chute to see how this affected the performance.

Test 7 Engine Idle Thrust

During the expected ferry mission of the Shuttle vehicle, there will be air breathing jet engines attached to the Shuttle. As happens on commercial jet transports engine idle thrust will provide some margin of accelerating thrust which will tend to add energy to the whole aircraft which the braking system must remove. This test subjected each system to this condition to assess its performance.

Data Recorded During Tests

The following data was recorded on pen recording charts to facilitate analysis and evaluation of the various antiskid systems.

- o Braked wheel speed
- o Pressure downstream of antiskid valve
- o Brake pressure
- o Brake torque
- o Developed ground coefficient
- o Strut displacement
- o Valve signal
- o Developed mu efficiency

The Mu-slip model will be monitored on the oscilloscope to observe the control system operation. This is also considered necessary to initiate some stability type tests.

Other measurements which are necessary to assess performance of the various skid control systems are:

- o Efficiency
- o Stopping distance
- o Skid index and cornering index

These will be measured by a digital voltmeter and recorded for all the tests. For purposes of these tests the developed Mu efficiency will be recorded. This efficiency measures the ability of a skid control system to produce a high ground coefficient of friction. Mu efficiency is determined by dividing the time integral of the developed coefficient divided by the time integral of the available maximum ground coefficient. Skid index and cornering index are both measurements dealing with how much any given skid control system skids the braked wheels. Skid index is a measured accumulation of the skids, the depths and the duration of each skid during each computer braking run. Cornering index is somewhat of an inverse measurement of the skid index. Whenever a braked wheel is driven into a deep skid, the resultant cornering efficiency is driven very low. For purposes of interpretation the lower the skid index, and the higher the cornering index the more efficient the antiskid system tends to be. However, the obvious case where the skid index is zero and the cornering index is 100 is not indicative of an efficient system. Its indicative of a free rolling unbraked wheel where no slip is developed.

EVALUATION OF LABORATORY RESULTS

Two antiskid vendors presented their systems to be evaluated, Hydro-Aire Mark III system and Bendix Slip Command System. Goodyear system and SPAD system vendors were each given an invitation to participate but both declined. Included also in this section was the Boeing Closed Loop System. This system was described in Section IV of this document and the reader is referred to that for more details. The tests have already been detailed so this section selected the more salient tests and described them. Four tests were selected for description and they represent the following:

- o .5 mi run with 4.5 Hz strut
- o .5 mi run with 11.5 Hz strut
- o Mu steps with 7.5 Hz strut
- o Wet runway curve 1 with 7.5 Hz strut.

These four tests were selected to represent both dry and wet runway braking runs. Both the low and high strut as well as nominal 7.5 Hz strut are represented in these tests. Also adaptability to step changes in μ was represented. These four tests are described for each of the three antiskid systems and the pen chart recordings are represented in Figures 56 through 67. The remaining tests conducted in this section are described with the aid of the tabulated data in Table V and further represented in bar chart form in Figures 68 through 108. The bar charts facilitate comparisons among the system's tested for each given test condition.

Discussion of Pen Chart Recordings

The Bendix test results are shown in Figures 56 through 59. Figure 56 represents a stabilized dry runway maximum effort stop with a nominal strut frequency of 4.5 Hz. The braking run began with the wheel rotating at synchronous velocity equivalent to 334 km/hr (180 knots). Since the Shuttle will be "brake-by-wire" type system, the brake pressure was brought on by a current ramp signal which went from full valve signal to zero in 300 ms. The resultant pressure rise is similar to that produced when the pilot rapidly applies full brakes at touchdown. In a matter of 400 ms the brake pressure was up to 211 kg/cm^2 (3000 lbs/in^2) which was more than sufficient to decelerate the braked wheel. It took the Bendix system approximately one second to adapt and stabilize to this braking condition. One skid went to a 34 percent slip and the second skid dropped to 27 percent slip. There were at least two full valve release signals which were unnecessary partly because the initial valve signal does not have sufficient authority to allow the wheel to recover and also because there was not sufficient pressure modulation. Referring back to Section III, the Bendix system is described. Initially when the wheel deceleration exceeded the decel limit the mono stable flip-flop triggered the slip command signal which did not have sufficient control for dry runway skids to allow full velocity recovery. The deceleration was momentarily halted but then

increased rapidly. This then caused a full valve release signal, dropped the brake pressure to retractor spring pressure which allowed rapid velocity recovery. However, when the full release signal vanished, insufficient pressure modulation took place and the brake pressure jumped back to 140 kg/cm^2 ($2,000 \text{ lbs/in}^2$), another valve full release signal then brought down the signal only 21 kg/cm^2 (300 lbs/in^2) before disappearing. The pressure then increased to 175 kg/cm^2 (2500 lbs/in^2) causing the slip command signal to retard the deceleration, but not sufficiently to stop the deceleration. As this increased again the valve signal pulled off insufficient pressure, the wheel decelerated again causing a full release signal and allowing complete wheel velocity recovery. This time after the full release signal was gone the pressure was modulated sufficiently to prevent another skid. As pressure was gradually brought on a skid was precipitated and the system is in smooth command of the wheel velocity. Skids were sampled at about 1.25 times per second, and the control exhibited proportional correction and adequate modulation. Except for some deflection associated with the first rapid skid cycling, the strut was exceptionally well damped.

Figure 57 represents a dry runway stop with the nominal strut frequency at 11.5 Hz. The pressure application was identical to that described for Figure 56. The system seemed to adapt to the rapid pressure application better in this case than the 4.5 Hz case. As soon as the pressure reached 211 kg/cm^2 (3000 lbs/in^2) the wheel went into a 25 percent slip skid and the system responded with a full brake release signal which allowed the wheel to recover. As no pressure modulation remained when the release signal departed, the wheel again went into a skid of 21 percent slip except that momentarily a partial release signal halted the deceleration. However, being insufficient the wheel continued its deceleration. This required another full release signal which allowed the wheel to recover its velocity. At that point came another partial release signal and the modulation level kept the wheel from going into another rapid skid. Pressure was then gradually increased until another skid was precipitated and the system

regained full control of the wheel velocity.

Skids were sampled at a rate of about 1.25 per second. This rate keeps up throughout the run until the stop was ended. In conjunction with the earlier rapid cycling when pressure was applied the Bendix system provided a two step response to skids that occurred during the low velocity portion of the braking run. Unless the braked wheel went into a deceleration as steep as possible the full release signal is not activated. Intermediate skid decelerations always cause just the slip command signal to react. Sensing that this is not enough correction to allow the full wheel recovery eventually the full release signal must provide complete wheel recovery. The time elapsed while this two-step reaction occurs is approximately 80 ms resulting in a deeper and wider skid than normal. For instance, if the proper brake release signal were initially provided, the skid would correspondingly be shorter and not as deep.

The strut motion was well damped reflecting the overall smooth control of the Bendix system.

The next test condition shown in Figure 58 involves dry runway adaptability by subjecting the system to sudden abrupt changes in μ . These μ changes drop the μ value from .54 down to .16. The duration of the low μ period is approximately .6 seconds upon which just as suddenly the μ increases to .54 again. These yield a μ -time profile of a non-symmetrical square wave. The time between repetitions is approximately six seconds. During the test each system is subjected to 4 or 5 of these stepdown changes. With this many μ changes the system's response can be observed under a variety of conditions. In this Bendix test, Figure 58, the first μ change caught the system in its recovery from a previous skid. Up until that first μ change the test resembled a .54 μ dry runway stop with the nominal 7.5 Hz strut frequency. When the μ suddenly dropped from a .54 to .16 this precipitated a maximum deceleration of the wheel since the brake pressure was considerably greater than what the tire-runway μ could

sustain. The skid caused a full release signal from the system which allowed the wheel to recover. This first low μ skid was about a 30 percent slip indicating the system was able to very rapidly recover since the skid was fairly shallow. Another skid came immediately after and its depth was only 25 percent slip. The system had fully adapted to the .16 μ condition and then the μ switched back to .54 μ . At this point the brake pressure was considerably below the required skid pressure so it was the task of the system to recognize this condition and raise the pressure up to the skidding level.

One problem any system must deal with is the strut activity. Because that first low μ skid required a full release signal the strut was fully released (this condition is more severe than real life since the space shuttle would have two wheels per strut and the interaction of those two separate brake systems might provide some strut damping; they might not release together) also causing the strut to oscillate considerably. This in turn caused velocity modulation of the wheel speed which could be interpreted as skids by the antiskid system. As soon as the μ switches back to .54 the remaining damped strut motion caused enough wheel modulation that the system kept the pressure low or unchanged for 1.8 seconds. After that the pressure rapidly increased from a level of 84 kg/cm^2 (1200 lbs/in^2) to 196 kg/cm^2 (2800 lbs/in^2) in just .7 seconds. This meant that 2.4 seconds elapsed after the μ switched up to .54 μ until the subsequent skid.

Normal skid sampling then continued for another three seconds at which time the μ switches down to .16 again. This time the wheel went into a 51% skid, the system responded with a full release signal allowed the wheel to fully spin up. Another skid of 32 percent slip depth required only a partial release signal to correct the deceleration condition. Before the wheel had time to recover under the .16 μ level the μ switched back up to its .54 μ level which very rapidly accelerated the wheel up to its synchronous velocity. This time the skidding pressure remained at the .16 μ level for 1.7 seconds with only slight

change.

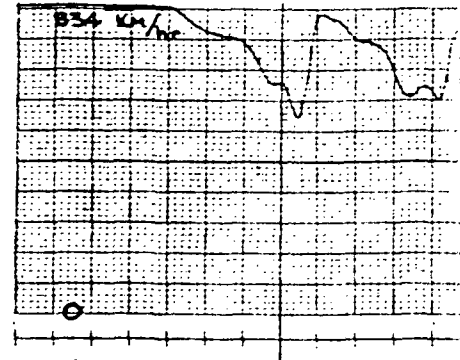
From that point on the pressure went from 105 kg/cm^2 (1500 lbs/in^2) to 207 kg/cm^2 (2950 lbs/in^2) in .5 seconds whereupon another skid was precipitated. Total elapsed time from the end of the low μ period to the next skid was 2.3 seconds. There was considerably less large amplitude strut oscillation with this particular μ change than the first. What lowered the overall performance efficiency was the delay time after every low μ period during which the pressure remained at a low level instead of increasing to the higher required level.

The fourth test is shown in Figure 59. It is a wet runway profile with the μ level varying as a function of aircraft velocity. Figure 55 shows the μ velocity profile used in this test. Basically the μ value starts out at .11 at brake application and goes up to .4 μ at the end of the computer stop. When pressure was applied at the beginning of the braking run, there was a period of 1.4 seconds in which 5 rapid skids took place. The deepest and first skid was a 40 percent slip followed rapidly by some more shallow ones. After each skid the modulation was increased until the pressure finally lowered to the retractor spring pressure and allowed the wheel to rotate at synchronous velocity for 2.5 seconds. No braking took place during this period until the modulation level finally decayed allowing the system to start skid sampling. The time starting from the beginning of the run until the system adapted and settled down to continuous control of the wheel velocity was four seconds. This could lead to a significant loss of efficiency although the system seems quite able to make up for this during the remainder of the run.

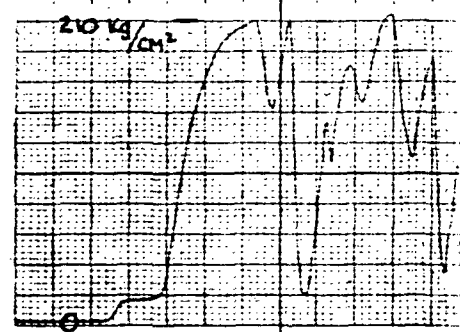
A velocity profile such as this wet runway test provides an excellent opportunity to see not only how the system adapts to very low μ start up conditions but also how smoothly the system can keep up with the ever-changing μ . There are obvious changes in the tire to ground wheel acceleration dynamics due to the decreasing wheel speed, but on a wet

34009

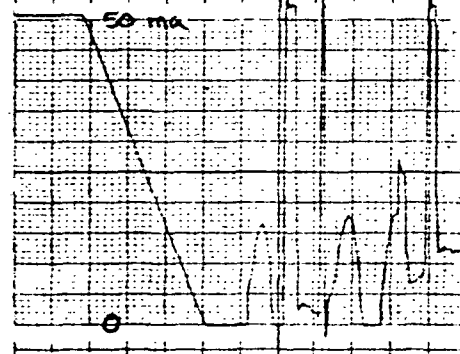
834 K_h/hr



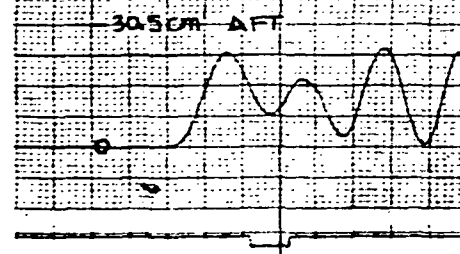
210 kg/cm²

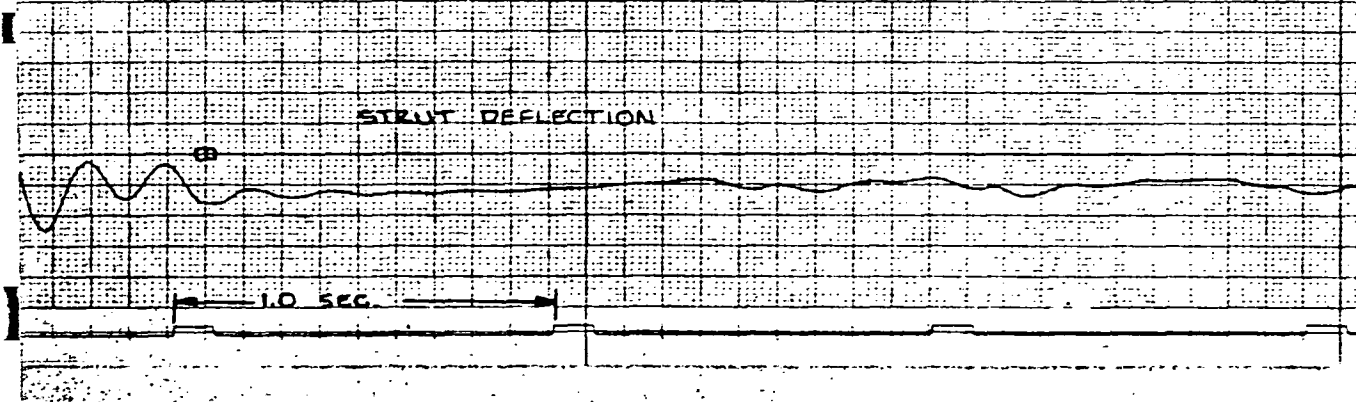
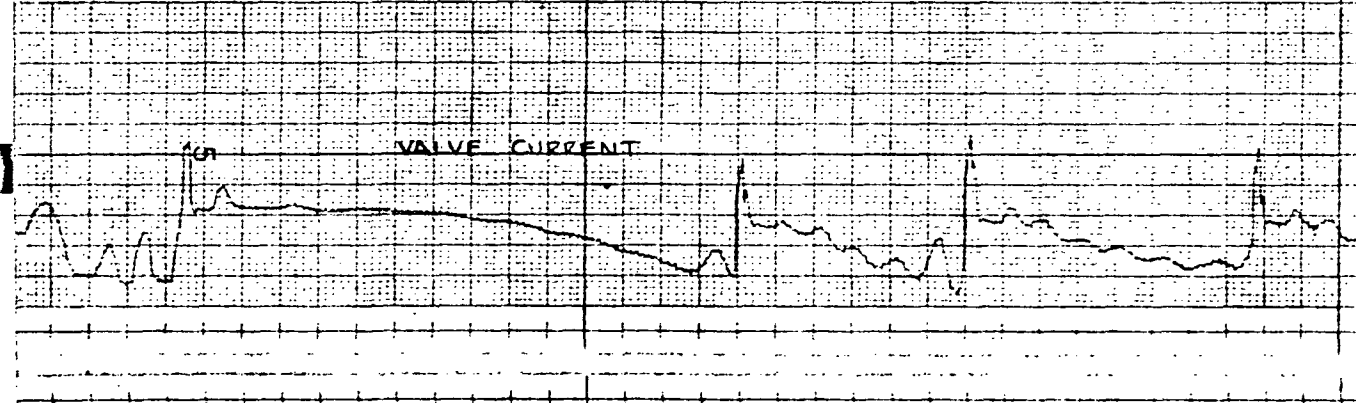
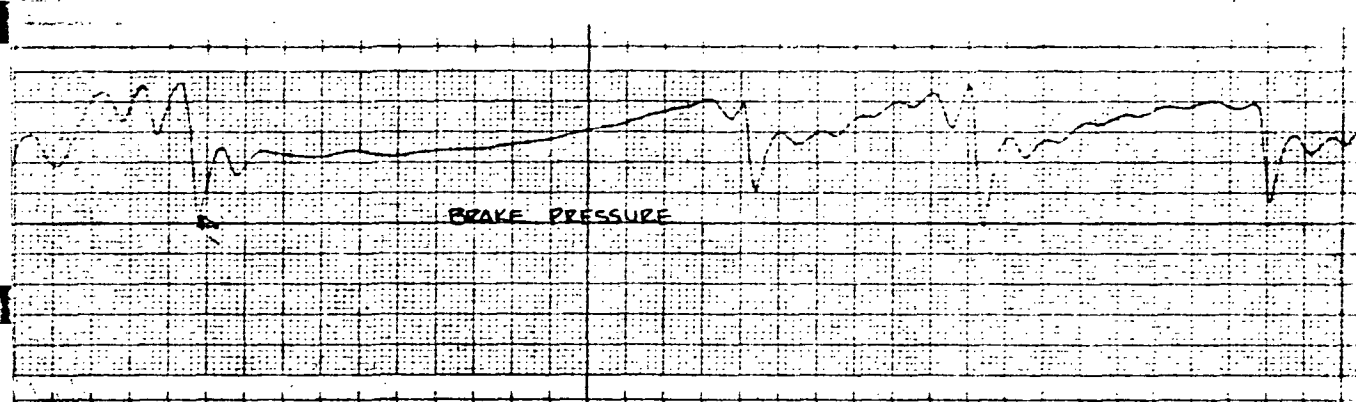
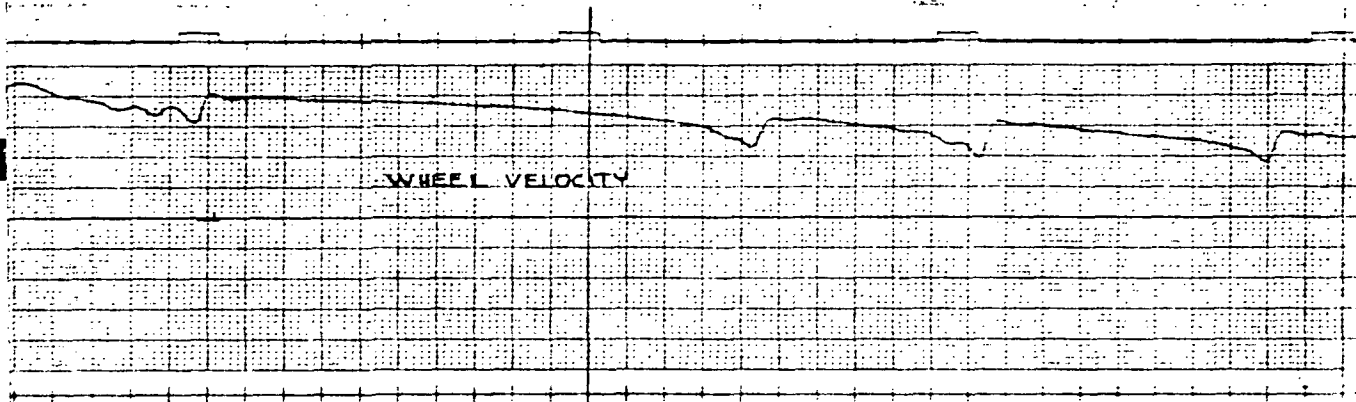


50 ma



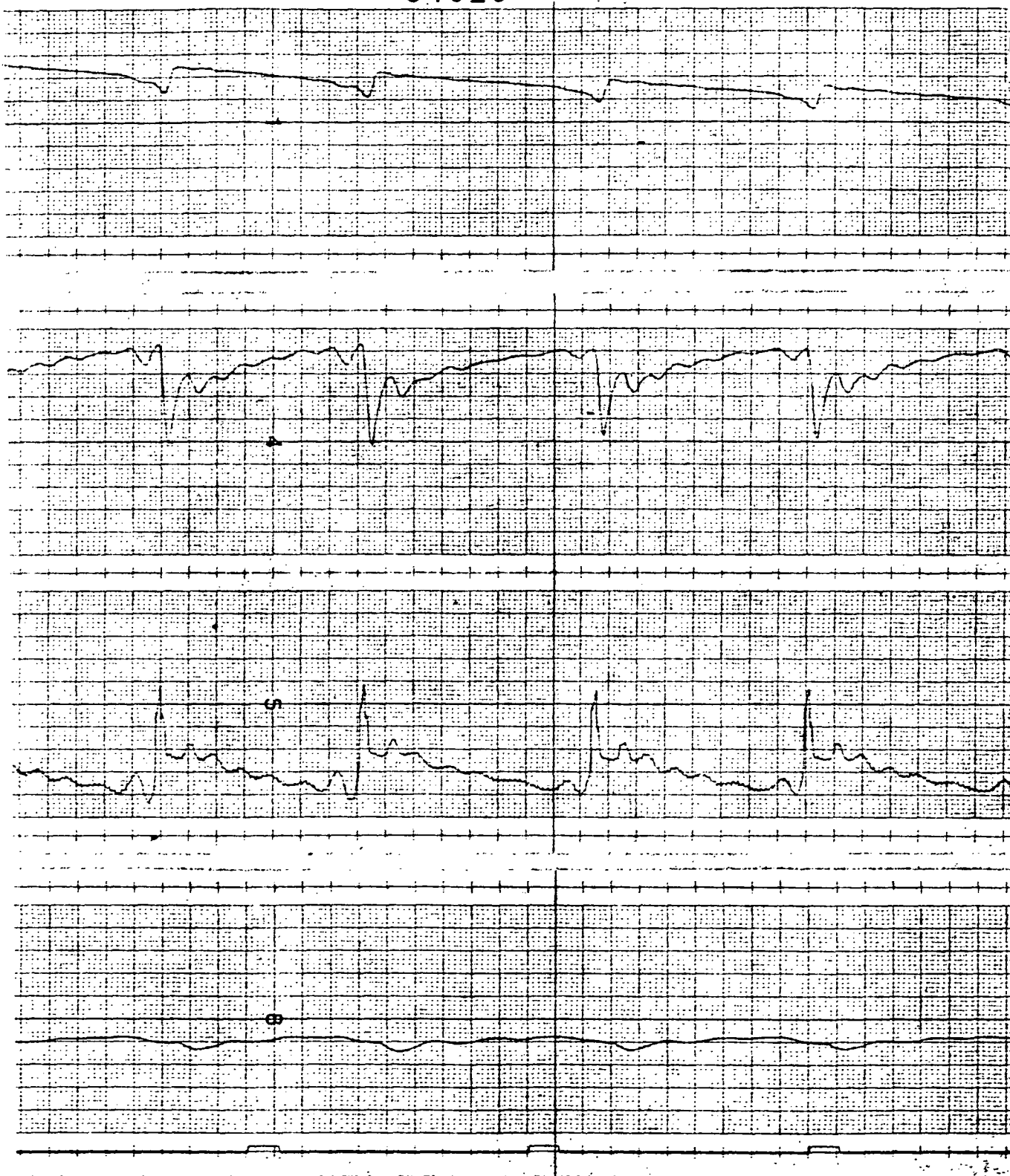
30.50R AFT





FOLDOUT FRAME

34010

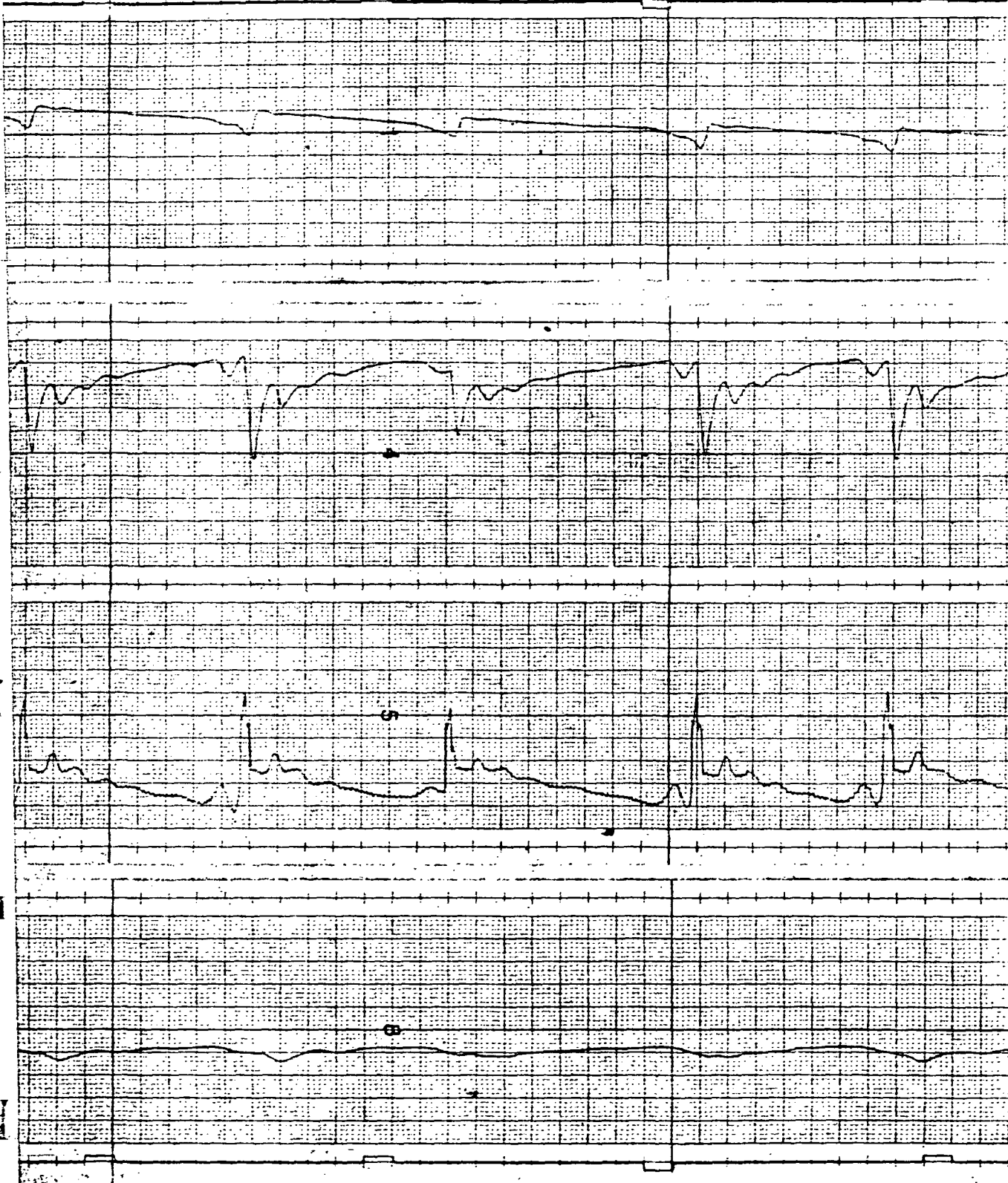


FOLDOUT FRAME 2

BRUSH INSTRUMENTS DIVISION, GOULD INC.

CLEVELAND, OHIO

PRINTED IN U.S.A.



FOLDOUT FRAME 3

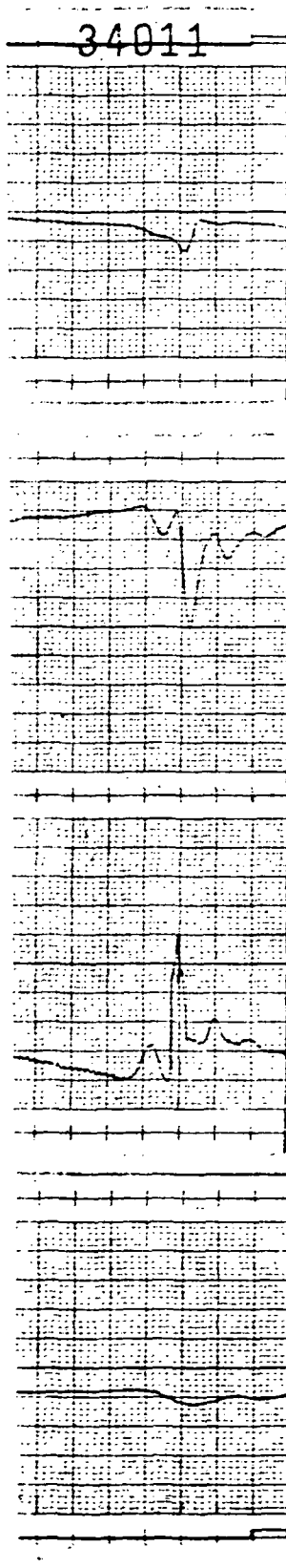
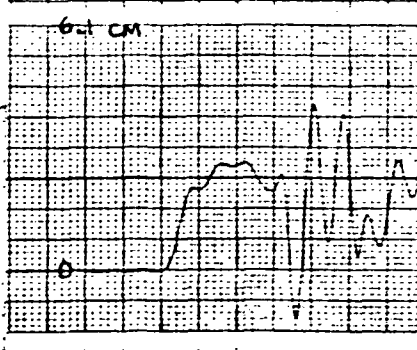
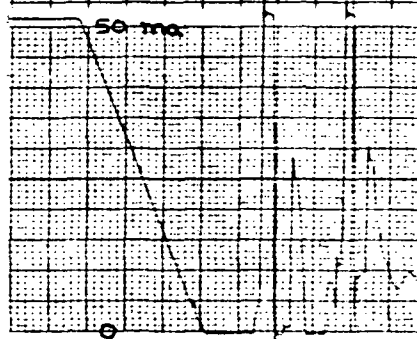
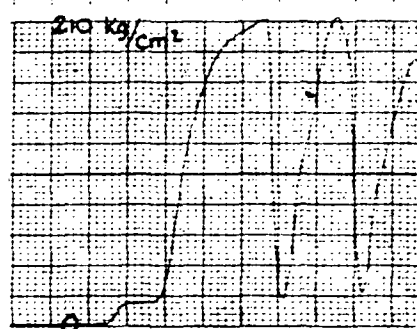
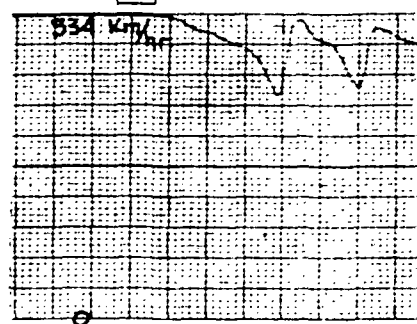


FIG. 56

.5 MU WITH 4.5 HZ STRUT
BENDIX SYSTEM

PRINTED IN U.S.A



18244

WHEEL VELOCITY

BRAKE PRESSURE

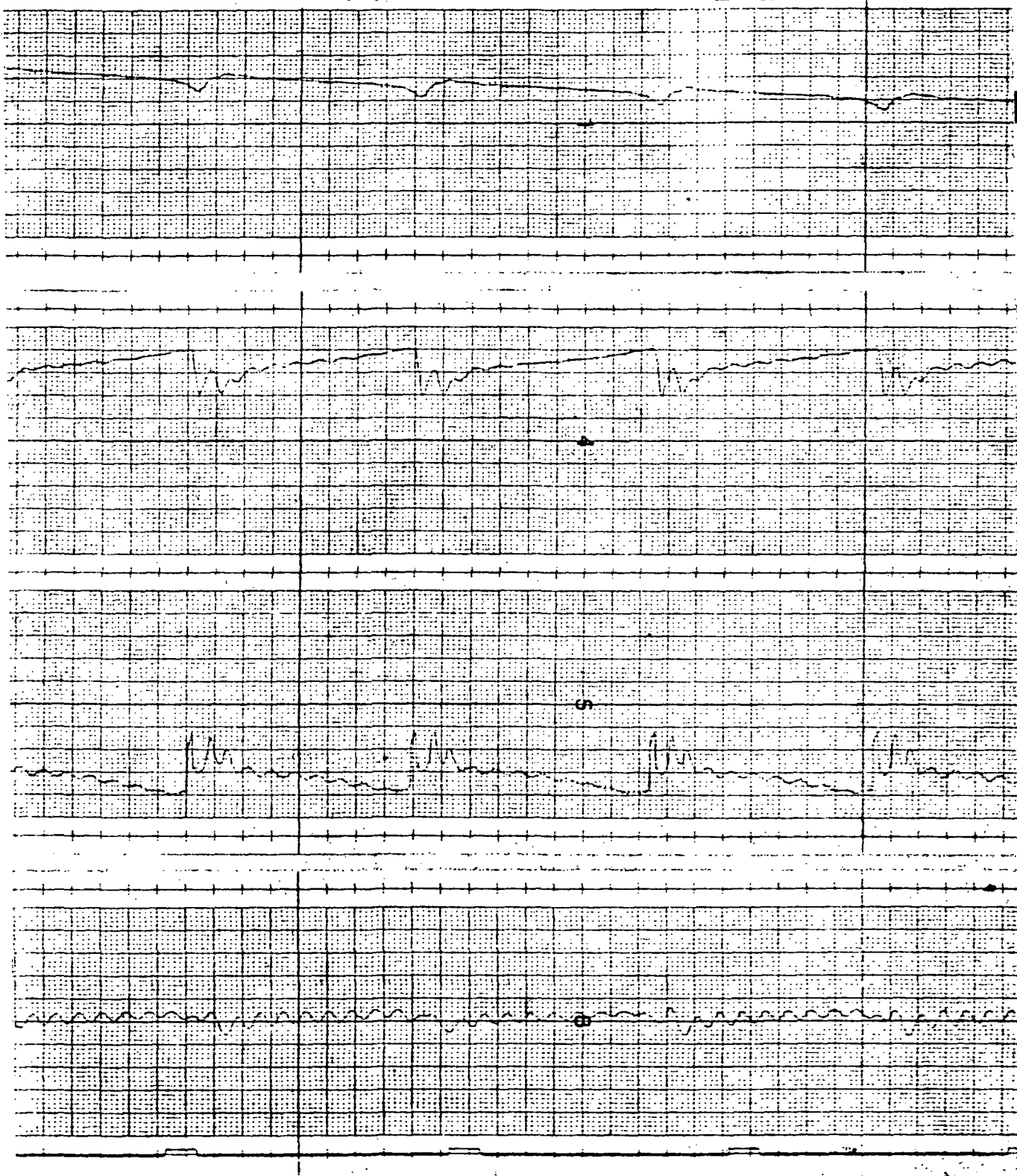
VALVE CURRENT

STRUT DEFLECTION

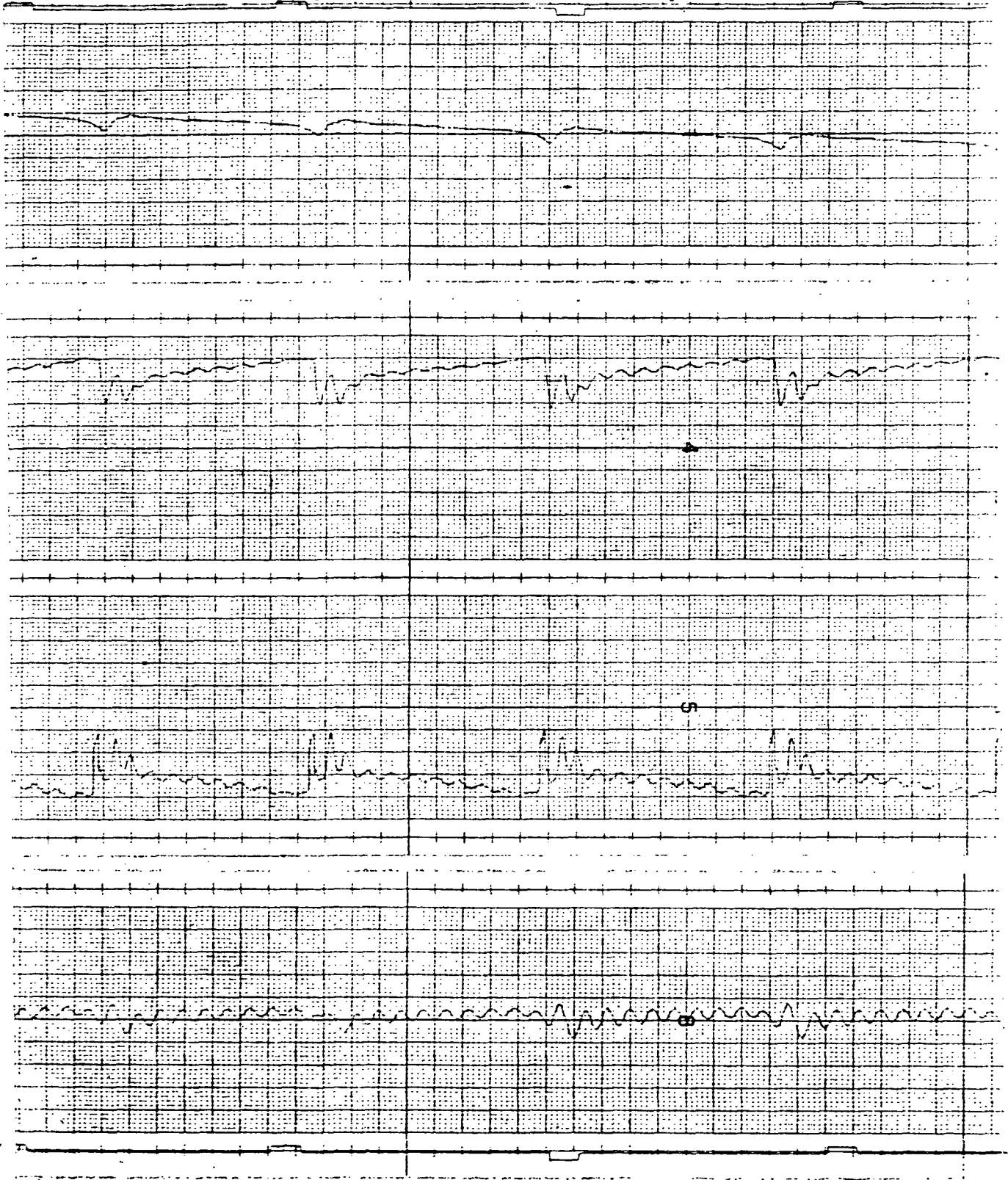
1.0 SEC.

FOLDOUT FRAME /

18245



FOLDOUT FRAME 2



FOLDOUT FRAME 3

OHIO

PRINTED IN U.S.A.

18246

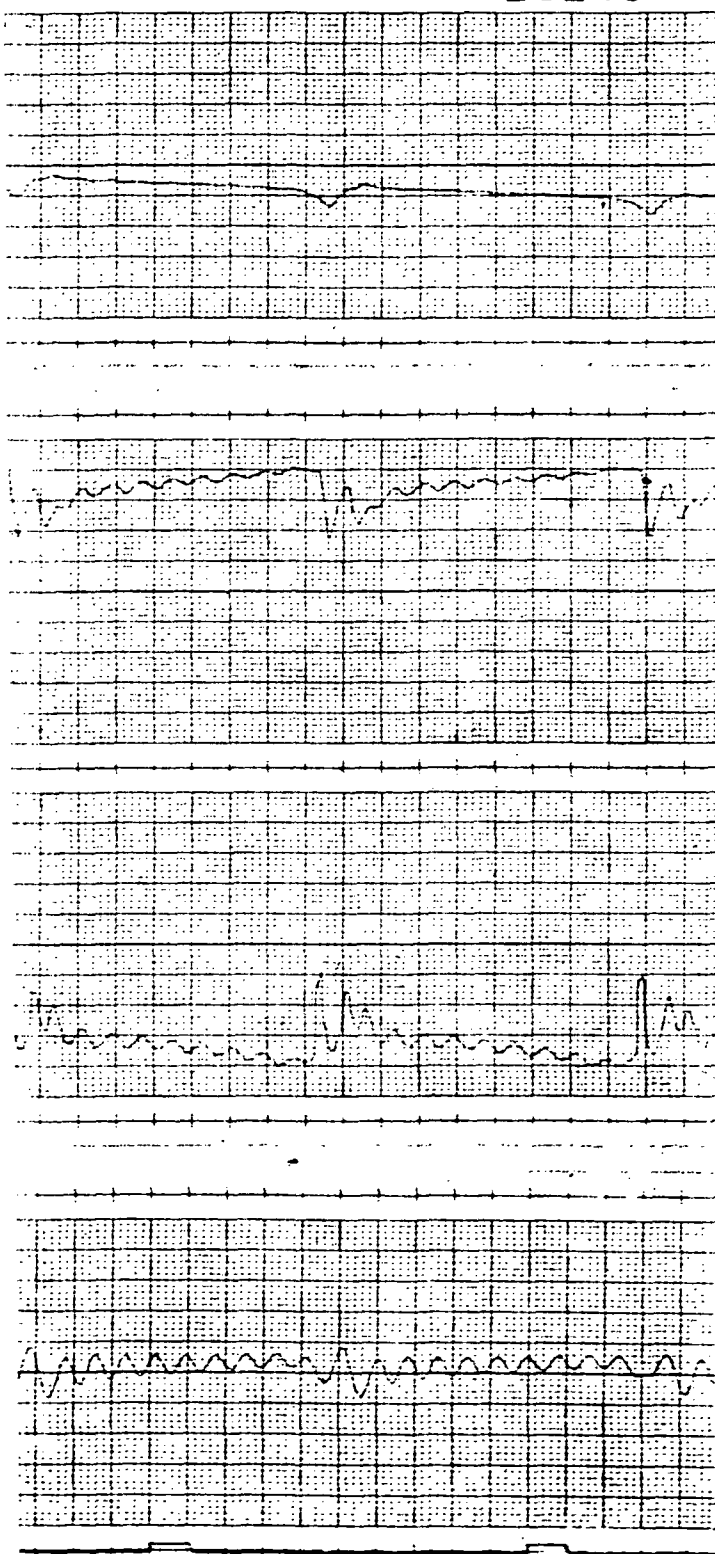
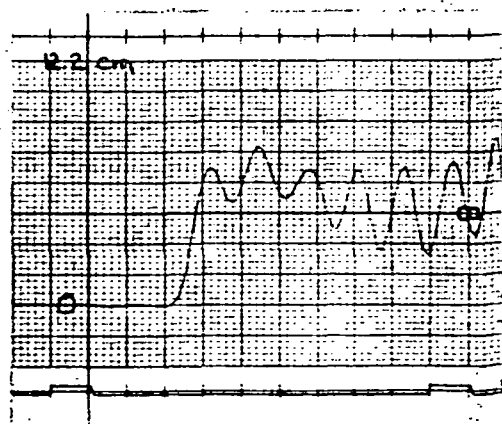
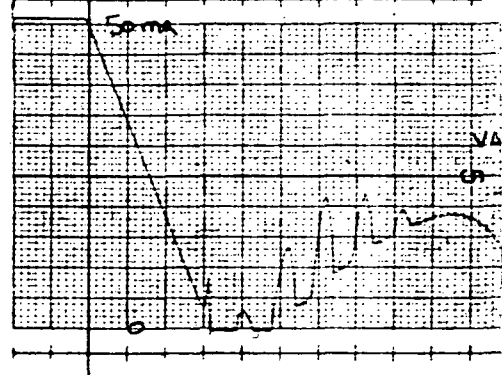
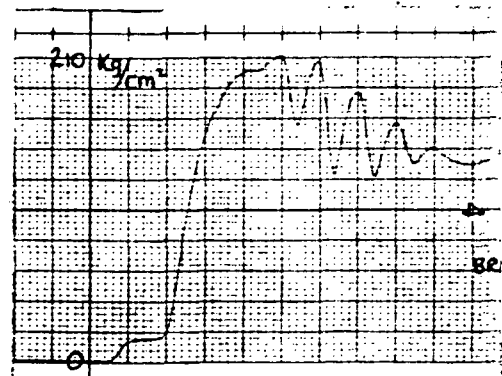
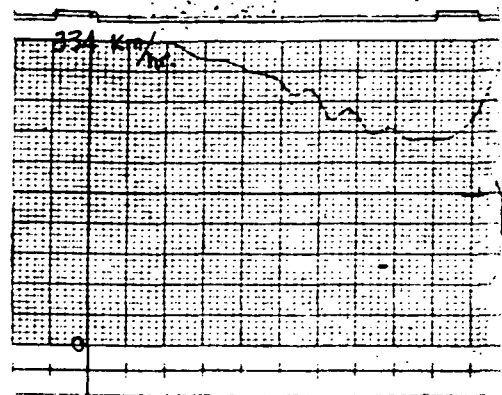


FIG. 57

.5 MU WITH 11.5 H₂ STRUT
BENDIX SYSTEM

FOLDOUT FRAME

133



18389

BRUSH INSTRUMENT

WHEEL VELOCITY

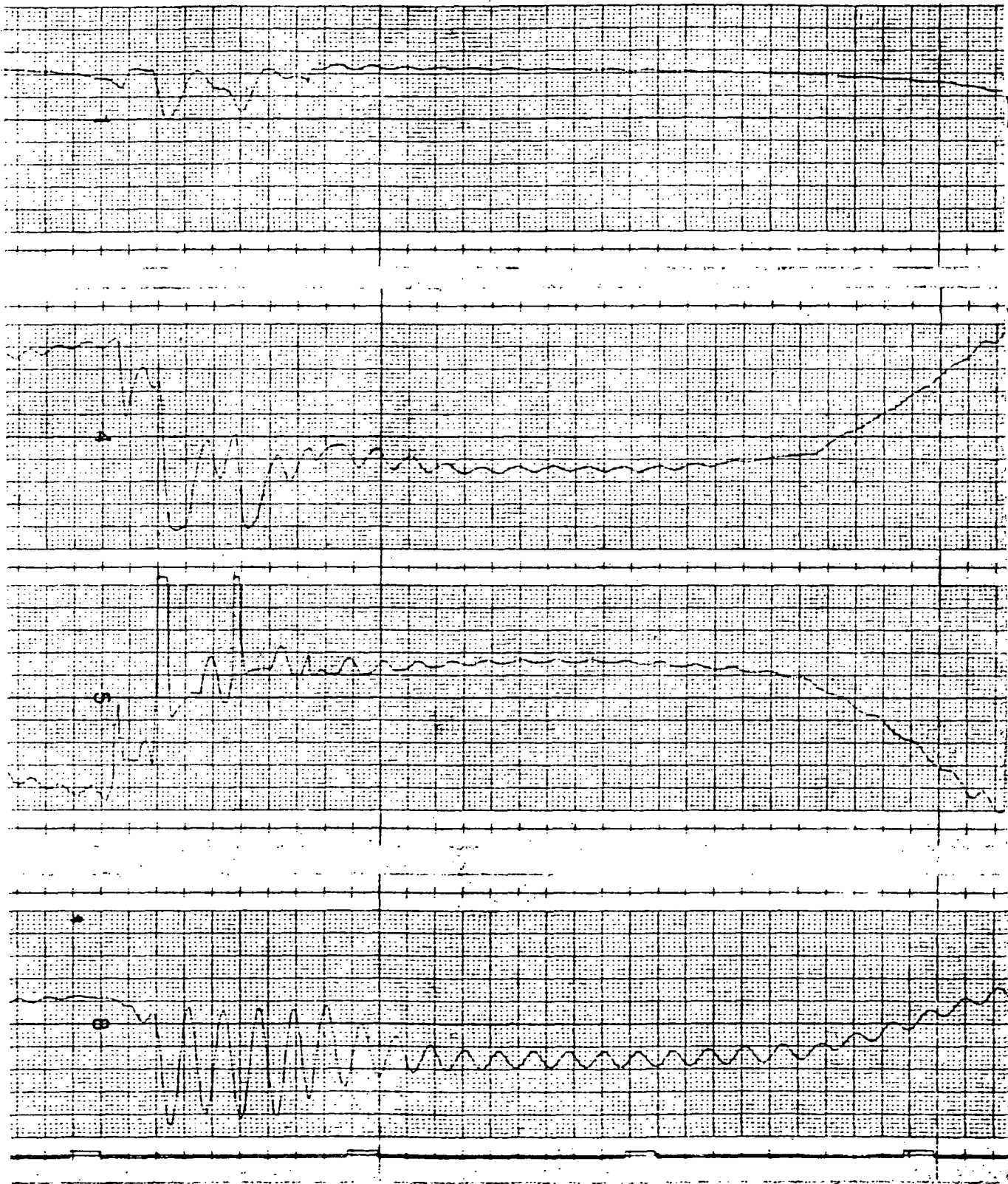
WHEEL PRESSURE

WHEEL CURRENT

STROUT DEFLECTION

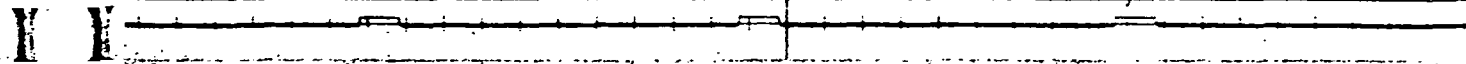
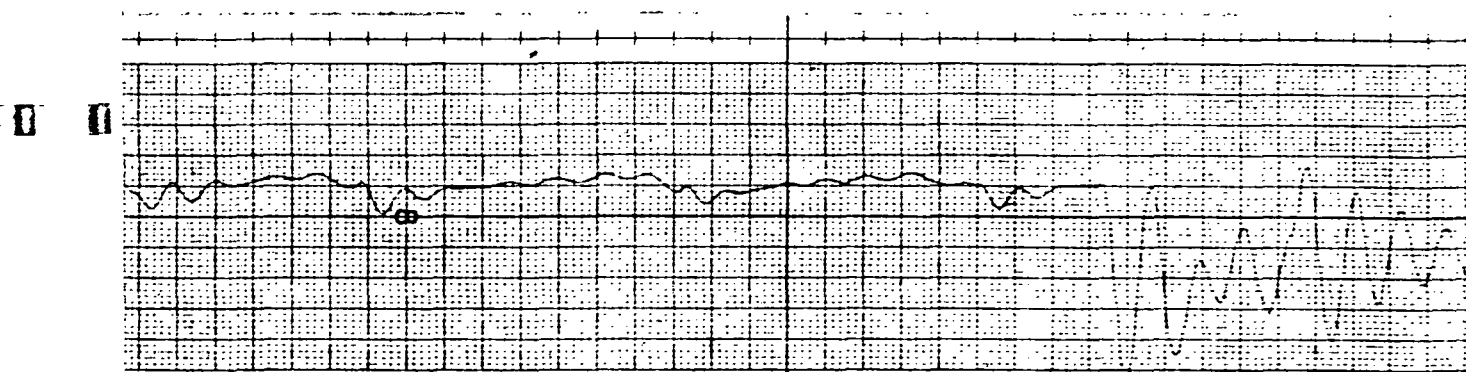
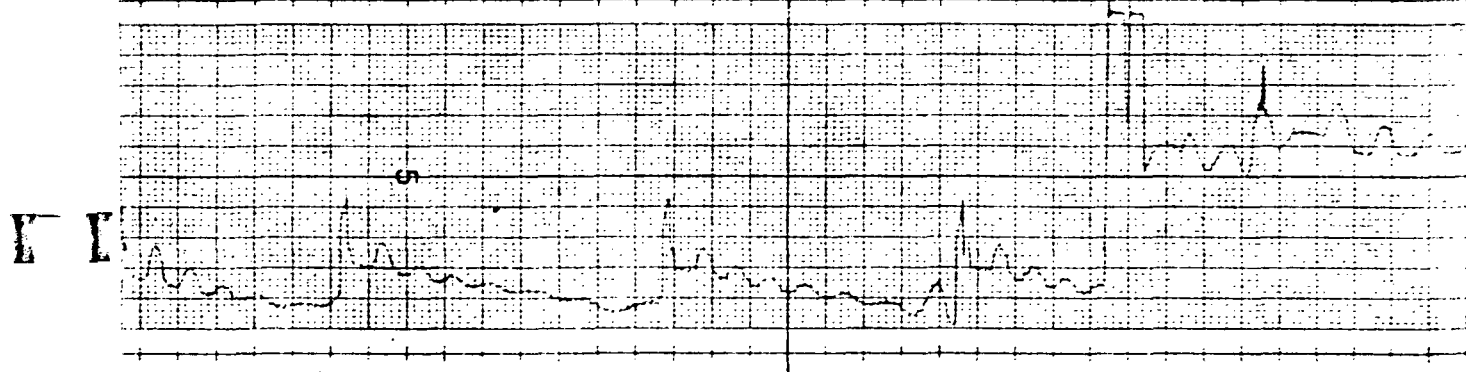
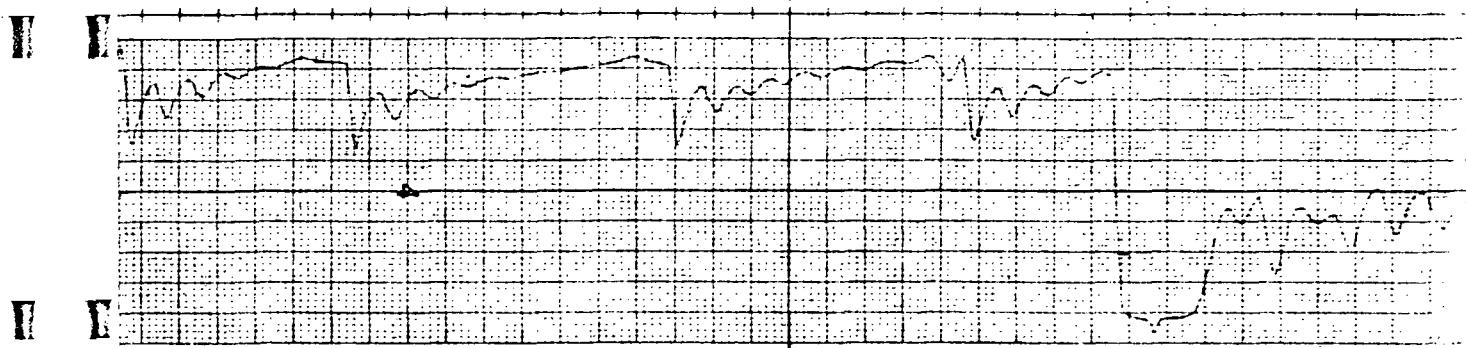
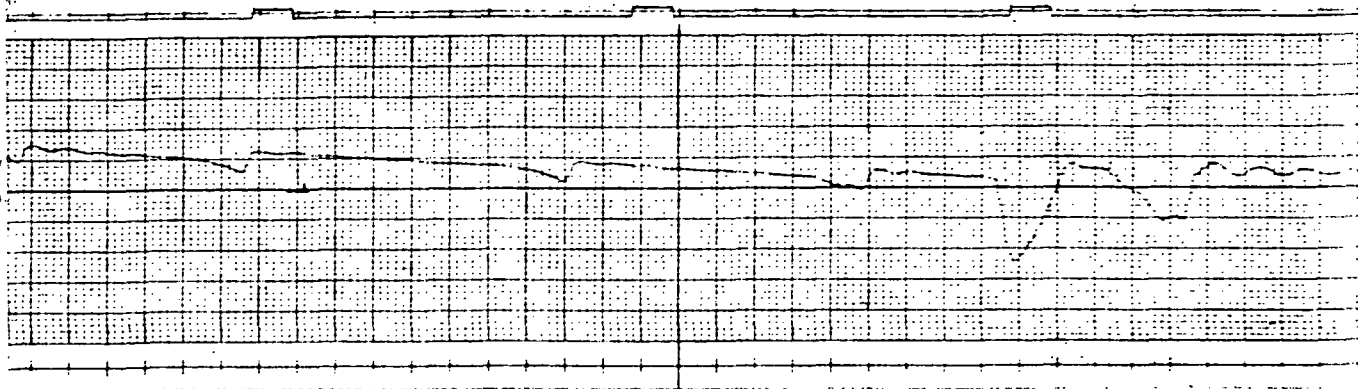
1.0 SEC

OLDOUT FRAME /



FOLDOUT FRAME

2



FOLDOUT FRAME 3

18391

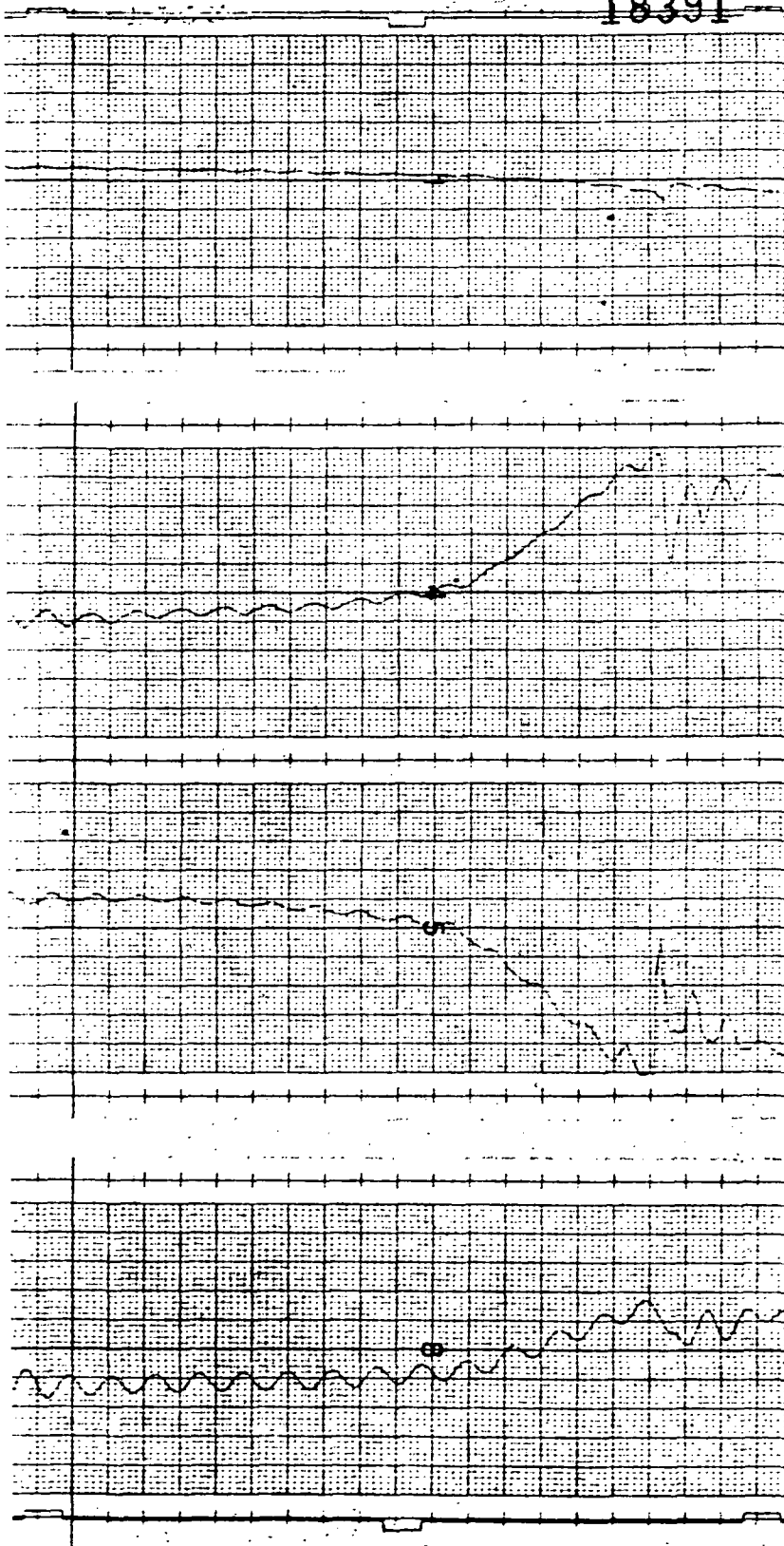
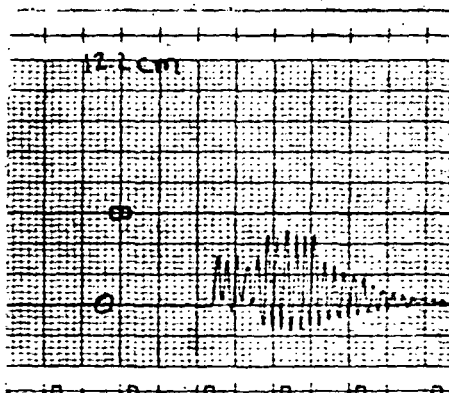
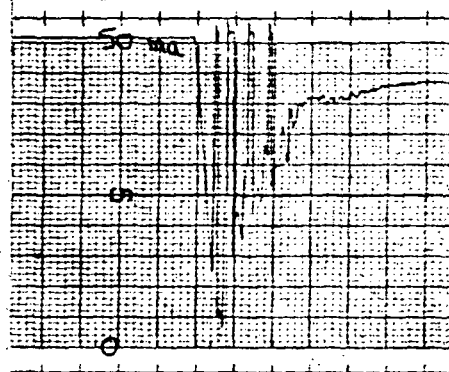
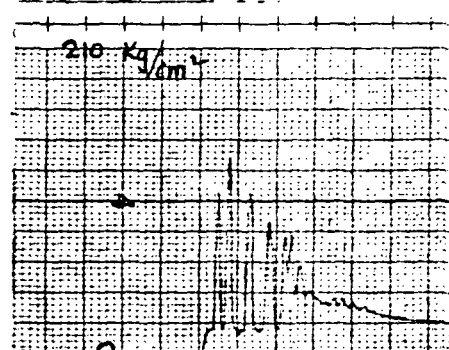
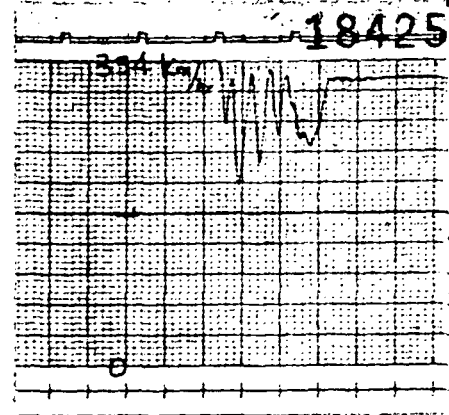


FIG. 58

MU STEPS WITH 7.5 HZ STRUT
BENDIX SYSTEM

FOLDOUT FRAME 4

18425



WHEEL VELOCITY

BRAKE PRESSURE

VALVE CURRENT

STRUT DEFLECTION

1 sec

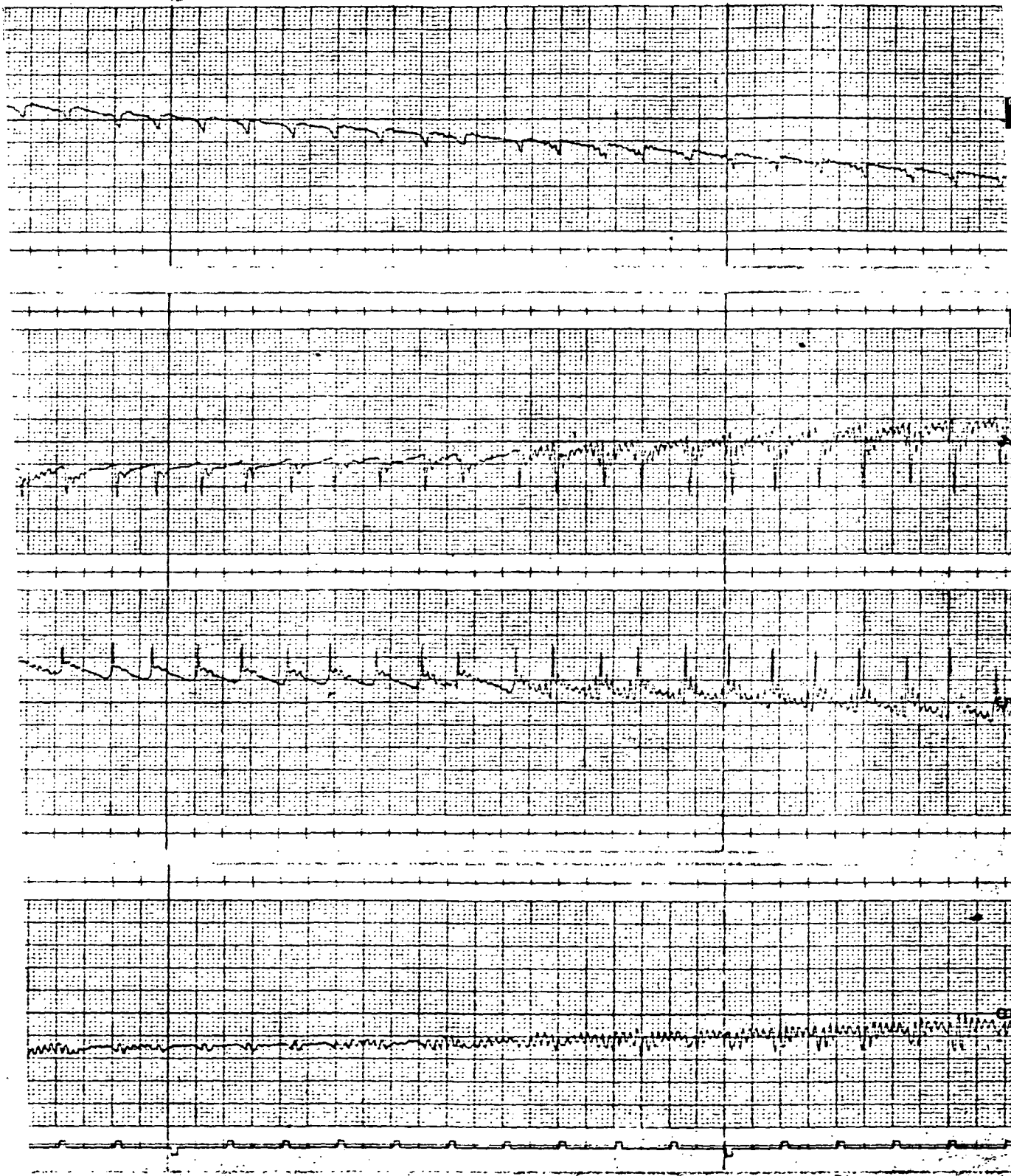
FOLDOUT FRAME

INC.

CLEVELAND, OHIO

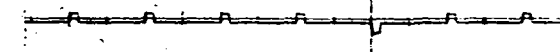
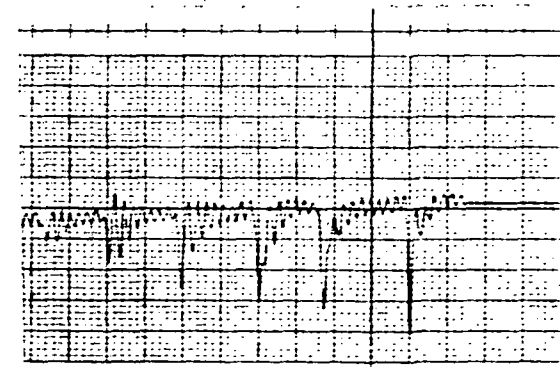
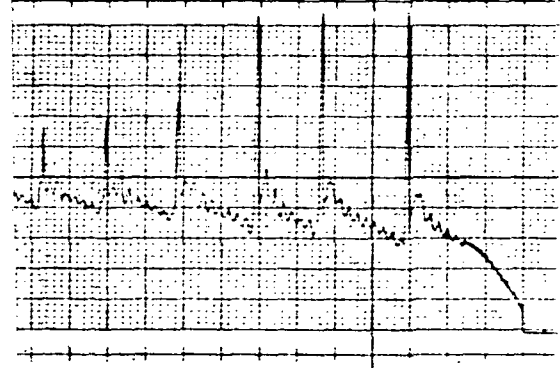
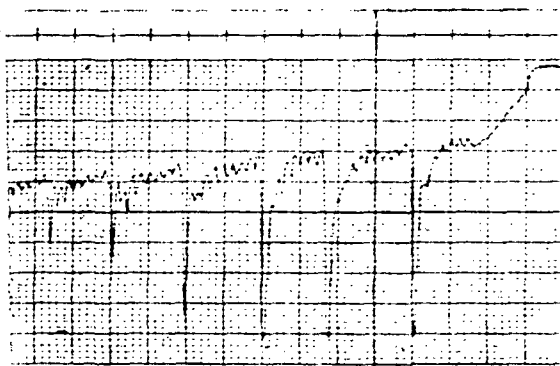
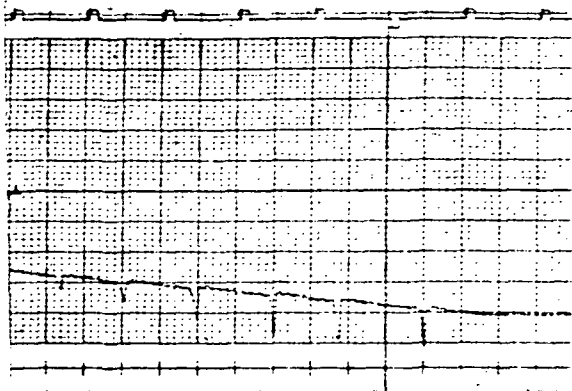
PRINTED IN U.S.A.

18426



FOLDOUT FRAME

2



FOLDOUT FRAME 3

FIG 59
WET RUNWAY CURVE 1 WITH
7.5 H₂ STRUT
BENDIX SYSTEM

135

FOLDOUT FRAME

4

runway the constantly changing μ also requires the system to further adapt. The skid sampling for this system is maintained constantly throughout the entire braking run, averaging 1.25 skids per second. Only those last few skids at the low velocity end of the braking run were complete lockups. The transition from the very low μ up to the higher μ 's for the Bendix system went smoothly. However, the poor start up characteristics and somewhat inefficient very low μ control left the overall performance down from what it might have been.

Stability considerations on the Bendix system were truly excellent. This system used both a notch filter (the attenuation notch is "tuned" in each case to the natural gear frequency) and a derivative lead control. Together these provide system damping to the brake control loop which in all cases actively damps the gear oscillations. Table VI shows that the Bendix stability was better overall with the exception of the 7.5 and 11.5 Hz gear stability of the Boeing Closed Loop system.

Figure 60 represents the .5 μ dry runway test with the 4.5 Hz gear and the Boeing Closed Loop system. Pressure was brought on with the 300 ms valve signal ramp and when the pressure reached 196 kg/cm^2 (2800 lbs/in^2) a skid was precipitated. The system responded quickly enough to where the wheel only went into a 12 percent slip on the first skid. It immediately adapted to the dry μ condition and proceeded with continuous control. In this particular test case where the strut frequency was 4.5 Hz the system did not exhibit very good stability. There are two reasons why this happened. First during the higher velocity part of the braking run the skid sampling rate was quite high, 2.5 cycles per second. It can be easily seen how this sampling rate could tend to excite the strut. The second problem deals with the skid detector scheme this system uses to control deep skids. (See Section III description of the Boeing Closed Loop system). Once the skid detector rate and velocity limits were exceeded the skid detector released all brake pressure immediately and also initialized the modulator to a very high level (low brake pressure). Once the level

was reached the modulator decay rate dictated the pressure reapplication rate. Although this rate was $53.2 \text{ kg/cm}^2/\text{sec}$ ($760 \text{ lbs/in}^2/\text{sec}$) the pressure started out at such a low level that it took three full seconds before another skid occurred. While the pressure was reduced the strut abruptly relaxed and oscillated. If the skid detector initialization did not leave the modulator at such a high level, the strut would remain more evenly and smoothly deflected, thus aiding the strut stability. Thus the system stability at this strut frequency was really deficient. The necessary inherent strut damping required even to make this system marginally stable was nearly as much as the other two systems needed to make them stable enough to complete the tests. (See Table VI for comparisons of damping ratios).

Performance at the beginning and the entire high speed end of the run was extremely good, but deteriorated rapidly at the low velocity end. Primarily the reason for this was the skid detector and its high modulation effect on the brake pressure. There was also a tendency for this system to lockup below the velocity of 37 km/hr (20 knots).

The next test shown in Figure 61 was also with a dry runway, .5 mu but with the gear frequency of 11.5 Hz. In this run the system stability and performance was extremely good. Again the low velocity end was hampered by the skid detector and the tendency to lockup at the end of the run.

The two final skids of this braking run made an effective contrast. Pressure reapplication after the next to the last skid helped to begin strut deflection and although there was strut oscillations the system was able to actively damp them. Contrast this to the last lockup skid where the system was unable to properly remove pressure with the net result the wheel locked up, never to recover. The strut oscillations were not large in magnitude, but the damping was effected because the last skid was a lock

up. The damping was considerably diminished because full lockup tire damping is negligible compared to the damping available on the stable front side of the tire-to-ground friction characteristics. This lockup condition also prevented the skid control system from any active damping role. Any strut damping that was exhibited must therefore be inherent in the strut structure.

Figure 62 represents the dry runway step mu tests. Only the first two steps are shown of the four that occurred during the tests. Before the first step mu change the Boeing Closed Loop system performed normally for a .54 mu dry runway condition. The pressure was brought on by the 300 ms valve signal ramp and as soon as the brake pressure rose to 203 kg/cm^2 (2900 lbs/in^2) the first skid occurred. It was a very shallow skid and the system adapted after it to maintain continuous highly efficient control. This continued for the first 4.5 seconds until the first step mu occurred. Once the mu dropped to .16 value the wheel decelerated into a 59% slip skid and the skid lasted 150 ms. Each low mu condition lasted approximately 600 ms but the Boeing Closed Loop system reduced pressure so completely during this skid that the brake pressure momentarily drained the brake, lowering the brake pressure to reservoir pressure. This meant a further delay in getting pressure re-applied and so the pressure did not even reach skidding pressure for the .16 mu condition before it went away. Once the mu switched back to .54 mu level the brake pressure was just that much more below skidding pressure. From the time the mu switched back to .54 until the system reached skidding pressure was 4.8 seconds.

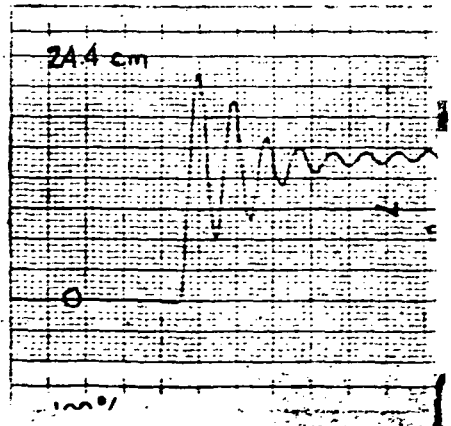
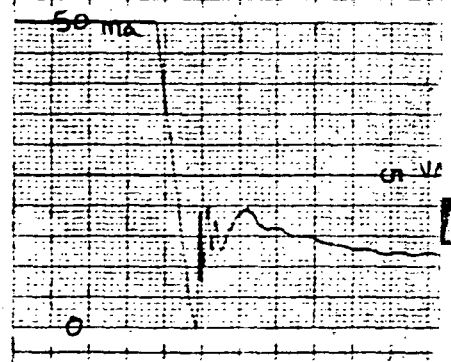
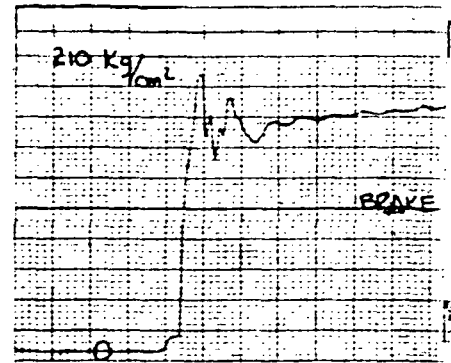
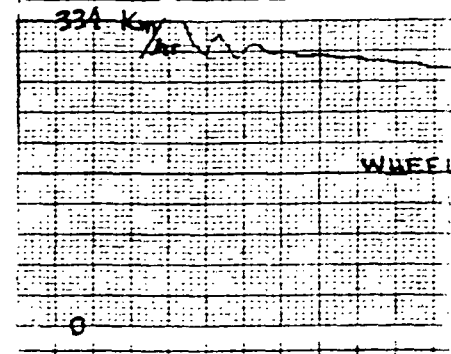
This situation caused a great reduction in efficiency since the brake pressure was low at the start of this period and had to gradually increase. The reason for this very poor adaptability centered around the skid detector and its initialization effect on the closed loop modulator. Much the same situation existed every time a deep skid occurred during low velocity. The system's response to the sudden drop in mu to .16 was adequate to prevent the wheel

from locking up but could still use some improvement. In other words, looking at the valve signal shows that it hesitated for nearly 100 ms before the complete full release signal was present. However, the real deficiency in the system was its inability to adapt to changing conditions. Once the skid detector initialized the modulator to a high value, it then had to decay at a fixed rate. This same situation occurred no matter what the runway conditions were.

To verify this lack of ability to adapt to conditions the next step mu change provided the needed evidence. This time when the mu suddenly stepped down to .16 the wheel dropped into a 78 percent slip skid that lasted for 350 ms. During the remainder of the .16 low mu period the system did not regain skidding pressure before the mu again switched back to .54 level. From that point until skidding pressure was regained took 4.4 seconds. This was nearly the same amount of recovery time that the system took during and after the first mu step. This inability to adapt quickly to sudden changes in mu not only hurt the system's efficiency but it also degenerated its ability to actively damp the strut oscillations. As long as brake pressure was kept below the brake retractor spring pressure the torque was negligible and therefore the system was not actively in the wheel speed loop and could not exert any control over the strut oscillations.

Not shown is the remaining two mu steps. The third step caused the wheel to go into an 84 percent slip which remained 300 ms. It took 3.9 seconds for the brake pressure to regain skidding level. The fourth step mu occurred just after a normal low velocity skid took place and the pressure was already moderated considerably. This meant that when the wheel went into the .16 mu skid, the system was already operating at a low pressure level so the low mu skid was responded to more rapidly. The skid was only a depth of 57 percent slip instead of a complete lockup that was expected. Since the skid was caught earlier in its deceleration, the skid depth and width was much lower. Not as much pressure was released to control the skid so that the

BRUSH INSTRUMENTS DIVISION.



GOULD INC.

CLEVELAND, OHIO

PRINTED IN U.S.A.

33615

VELOCITY

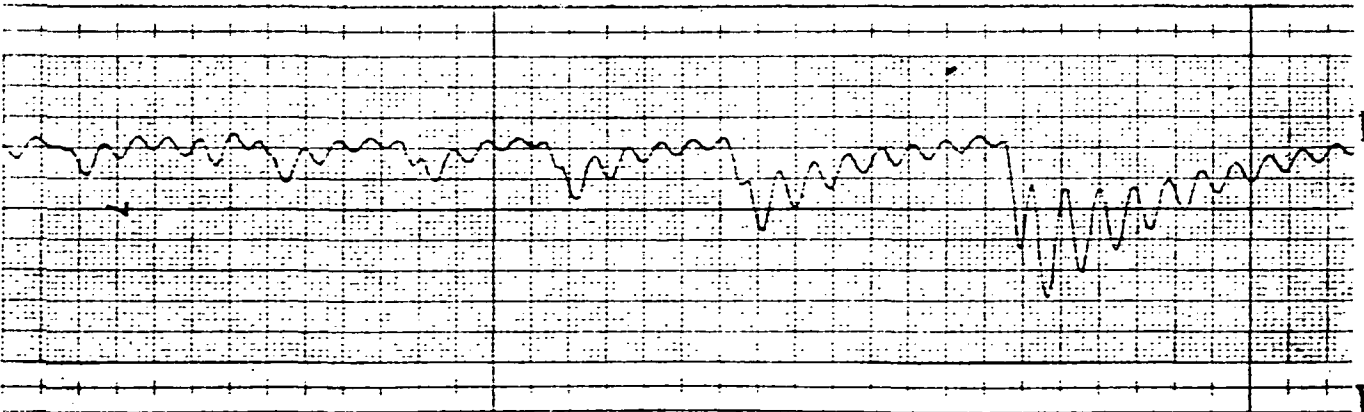
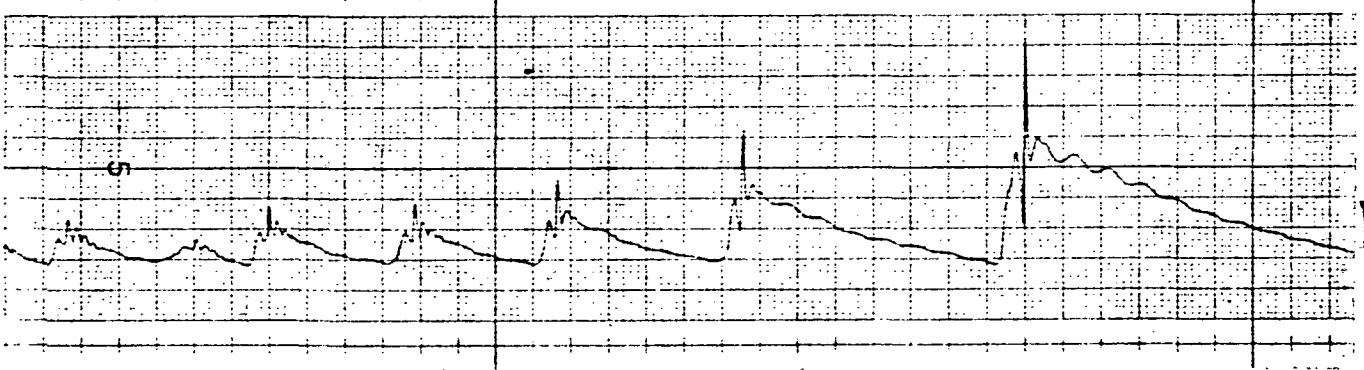
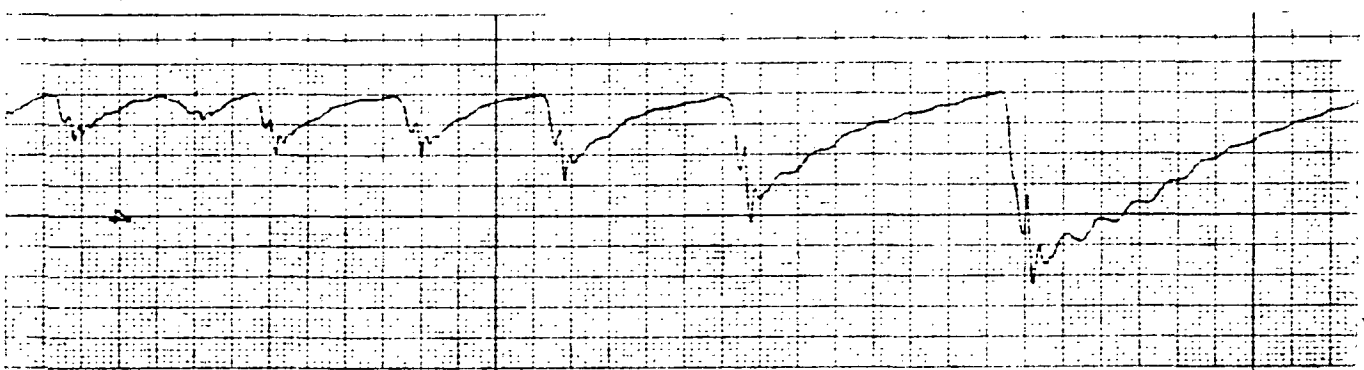
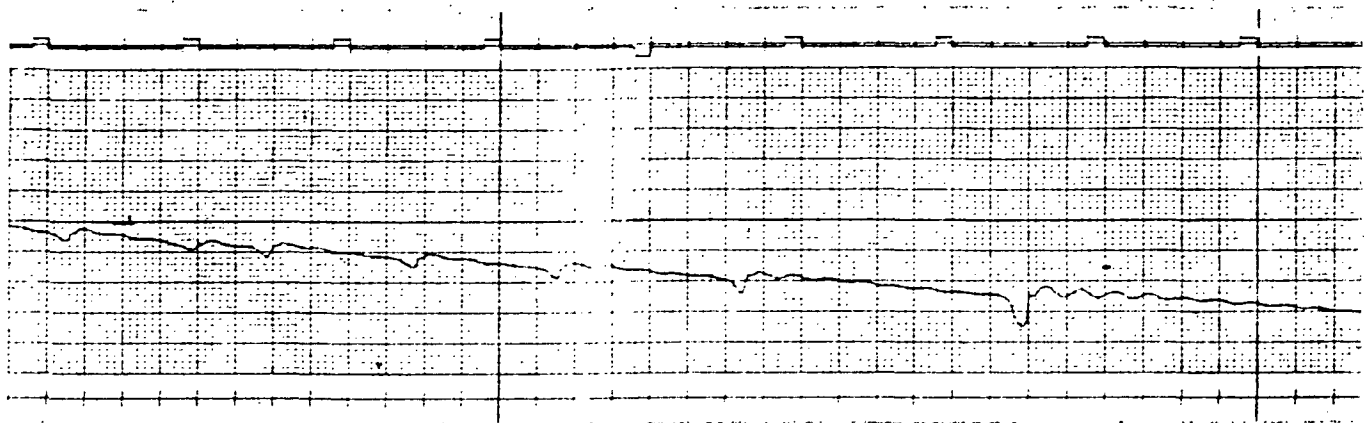
PRESSURE

LIVE CURRENT

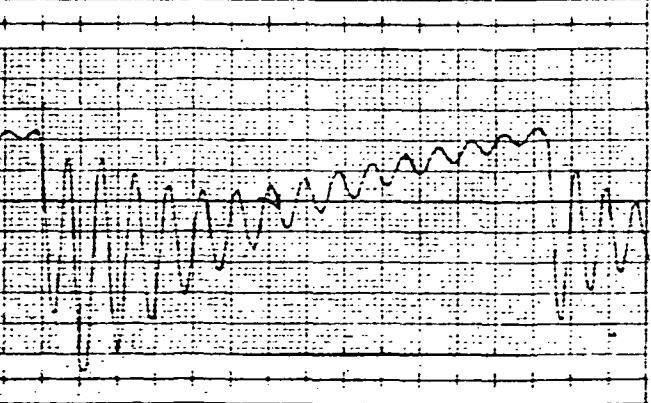
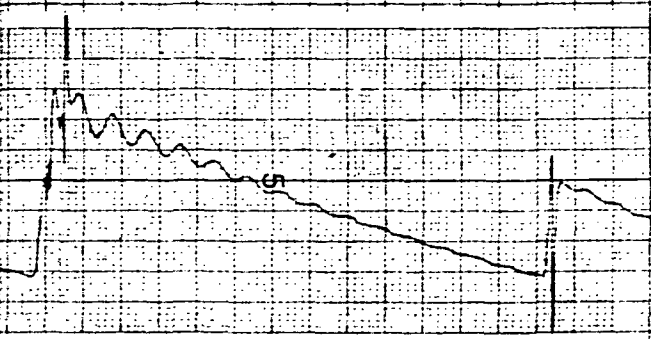
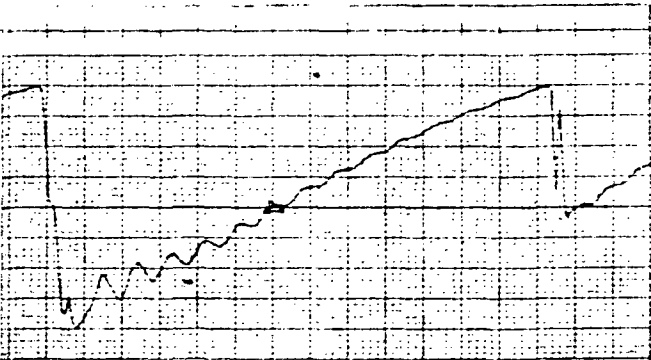
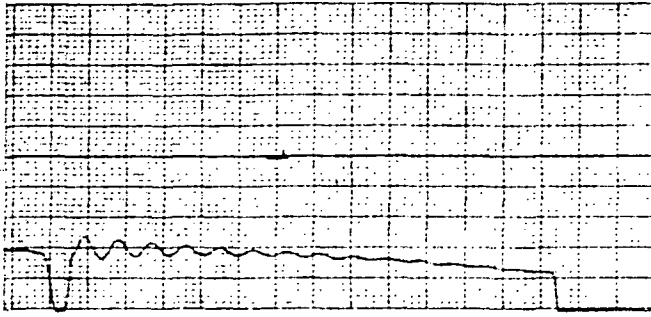
STRUT DEFLECTION

10 sec.

FOLDOUT FRAME



33616

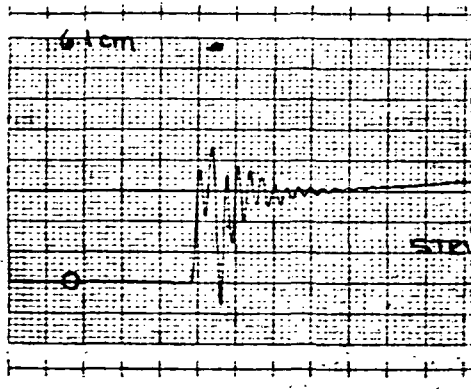
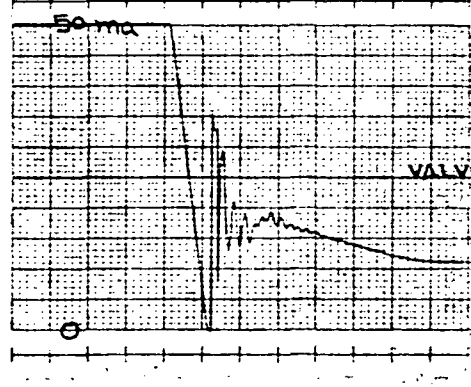
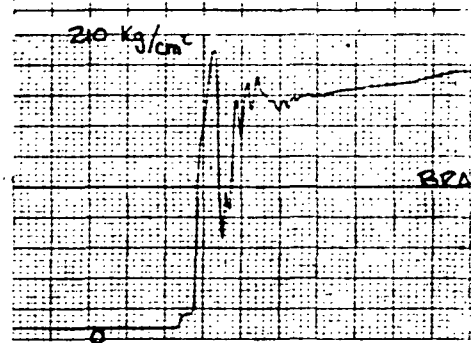
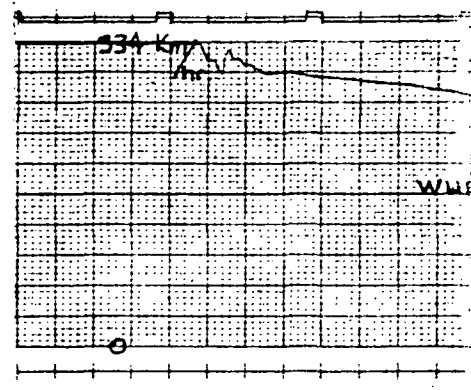


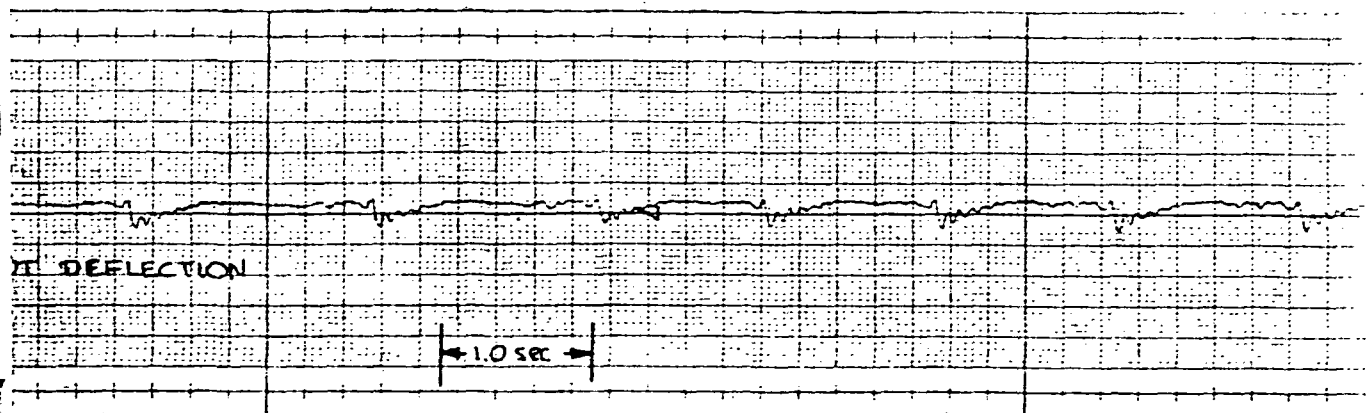
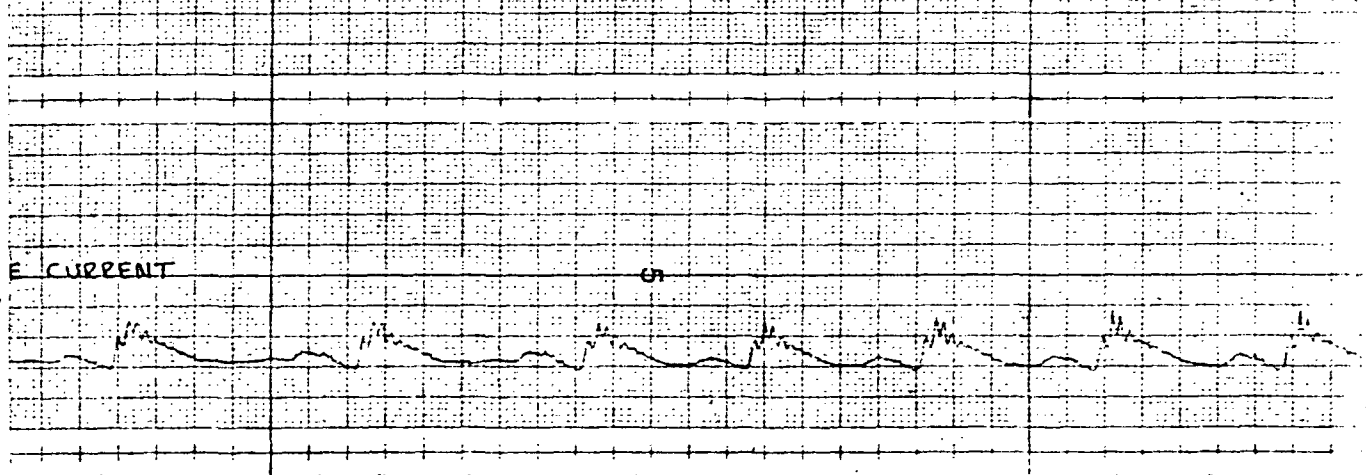
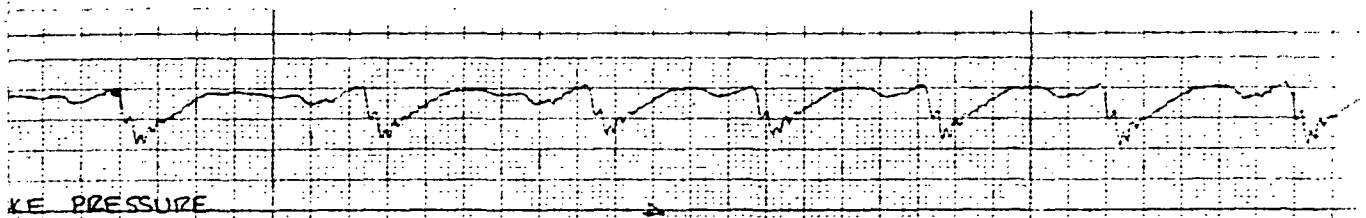
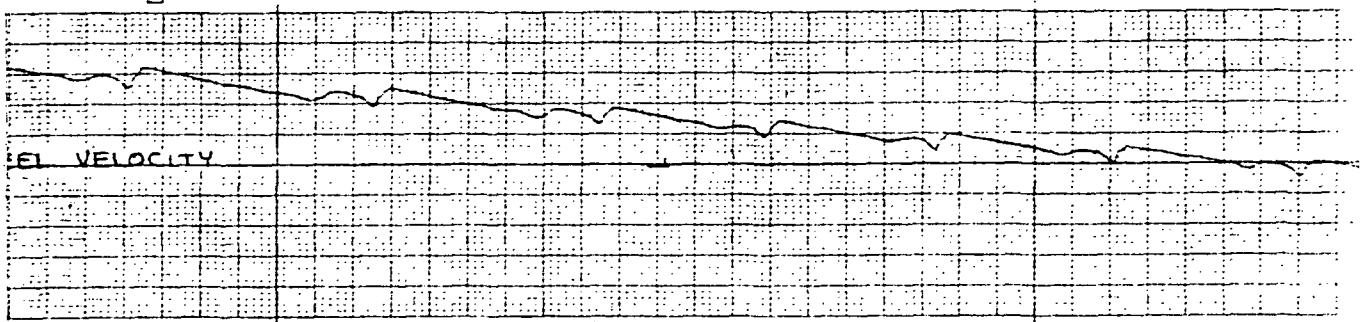
FOLDOUT FRAME 3

FIG. 60
.5 MU WITH 4.5 HZ STRUT
BOEING CLOSED LOOP SYSTEM

140

FOLDOUT FRAME 4

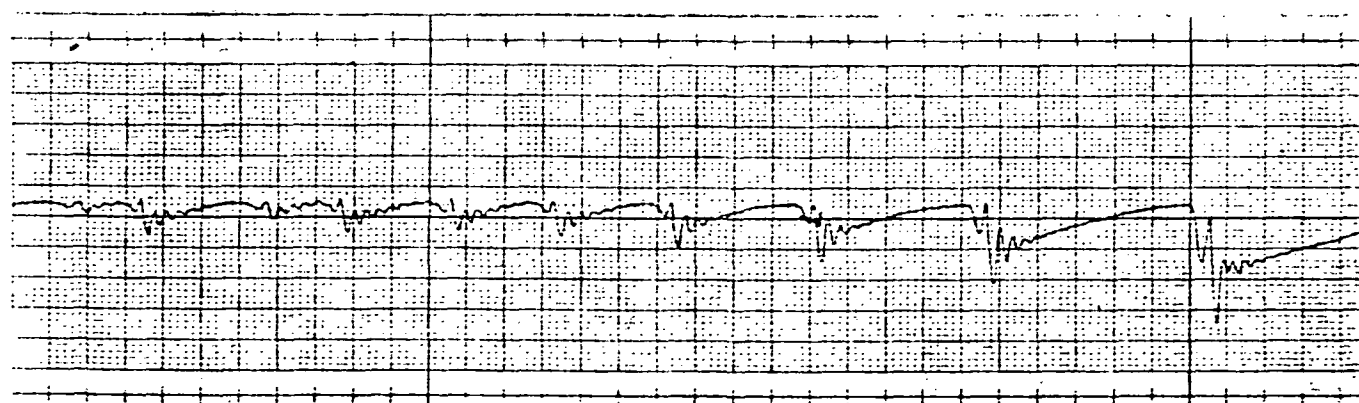
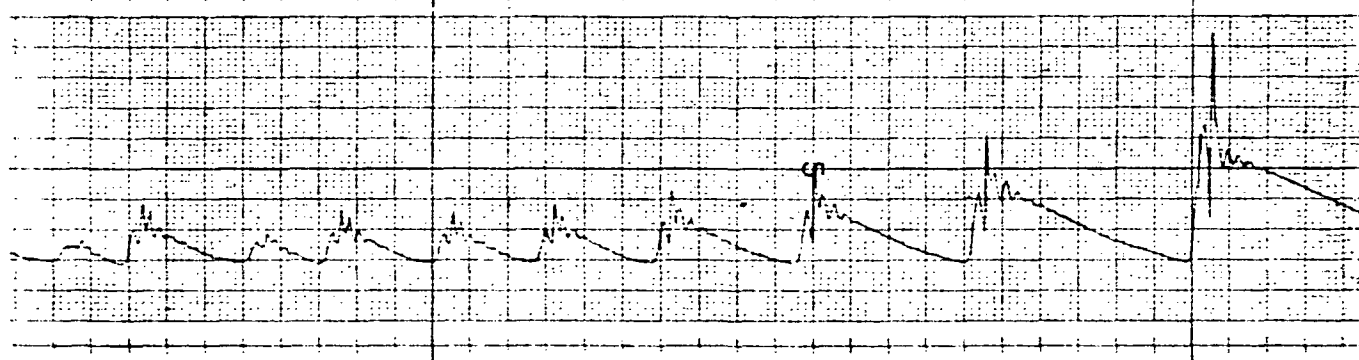
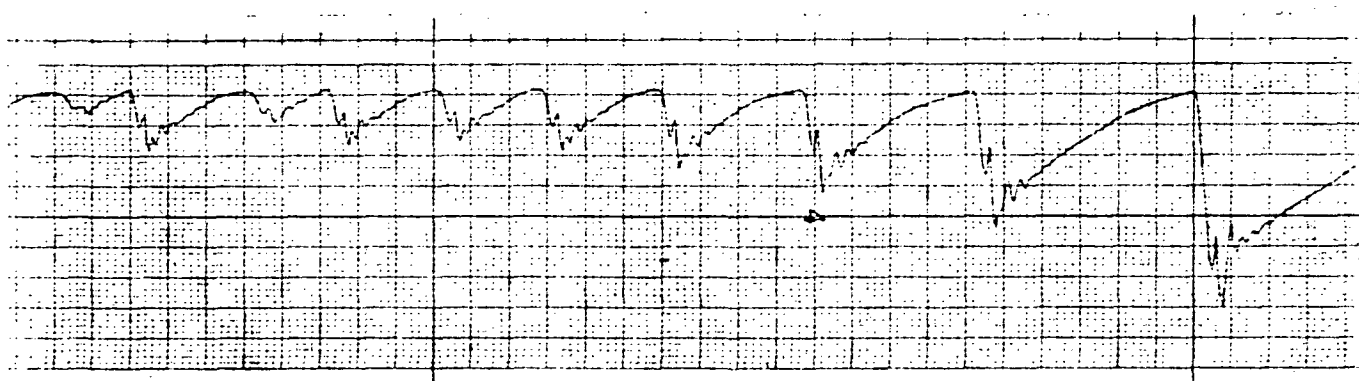
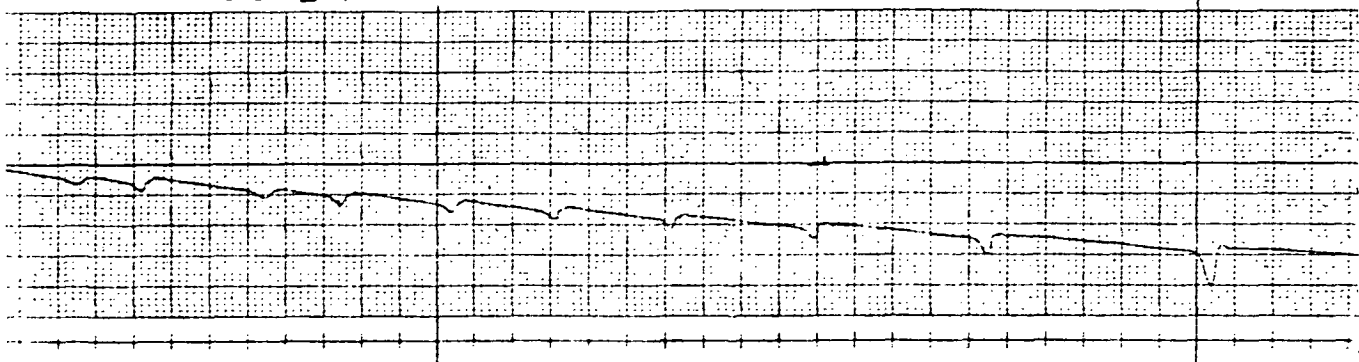




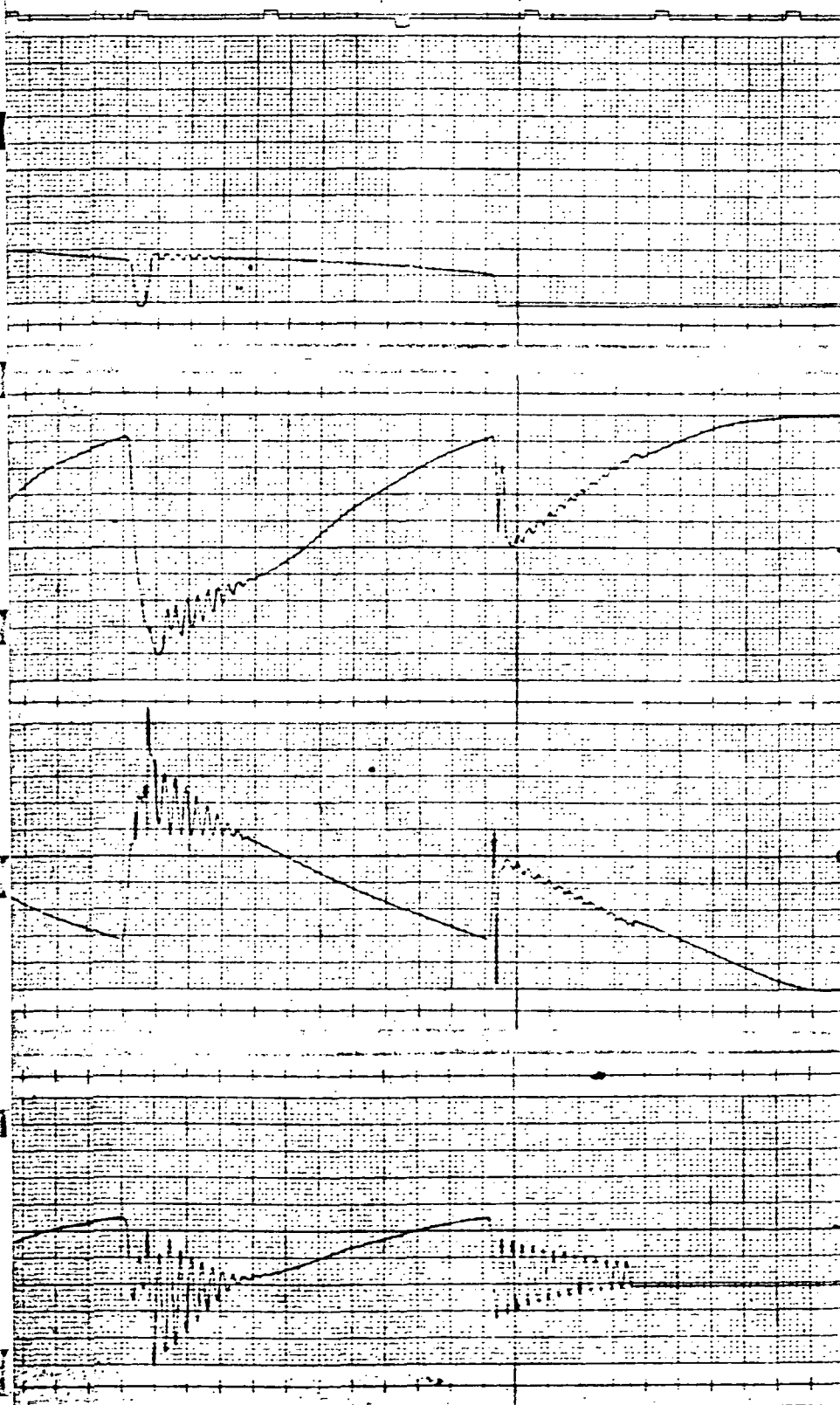
FOLDOUT FRAME /

1A

33667



FOLDOUT FRAME 2



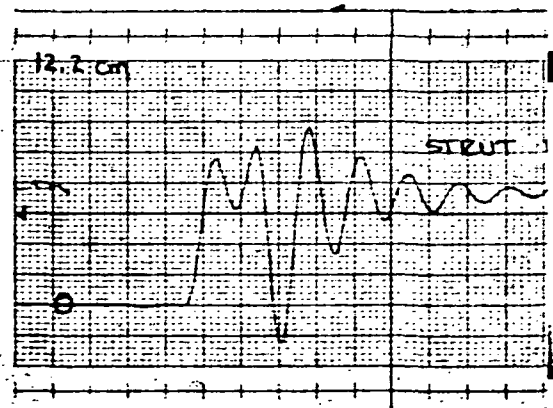
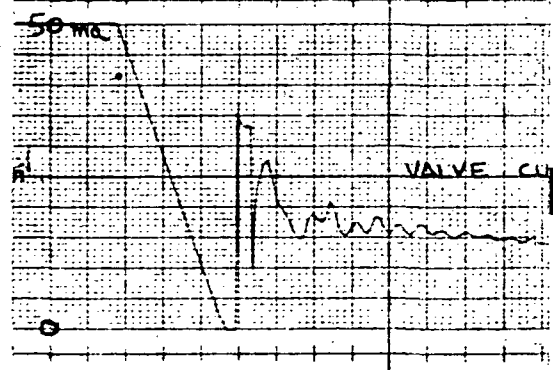
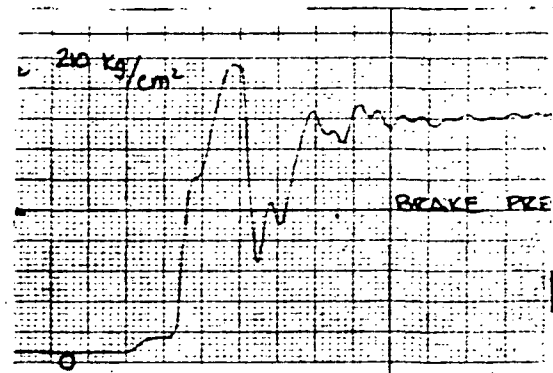
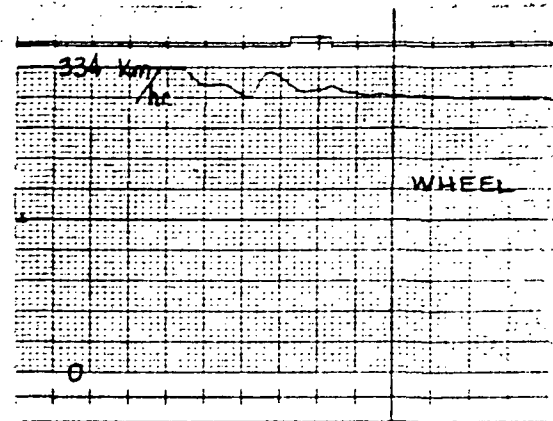
FOLDOUT FRAME

3

• FIG. 61
.5 MU WITH 11.5 HZ STRET
BOEING CLOSED LOOP SYSTEM

141

FOLDOUT FRAME 4



33766

VELOCITY

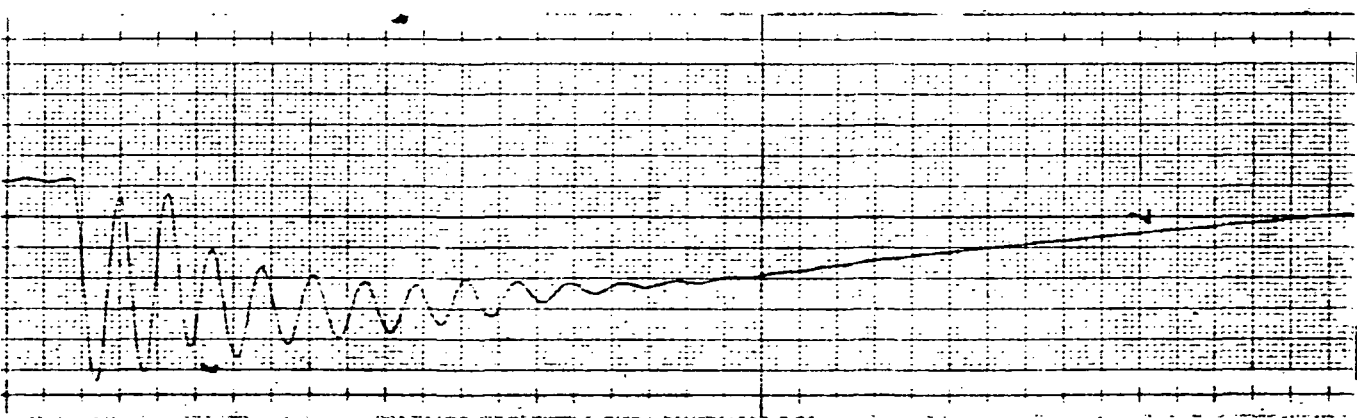
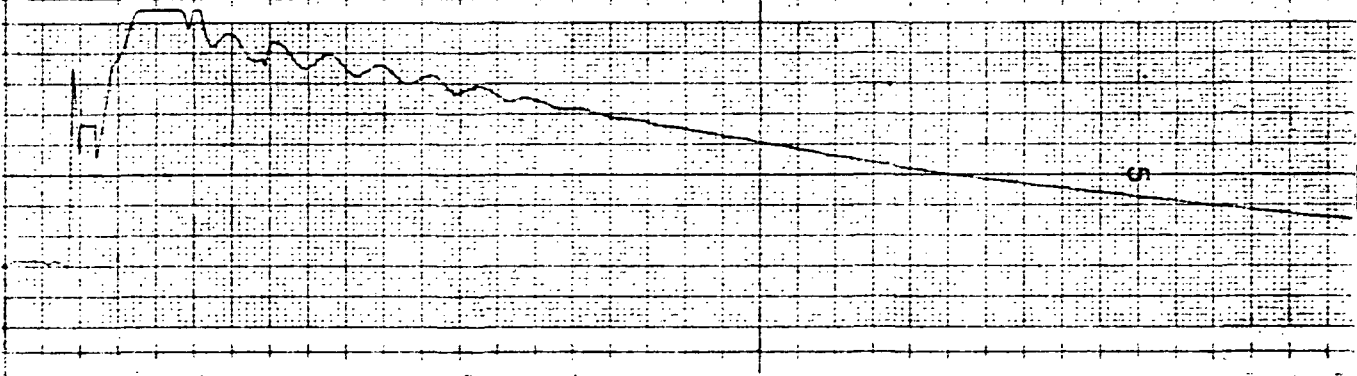
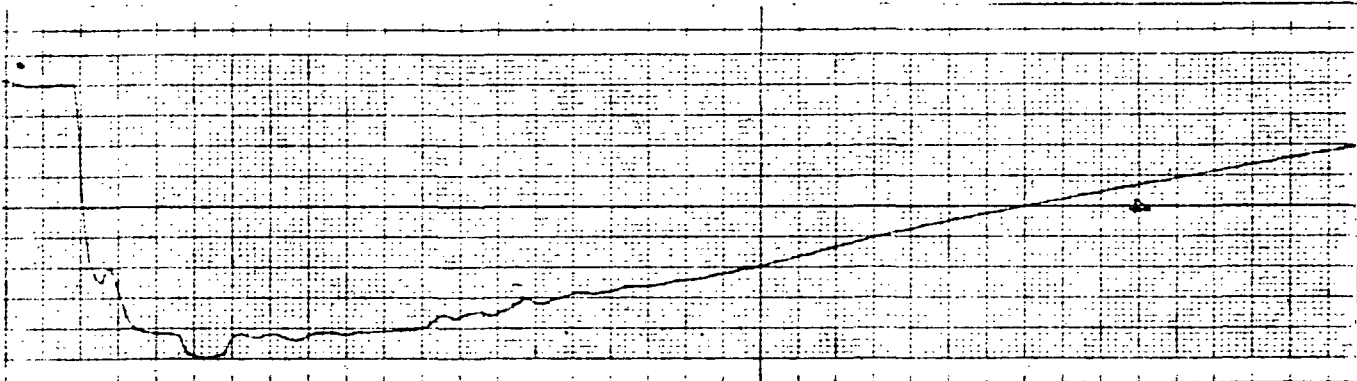
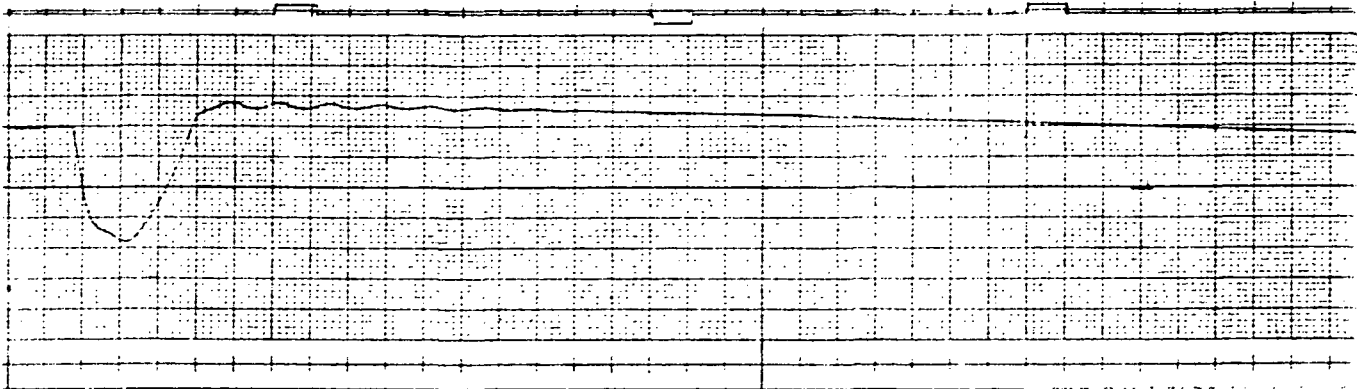
SSURE

URRENT

DEFLECTION

1.0 sec

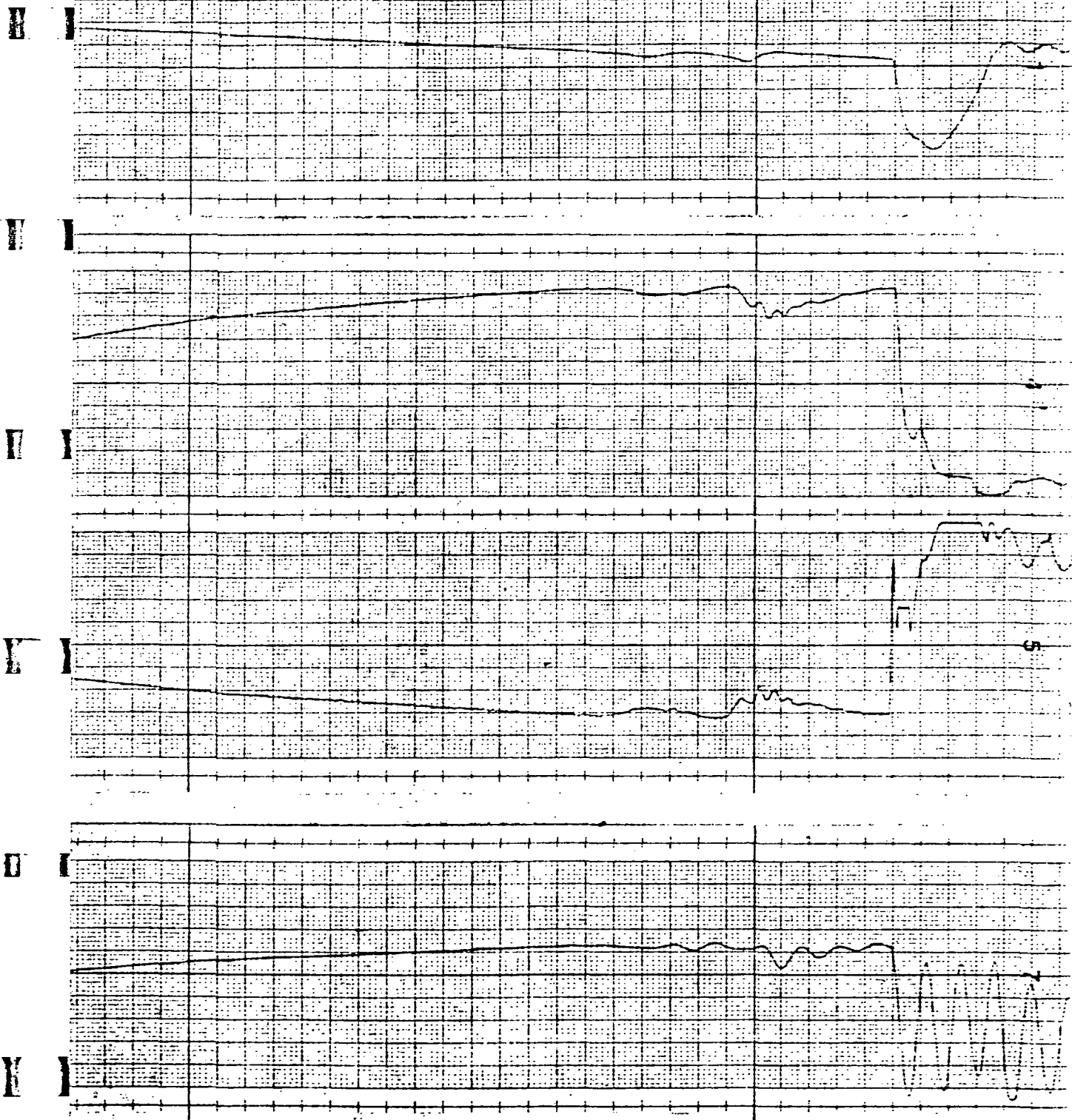
FOLDOUT FRAME /



CLEVELAND, OHIO

PRINTED IN U.S.A.

33767



FOLDOUT FRAME

3

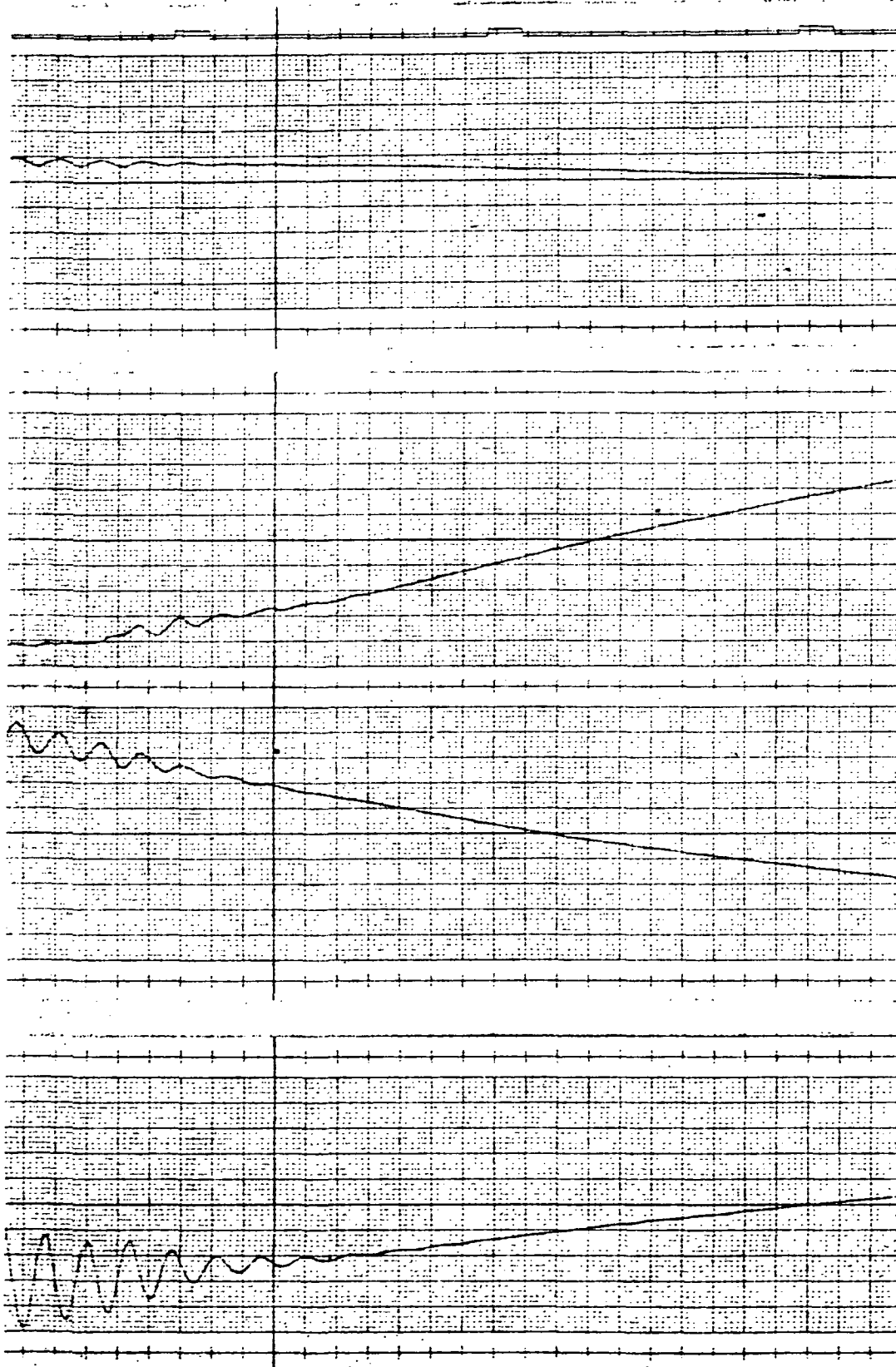
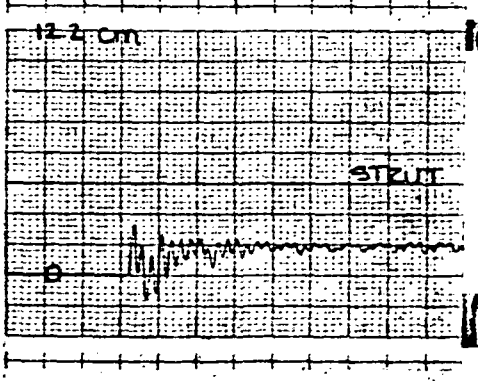
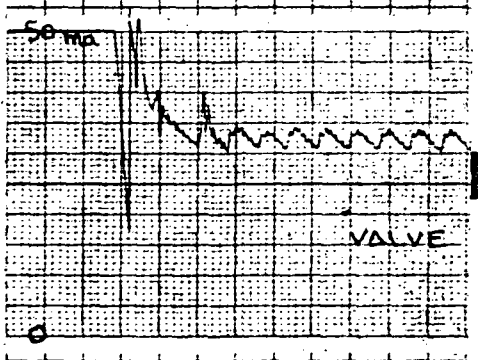
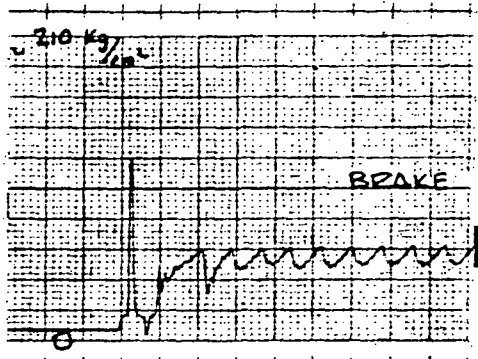
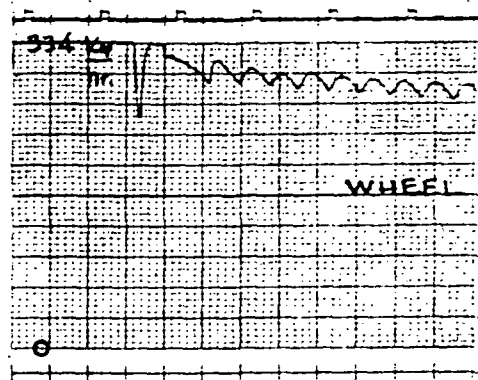


FIG. 62

MU STEPS WITH 7.5 HZ STRUT
BOEING CLOSED LOOP SYSTEM



VELOCITY

PRESSURE

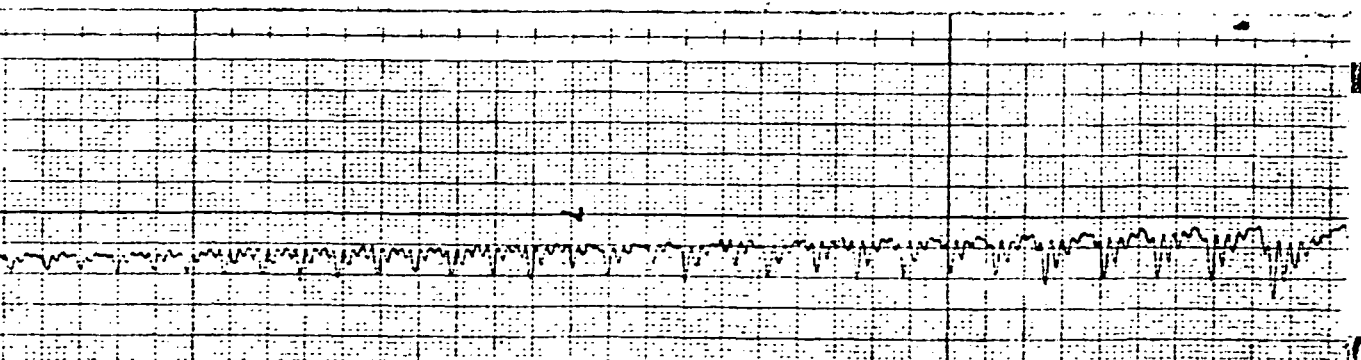
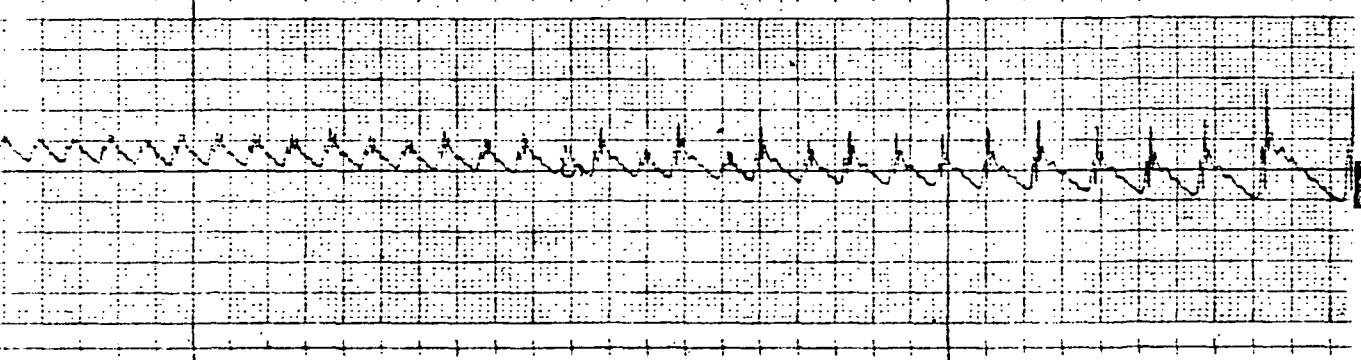
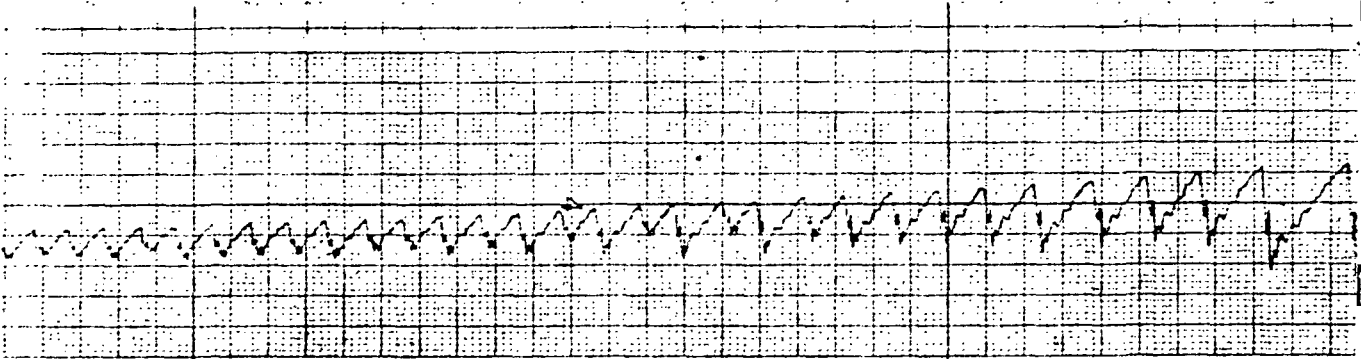
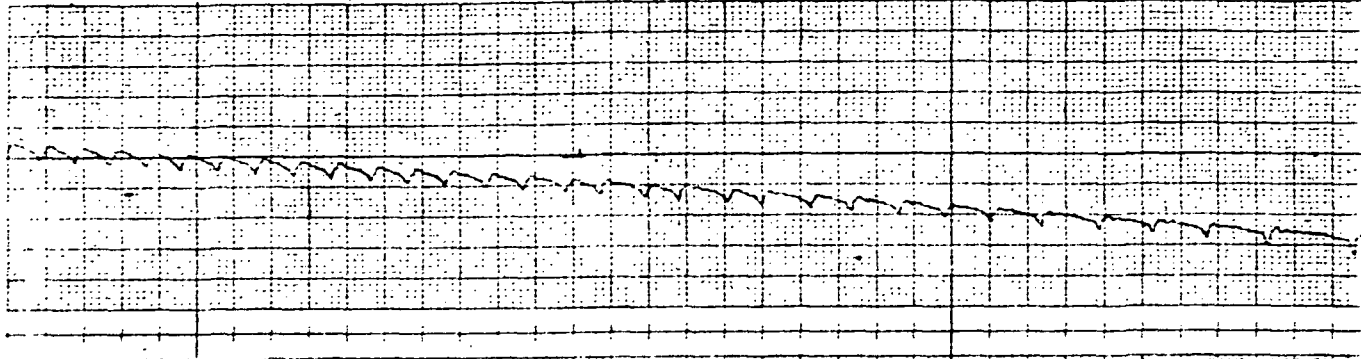
CURRENT

DEFLECTION

10 sec

FOLDOUT FRAME /

3797



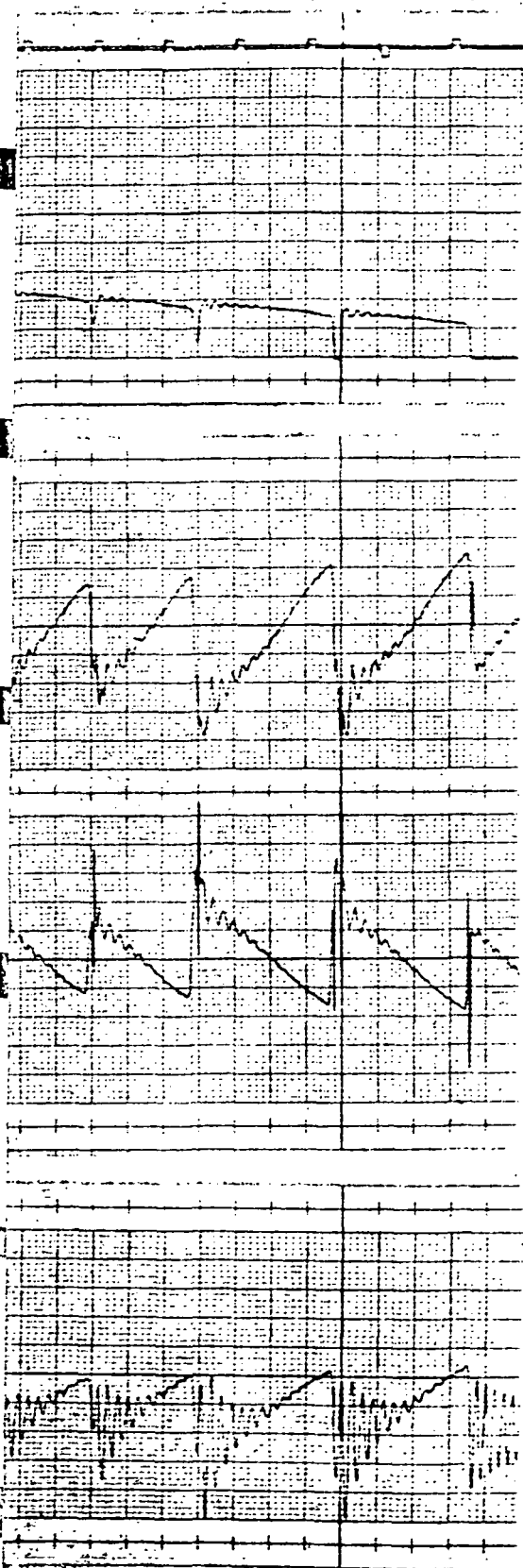


FIG. 63
WET RUNWAY CURVE 1 WITH 7.5 STRUT
BOEING CLOSED LOOP SYSTEM

143

FOLDOUT FRAME

4

time to recover and regain skidding pressure was much less. 2.8 seconds was all it took to regain skidding pressure. This apparent improvement in adaptability really was just the result of the timing of the step μ change and apparently not the capability of the system.

Figure 63 represents the wet runway profile test. The μ level started out at .11 and increased up to about .40 at the end of the braking run. The brake pressure was brought on with the usual 300 ms valve signal ramp, but of course, at this low μ level a skid occurred immediately. Its depth was only 25 percent slip and the system recovered within 100 ms and continued controlling the wheel velocity. Initially the efficiency was not at its best during the portion of the run where μ was below .15. As the μ value increased above .15 the efficiency steadily improved until the low velocity end where the skid detector came into play. Strut damping was good until the very last skid where the system never recovered and the wheel stayed locked up for 250 ms until the braking run ended. As before the low wheel lockup caused the strut to oscillate and damp out very slowly. With the system effectively out of the loop because of the locked wheel it had no further possibility of actively damping the strut, thus the slower damped oscillations.

The first Hydro-Aire Mark III test is shown in Figure 64. It is a .5 μ dry runway test with the 4.5 Hz strut frequency. Pressure was brought on by the 300 ms valve signal ramp and when the brake pressure reached 193 kg/cm^2 (2750 lbs/in^2) the wheel went into a very shallow skid of only about 10 percent slip. However, there was considerable ringing in the valve signal, brake pressure, wheel velocity and strut. Since the frequency of the oscillations was 13 cycles per second the 4.5 Hz strut did not follow the brief excitation. However, the six cycles of oscillation caused the system to reduce brake pressure some 42 kg/cm^2 (600 lbs/in^2) but which was then increased to resume skidding. From this point on the control was very highly efficient. The strut was kept oscillating but this was because of the skid sampling rate of about

2.5 skids per second. These strut oscillations were damped at all times. Even during the low velocity skids the system was able to prevent complete lockup skids. Pressure recovery after a deep skid was extremely rapid serving to minimize strut oscillations and allowing the system to actively damp the oscillations. This braking run yielded very high efficiency throughout the entire velocity profile. Damping appeared adequate although the test was run with a 4 percent system damping.

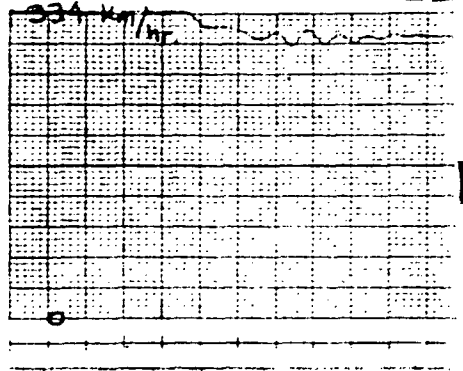
Figure 65 represents a .5 mu dry runway with a 11.5 Hz strut. Pressure was brought on by the 300 ms valve ramp signal and the pressure rose to 196 kg/cm^2 (2800 lbs/in^2) causing the first of many skids. Actually, the skids are just the result of excessive ringing in the wheel velocity, brake pressure, valve signal and strut oscillation. The strut oscillations diverged for 300 ms but then converged although it took 1.6 seconds before the strut was finally damped. After this first period the pressure regained skidding level and continued efficient control throughout the remainder of the run. With the smooth continuous control that the system exhibited the strut motion was well damped. The low velocity end of the run caused progressively deeper skids which in turn caused more strut activity. Although the strut motion was damped it took progressively longer to damp out the oscillations as the skids got deeper.

Figure 66 represents the step mu test. Initially the mu value was .54 and the brake pressure was increased by means of a 300 ms valve signal ramp. Pressure increased to 200 kg/cm^2 (2850 lbs/in^2) and the system reached skidding pressure and again precipitated about 8 cycles of oscillation. This had the effect of lowering the brake pressure some 42 kg/cm^2 (600 lbs/in^2) but as soon as the oscillation damped out the pressure again reached skidding level. Although the oscillations showed up in the wheel velocity, brake pressure, valve signal and strut, the amount of wheel velocity modulation was slight; the skids averaging only 10 percent slip values. Control continued

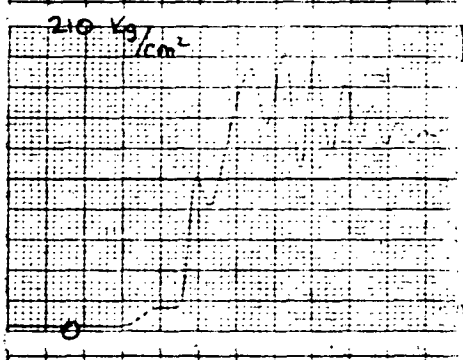
normally until the first step μ . When the μ dropped to .16, the wheel velocity dropped into a skid with a slip value of 49 percent and lasted only 200 ms. The system adapted to this so rapidly that it began skid cycling while the .16 μ period remained. This .16 μ skid cycling was very oscillatory but before the strut oscillations grew or the brake pressure increased, the μ switched back to .54 which abruptly stopped all skid activity. From the switching point to the resumption of skidding took only 2.2 seconds. Skid sampling continued as normal then until the second step μ took place. This caused a skid which had a slip value of 67 percent and width of 200 ms. Again the system was able to adapt and began .16 μ level skid sampling while still operating in this .16 μ region. The strut was more oscillatory during this second step μ and kept oscillating until the μ switched back to the .54 level. From that point until skidding resumed was 1.8 seconds. Skid sampling continued as normal until the third step μ . This skid was very deep reaching a slip value of 97 percent and lasting 240 ms. This time the system was not able to regain skidding level during the remainder of the .16 μ region. The strut oscillated violently during this low μ period and did not damp out until the .54 μ level was switched to again. Elapsed time was 2.2 seconds until skidding pressure was reached again. Since this .54 μ period was now during much lower wheel velocity, the skid sampling caused the skids to get deeper progressively until the fourth step μ caused a lockup skid. The width of the skid was still only 200 ms even though the wheel was caused to lockup for 40 ms. The system was not able to regain skidding during the remainder of the .16 μ period although only 2.9 seconds was required to cause another skid once the μ switched back to .54 region.

Figure 67 represents the wet runway curve 1 profile. The characteristics of this curve have been mentioned before in conjunction with Figures 59 and 63 but basically the μ starts at .11 and increases up to about .4 value at the completion of the braking run. Pressure was brought on by the 300 ms valve signal ramp but being a low μ a skid was precipitated almost immediately. The depth of the skid was 38 percent

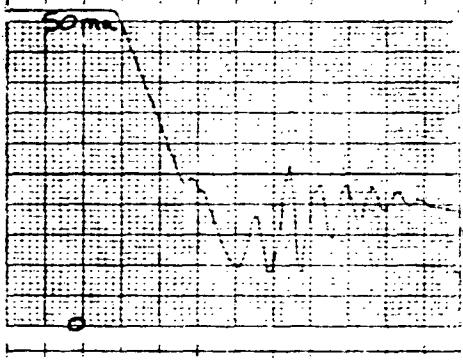
334 km/hr



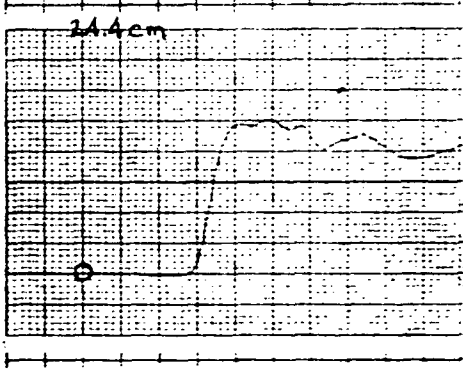
210 kg/cm²



50 mc



24.4 cm



464

WHEEL VELOCITY

BRAKE PRESSURE

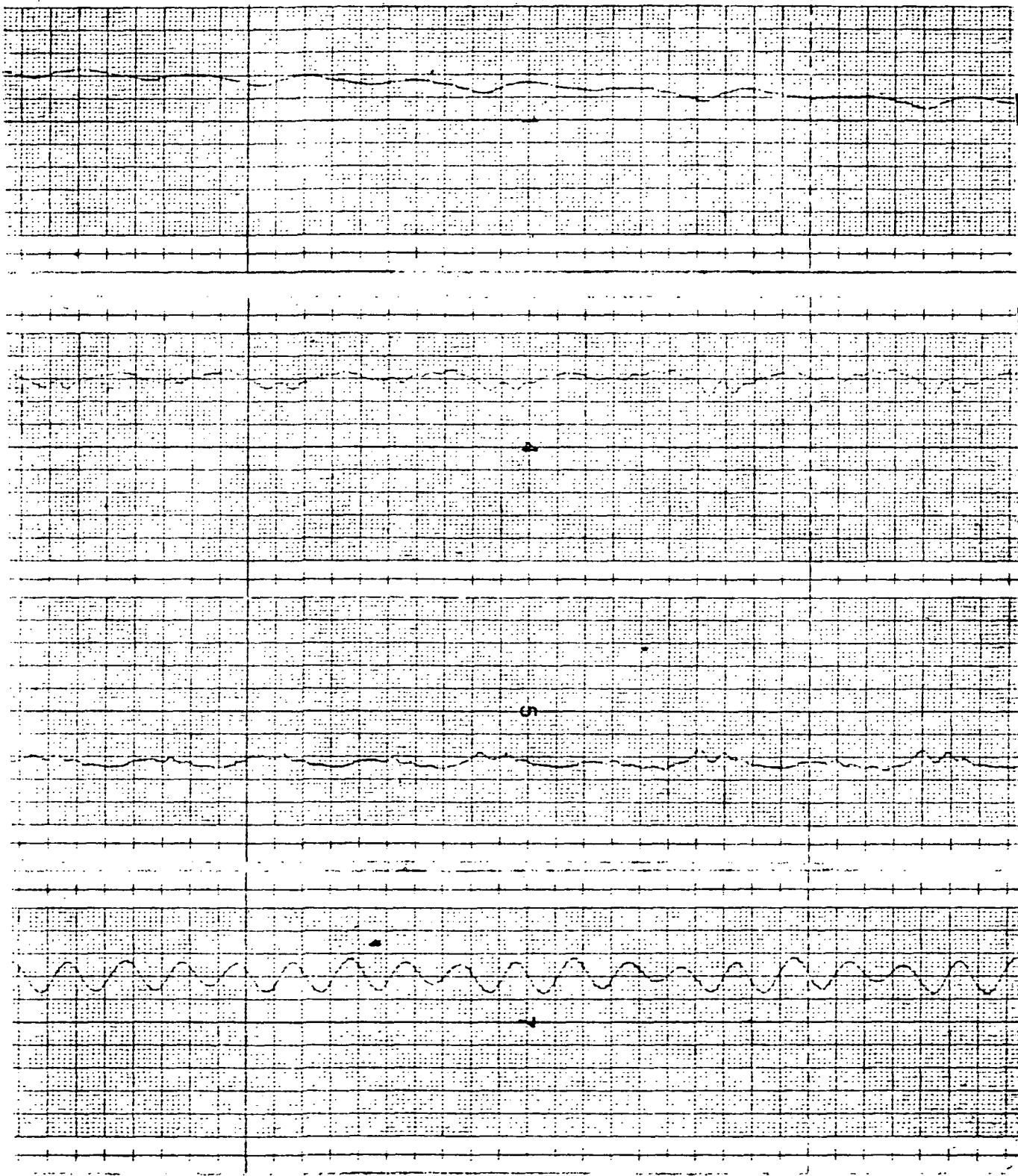
VALVE CURRENT

STRUT DEFLECTION

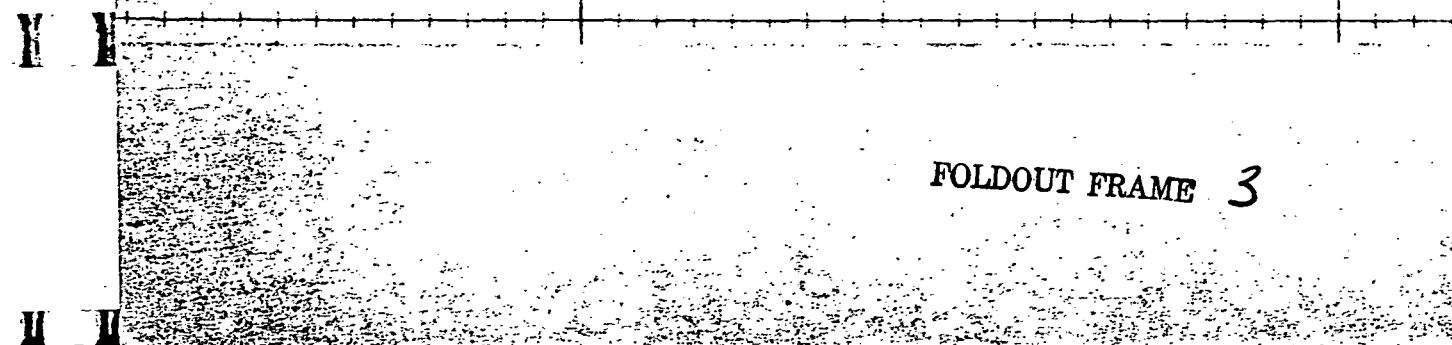
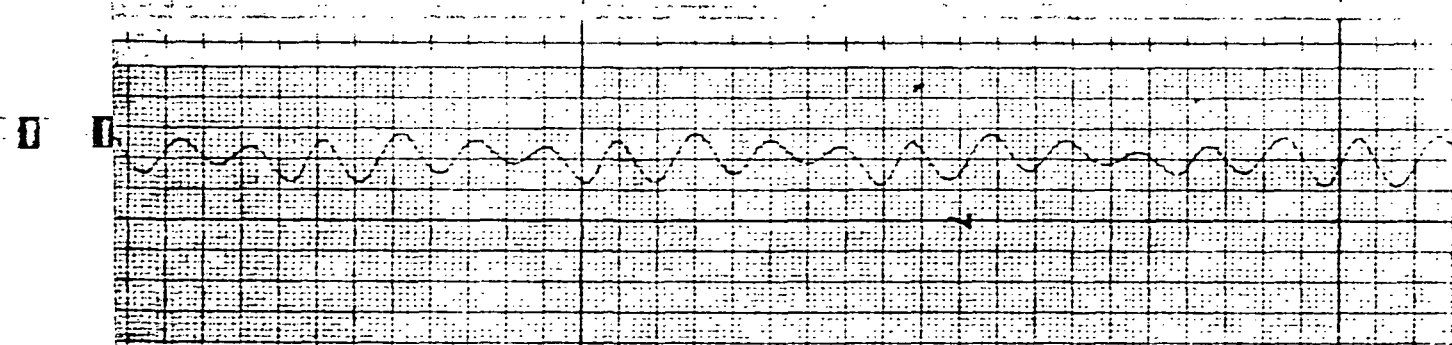
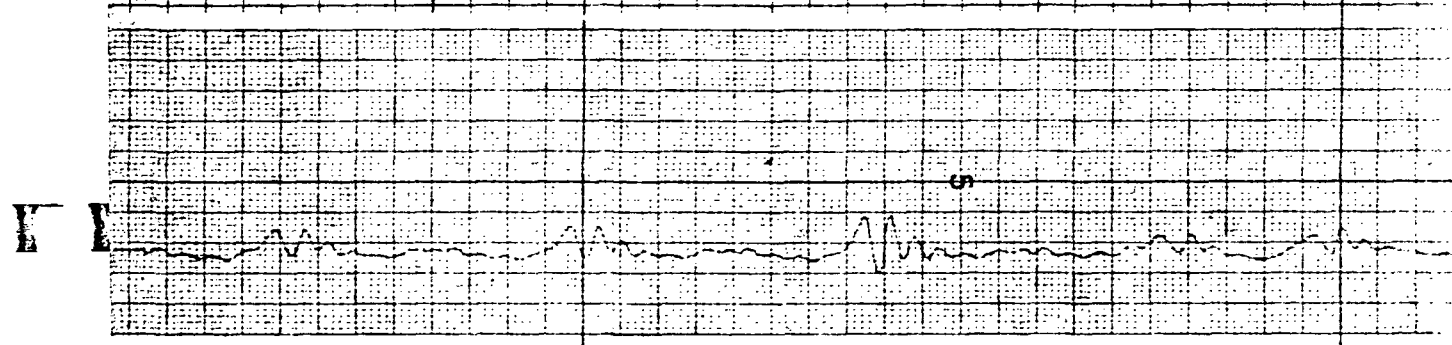
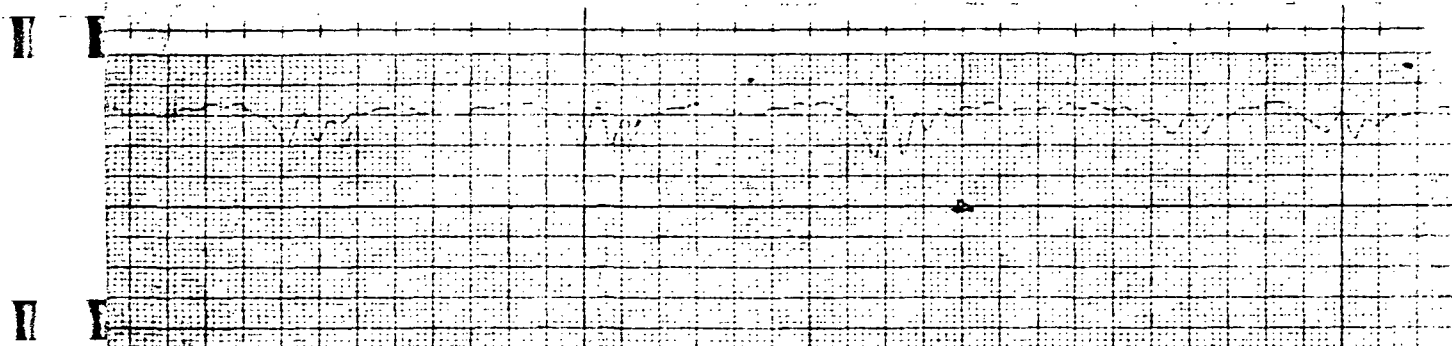
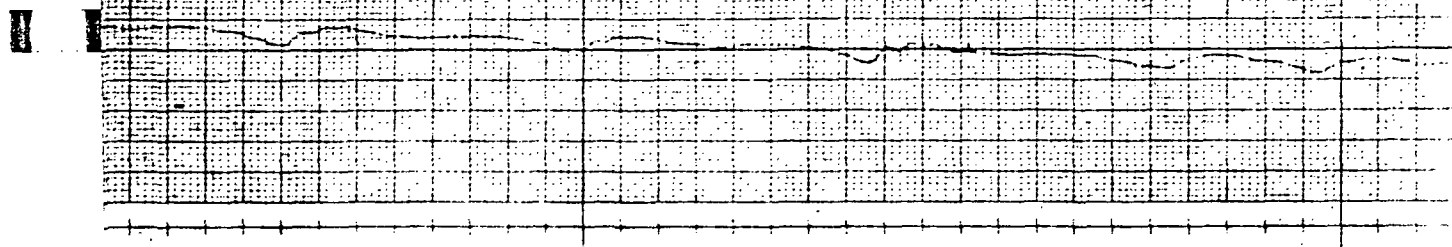
1.0 Sec

FOLDOUT FRAME

15465



FOLDOUT FRAME 2



FOLDOUT FRAME 3

PRINTED IN U.S.A.

15466

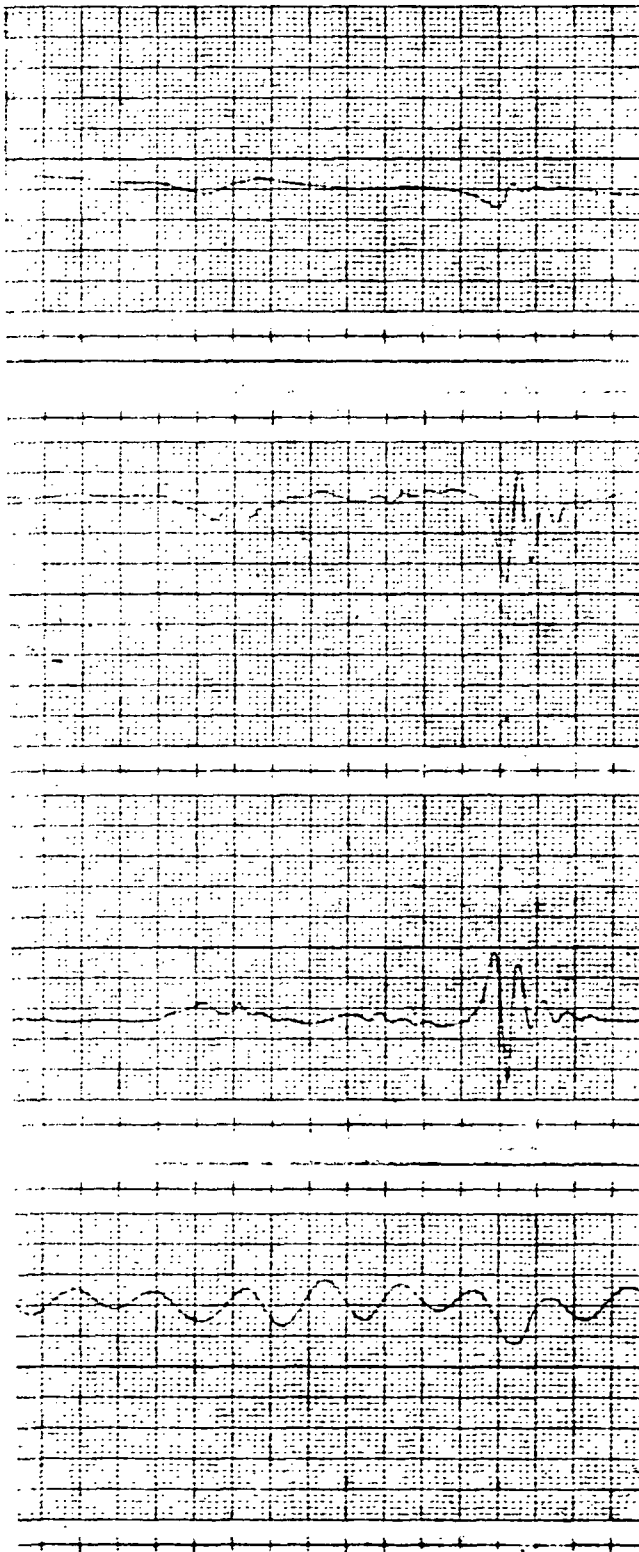
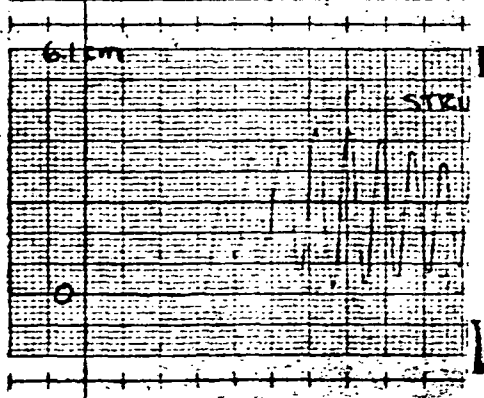
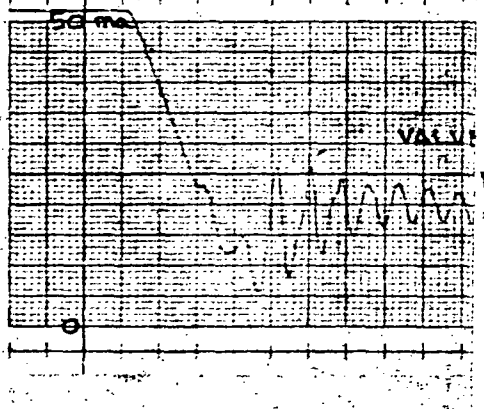
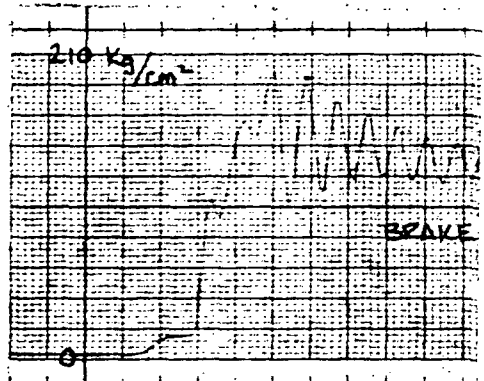
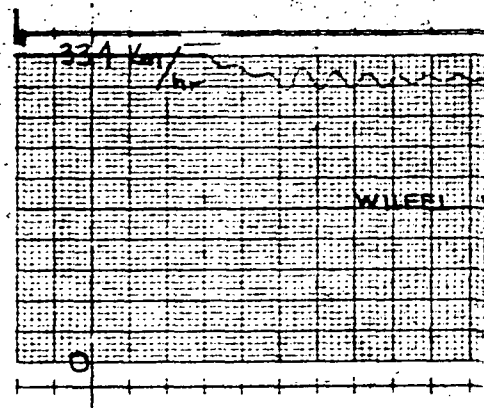


FIG. 64

.5 MU WITH 4.5 H₂ STRUT
HYDRO-AIRE MARK III SYSTEM

FOLDOUT FRAME 147

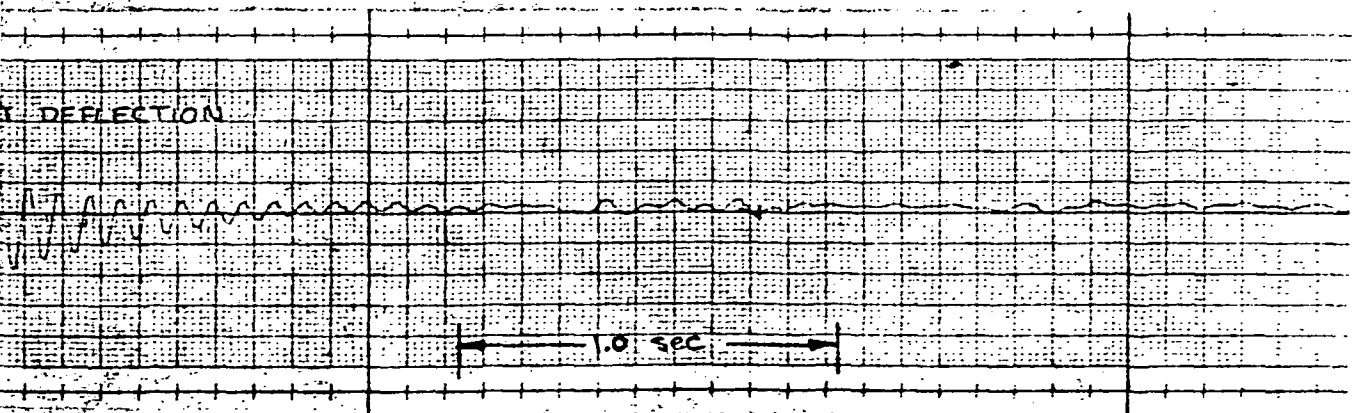
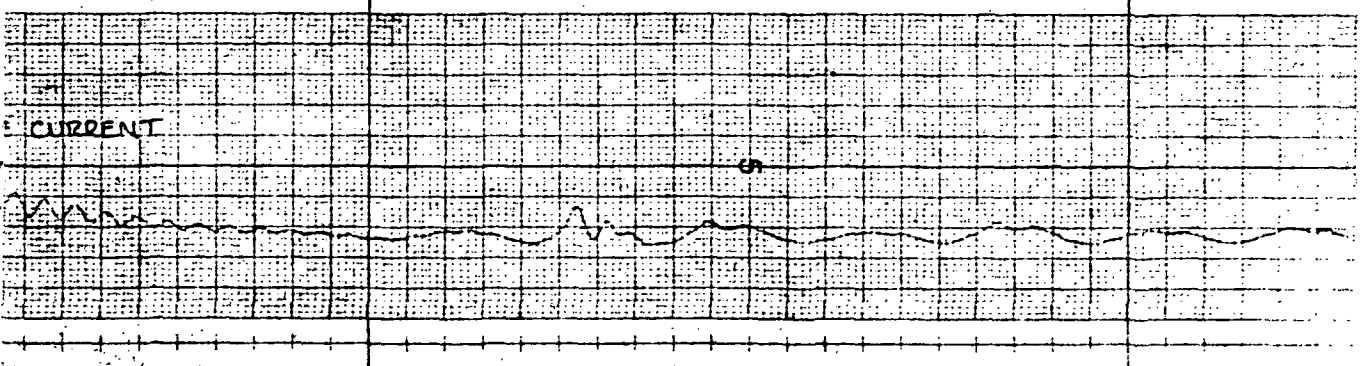
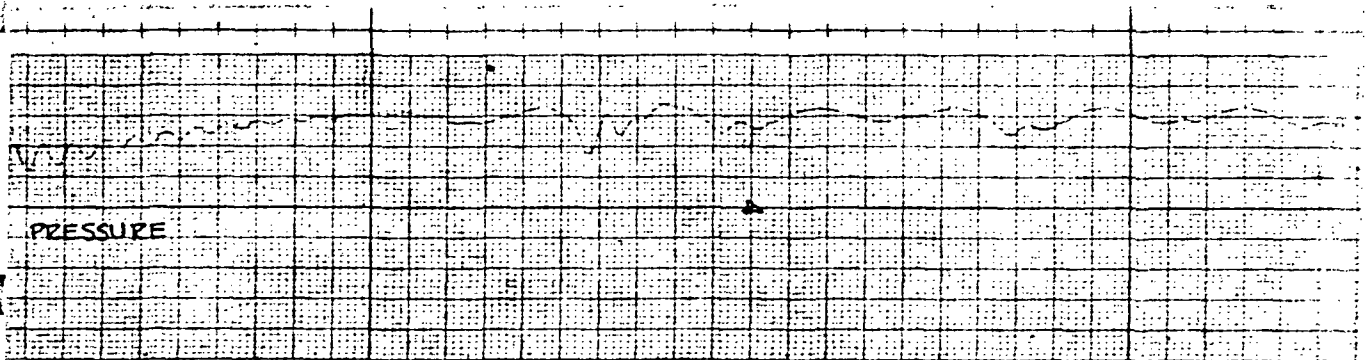
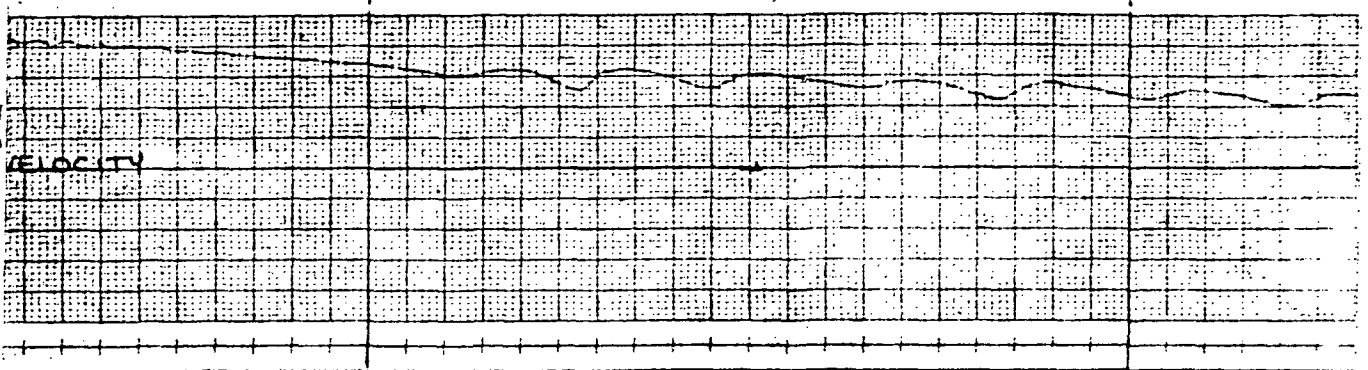
4



BRUSH INSTRUMENTS DIVISION, GOULD INC.

CLEVELAND, OHIO

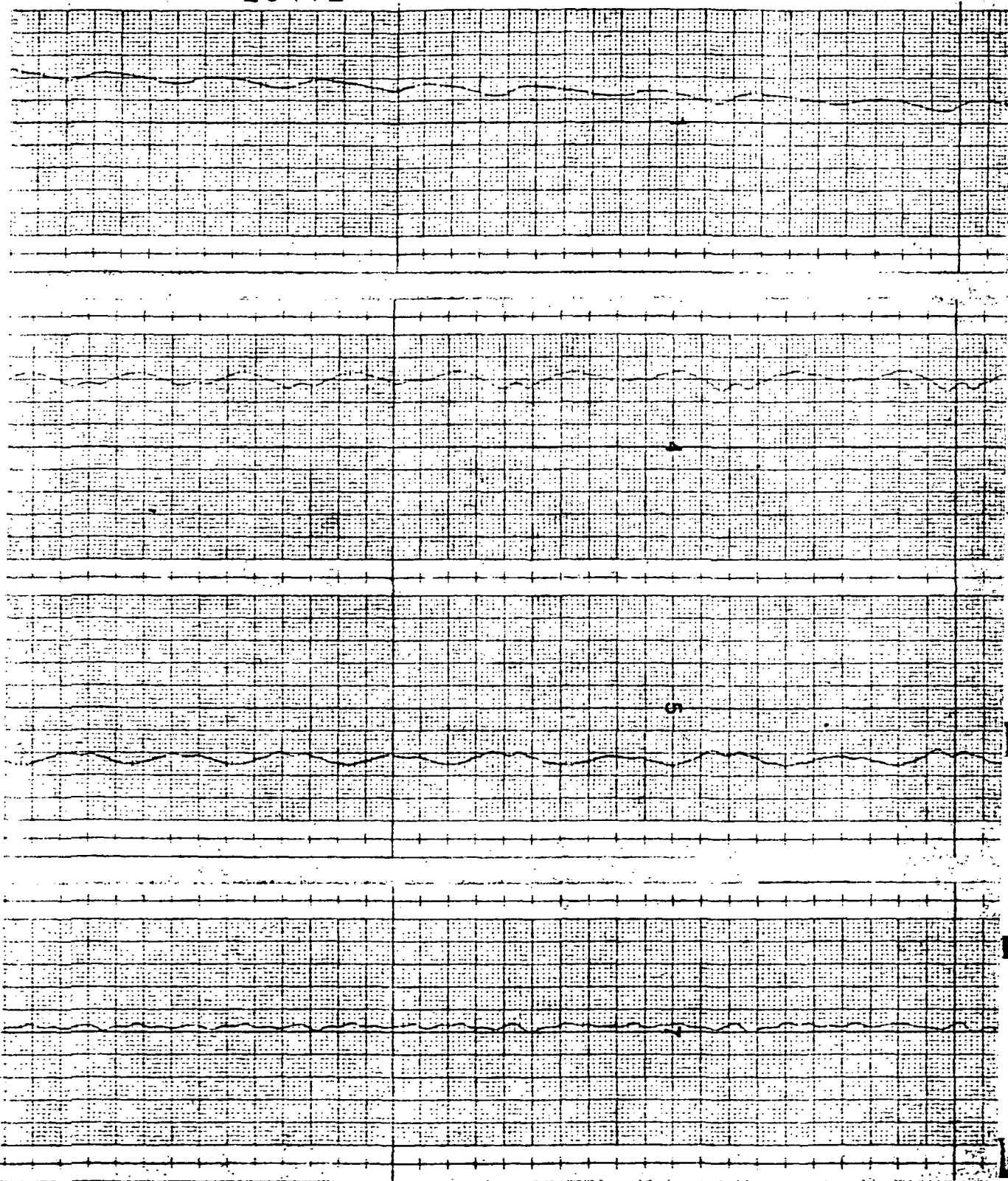
PRINT



FOLDOUT FRAME

ED IN U.S.A.

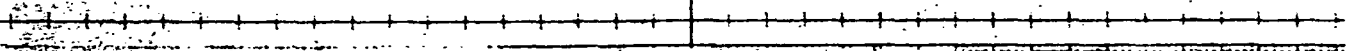
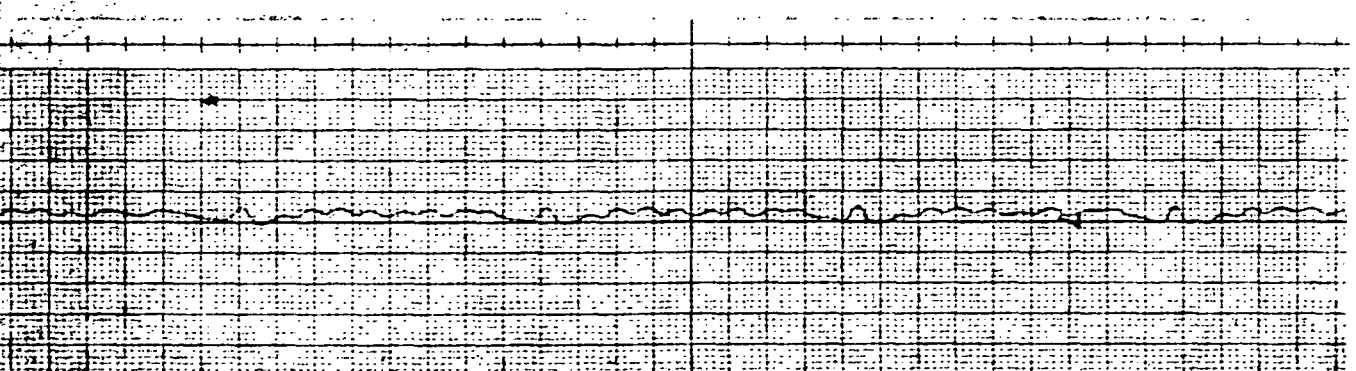
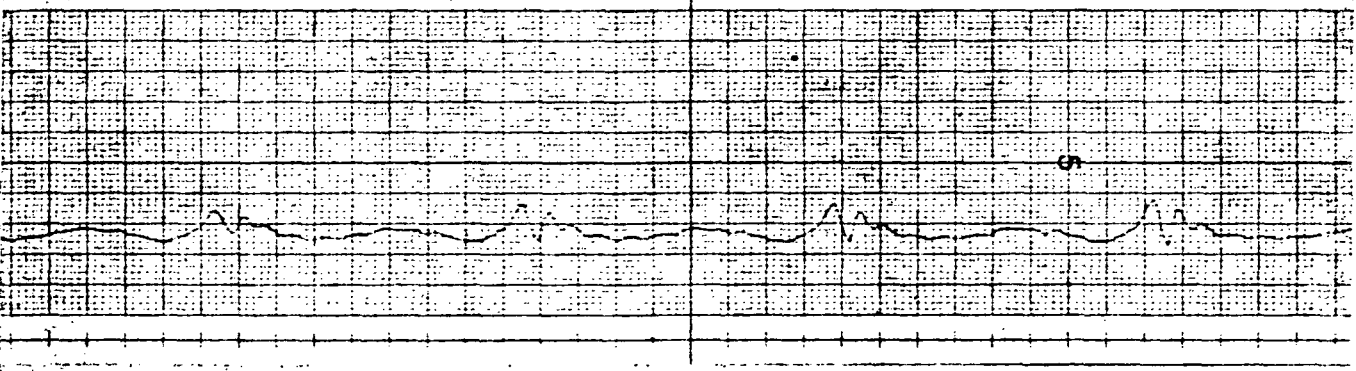
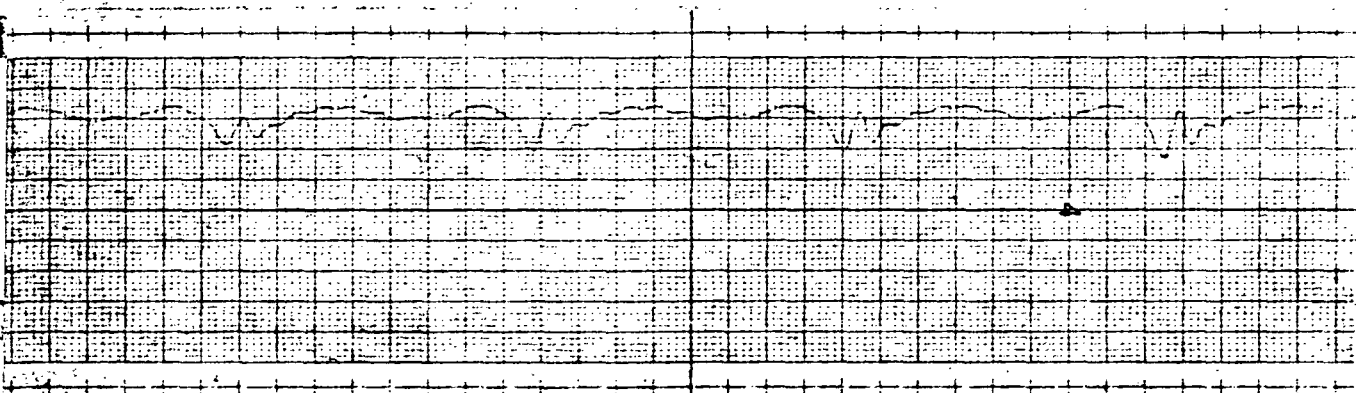
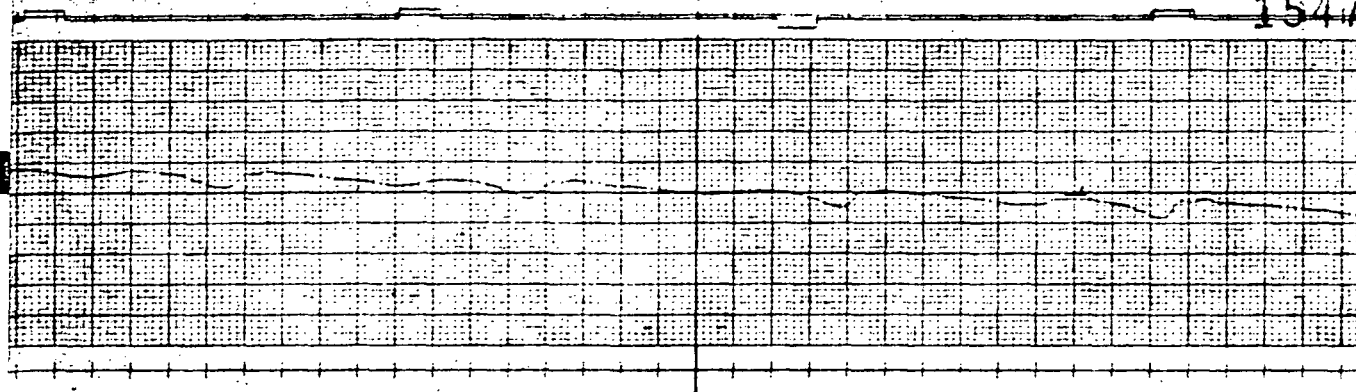
15472



FOLDOUT FRAME

2

1547



FOLDOUT FRAME 3

3

BRUSH INSTRUMENT

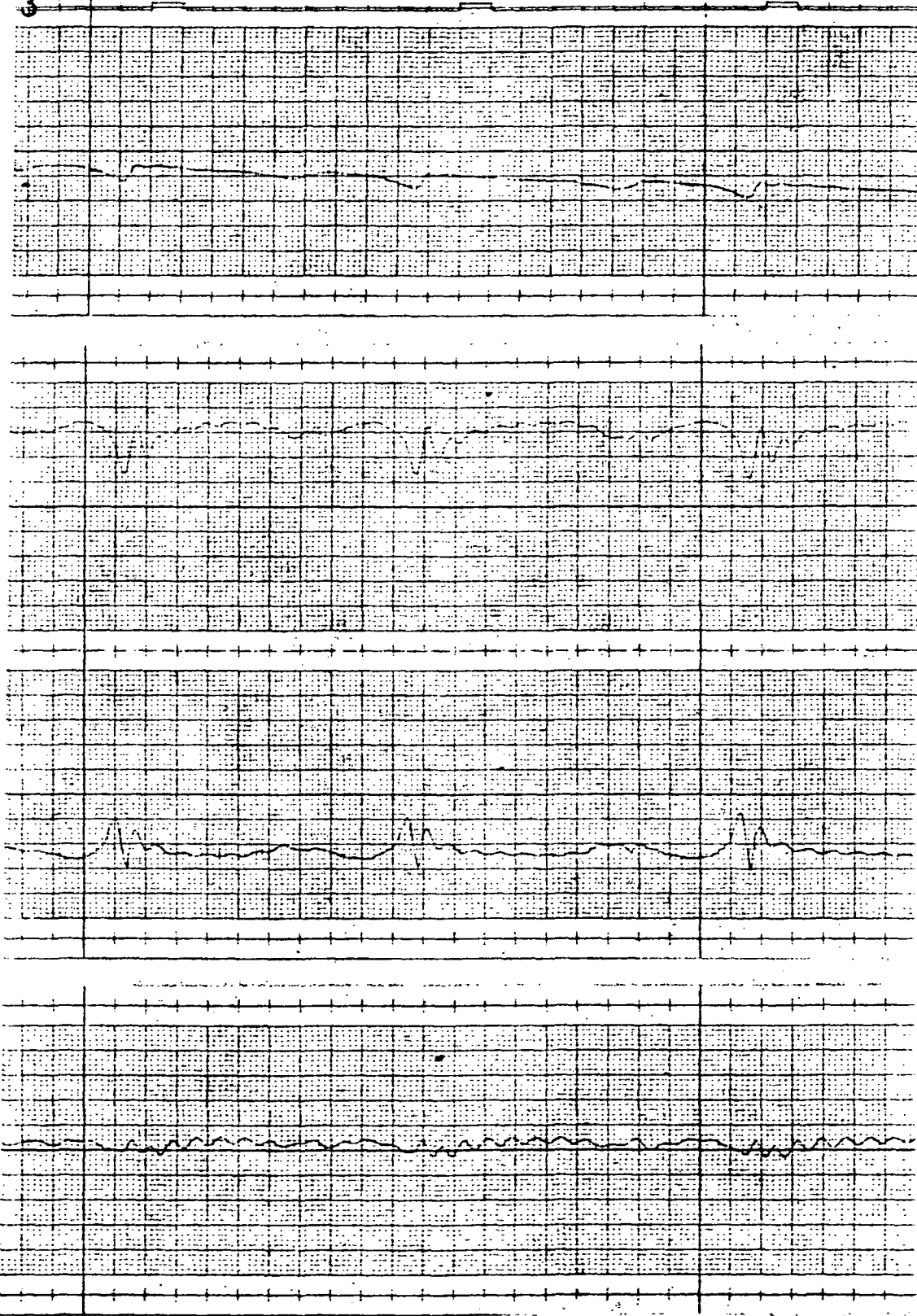
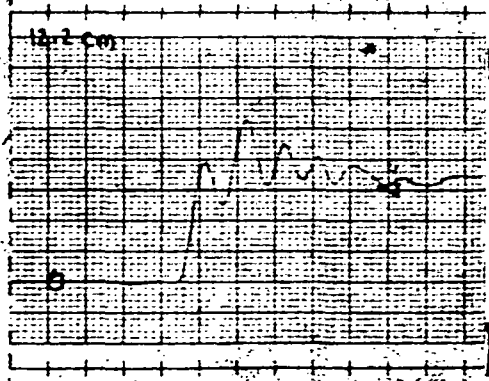
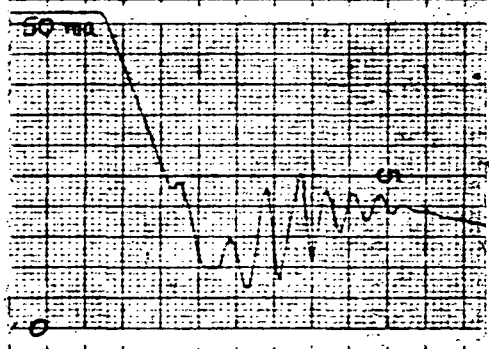
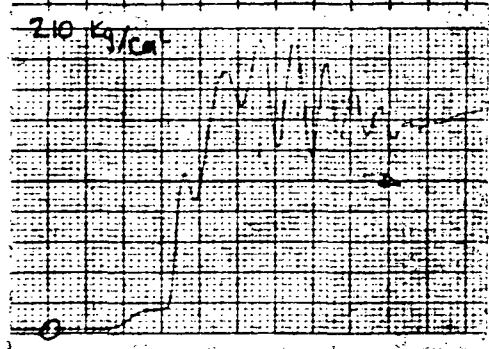
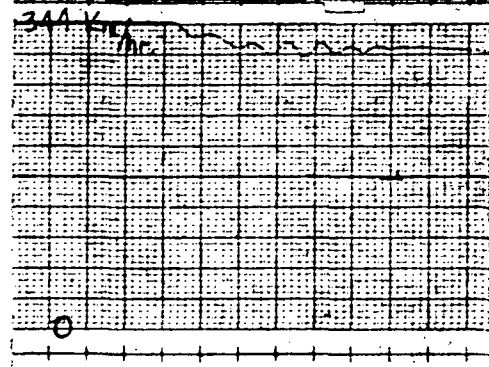
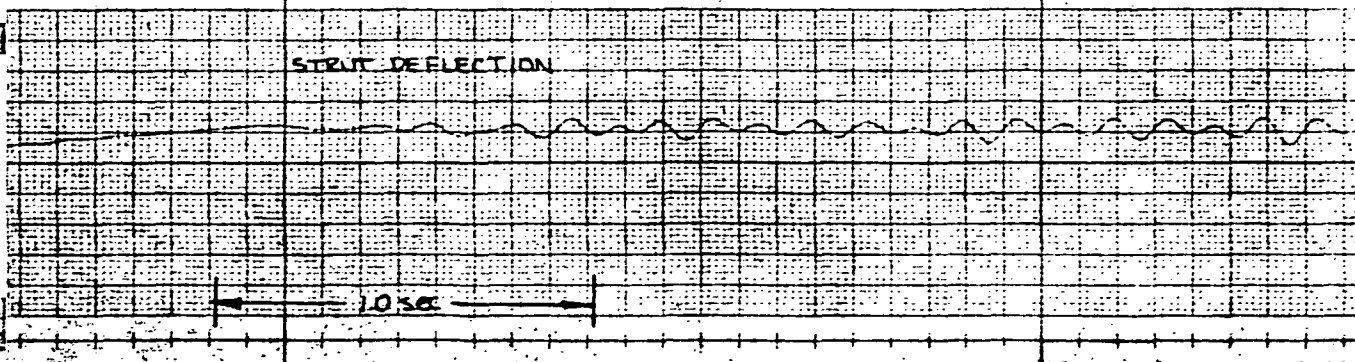
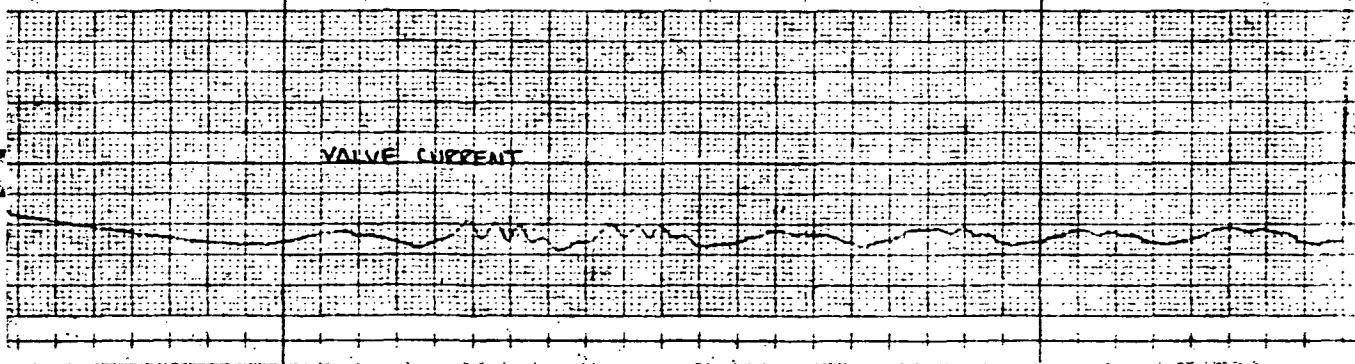
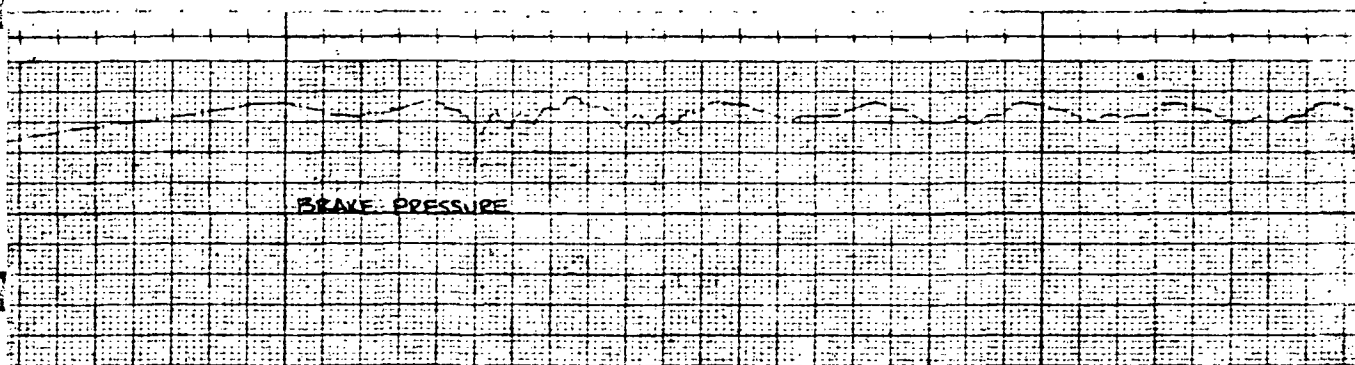
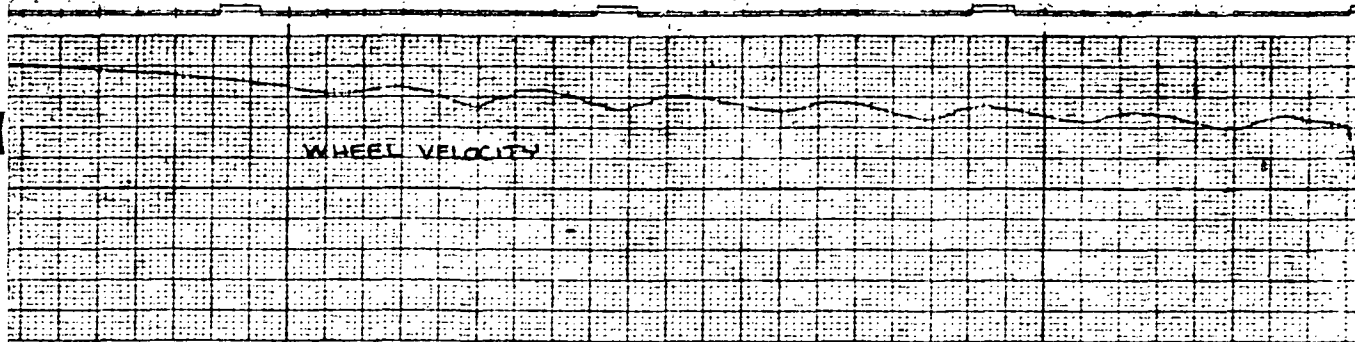


FIG. 65

.5 MU WITH 11.5 42 STRUT
HYDRO-AIRE MARK III SYSTEM

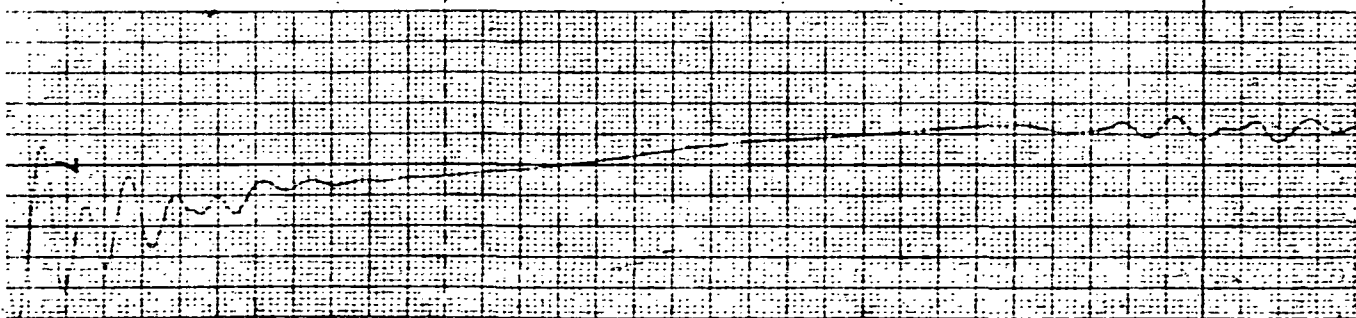
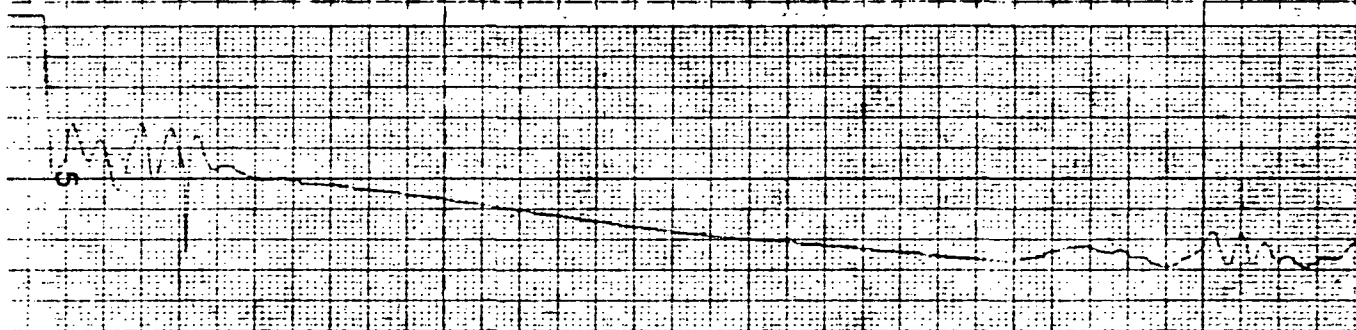
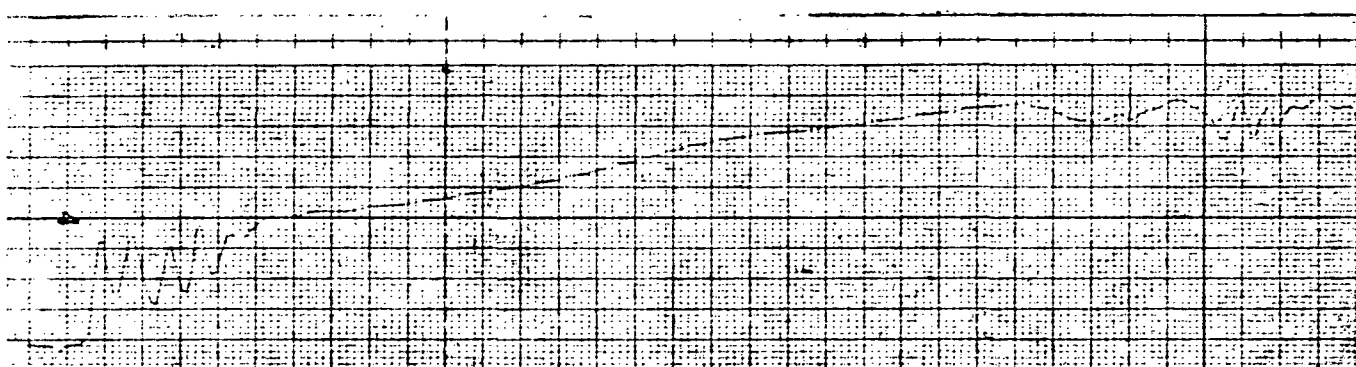
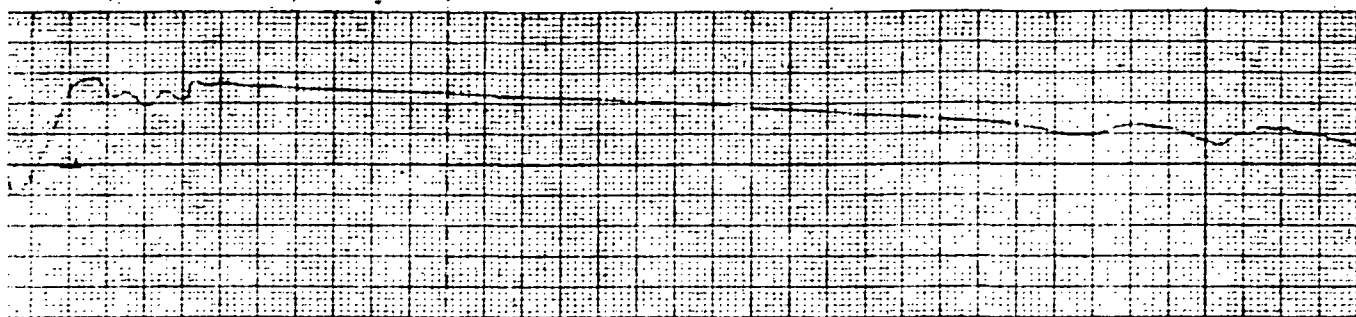




FOLDOUT FRAME

15447

BRUSH INS



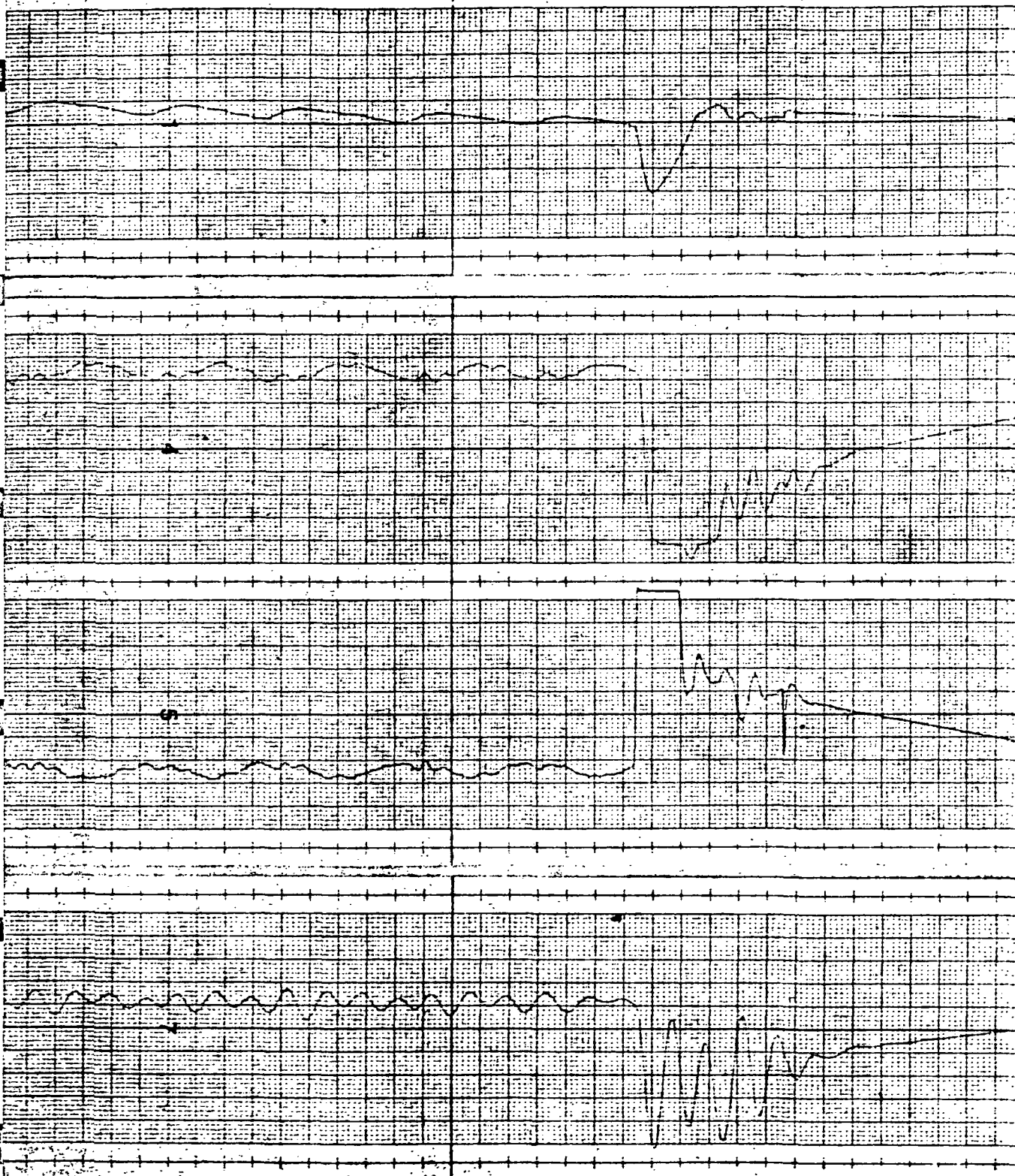
FOLDOUT FRAME 2

INSTRUMENTS DIVISION, GOULD INC.

CLEVELAND, OHIO

PRINTED IN U.S.A.

15448



FOLDOUT FRAME 3

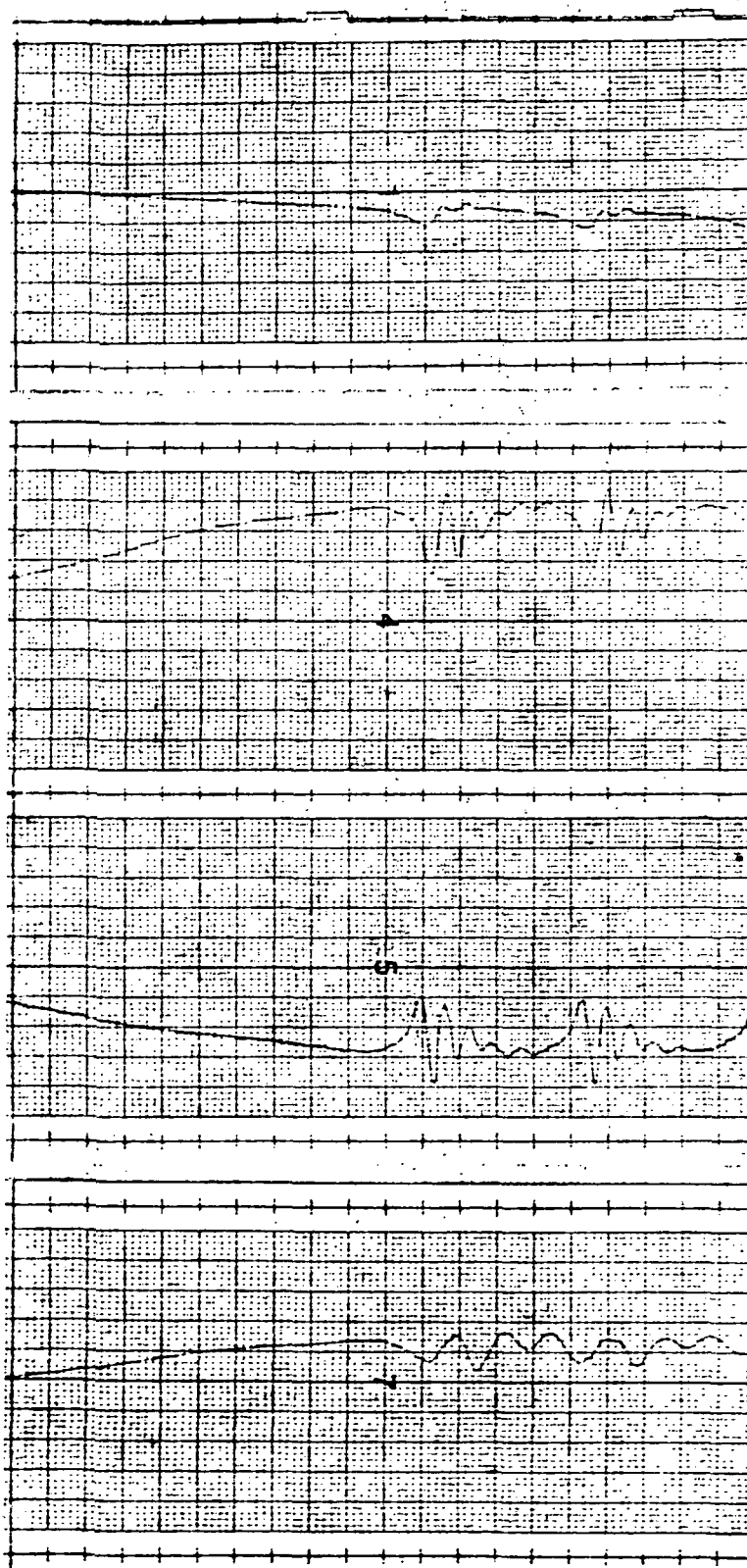
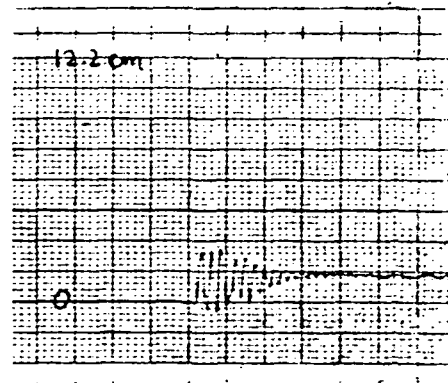
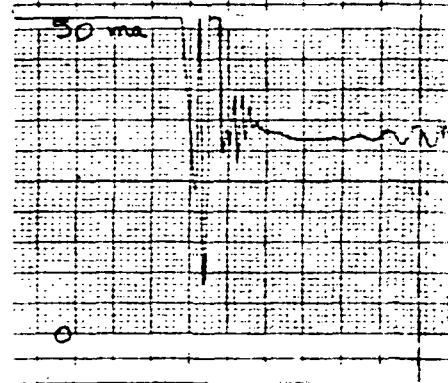
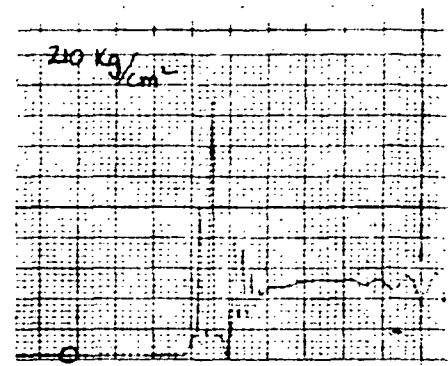
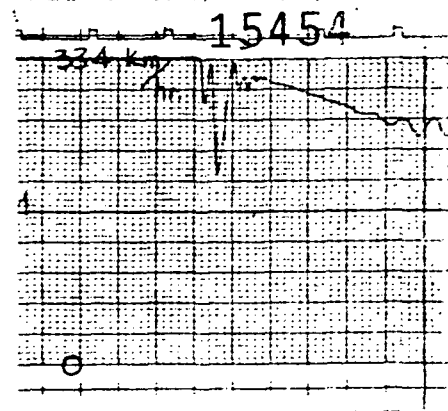


FIG. 66

MU STEPS WITH 7.5 HZ STRUT
HYDRO-AIRE MARK III SYSTEM



WHEEL VELOCITY

BRAKE PRESSURE

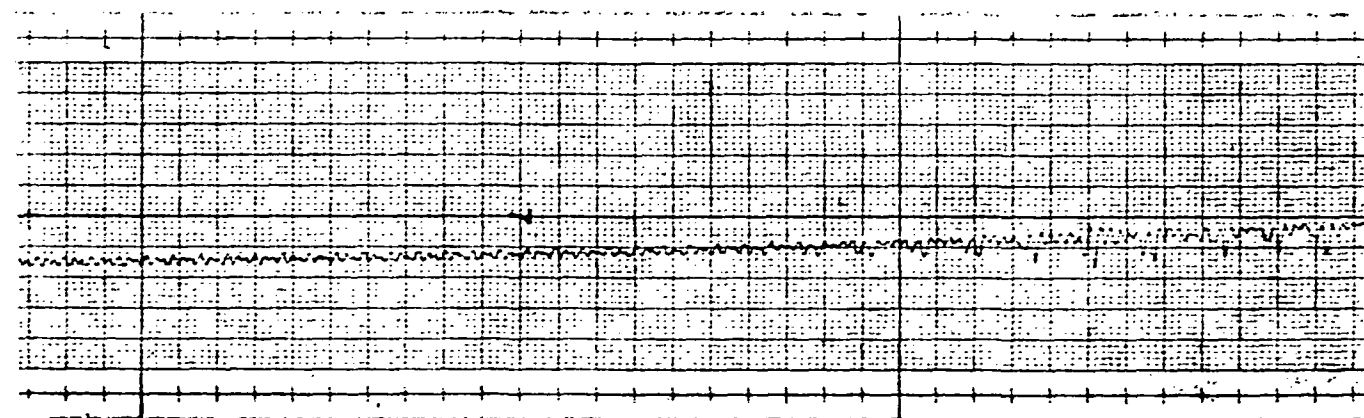
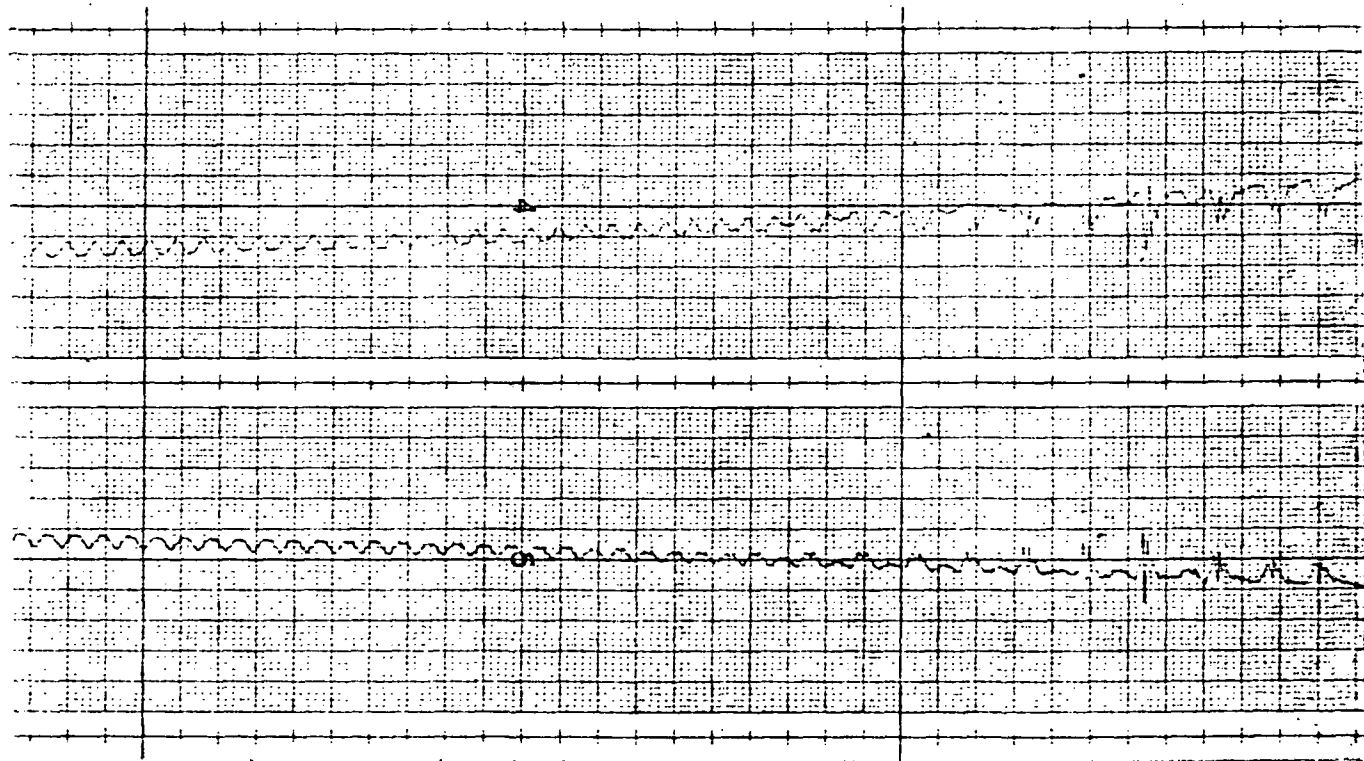
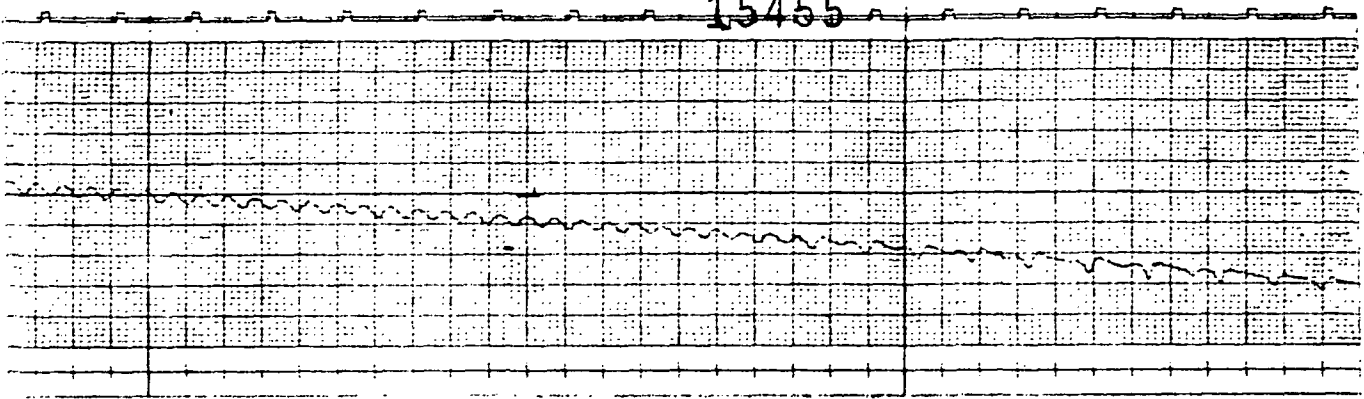
VALVE CURRENT

STRUT DEFLECTION

10X

FOLDOUT FRAME

15455



FOLDOUT FRAME

2

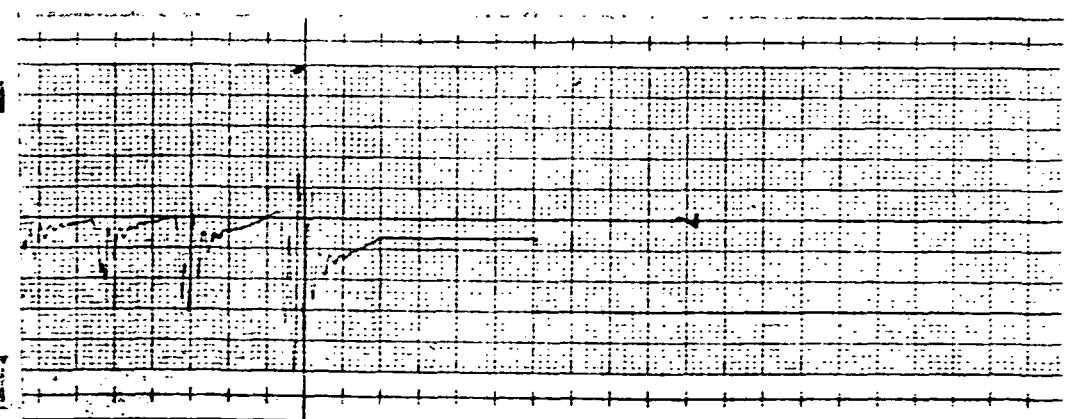
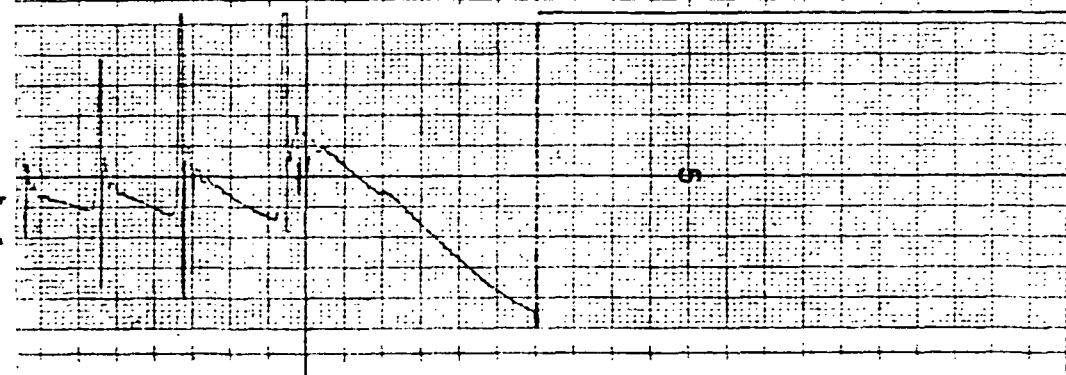
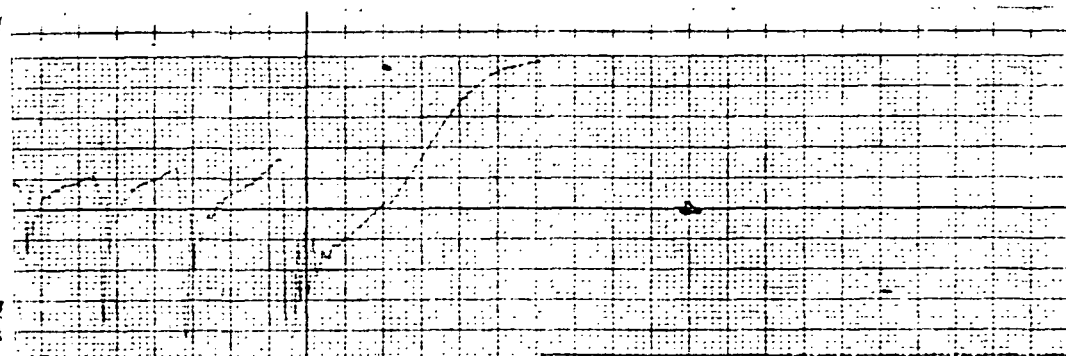
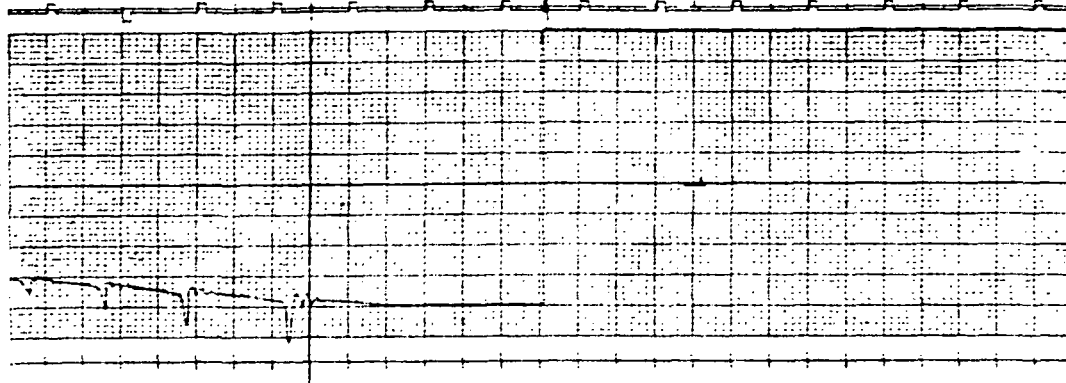


FIG. 67
WET RUNWAY CURVE 1 WITH 7.5 Hz STRUT
HYDRO-AIRE MARK III SYSTEM

150

FOLDOUT FRAME 4

and it lasted only 45 ms. To control this skid the brake pressure was dropped all the way to reservoir pressure but then jumped back to approximately 42 kg/cm^2 (600 lbs/in^2) and in the next two seconds increased to 56 kg/cm^2 (800 lbs/in^2) and resumed skidding. The skid sampling occurred at approximately three skids per second and kept this pace until the lower velocity end where the sampling slowed down to less than one skid per second. Transition for this system from low μ high velocity to high μ low velocity was extremely smooth. There was a small amount of strut oscillation at the beginning of the run but during the rest of the time except the very last three skids the strut was very well damped. One thing that caused a slight loss in stability at the beginning of this run was the system's tendency to operate on the backside of the μ -slip curve. In other words, the wheel velocity was momentarily kept from operating about the 10 percent slip or maximum μ peak.

This condition lasted but four seconds and meant little or no efficiency loss since the average slip value the system was controlling to was not that significantly more than 10 percent slip. The efficiency was very high overall throughout the wet runway run.

Discussion of Tabulated Test Data

The twelve figures just previously discussed (Figures 56 through 67) dealt only with four selected tests from each system. No attempt was made to compare the system's performance within a given test among themselves. This section will be devoted entirely to making performance comparisons. Bar charts will be used extensively to aid in interpreting all the laboratory test data. The bar charts are found in Figures 68 through 84. They compare the three antiskid systems tested for each test condition, indicating actual stopping distance, landing distance efficiency and developed μ efficiency. Figures 68 through 81 deal with Performance-Adaptability Tests.

Figures 68 through 70 compare results of the 4.5 Hz strut stabilized stops. Both the Closed Loop and Bendix systems were less efficient than Mark III, with the Closed Loop being the lowest. Figures 71 through 73 represent the 11.5 Hz strut stabilized stops. The Mark III system was more efficient with a shorter stopping distance than the other two systems. But the Bendix system had more trouble with these tests than the Closed Loop system and thus came out the same distance on dry runway as the Closed Loop but longer on the .2 mu and wet runway tests. All three systems stopped shorter with this higher strut frequency than with the lower frequency.

Figures 74 through 79 represent the nominal strut frequency of 7.5 Hz and also a range of operating mu's of .5 down to .075 in six steps. In all these tests the Mark III system had the shortest distance except Figure 75 which represents the .4 mu stabilized stop. Except for the .2 mu run, Figure 77 the Closed Loop system had the longest stopping distance. Figure 108 is a plot of the stabilized landing efficiencies. Basically the Mark III and Bendix systems were the two top performers and the Closed Loop system produced the longest stopping distance and lowest efficiencies. The only exception was at .2 mu the Bendix stopping efficiency dipped below the Closed Loop efficiency.

Figure 80 represents the touchdown tests where the braked wheels spin up upon touchdown but then leave the ground because of airplane bounce. It's a test of adaptability and as such shows that the Bendix and Mark III systems are equally efficient. The Closed Loop system is relatively intolerant to changes in operating conditions. The next test is the step mu test represented by Figure 81. It shows the same trend for the Closed Loop system. Although all three systems lost efficiency the Closed Loop lost the most. The Bendix system was less efficient in adapting to the steps while the Mark III system was the most efficient.

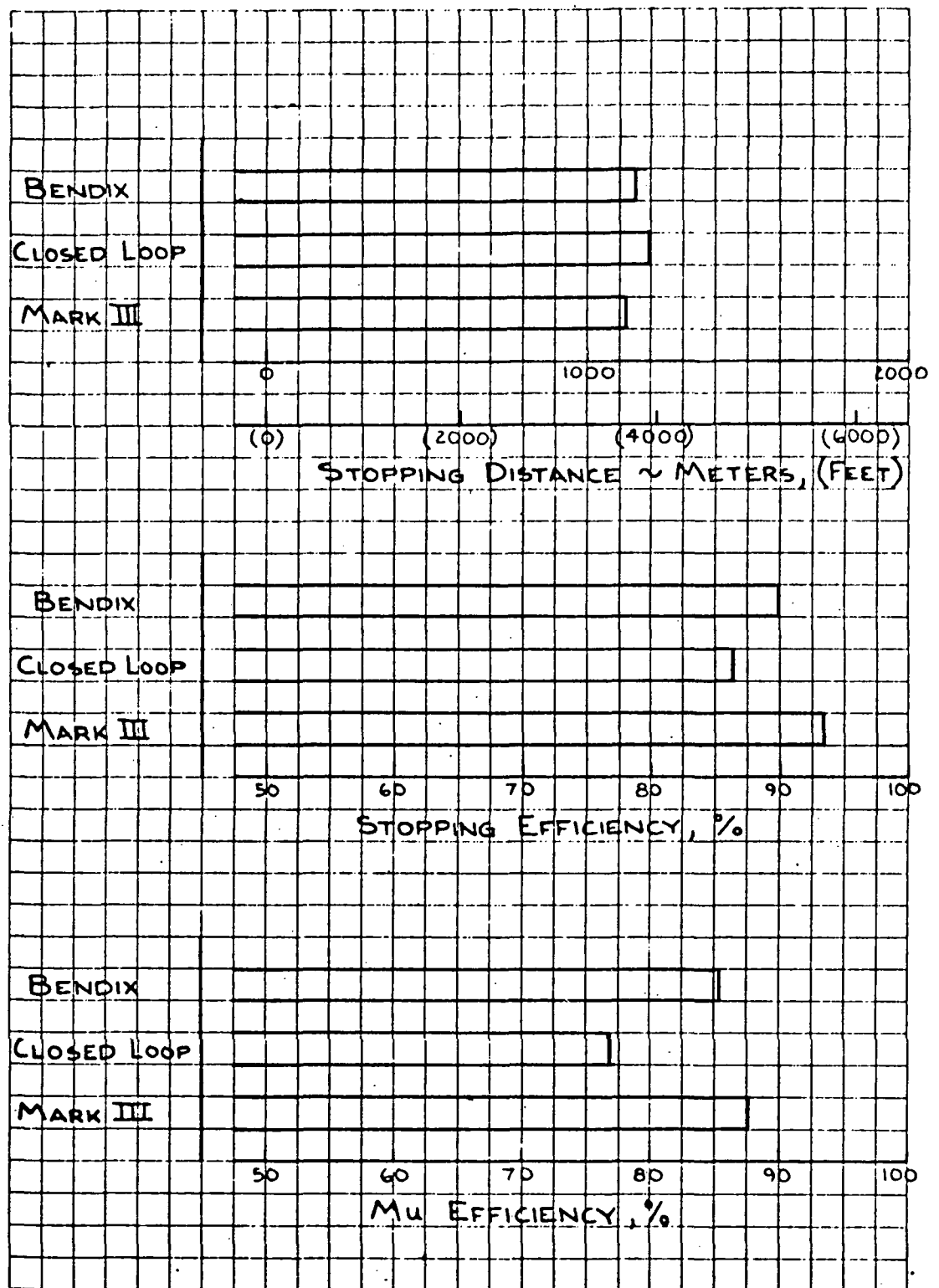


FIGURE 68. PERFORMANCE - ADAPTABILITY TEST 1, .5 MU, 4.5 HZ. STRUT

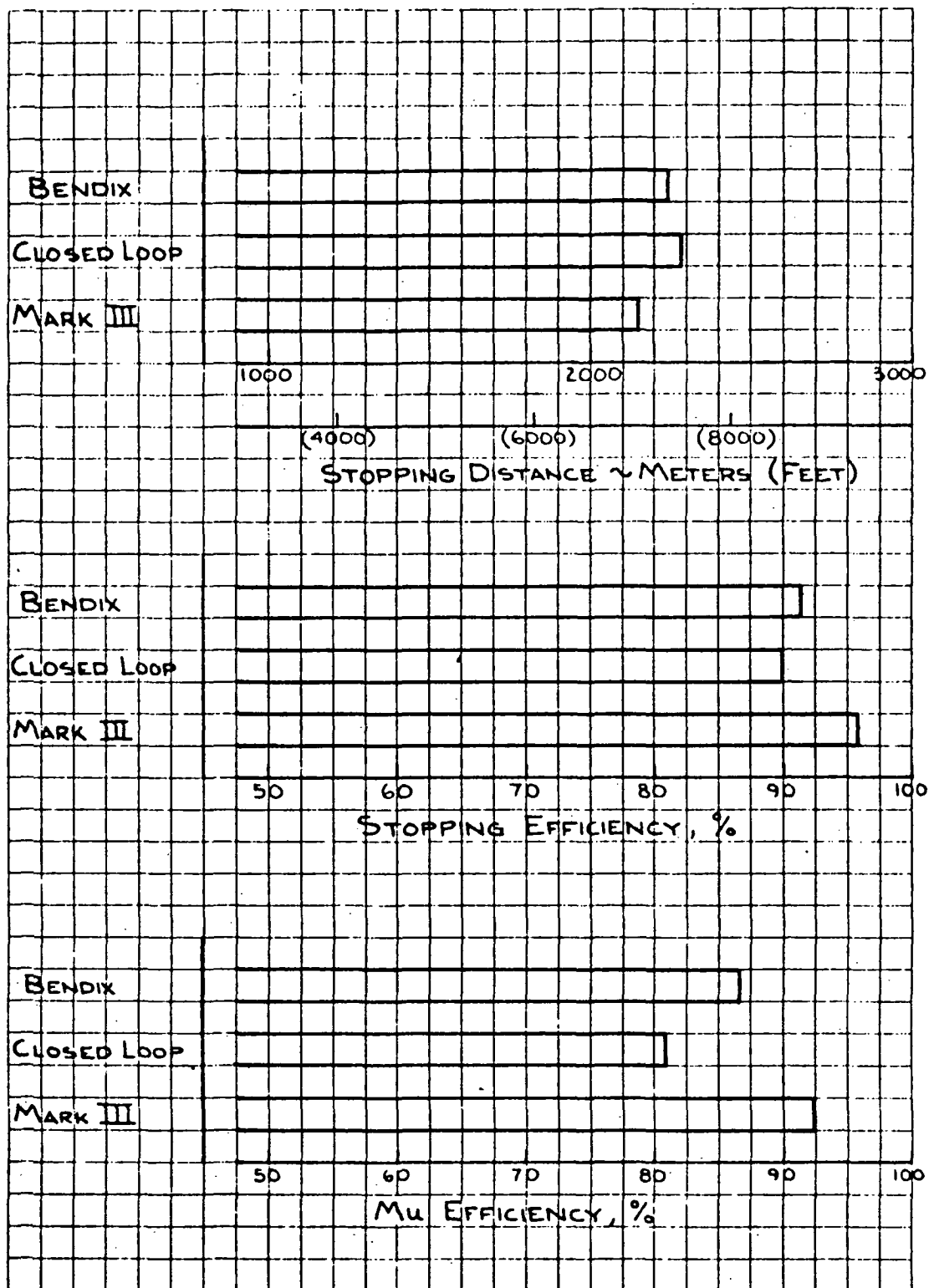


FIGURE 69. PERFORMANCE - ADAPTABILITY TEST 1, .2 MU, 4.5 HZ. STRUT

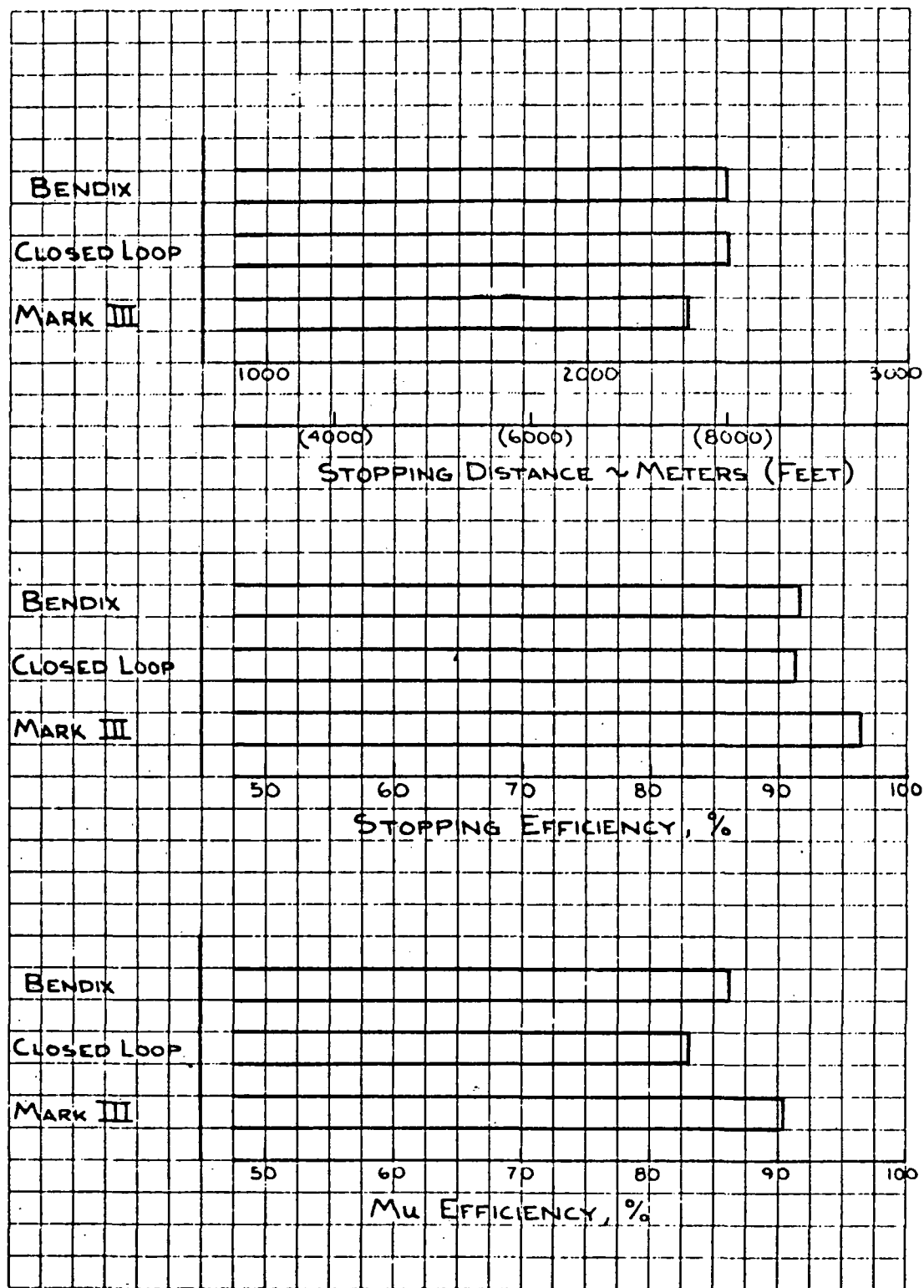


FIGURE 70. PERFORMANCE - ADAPTABILITY TEST 1, CURVE 1, 4.5 HZ. STRUT

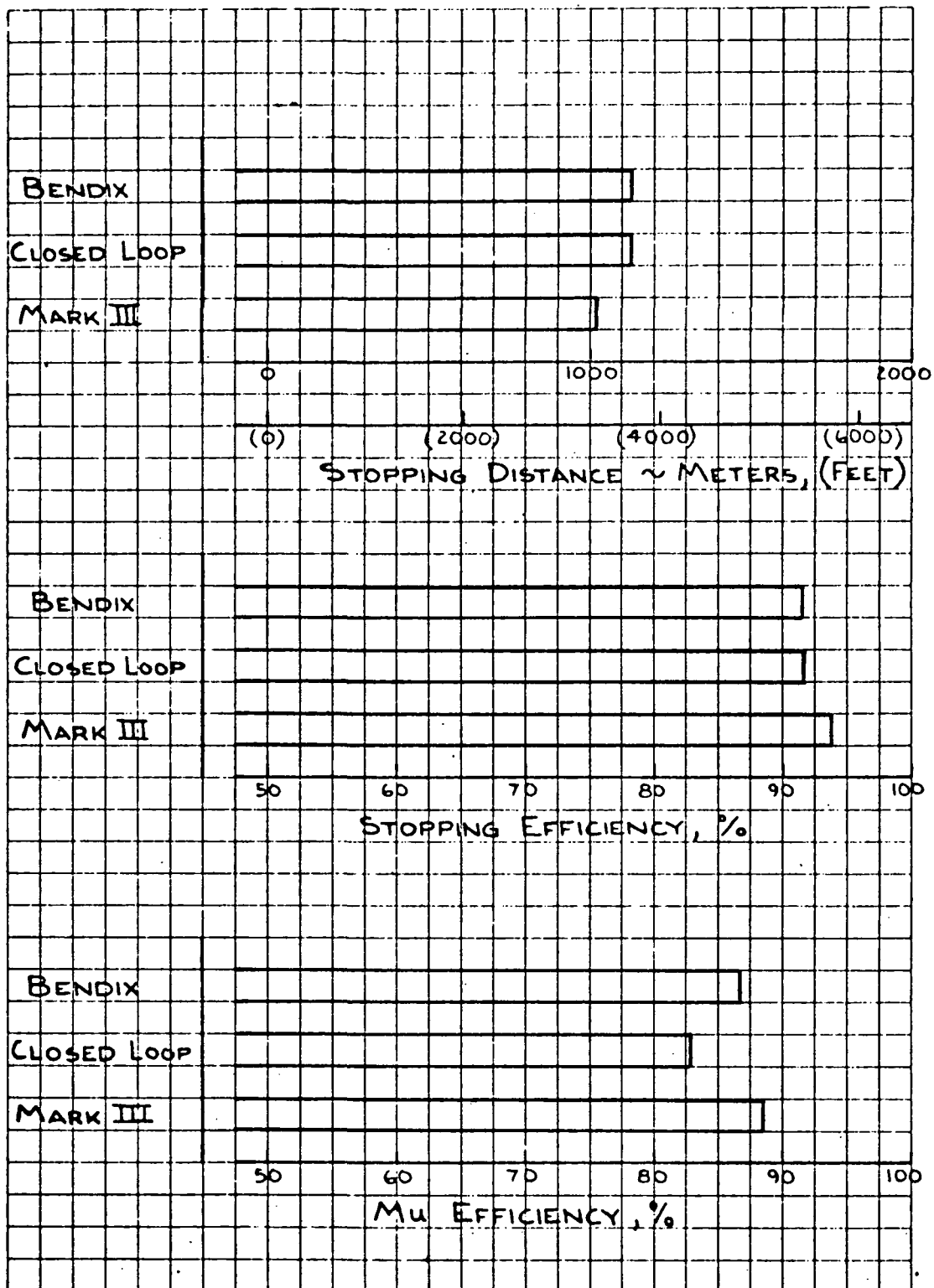


FIGURE 71. PERFORMANCE - ADAPTABILITY TEST 1, .5 MU, 11.5 HZ. STRUT

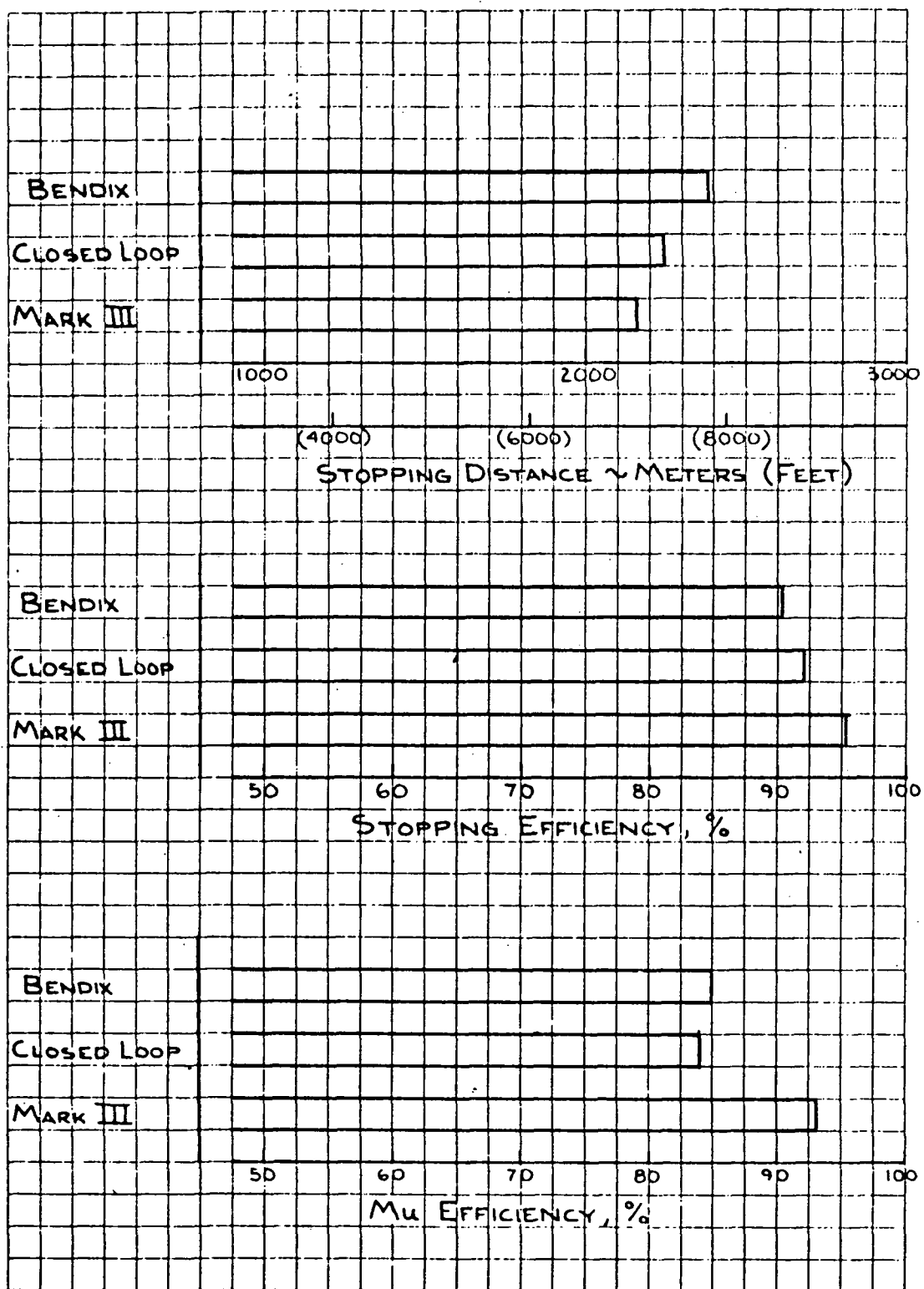


FIGURE 72. PERFORMANCE - ADAPTABILITY TEST 1, .2 MU, 11.5 HZ. STRUT

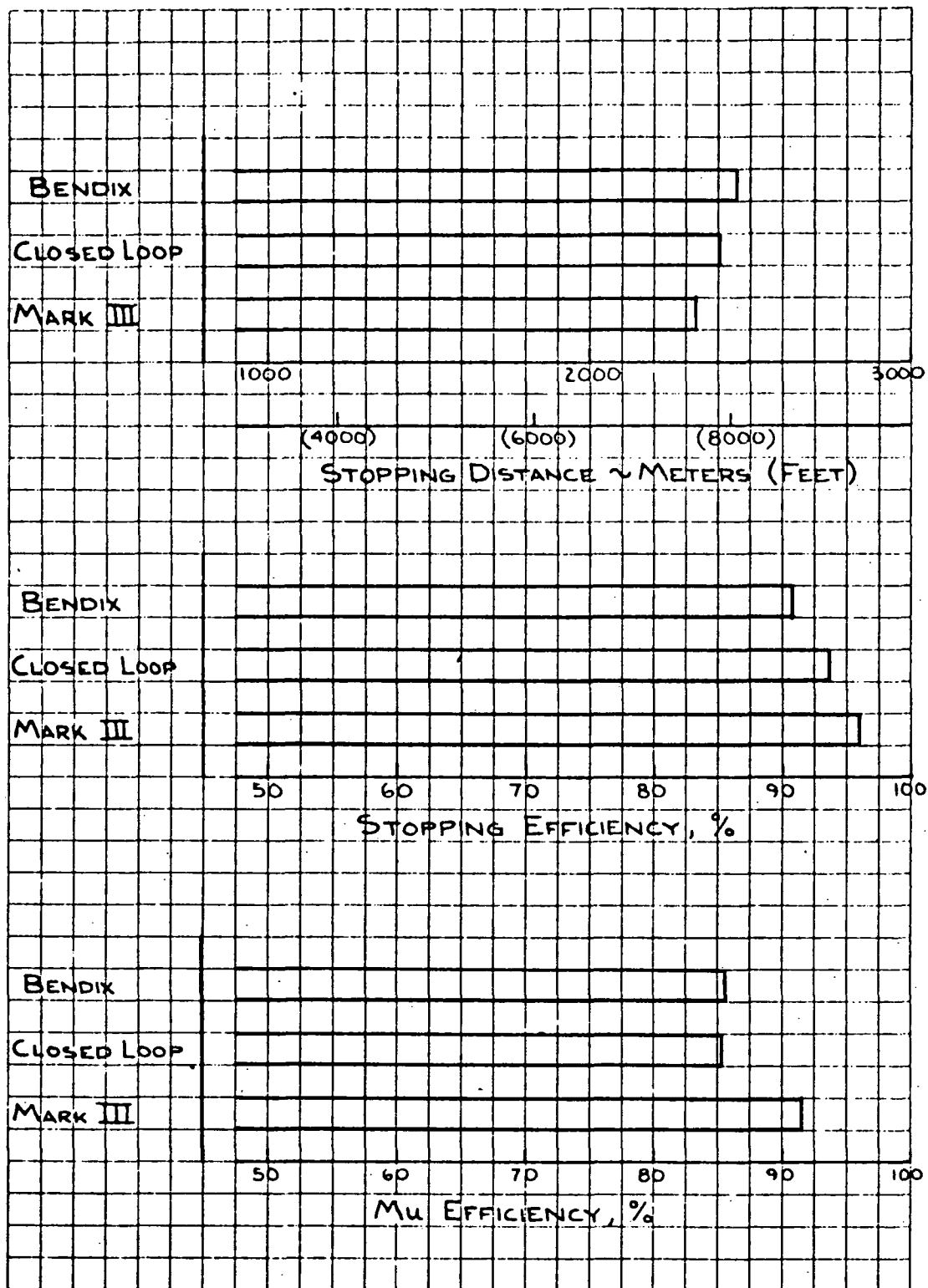


FIGURE 73. PERFORMANCE - ADAPTABILITY TEST 1, CURVE 1, 11.5 HZ. STRUT

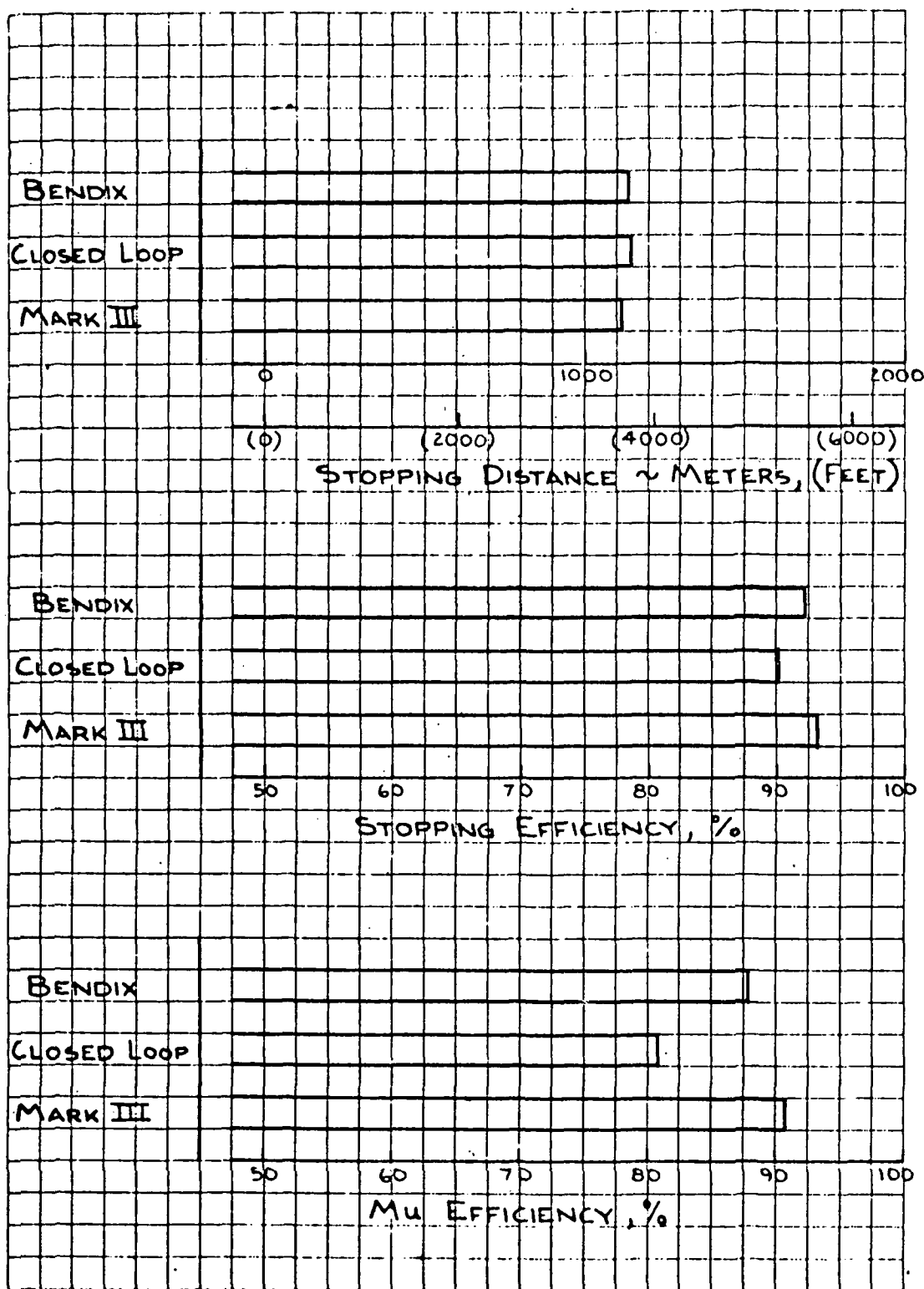


FIGURE 74. PERFORMANCE - ADAPTABILITY TEST 1, .5 MU, 7.5 HZ. STRUT

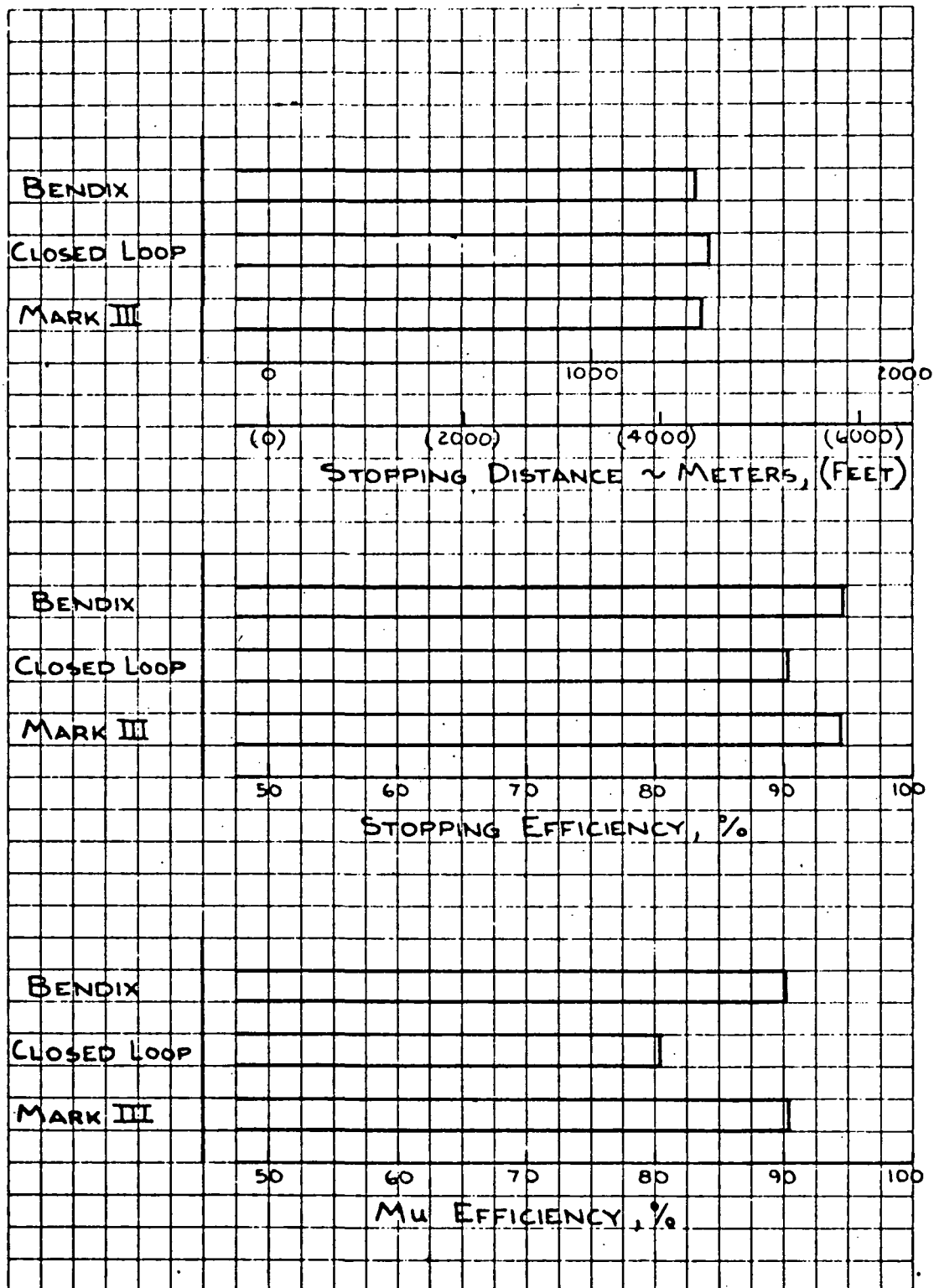


FIGURE 75. PERFORMANCE - ADAPTABILITY TEST 1, .4 MU, 7.5 HZ. STRUT

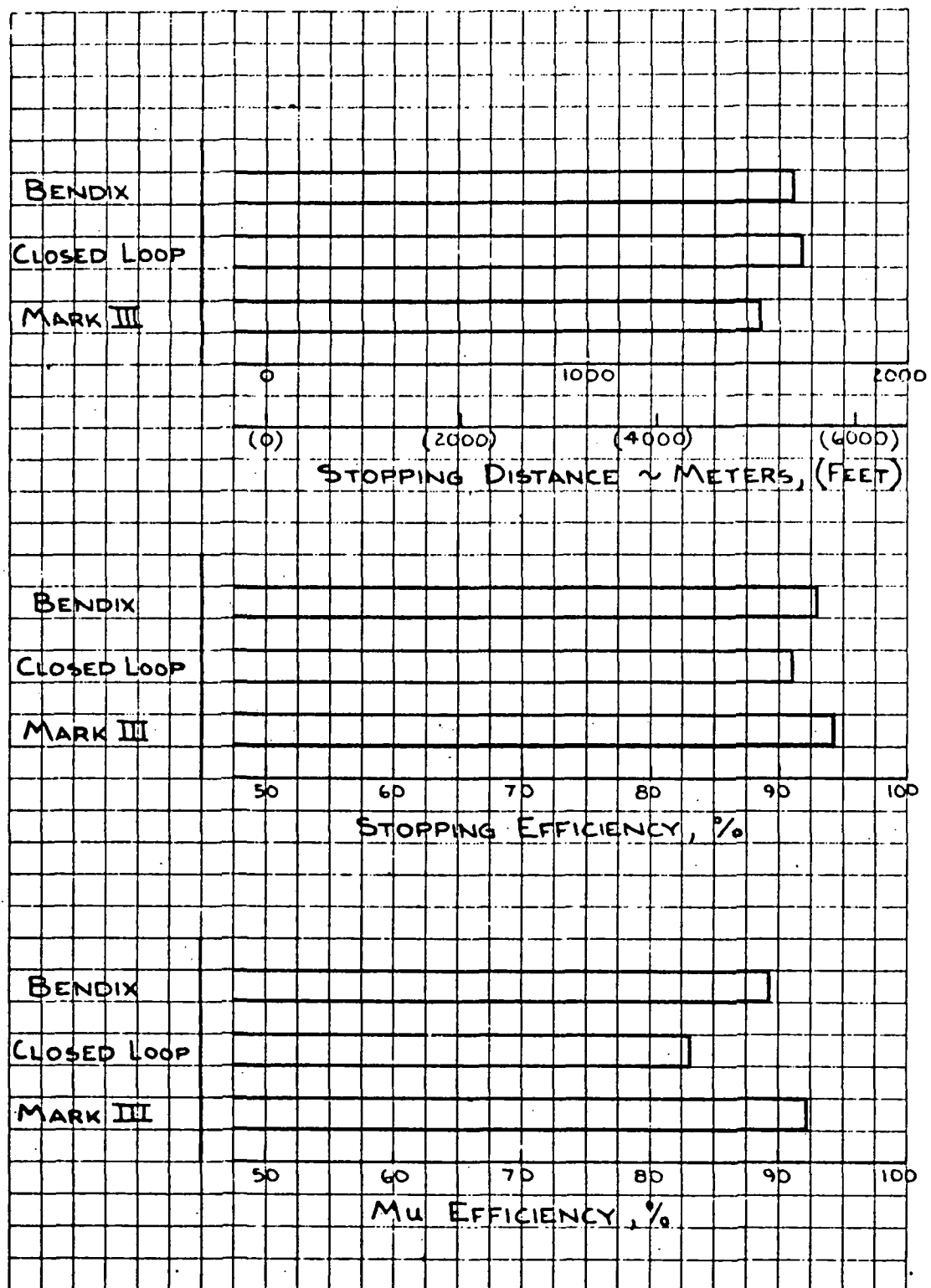


FIGURE 76. PERFORMANCE - ADAPTABILITY TEST 1, .3 MU, 7.5 HZ. STRUT

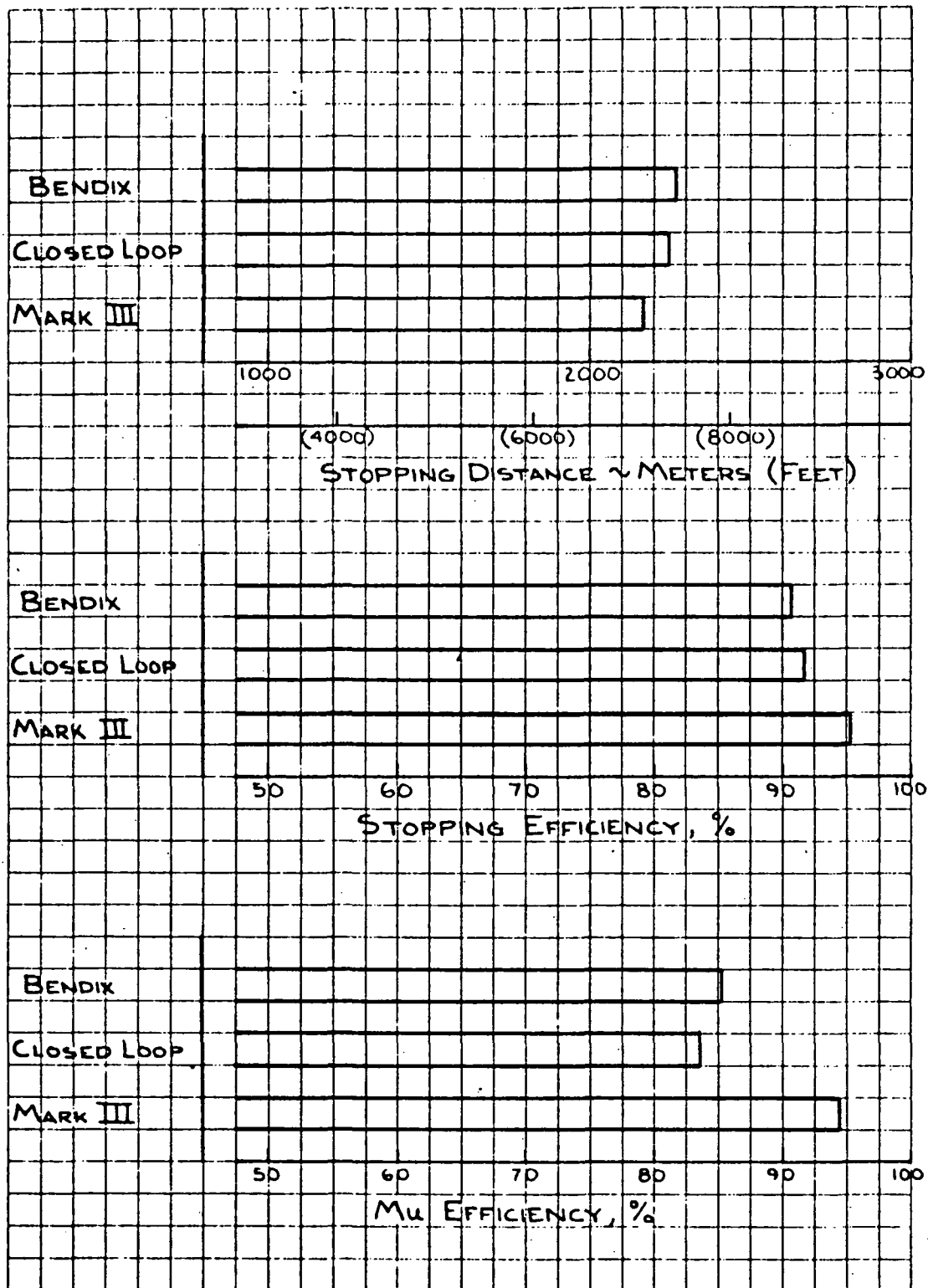


FIGURE 77. PERFORMANCE - ADAPTABILITY TEST 1, .2 MU, 7.5 HZ. STRUT

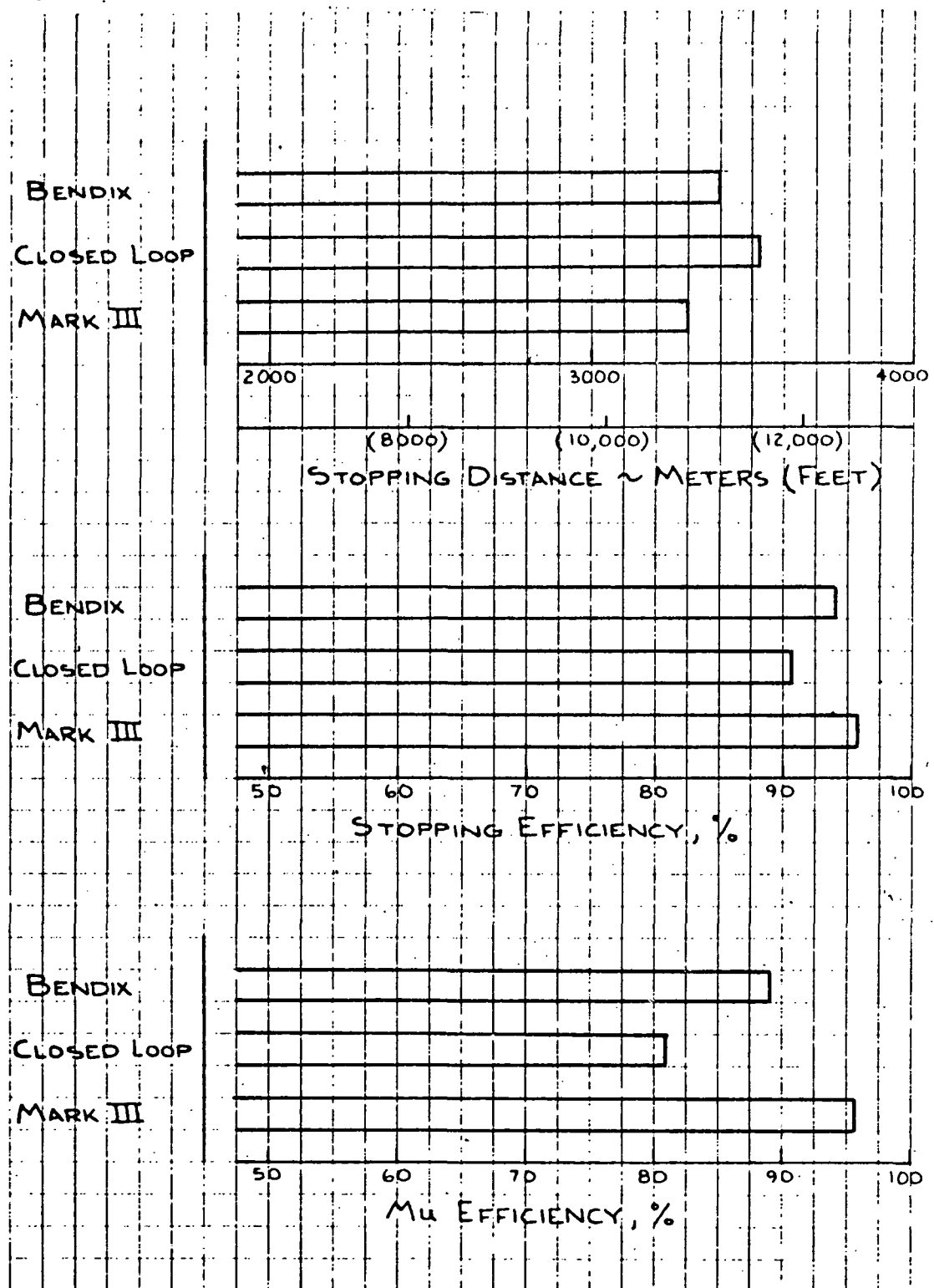


FIGURE 78. PERFORMANCE - ADAPTABILITY TEST 1, .1 MU, 7.5 HZ. STRUT

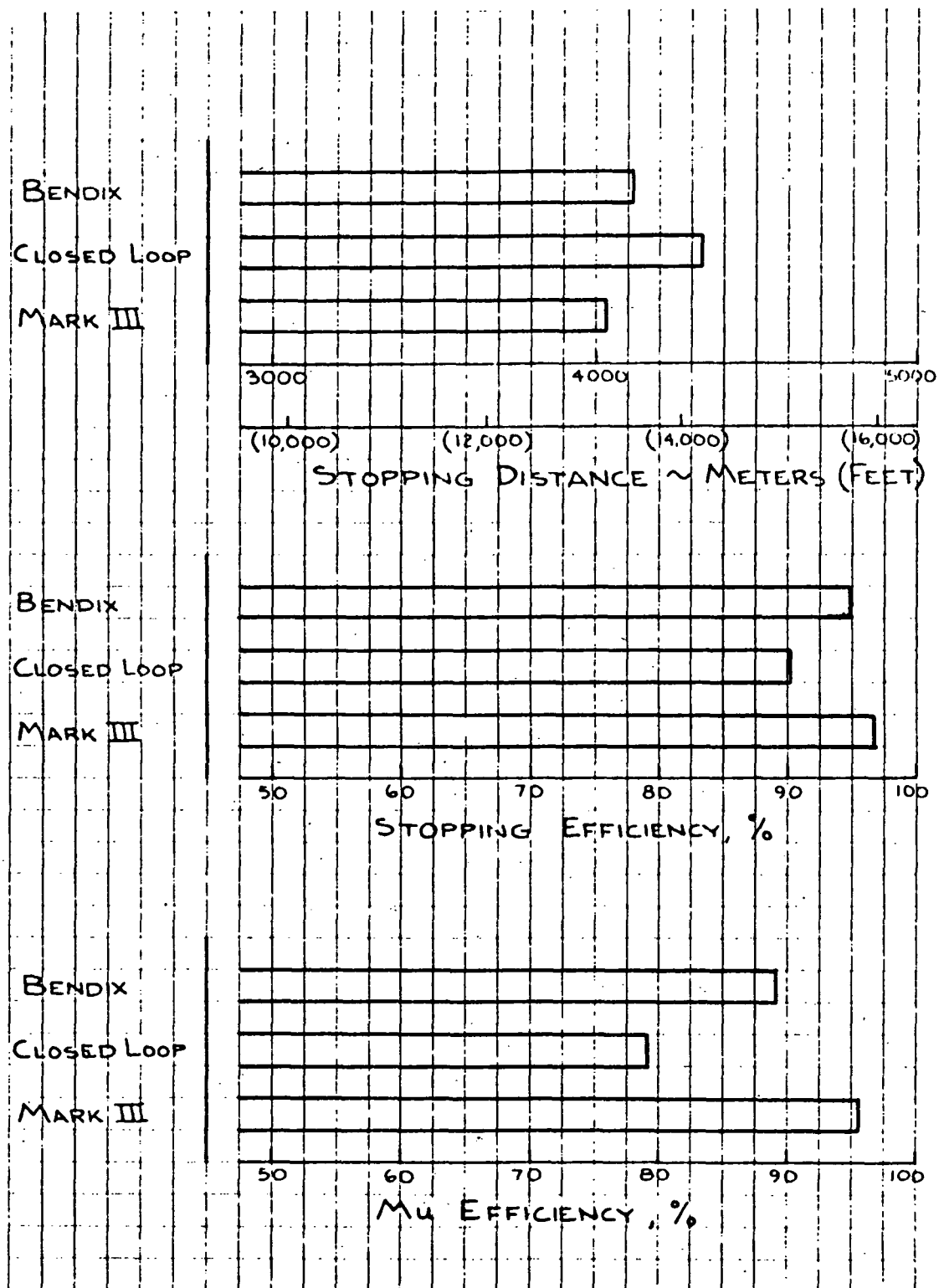


FIGURE 79. PERFORMANCE - ADAPTABILITY TEST 1, .075 MU, 7.5 HZ. STRUT

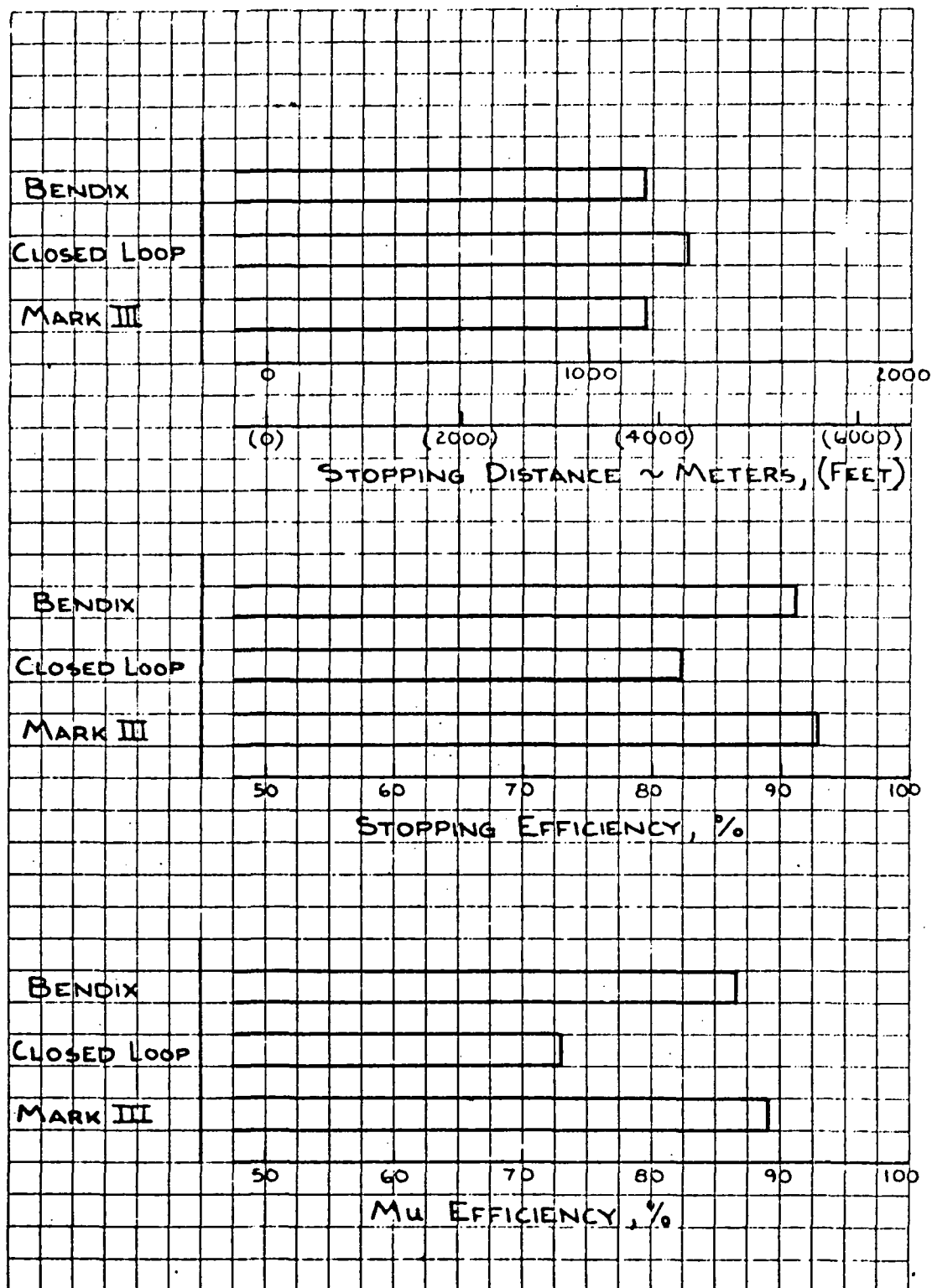


FIGURE 80. PERFORMANCE - ADAPTABILITY TEST 2, .5 MU, 7.5 HZ. STRUT

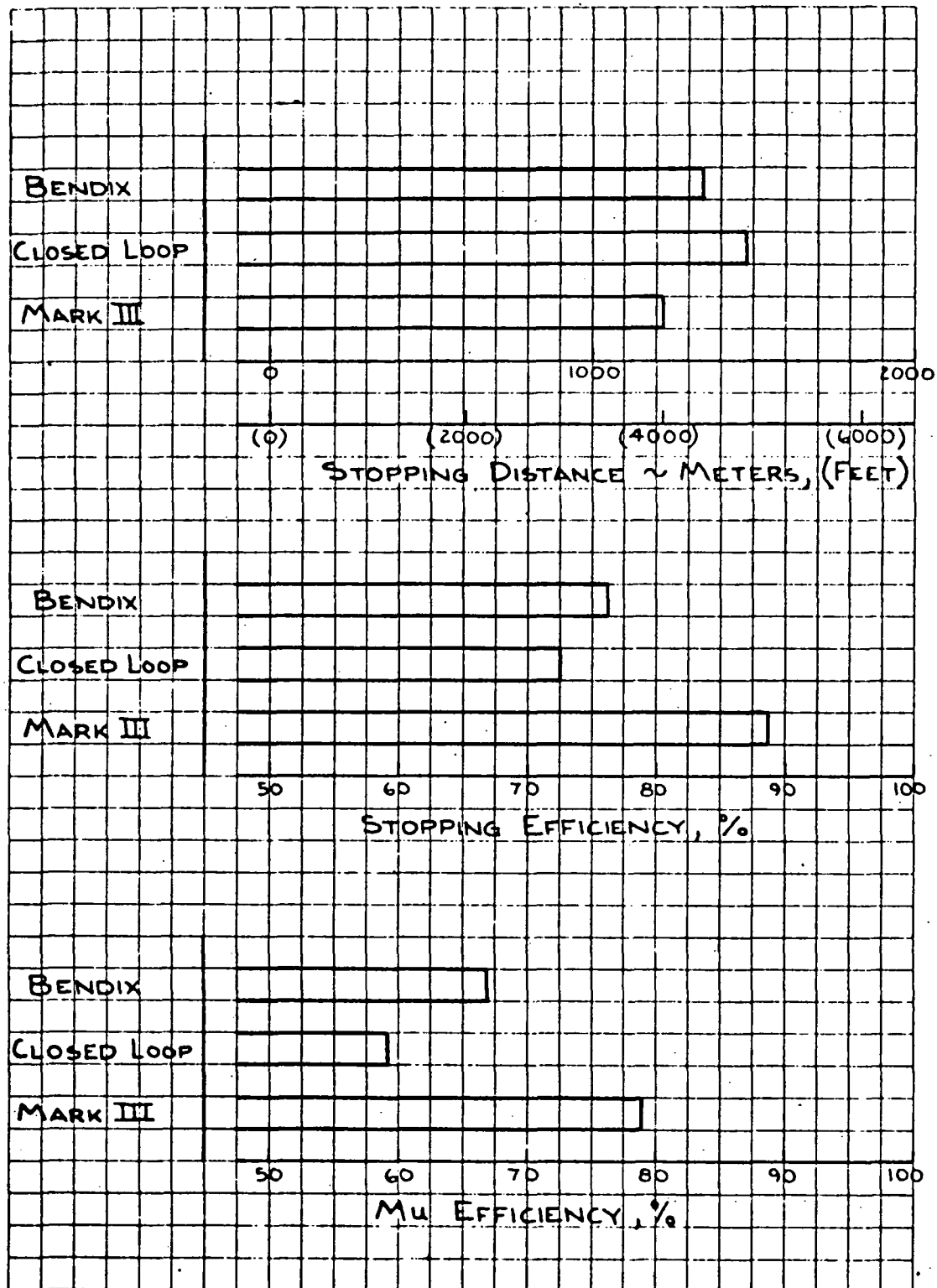


FIGURE 81. PERFORMANCE - ADAPTABILITY TEST 3, 7.5 HZ. STRUT

The remaining tests are called Operational Studies and comprise seven different test configurations. The first test represents wet runway studies and the results of both tests are shown in Figures 82 and 83. Both μ curves used in these tests are velocity dependent and their profiles can be seen in Figure 55. All systems showed relatively high efficiencies. Mark III system showed the highest efficiency and Closed Loop the lowest. Bendix and Closed Loop system had nearly the same stopping distance during the Curve 1 wet runway test. Bendix and Mark III system had nearly the same stopping distance during the same curve 2 wet runway test.

Results of tests 2 through 7 can be obtained by consulting Table V which is the tabulated data. Test 2 represents both the higher and lower gross weights of the Space Shuttle. In general the Closed Loop system showed the least efficiency and both the Bendix and Mark III systems showed the most.

Test 3 represents both the lower and higher wheel inertia. In these tests the Closed Loop system had the lowest efficiency and the Mark III the highest. On the tests with the higher wheel inertia the Bendix system efficiency fell down to the Closed Loop system level on the .2 μ and wet runway curve 1 tests.

In Test 4 the sensitivity to brake torque peaking was tested. Here the Mark III system was the best in stopping distance and efficiency. The Bendix system performed better than the Closed Loop system on .5 μ test but the .2 μ and wet runway tests, the two systems performed the same. In other words the Bendix system suffered more performance loss than expected.

Test 5 represents a tire efficiency heating loss test. Again the same pattern held, namely the Mark III system was the most efficient with the Bendix less than Mark III but better than Closed Loop. The Bendix and Closed Loop systems showed more tendency

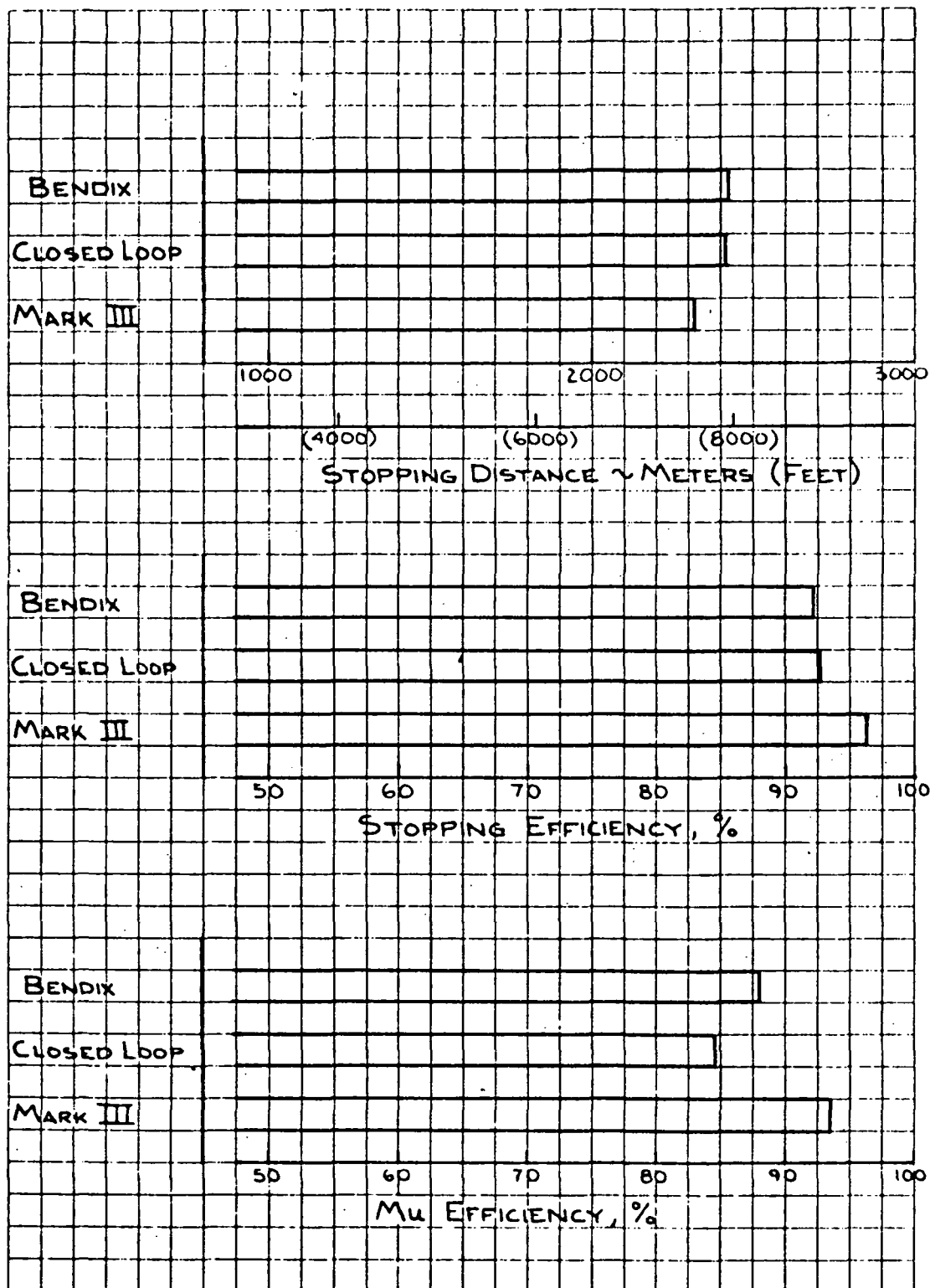


FIGURE 82. OPERATIONAL STUDIES TEST 1, CURVE 1, 7.5 HZ. STRUT

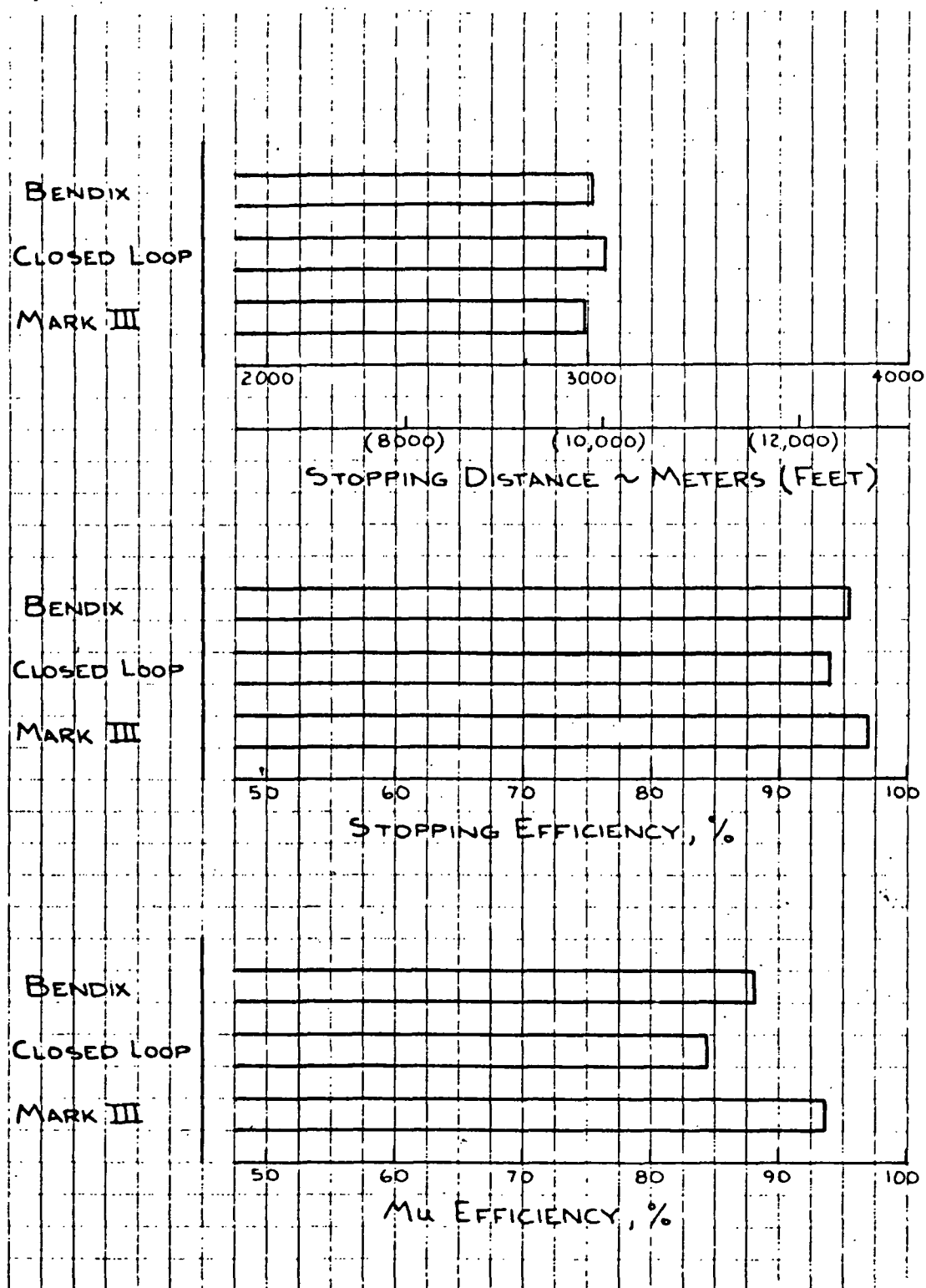


FIGURE 83. OPERATIONAL STUDIES TEST 1, CURVE 2, 7.5 HZ. STRUT

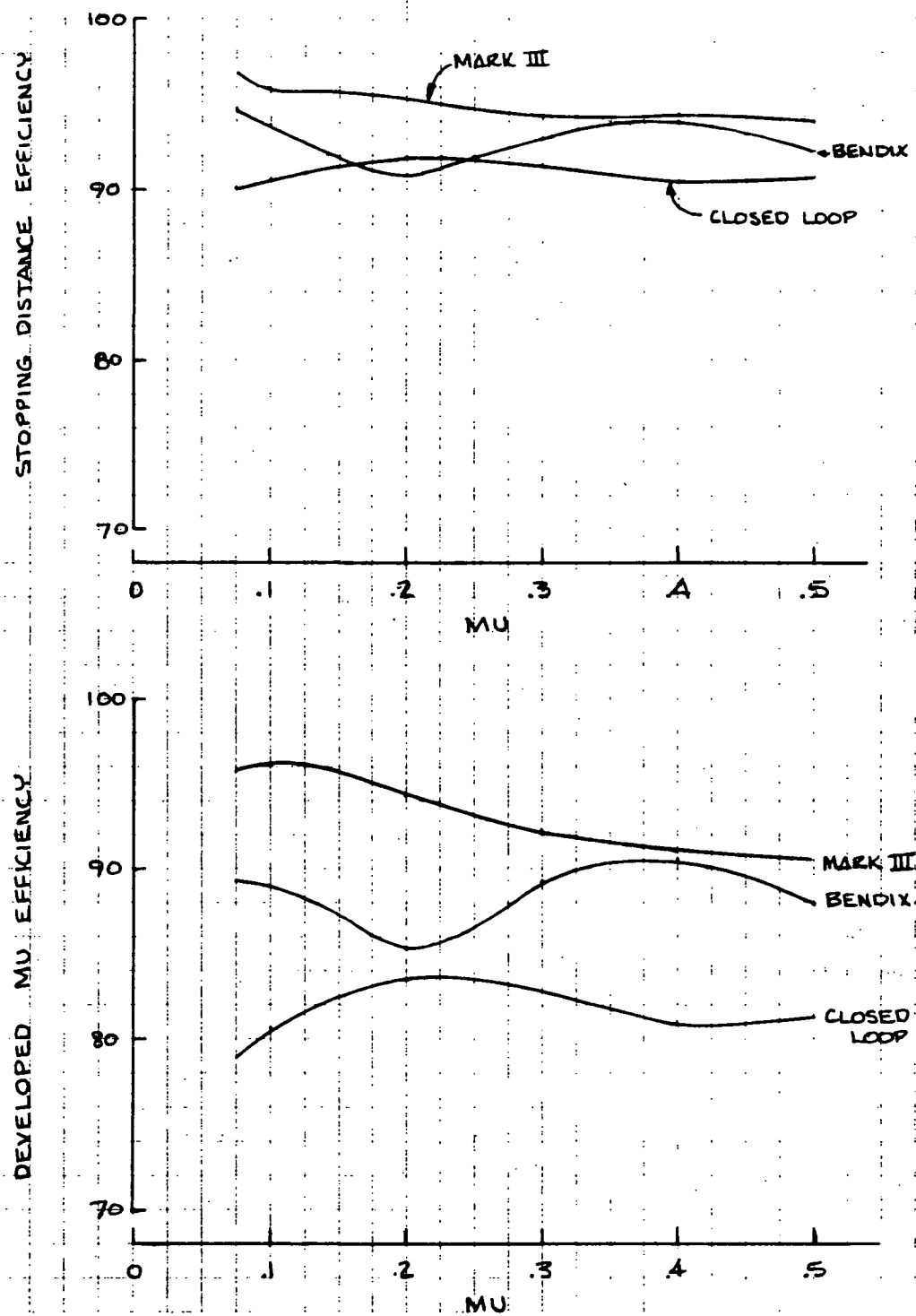


FIGURE 84. EFFICIENCY COMPARISON STABILIZED LANDINGS

to lose performance on the low mu and wet runway tests.

The next two groups of tests dealt with addition and subtraction of energy to the shuttle vehicle. Test 6 deals with deployment of a drag chute while landing while Test 7 deals with the added thrust during braking from engine idle. In general these tests verified the findings earlier that showed Mark III system to be the most efficient of the three with Bendix next and Closed Loop the last. Both Bendix and Closed Loop systems lose efficiency on the .2 mu and wet runway tests.

Discussion of Grading

The grading system used involved assigning certain points to each system for each test condition. The weighting of the points reflects the fact that some tests are considered much more important than others. For instance a system's stability and adaptability are considered far more important than its performance during an ideal stabilized stop. In actual use the antiskid system will be subjected to conditions that are constantly changing. These changes will tax the ability of the system to adapt and stabilize where necessary. Thus the grading points are assigned to grade stability and adaptability tests heavier than the operational tests.

Grading Criteria

To facilitate the interpretation of the results, a grading system based on a total of 230 possible points was used. This grading system was the method used in rating the participating vendors' systems. Each category is broken down into individual tests and the distribution of points was as follows:

| <u>Stability Studies</u> | <u>Points</u> |
|--------------------------|---------------|
| 4.5 Hz. gear | 25 |
| 7.5 Hz. gear | 50 |
| 11.5 Hz. gear | <u>25</u> |
| | 100 Total |

| <u>Performance-Adaptability Studies</u> | <u>Points</u> |
|---|---------------|
| Test 1, 4.5 Hz. gear | 10 |
| Test 1, 7.5 Hz. gear | 25 |
| Test 1, 11.5 Hz. gear | 10 |
| Test 2, | 25 |
| Test 3, | <u>25</u> |
| | 95 Total |

| <u>Operational Studies</u> | <u>Points</u> |
|----------------------------|---------------|
| Test 1, | 5 |
| Test 2, | 5 |
| Test 3, | 5 |
| Test 4, | 5 |
| Test 5, | 5 |
| Test 6, | 5 |
| Test 7, | <u>5</u> |
| | 35 Total |

Grading results shown in Table VII were arrived at by applying the point schedule to Tables V and VI. For each test run the landing efficiency was multiplied times the total points for that test condition. This procedure was used for tests under Performance-Adaptability tests and Operational tests. Grading under Stability tests was more subjective. Consulting Table VI shows what level of computer strut damping was required to reach the limit of operational stability called marginal stability in the table. Since tests could not be run at these low damping ratios another level of damping was chosen for each

TABLE VI COMPARISON OF SYSTEM STRUT DAMPING RATIOS

| ANTISKID SYSTEM | GEAR FREQUENCY | DAMPING RATIO % | COMMENT |
|---------------------|-------------------|--------------------|---------------------------|
| Bendix Slip Command | 4.5 Hz | 0.0% | Marginal stability |
| | | 3.0% | Test run at this damping |
| | 7.5 Hz | 0.3% | Marginal stability |
| | | 3.4% | Tests run at this damping |
| | 11.5 Hz | 1.6% | Marginal stability |
| | | 3.5% | Tests run at this damping |
| Boeing Closed Loop | 4.5 Hz | 3.0% | Marginal stability |
| | | 5.0% | Tests run at this damping |
| | 7.5 Hz | - .6% | Marginal stability |
| | | 3.5% | Tests run at this damping |
| | 11.5 Hz | 0.8% | Marginal stability |
| | | 4.0% | Tests run at this damping |
| Hydro-Aire Mark III | 4.5 Hz | 0.0% | Marginal stability |
| | | 4.0% | Tests run at this damping |
| | 7.5 Hz | 0.8% | Marginal stability |
| | | 4.0% | Tests run at this damping |
| | 11.5 Hz | 2.7% | Marginal stability |
| | | 5.0% | Tests run at this damping |

system to conduct the rest of the tests. Both damping ratios were taken into consideration when the grading was done.

The total points each system earned appears at the bottom of Table VII. It shows that both the Bendix and Hydro-Aire Mark III system to be nearly equal in points total. This should not be construed to mean that their performance was equal. In the majority of tests the Mark III system was the better performer in terms of landing distance but also noteworthy, the spread in distance was not great. Where the Bendix system excelled over Mark III was stability. It provided more active damping to the overall system such that a lower damping ratio could be sustained in the simulation.

The results of the Boeing Closed Loop system in the grading was third place. This system in its present state of development has not been flight tested. Before the present improvements were made, the system was never certified, although it was flight tested. The improved system is also not certified, but it does show promise and with some further work could easily become a credible brake control system.

TABLE VII SPACE SHUTTLE GRADING

Stability Studies

| | BENDIX | BOEING C.L. | H.A. MK III | TOTAL POSSIBLE |
|---------------------|-----------|-------------|-------------|-------------------|
| Test 1 4.5 Hz | 23 | 10 | 21 | 25 |
| Test 2 7.5 Hz | 43 | 47 | 40 | 50 |
| Test 3 11.5 Hz | <u>21</u> | <u>23</u> | <u>20</u> | <u>25</u> |
| Subtotal | 87 | 80 | 81 | 100 |

Performance - Adaptability Studies

| | | | | |
|---------------------|-------------|-------------|-------------|-----------|
| Test 1 4.5 Hz | 9.1 | 9.0 | 9.5 | 10 |
| Test 1 11.5 Hz | 9.1 | 9.2 | 9.5 | 10 |
| Test 1 7.5 Hz | 23.3 | 22.7 | 23.8 | 25 |
| Test 2 | 22.8 | 20.6 | 23.4 | 25 |
| Test 3 | <u>19.1</u> | <u>17.5</u> | <u>22.2</u> | <u>25</u> |
| Subtotal | 83.4 | 79.0 | 88.6 | 95 |

Operational Studies

| | | | | |
|----------|------------|------------|------------|----------|
| Test 1 | 4.1 | 4.0 | 4.1 | 5 |
| Test 2 | 4.0 | 3.7 | 4.5 | 5 |
| Test 3 | 3.9 | 3.7 | 4.3 | 5 |
| Test 4 | 3.8 | 3.7 | 4.2 | 5 |
| Test 5 | 3.8 | 3.5 | 4.1 | 5 |
| Test 6 | 4.0 | 3.8 | 4.3 | 5 |
| Test 7 | <u>3.8</u> | <u>3.6</u> | <u>4.2</u> | <u>5</u> |
| Subtotal | 27.4 | 26.0 | 29.7 | 35 |
| Totals | 198 | 185 | 199 | 230 |

VII. SPACE SHUTTLE HARDWARE CRITERIA

What in the way of hardware is needed to implement an antiskid system for the space shuttle? Assume for the sake of this discussion that such design items as the tire, wheel, brakes, main gear strut, aerodynamics and hydraulic system are already firmly determined. This leaves the brake actuation system, hydraulic supply and return, wheel speed transducer and antiskid control card, antiskid valve and brake (its dynamic related properties) to be selected and determined. Each of these items will be discussed separately and where practical, supporting laboratory data presented. The Boeing Closed Loop system was used to conduct a sensitivity analysis to determine what effect these hardware components have on the total system performance, stability and safety.

It is assumed that this Space Shuttle system will utilize a "brake-by-wire" actuation system. The normal pilot control cables will not be used to meter or actuate brake pressure. Instead pedal transducers will receive pedal inputs from the pilot. The electrical signal from the transducers will be processed and transmitted to the antiskid valves individually or to a separate metering valve if it is used.

Instead of the conventional cable rigging originating at the pilot's pedals and transmitting signals to a metering valve, the individual valves become metering valves. In other words an additional electrical signal is sent to each valve relaying pilot's input signals. In conjunction with this signal is the conventional antiskid signal which is free to modulate brake pressure in the event the pilot's signal exceeds the ground mu capability of the braked wheel and it begins to decelerate too rapidly.

Since this system would eliminate the metering valves and cable rigging and replaces them with this electrical transmitting system, certain safeguards must be built into the systems. One proposal would be to have tripple redundant pedal transducers attached to each

pilot's pedals. All position transducers would transmit their respective signals to a receiving circuit which would then vote or select which signal or pair of signals to send to the valves. This voting scheme is necessary to eliminate one bad signal from disturbing the true pedal position signal. An accepted means of implementing this is called "mid-value logic" and it requires tripple redundant input signals. It chooses the correct signal by comparing any two agreeing signals and rejects the third. An exhaustive analysis of a brake-by-wire system is really outside the scope of this discussion except that it is mentioned here for the sake of completeness. The pilot brake pedal input will be assumed available to the antiskid system throughout the rest of this analysis. If the actuation system incorporates a separate metering valve, it will be assumed to have sufficient flow and to have no tendency to self excite or oscilate that portion of the hydraulic system pertinent to the brake control system.

Items that do have significant importance in the antiskid system are the servo valve, wheel speed transducer, brake assembly and hydraulic system. These hardware items play an extremely important function in determining the antiskid performance. Their total impact will also depend on which antiskid control circuit is used. For this study the Boeing Closed Loop system was the only one used.

ANTISKID VALVE

The antiskid valve chosen for the space shuttle must meet some tolerance or sensitivity objectives. Some of the more important ones deal with sensitivity to vibration and hydraulic back pressure. The successful valve must not show failure or loss of performance to expected levels of mechanical vibration or hydraulic back pressure. In addition there are different types of valves such as pressure control or flow control, overlap or underlap, and jet pipe or flapper nozzle. The conventional valve used in commercial jet transport antiskid systems is the pressure control type and most systems use a flapper type first stage design. Although the Bendix system uses a

jet pipe first stage its second stage is the conventional pressure control type.

These specific details of valve design are not intended for discussion in this report except to indicate that the valve type used must be capable of efficient pressure modulation in the expected frequency range and step function response range. Quiescent antiskid valve leakage is an important aspect in commercial aircraft from the standpoint of parking. When all hydraulic power is shut off the accumulator in the hydraulic system maintains sufficient pressure to the brakes to allow a locked brake parking mode. Excessive antiskid valve leakage would prevent the accumulator from maintaining its charge for any length of time. This parking mode might not be a consideration for the space shuttle so the discussion will continue with other performance aspects of the antiskid valve.

Two different valve types will be compared in this study, overlapped and underlapped. The Boeing Closed Loop system was run with both valves and comparative data will be presented. Pressure gain plots were taken with each valve as well as brake release and fill pressure recordings were taken. In addition, brake pressure frequency response data were taken for each valve. Comparing and analyzing these data will demonstrate the performance and dynamic differences of these two valve types.

In describing these different hydraulic, brake and antiskid valve configurations, keep in mind that the normal configuration referred to in this study consists of the 432 cm (170 in.) brake line length, 3-way antiskid valve, 747A brake and Boeing Closed Loop System. This is the system configuration used during testing of the Boeing Closed Loop system conducted and reported in Section VI.

The pressure gain curve shown in Figure 85 is representative of an underlapped valve (See Figure 8 for more details on this 3-way valve). Pressure change from fully opened 211 kg/cm^2 (3000 lbs/in^2)

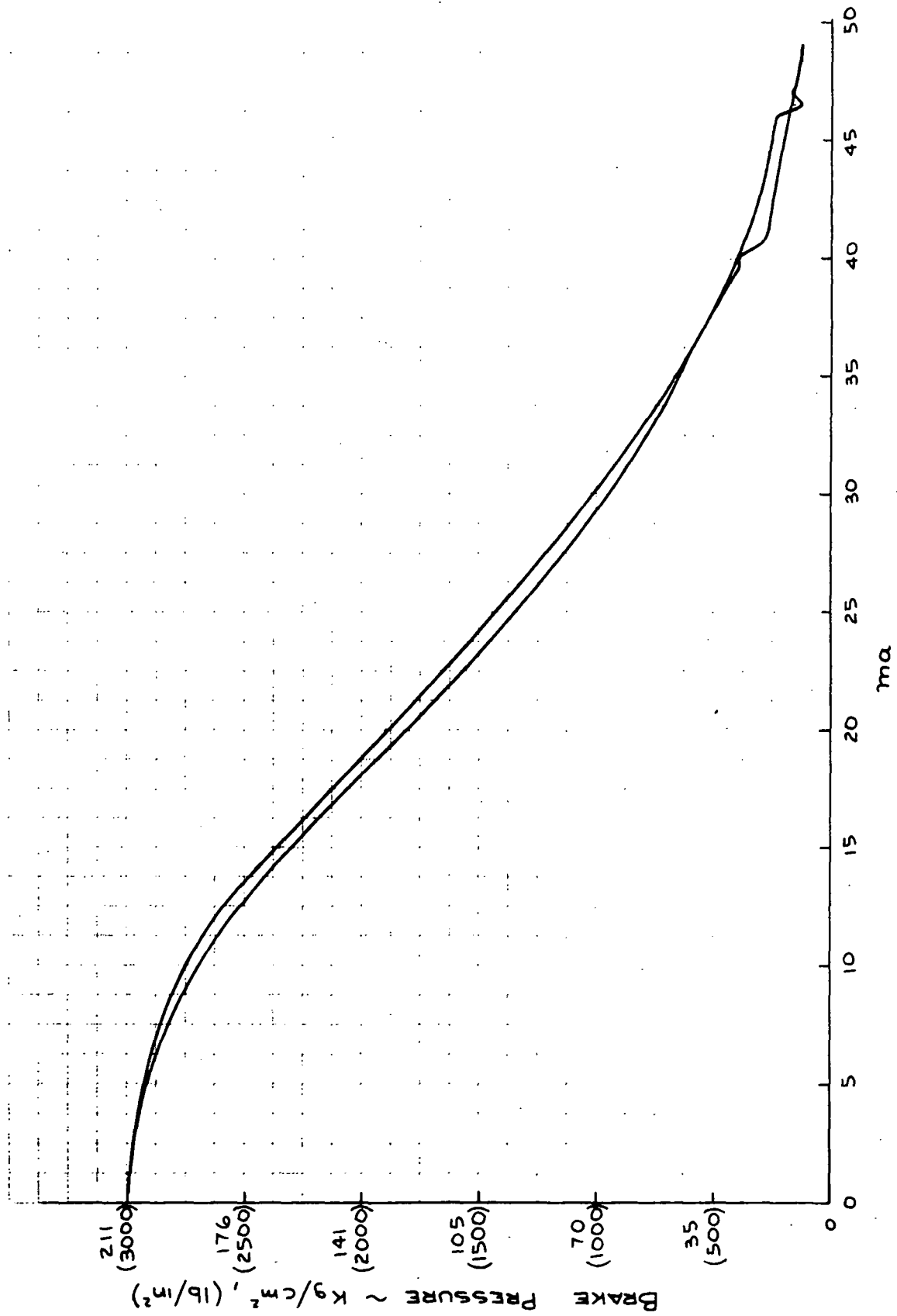


FIG. 85 SPACE SHUTTLE 3-WAY VALVE SN 211

pressure down to reservoir pressure is characterized by a smooth transition. Hysteresis throughout the operating range of the valve is kept to a minimum so that whether the direction of pressure change is from low to higher or high to lower, any given current signal to the first stage will yield a closely determined pressure. This becomes especially important for wet runway performance. The pressure gain plot of the 737 Goodyear overlapped valve is shown in Figure 86. This valve functionally is the same as the valve used on the Boeing 747 antiskid system and is shown in Figure 5. Where the Goodyear valve differs is that it has an overlapped spool design whereas the 747 anti-skid valve is underlapped. Comparing the pressure gain curve in Figure 86 with the curve in Figure 85 indicates the differences in the valve designs. The overlapped valve has a characteristic lack of smoothness plus some very wide hysteresis at the low pressure, high current region. (Note that this valve requires only 20 milliamperes full signal while other valves require 50. This just reflects the difference in the first stage electrical impedance). Also the characteristic "S" shape of the three way valve is not necessarily characteristic of an underlapped valve in general. It is the particular shape and characteristic of this three way valve only.

The normal Space Shuttle hydraulic system with the 747 brake was operated with both the Hydro-Aire 3-way valve and the Goodyear valve. Figures 87 and 111 are the resultant frequency response plots. Since both plots were made by operating the system about 105 kg/cm^2 (1500 lbs/in^2) the overlap characteristic of the Goodyear valve was not apparent. This pressure as seen in Figure 86 is in a region of very little hysteresis. The Goodyear valve has less damping (See Figure 87) than the 3-way valve (See Figure 21). This means the gain is higher in the Goodyear valve up to about 12 Hz and the phase lag is lower with the Goodyear valve up to about 8.5 Hz. than the 3-way valve. The 3-way valve has more damping and above 9 Hz. has less phase lag than the Goodyear valve. These characteristics translate themselves into the performance shown in Figure 88. The Closed Loop system

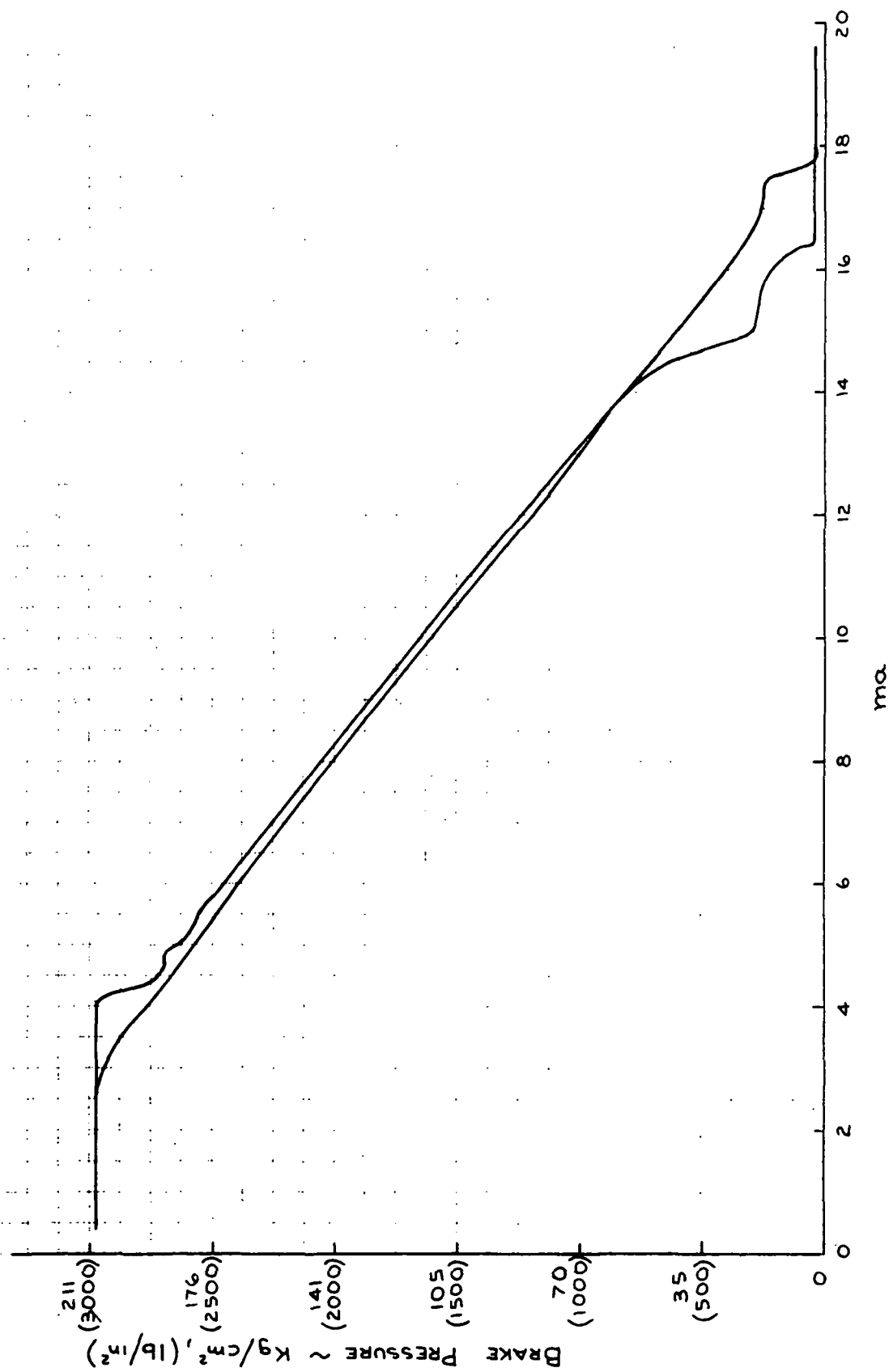


FIG. 86 SPACE SHUTTLE GOODYEAR 737 VALVE

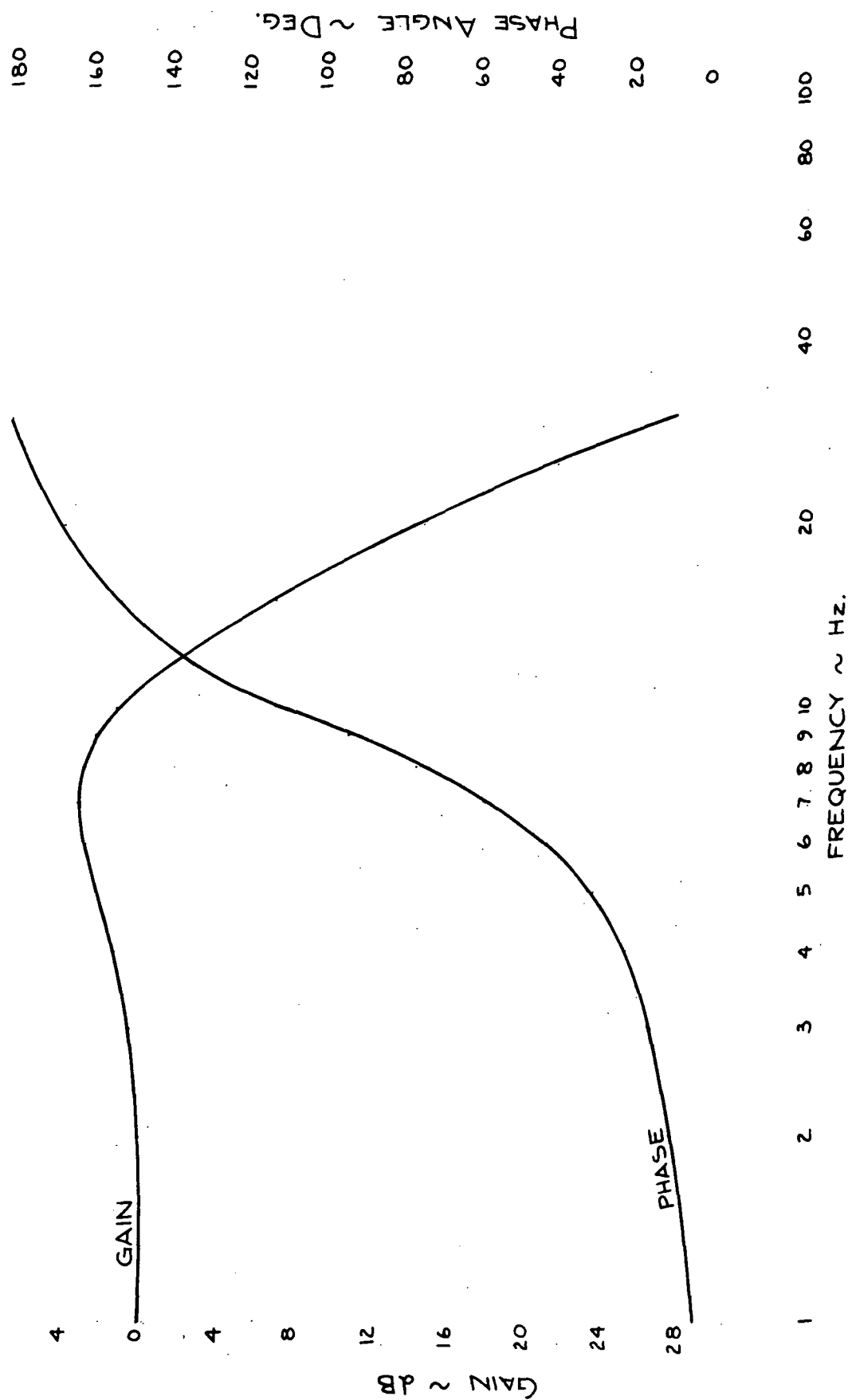


FIG. 87 SPACE SHUTTLE HYDRAULIC FREQUENCY RESPONSE
WITH GOODYEAR 737 VALVE S.N. 99

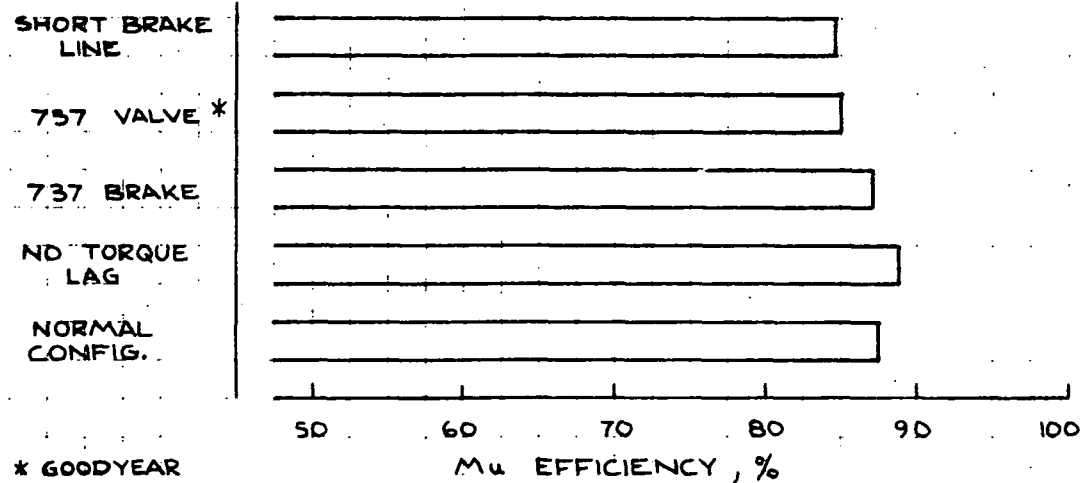
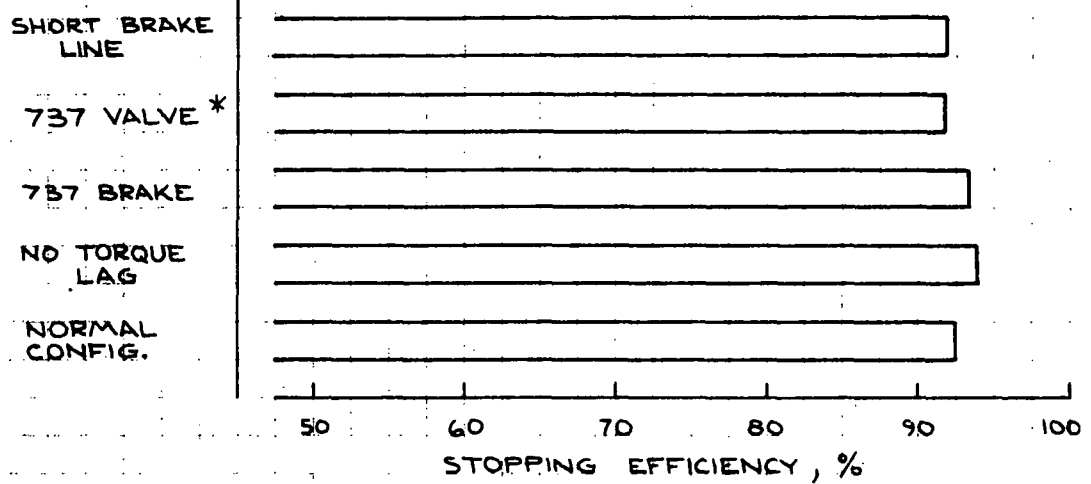
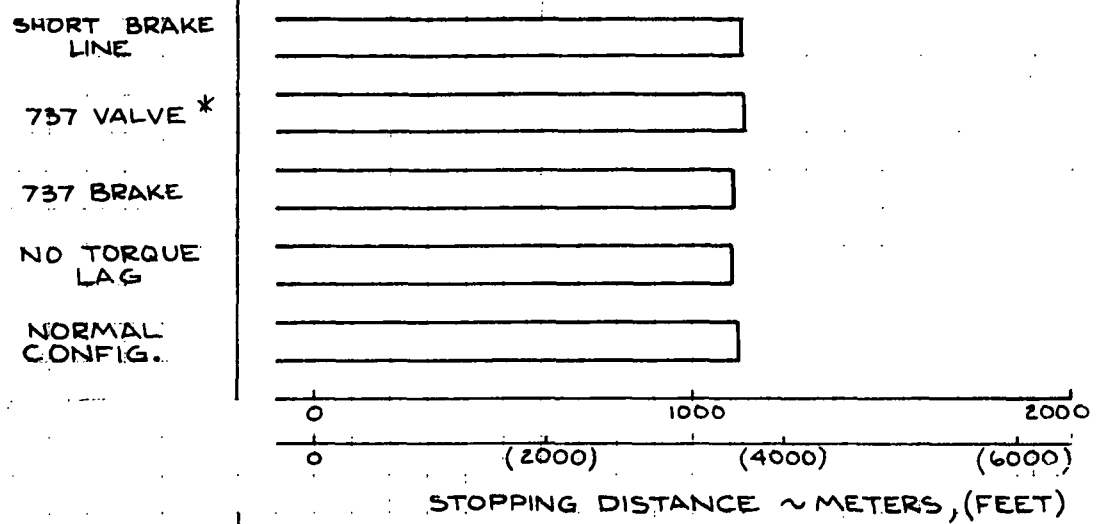


FIG. 88 .5 MU CLOSED LOOP SYSTEM SENSITIVITY STUDY

was run with each valve (tuned for maximum performance for each condition run) and the results on dry runway are very similar. The 3-way valve just slightly out performs the Goodyear valve.

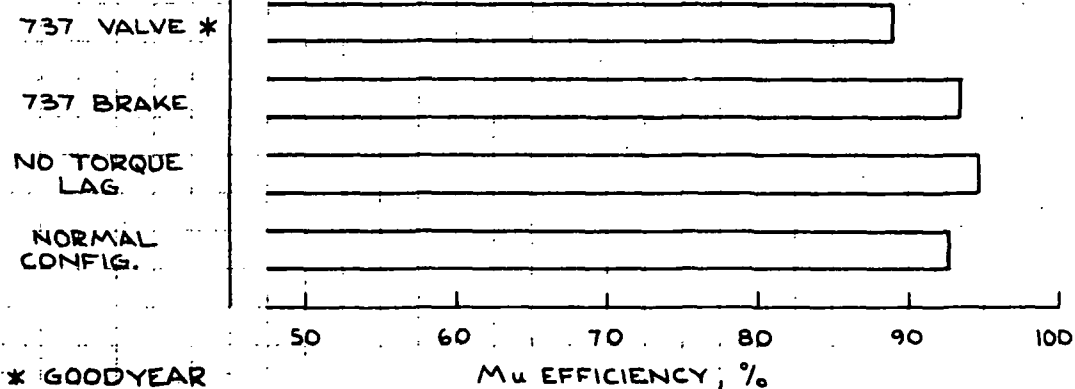
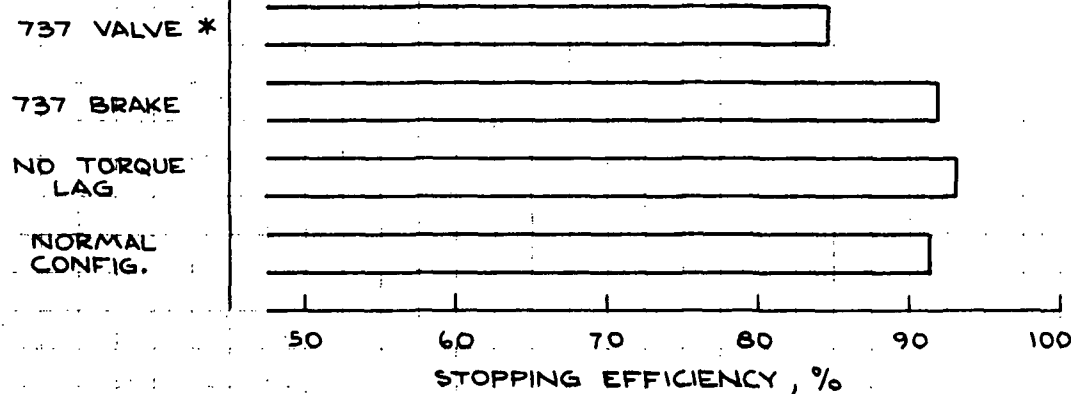
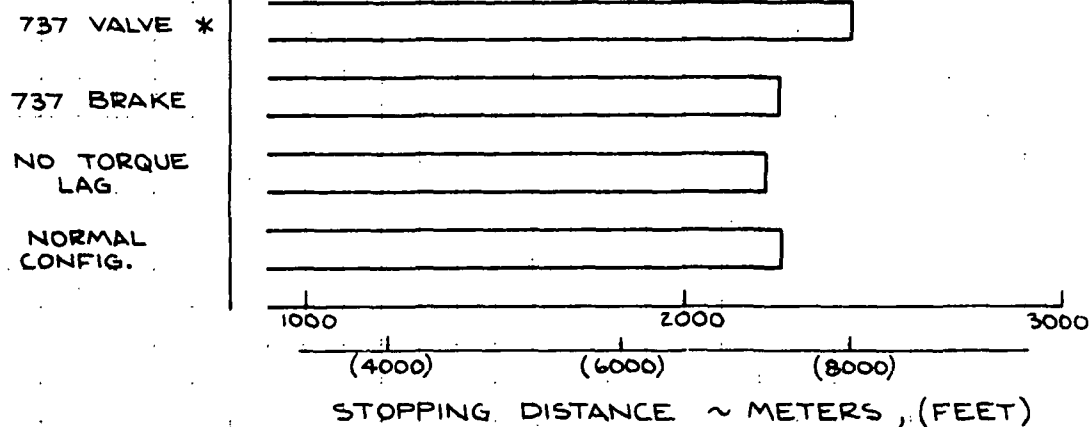
Figures 89 and 90 show the performance on low μ and wet runway conditions. Here the 3-way valve is decidedly superior. The 3-way valve can also be expected to provide better stability for a system since its phase lag above 9 Hz. is less than the Goodyear valve.

Stepdown and step up response tests with the 747 brake and Goodyear valve (see Figure 92 and 93) are compared with the response of the 3-way valve and 747 brake. The Goodyear valve is more sluggish to respond both up and down than the 3-way valve. This test really shows up the performance difficulty with an overlapped valve. This also helps explain the wet runway and low μ performance deterioration of the Goodyear valve.

BRAKE DYNAMICS

Assuming that Space Shuttle brake energy requirements dictate the brake heat sink weight and remaining torque requirements, what can the antiskid system expect from the brake in the way of hydraulic brake actuation response? To maximize braking efficiency the antiskid system wants a brake that gives good frequency response and good step function response. It also wants a brake that doesn't provide excessive squeal or chatter or has unnecessary hysteresis or torque peaking. Several test combinations were set up and run to show what trends and what extent the brake features into antiskid performance.

Figure 91 shows a plot of brake pressure versus volume for the 737 and 747 brake. Physically the 737 brake is much smaller than the 747 and as might be expected there exists considerable difference in the brake volumes. This difference translates into step response performance difference. Using the same 3-way valve the step down response (see Figure 92) and step up response (see Figure 93) tests were



* GOODYEAR

FIG. 89 .2 MU CLOSED LOOP SYSTEM SENSITIVITY STUDY

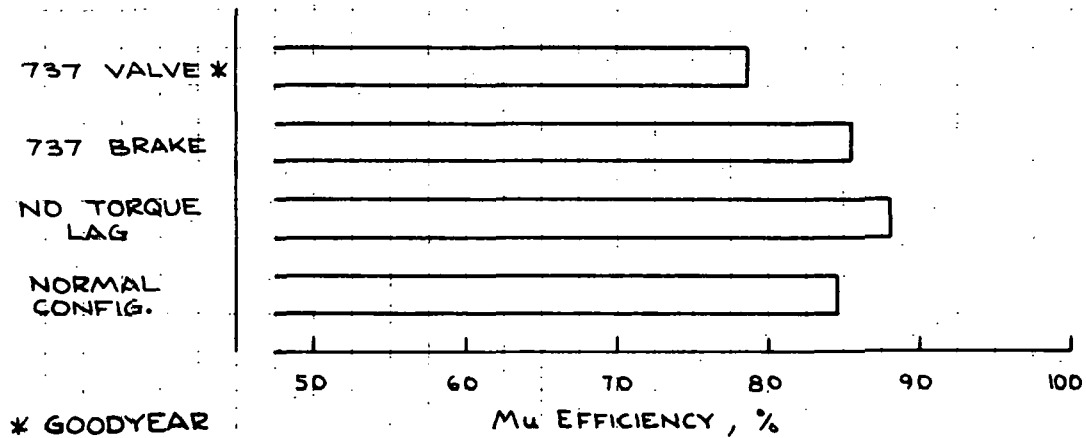
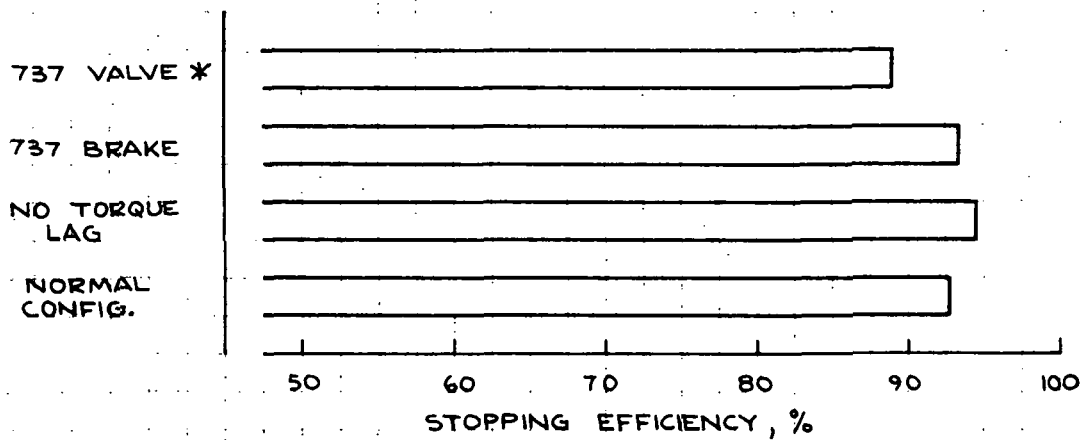
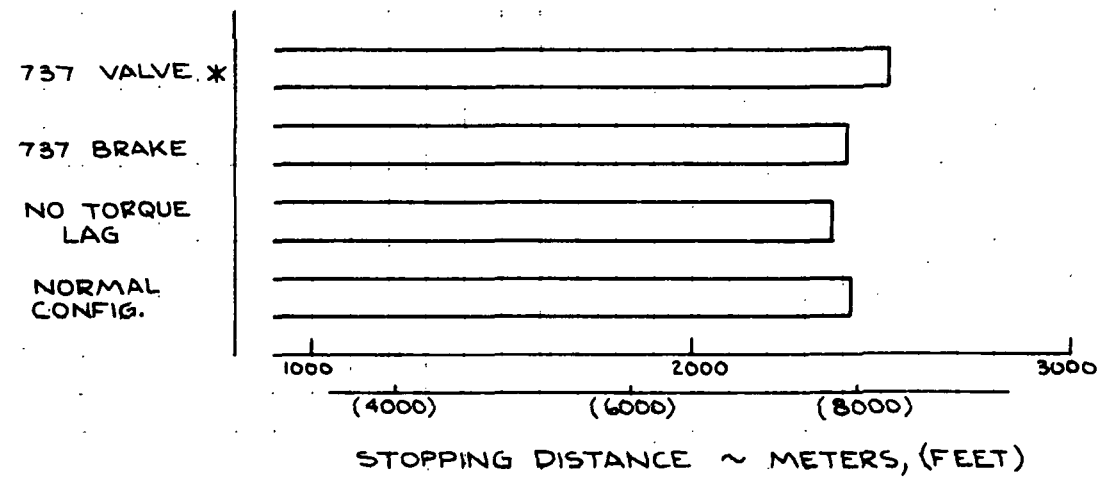


FIG. 90 WET RUNWAY (CURVE 1) CLOSED LOOP SENSITIVITY STUDY

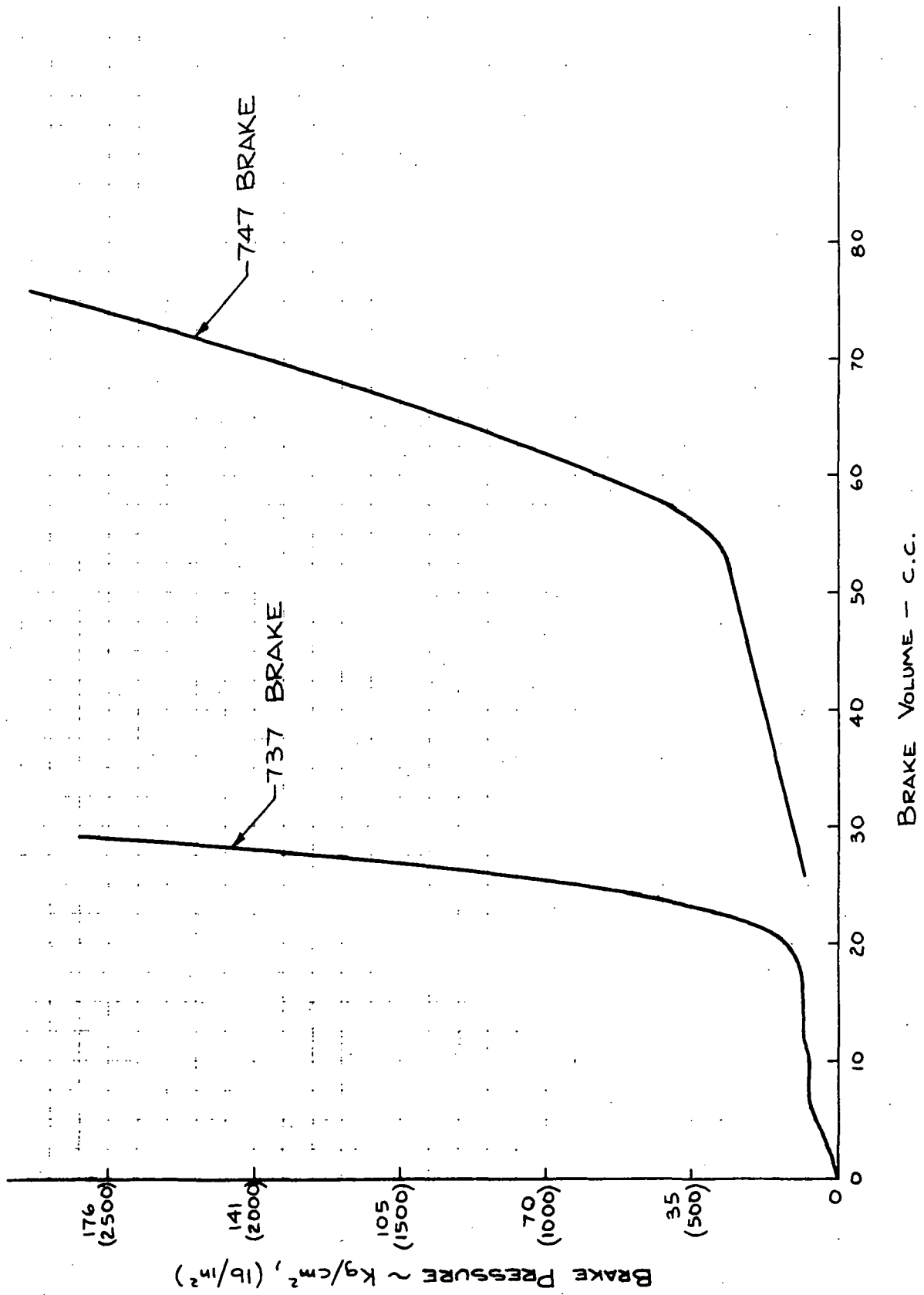


FIG. 91 SPACE SHUTTLE - 737 AND 747 BRAKE

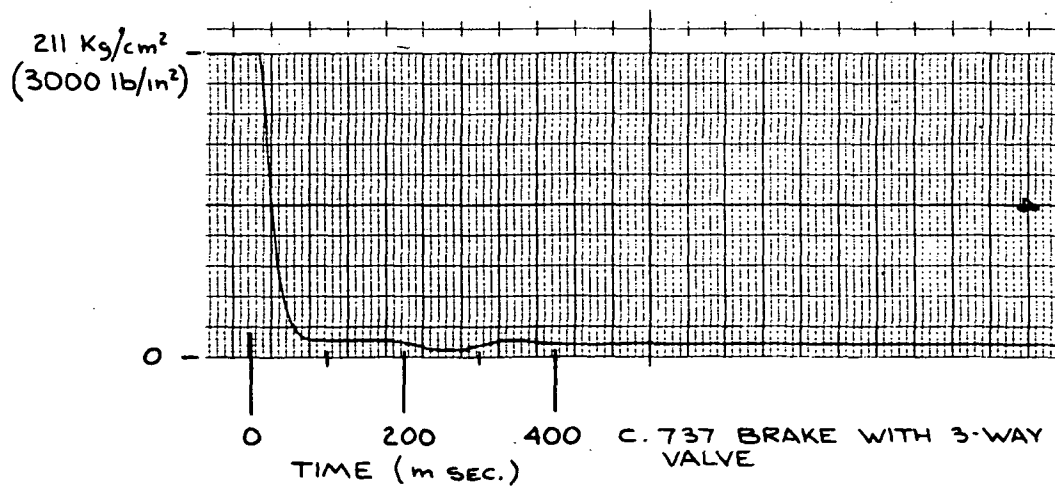
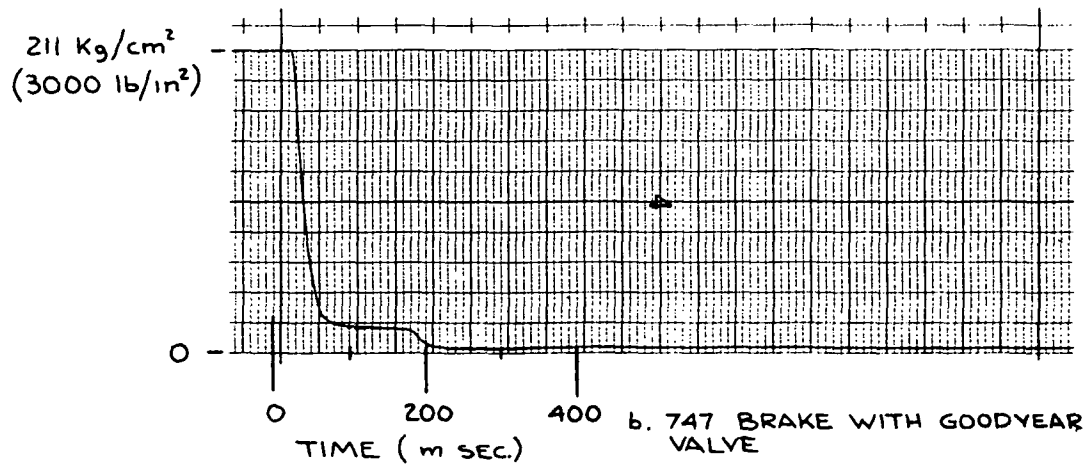
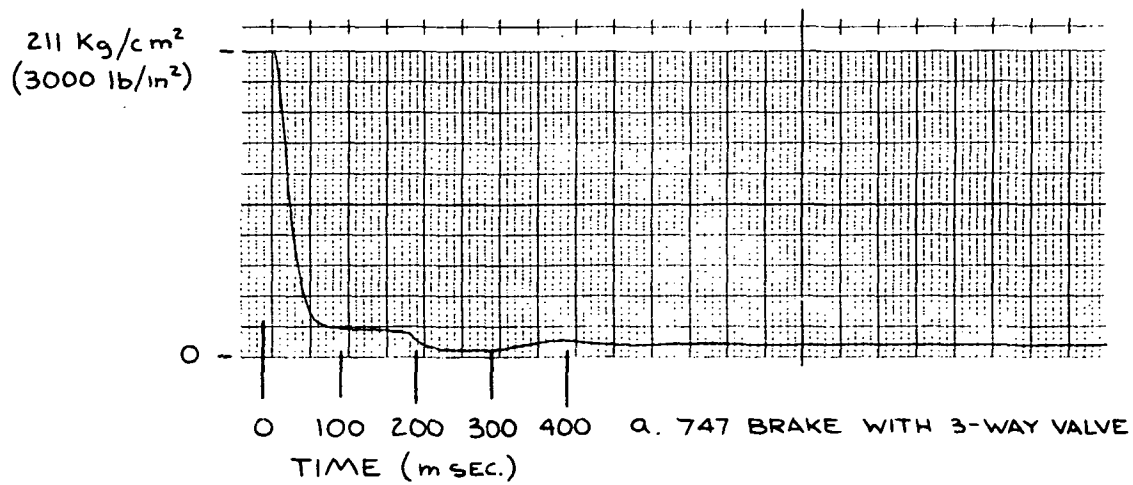


FIG. 92 BRAKE PRESSURE STEP DOWN RESPONSE TEST

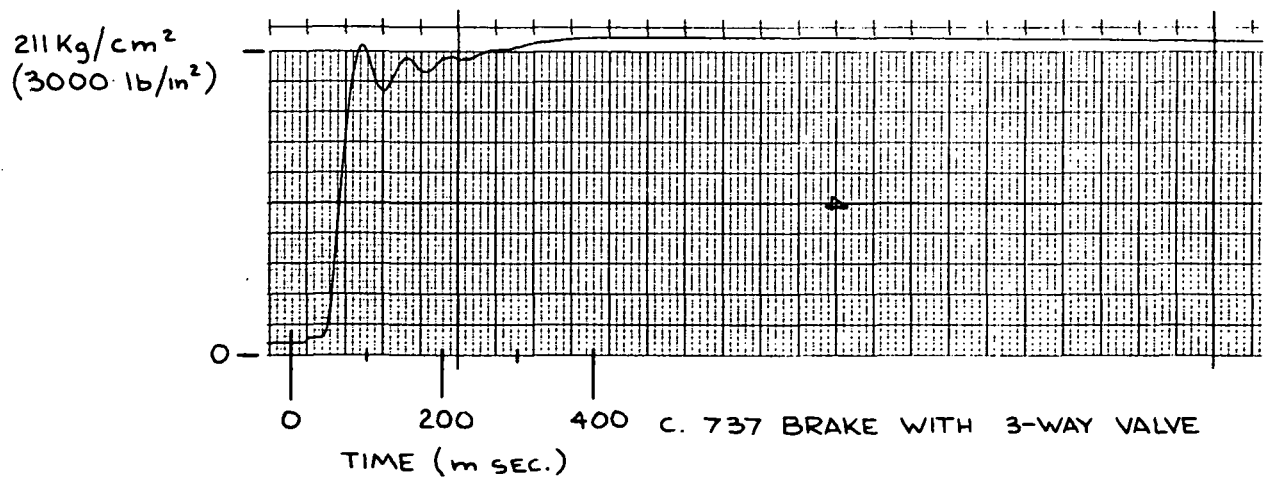
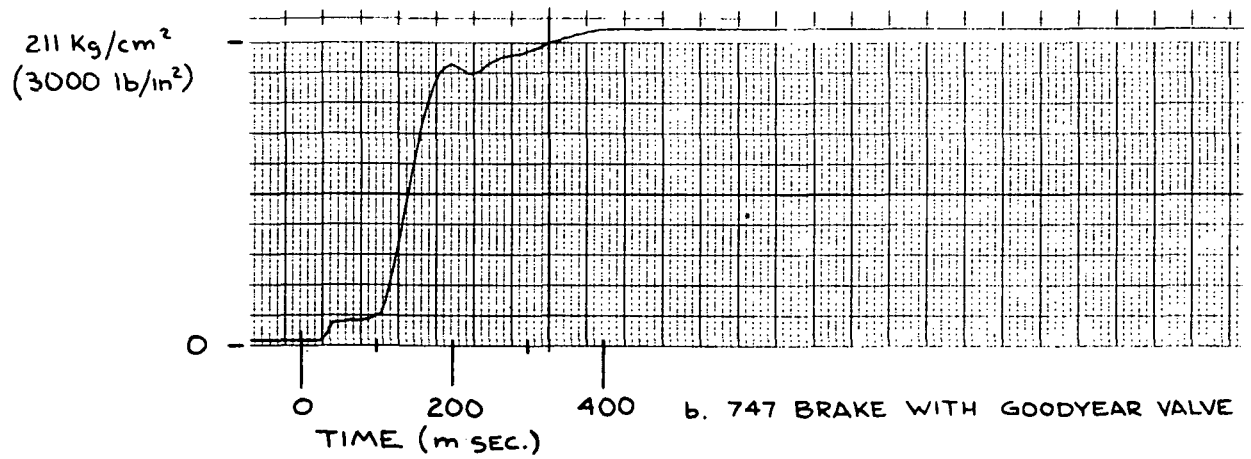
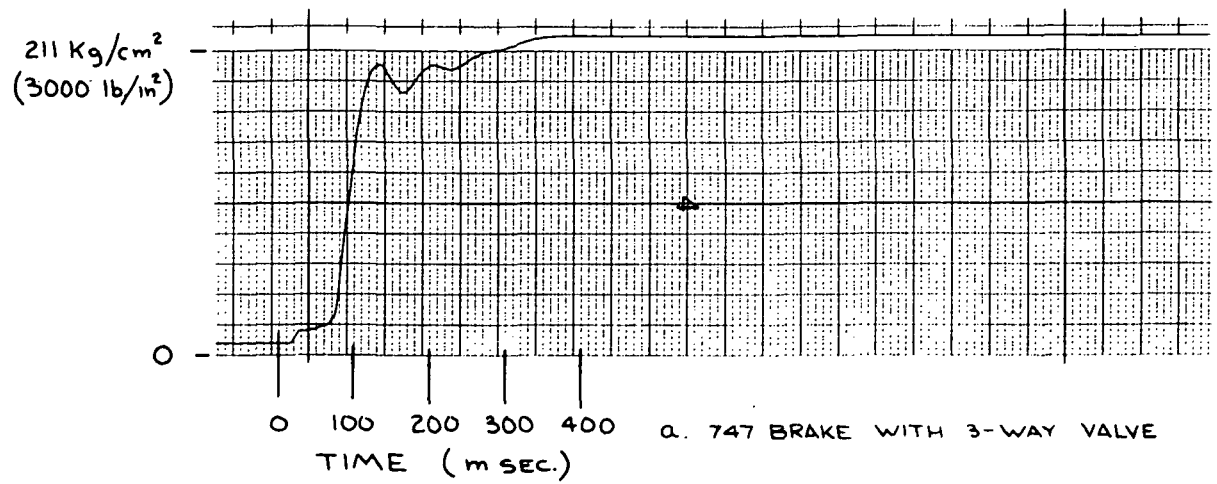


FIG. 93 BRAKE PRESSURE STEP UP RESPONSE TEST

conducted both with the 737 and 747 brake. It can be seen that the 737 brake is quicker to respond to step function commands than the 747 brake.

When the Closed Loop system was run with the 737 brake the performance difference can be seen in Figures 88 through 90. Only very slight performance improvement can be seen. So it seems that although differences can be detected in the two brakes as far as step function responses are concerned the performance improvement from using the 737 brake is not significant.

There are also differences in these two brakes concerning the brake torque response. Recently conducted tests have verified that the 737 brake torque response phase lag up to 20 Hz can easily be neglected. The 747 brake on the other hand has more response lag. The simulated brake torque response used throughout the Space Shuttle testing has the characteristics shown in Figure 94. Figures 88 through 90 show what the performance effect is by having the brake torque response in the simulation (observe the performance under "normal configuration") and removing this response entirely. Removing the lag produces improved performance on dry and even more performance on .2 mu and wet runway. This indeed shows a clear trend that brake torque lag hurts the system efficiency. It also plays a destabilizing effect as far as strut stability is concerned.

HYDRAULIC SYSTEM

Another important aspect of the brake control system involves some form of criteria about the hydraulic system (that portion of the hydraulic system or systems that contribute to the antiskid system). Hydraulic system flow and supply pressure will be designed by some other criteria such as flight control system or landing gear actuation system needs. But such things as line length and diameter especially from the antiskid valve to the brake and return line away from the valve can and do play an important part in the system's overall

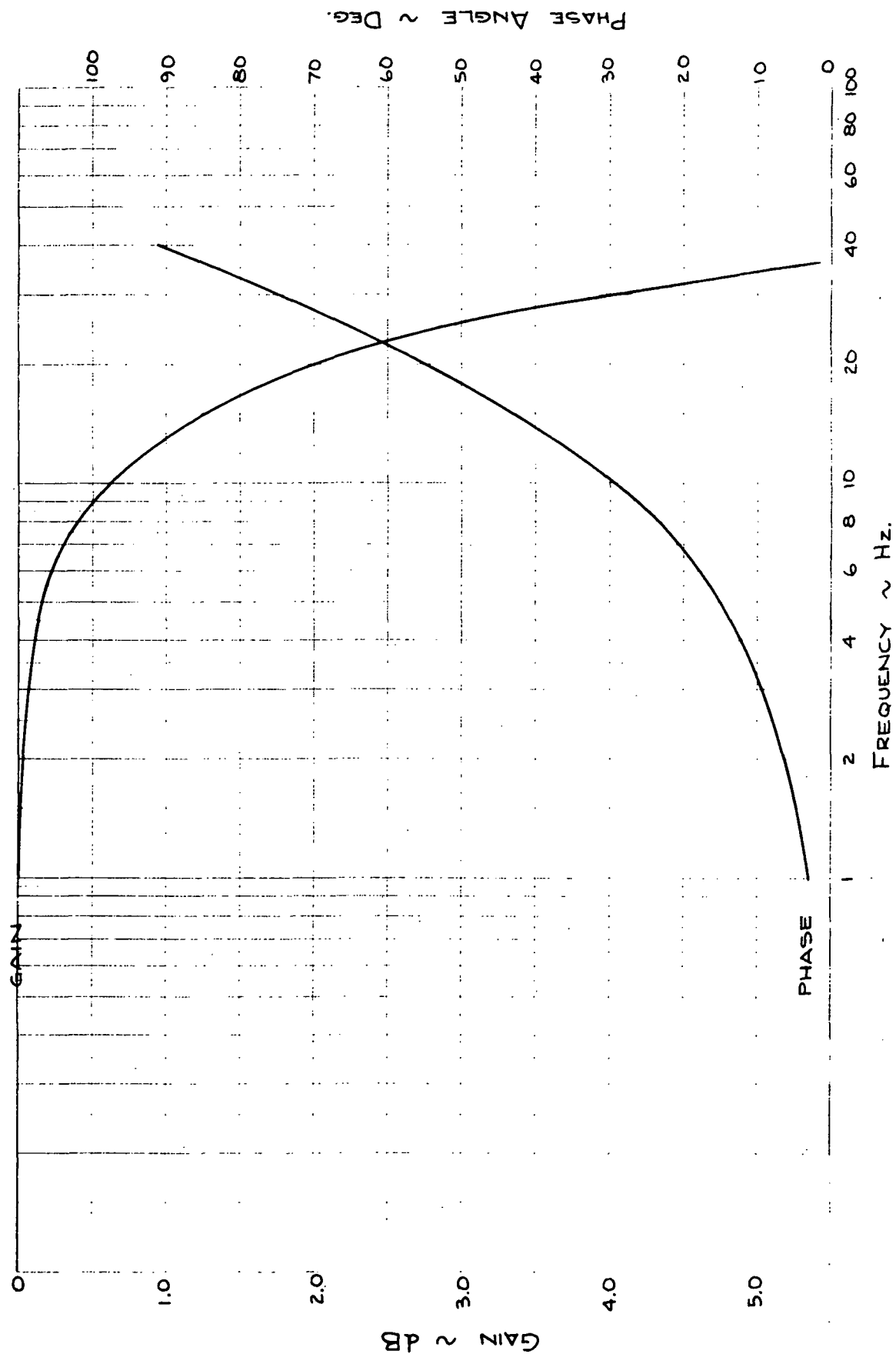


FIG. 94 SPACE SHUTTLE BRAKE TORQUE FREQUENCY RESPONSE SIMULATION

performance. In some applications return line accumulators have been used to aid the valve response.

One item was looked at and that deals with brake line length. Referring back to Figure 52, 432 cm (170 in.) of brake line exist between the antiskid valve and the 76 cm (30 in) flex line in the normal testing configuration. For this test the entire 432 cm (170 in) line was removed leaving only the flex line between the valve and brake. The results show up in Figure 95 in the hydraulic frequency response. Compared to the normal response plot in Figure 21 the response is considerably quicker. For instance at 10 Hz. the phase lag is nearly 18 degrees less. The Closed Loop system was run with this short line configuration with the results shown in Figure 88. This shows that performance wise the change made virtually no improvement, in fact a slight loss in performance. This reduced phase lag could be used to great advantage to help stabilize a system.

WHEEL SPEED TRANSDUCER

Although no formal testing was done with any wheel speed transducers it was felt that any discussion of criteria could not be complete without a discussion of them. Some aspects of the transducers were mentioned in conjunction with the system description in Section III. Again under the ratings that were conducted in that section aspects such as signal to noise ratio, concentricity, signal strength were mentioned. Along with the desirability of the transducer wheel speed signal to be free of objectionable noise, sensitivity to electro-magnet interference, the unit must also tolerate moisture, vibration and be relatively maintenance free. A very highly successful design has been the inductive FM alternator type.

Not all aspects of antiskid system criteria have been dealt with here. The task of integrating all details of a complete brake control system are numerous and complicated. It is hoped that this section

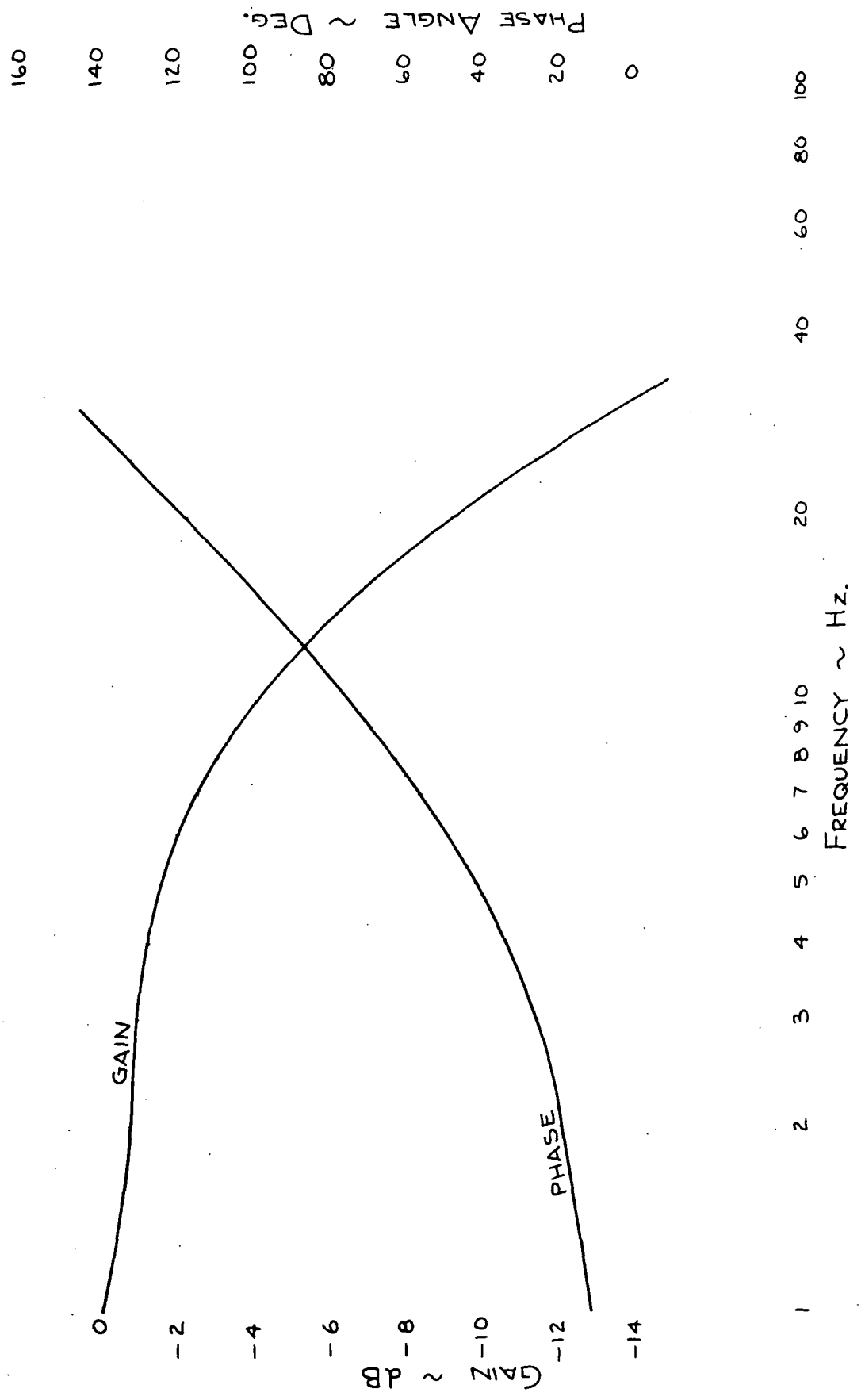


FIG. 95 SPACE SHUTTLE HYDRAULIC FREQUENCY RESPONSE WITH SHORT BRAKE LINE AND 3-WAY VALVE

has shown at least some of the trends that changes in hardware design have on the system. Not the least of the design choices is which antiskid system to use. Two commercially available systems were tested and the results described in Section VI. Depending on which system is chosen for use, some of the other component criteria may or may not be as important as when some other system is chosen for use.

In summary:

- o Antiskid Valve - Optimize frequency response; minimize leakage.
- o Brake Dynamics - Minimize brake actuator volume to improve response time.
- o Torque Dynamics - Minimize brake torque lag
- o Hydraulic System - Minimize brake line length, minimize return back pressure, optimize line size.
- o Wheel Speed Transducer - Strong signal to noise output, insensitivity to electromagnetic interference and vibration.

VIII. CONCLUSIONS

This contract investigated the subject of applying commercial airplane type brake control systems to the Space Shuttle. The two systems that fully participated in this contract were Hydro-Aire and Bendix. Both systems were found to be applicable to the Space Shuttle both in design and in observed performance. Both systems would have to be upgraded to space flight specifications but no impediment was seen to prevent this.

It was also concluded that to achieve fully implemented Fo/Fo/Fs electronical and Fo/Fs hydromechanical capability would entail a significant increase in system complexity, cost and weight over the conventional commercial aircraft rated system.

Further it was concluded that any judgment of the two systems (Goodyear L-1011 System and SPAD Concorde System) that did not participate in the lab screening (Section VI) would be premature and incomplete. To be adequately compared and judged, the tests conducted on the antiskid simulation with actual antiskid vendor hardware are necessary. The only information that was available about these two systems was furnished by their manufacturers and in the form of system description.

Based on the grading system used in Section VI the Hydro-Aire Mark III system and Bendix SST Systems accumulated scores only one point apart out of a total of 230 possible. Based on the compatibility study grading in Section III the Hydro-Aire Mark III system scored ten points higher than the Bendix SST system out of a total possible of 75. This would give a slight edge to the Hydro-Aire Mark III System based on overall system complexity, reliability, performance and stability.

IX. RECOMMENDATIONS

The value of an antiskid simulation to the development of an aircraft braking system is its ability to simulate the vehicle dynamics itself. This enables changes to be made to the brake control system readily without incurring the high penalty for operating a flight test aircraft for the same test. Chiefly the properly conducted simulation and brake control development program can vastly reduce the technical risks and economic expenditures of a flight test development program. In fact the timely use of a brake control simulation can greatly reduce the design risks and prevent delays in the Space Shuttle vehicle development.

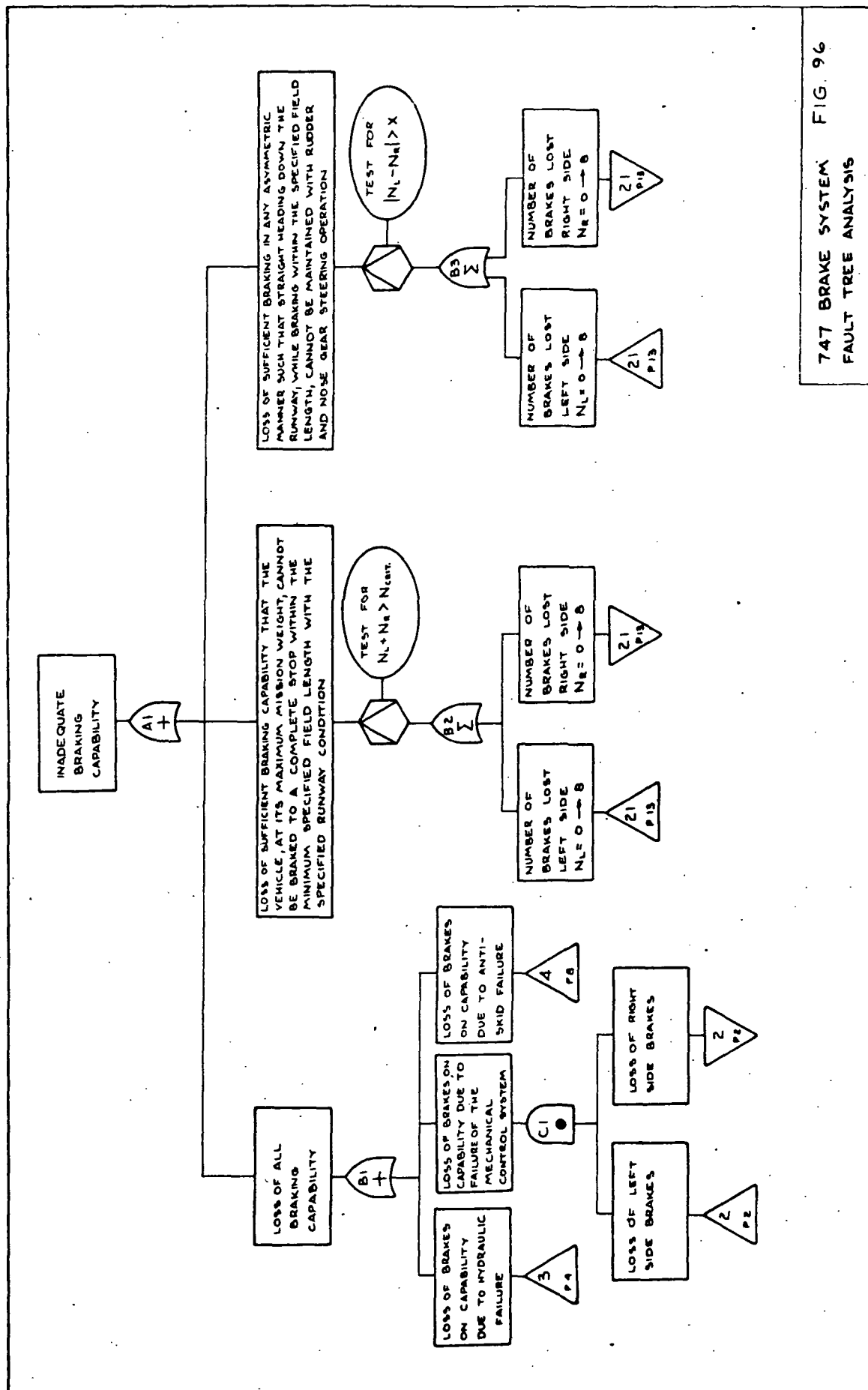
Eventually, when a flight test vehicle is available, actual vehicle braking performance data can be generated and compared to simulator data. Minor adjustments to the simulation can then be made as required for final antiskid system fine tuning. Thus, optimum brake control system performance can be achieved through minimum flight test effort and minimum risk.

Finally it is recommended that the results from this study be utilized in gaining familiarity and knowledge about the subject antiskid systems in this report. Also use of laboratory tests such as described and used throughout this study be made to assist in selecting an antiskid system that best matches the needs of the Space Shuttle.

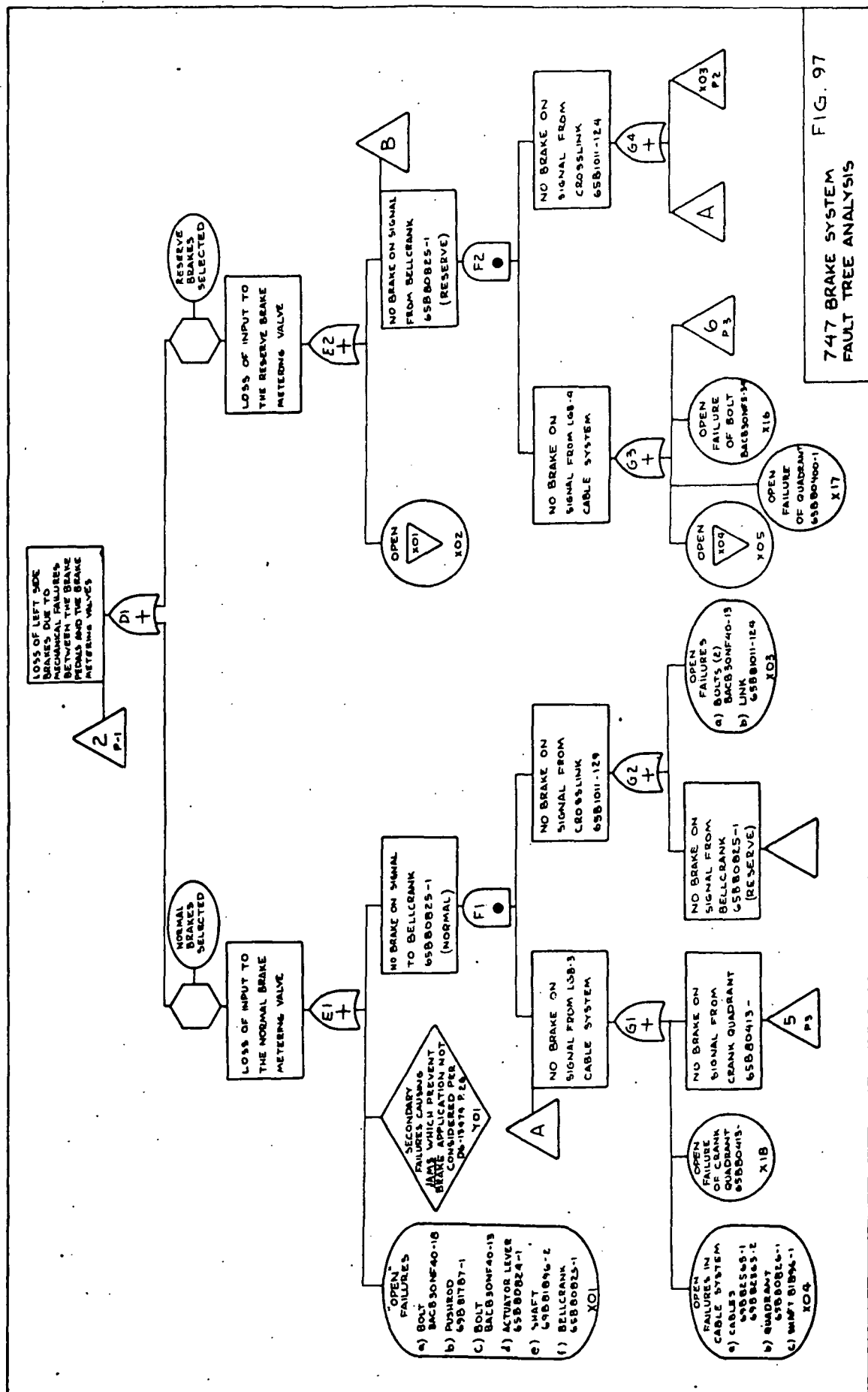
APPENDIX I

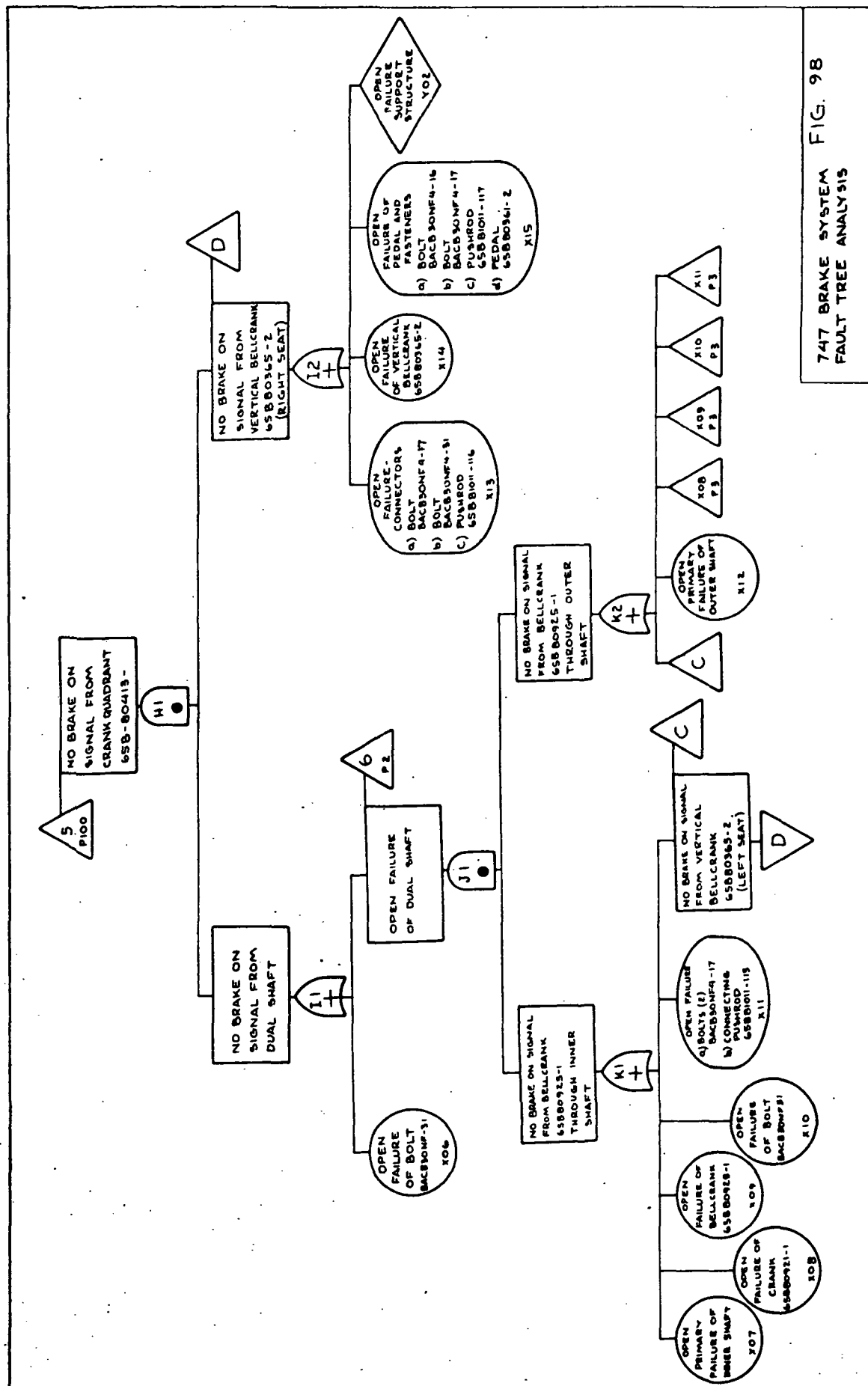
747 BRAKE SYSTEM FAULT TREE ANALYSIS

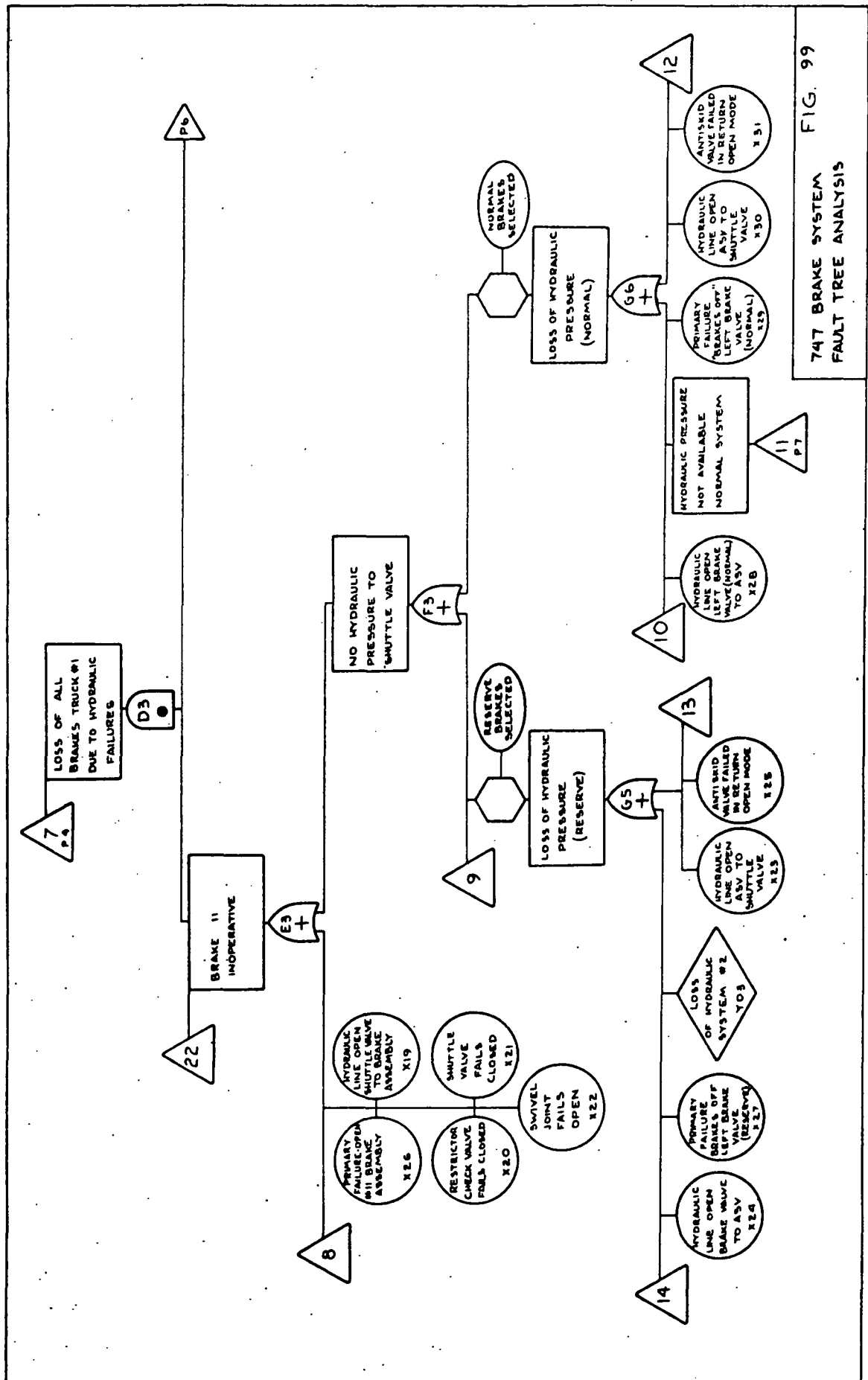
Figures 96 through 106 represent the 747 antiskid system, Hydro-Aire Mark III, Fault Tree.

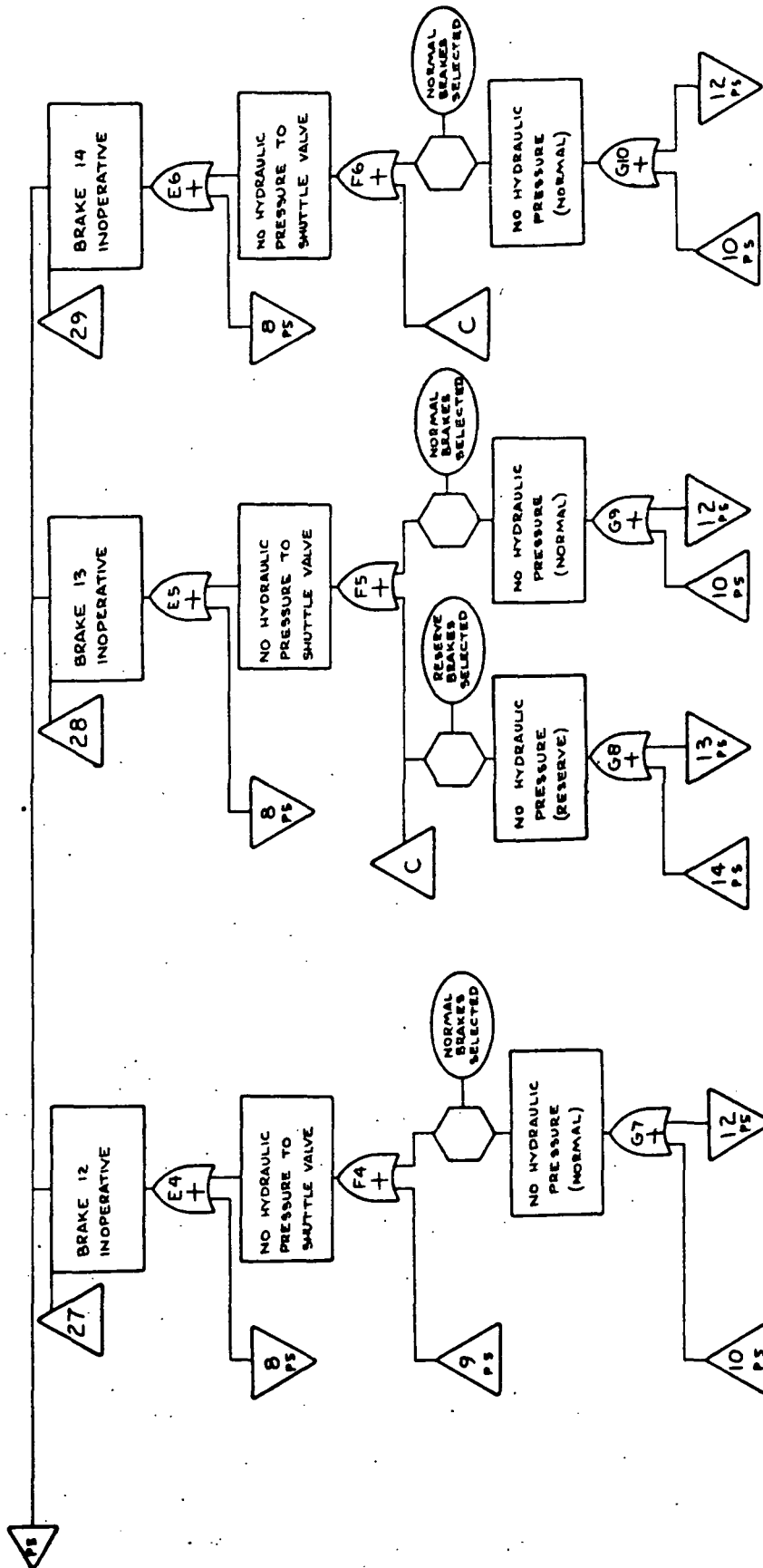


747 BRAKE SYSTEM FAULT TREE ANALYSIS FIG. 96









747 BRAKE SYSTEM
FAULT TREE ANALYSIS

FIG. 100

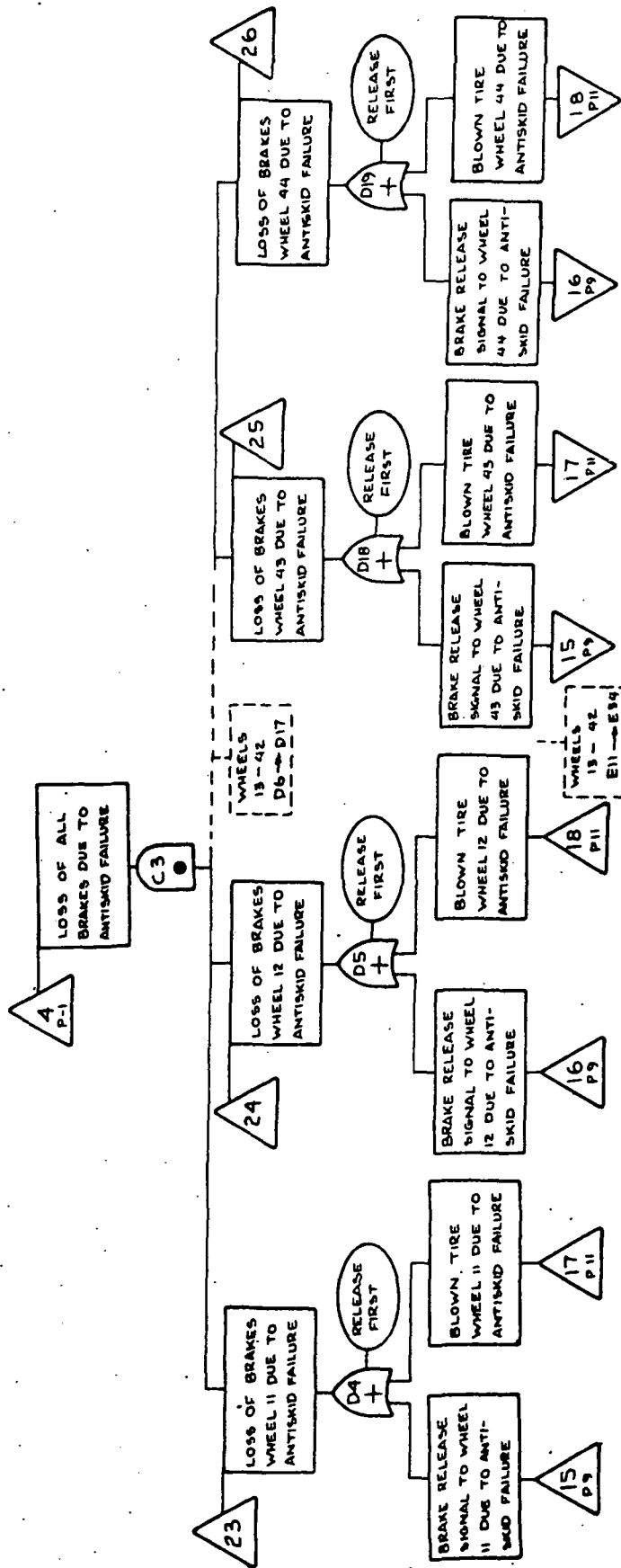
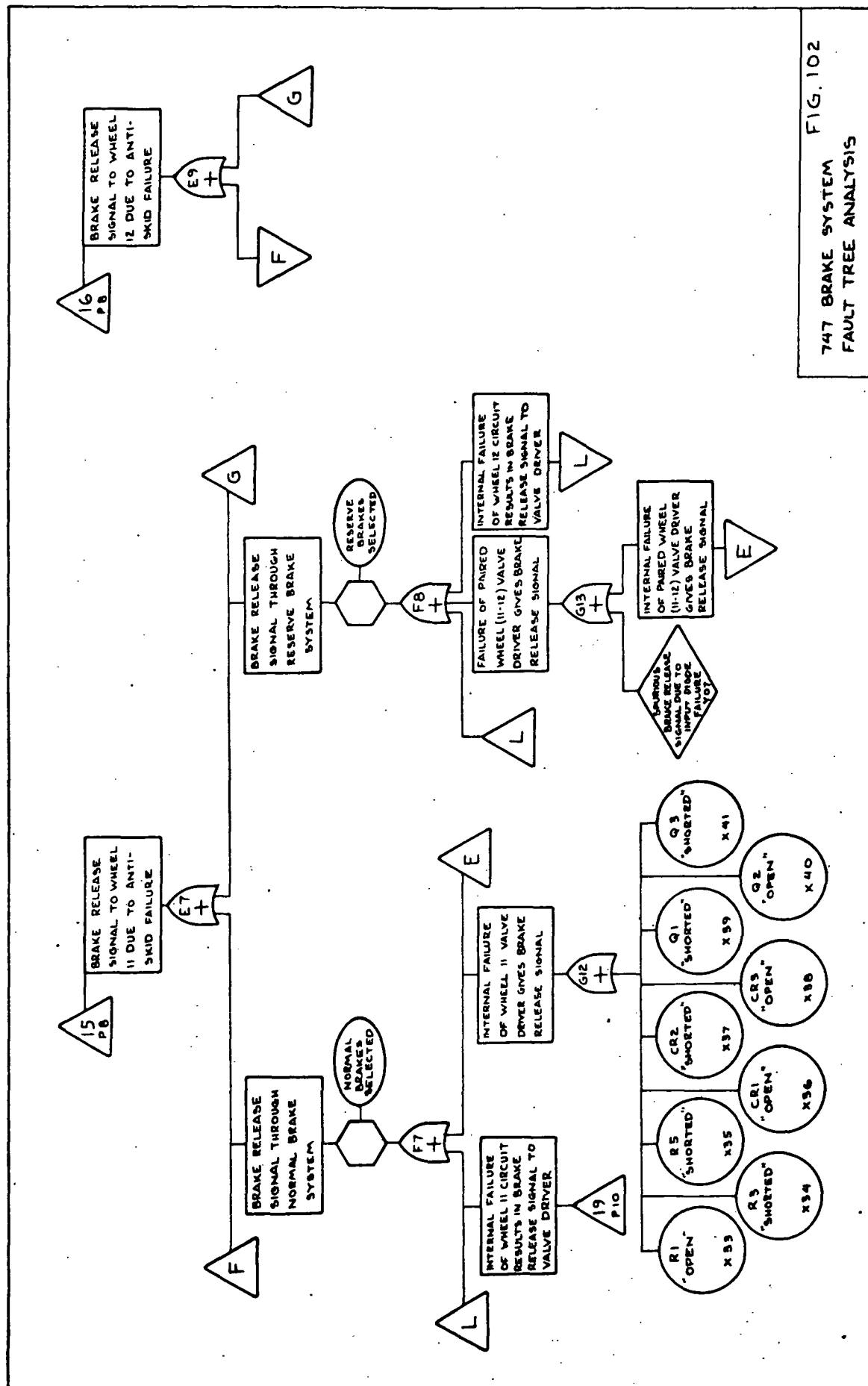
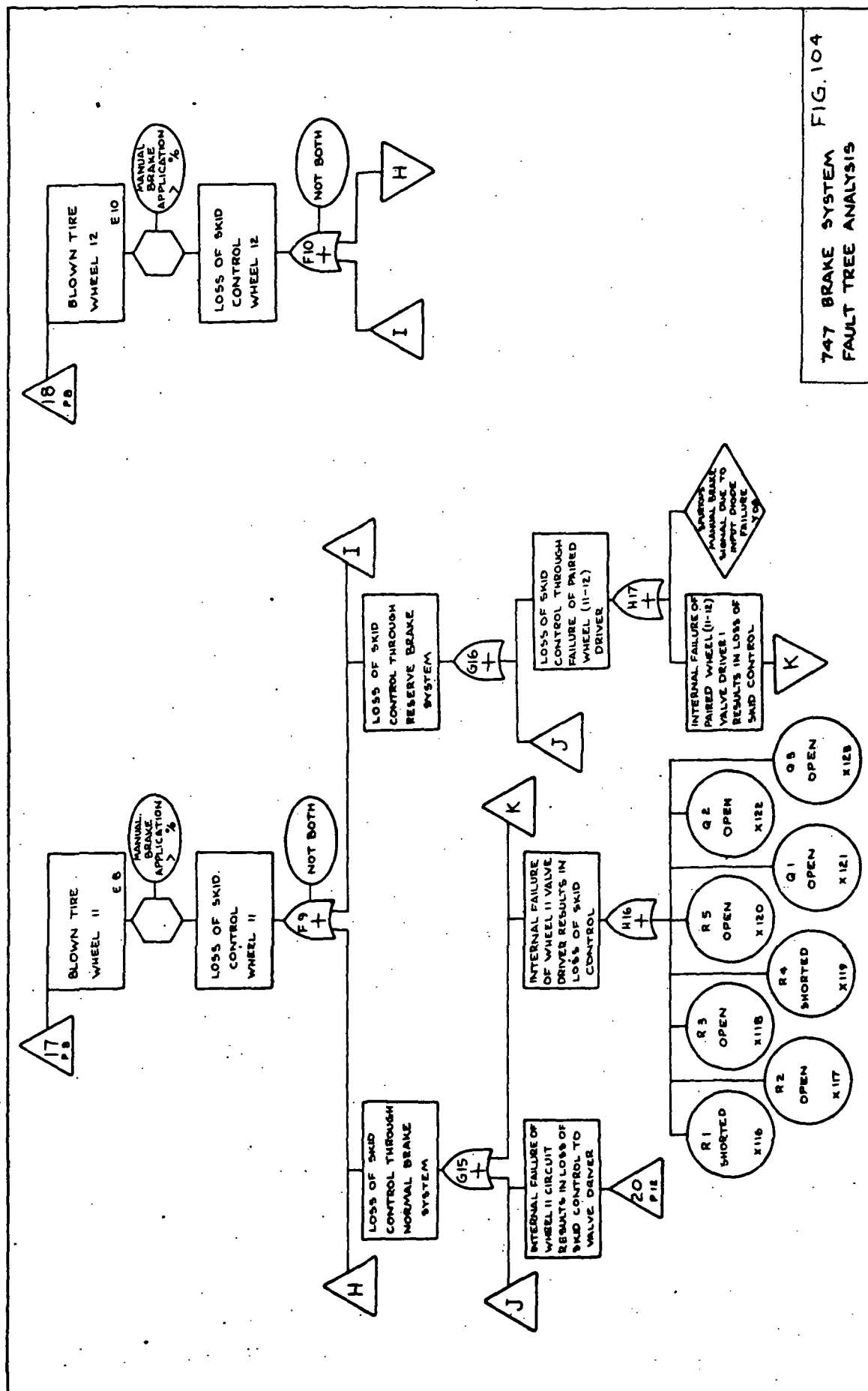
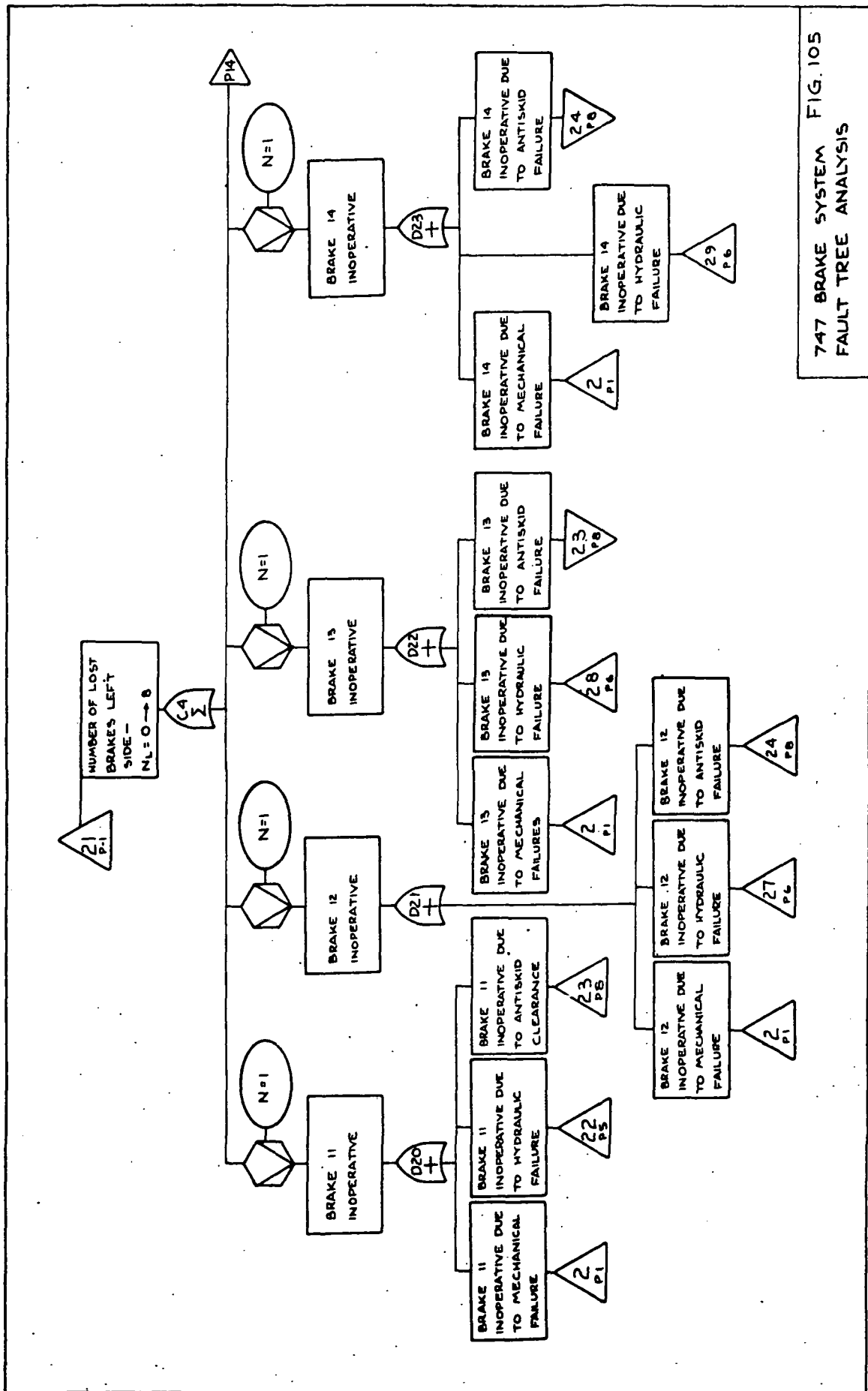


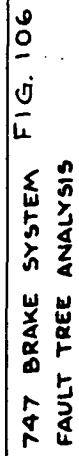
FIG. 101
747 BRAKE SYSTEM
FAULT TREE ANALYSIS







747 BRAKE SYSTEM FIG. 105
FAULT TREE ANALYSIS



APPENDIX II

TABLE IV. SPACE SHUTTLE PARAMETERS FOR SKID CONTROL SIMULATION

| | |
|---|--|
| Effective wing area | 260.1m ² (2800 ft ²) |
| Drag coefficient (landing configuration during braking roll) | 0.08 |
| Lift coefficient (landing coefficient during braking roll) | 0.037 |
| Engine idle thrust (sea level, Mach .3) | 132 n/eng. (600 lbs/eng.) |
| Engine idle thrust (sea level, zero velocity) | 308 n/eng. (1400 lbs/eng.) |
| Number of Engines (for ferry flight) | 4 |
| Drag Coefficient (Drag Chute) | 0.5 |
| Area of Chute (two 6.1m (20 ft) diameter chutes) | 58.4m ² (628 ft ²) |
| Height of Vehicle Center of Gravity Above Ground | 4.57m (15 ft) |
| Mass moment of inertia of stationary portion of brake per strut | 5.9 kg-m ² (8 slug-ft ²) |
| Strut Natural Frequency | 4-12 Hz (range) |
| Mass moment of inertia of wheel, tire and brake rotor assembly about axle center line | 8.85 - 14.75 kg-m ² (12-20 slug-ft ²) |
| Mass moment of inertia of the vehicle in pitch about the center of gravity | 3.79 x 10 ⁶ kg-m ² (5.14 x 10 ⁶ slug-ft ²) |
| Rate of change of engine idle thrust with airplane velocity | 36.1 $\frac{\text{n-sec}}{\text{m}}$ (2.42 $\frac{\text{lb-sec}}{\text{ft}}$) |
| Strut fore and aft spring rate | Empirical n/m |

APPENDIX II (continued)

TABLE IV. SPACE SHUTTLE PARAMETERS FOR SKID CONTROL SIMULATION

| | |
|---|---|
| Vertical spring rate of main gear tire (44x13-20) 18.2 kg/cm ² (260 psi) | 3.13 x 10 ⁶ n/m (2.1 x 10 ⁵ lb/ft) |
| Vertical spring rate of main gear oleo | 2.415 x 10 ⁶ n/m (1.62 x 10 ⁵ lb/ft) |
| Vertical spring rate of nose gear oleo | 8.95 x 10 ⁵ n/m (6 x 10 ⁴ lb/ft) |
| Vertical spring rate of the nose gear tire (29 x 7.7-15) 18.2 kg/cm ² (260 psi) | 2.013 x 10 ⁶ n/m (1.35 x 10 ⁵ lb/ft) |
| Effective length of main gear strut | 2.74m (9 ft) |
| Horizontal distance between nose gear and vehicle center of gravity | 13.2m (43.3 ft) |
| Horizontal distance between main gear and vehicle center of gravity | 2.54m (8.33 ft) |
| Total mass of vehicle | 91,000 kg (200,000 lbs) |
| Total effective mass at end of strut | 500 kg (34.2 slug-ft ²) |
| Total effective mass of tire, wheel and brake rotor assembly | 189 kg (13 slug-ft ²) |
| Brake retractor spring pressure | 17.58 kg/cm ² (250 psi) |
| Roll radius of the tire (free radius minus 1/3 deflection) | 0.518m (1.7 ft) |
| Torque radius of the tire (free radius minus deflection at 32%) | .466m (1.53 ft) |
| Brake torque gain (torque per unit pressure) | 1.163 $\frac{\text{n-m}}{\text{kg/cm}^2}$ (12 $\frac{\text{ft-lb}}{\text{sec}}$) |
| Vehicle weight | 44000 n (200,000 lbs) |
| Angular velocity at beginning of torque peaking | 30 rad/sec |

APPENDIX III

TABLE V. SPACE SHUTTLE SCREENING DATA

| VENDOR | MU | STOPPING DISTANCE | | STUDIES | 4.5 Hz | STOPPING EFFICIENCY | MU EFFICIENCY | SKID INDEX | CORNERING INDEX |
|----------------------------------|---------|-------------------|--------|---------|---------|---------------------|---------------|------------|-----------------|
| | | METERS | (FEET) | | | | | | |
| Performance-Adaptability Studies | | | | | | | | | |
| | | | | Test 1 | | | | | |
| Bendix | .5 | 1149 | (3770) | | 90.7 | 85.5 | 12.9 | 70.8 | |
| Boeing Closed Loop | .5 | 1202 | (3942) | | 86.8 | 76.5 | 12.6 | 73.6 | |
| Hydro-Aire Mk III | .5 | 1123 | (3683) | | 93.4 | 87.5 | 12.5 | 68.6 | |
| Bendix | .2 | 2251 | (7383) | | 91.7 | 86.5 | 27.2 | 64.6 | |
| Boeing Closed Loop | .2 | 2283 | (7490) | | 90.4 | 80.9 | 20.1 | 72.6 | |
| Hydro-Aire Mk III | .2 | 2168 | (7085) | | 96.0 | 92.4 | 20.7 | 64.5 | |
| Bendix | Curve 1 | 2441 | (8008) | | 91.8 | 86.3 | 28.9 | 64.7 | |
| Boeing Closed Loop | Curve 1 | 2449 | (8034) | | 91.5 | 83.0 | 21.1 | 71.2 | |
| Hydro-Aire Mk III | Curve 1 | 2320 | (7627) | | 96.6 | 91.3 | 23.5 | 63.9 | |
| Performance-Adaptability Studies | | | | | | | | | |
| | | | | Test 1 | 11.5 Hz | | | | |
| Bendix | .5 | 1134 | (3721) | | 91.9 | 86.8 | 12.6 | 70.6 | |
| Boeing Closed Loop | .5 | 1135 | (3723) | | 91.9 | 82.5 | 12.5 | 70.2 | |
| Hydro-Aire Mk III | .5 | 1123 | (3677) | | 93.6 | 88.5 | 11.9 | 67.8 | |
| Bendix | .2 | 2284 | (7492) | | 90.3 | 84.5 | 21.7 | 66.2 | |
| Boeing Closed Loop | .2 | 2243 | (7358) | | 92.0 | 83.4 | 18.9 | 71.1 | |
| Hydro-Aire Mk III | .2 | 2168 | (7064) | | 96.3 | 93.1 | 20.2 | 63.5 | |
| Bendix | Curve 1 | 2448 | (8030) | | 91.5 | 85.5 | 22.6 | 67.7 | |
| Boeing Closed Loop | Curve 1 | 2402 | (7881) | | 93.3 | 84.9 | 20.8 | 69.3 | |
| Hydro-Aire Mk III | Curve 1 | 2320 | (7664) | | 96.2 | 92.1 | 25.6 | 63.7 | |

TABLE V. SPACE SHUTTLE SCREENING DATA (Continued)

APPENDIX III

| VENDOR | MU | DISTANCE | | STOPPING | MU | SKID | CORNERING |
|--|------|----------|---------|----------|------|------|-----------|
| | | METERS | (FEET) | | | | |
| Performance-Adaptability Studies Test 1 7.5 Hz | | | | | | | |
| Bendix | .5 | 1132 | (3715) | 92.1 | 87.8 | 12.5 | 71.1 |
| Boeing Closed Loop | .5 | 1150 | (3773) | 90.6 | 81.2 | 12.4 | 70.4 |
| Hydro-Aire Mk III | .5 | 1127 | (3663) | 93.9 | 90.4 | 12.9 | 67.4 |
| Bendix | .4 | 1314 | (4312) | 94.0 | 90.4 | 14.0 | 70.0 |
| Boeing Closed Loop | .4 | 1366 | (4483) | 90.4 | 80.7 | 14.2 | 68.6 |
| Hydro-Aire Mk III | .4 | 1323 | (4308) | 94.3 | 90.9 | 14.4 | 66.8 |
| Bendix | .3 | 1647 | (5404) | 93.0 | 89.2 | 16.1 | 69.7 |
| Boeing Closed Loop | .3 | 1675 | (5494) | 91.5 | 82.7 | 15.2 | 70.9 |
| Hydro-Aire Mk III | .3 | 1629 | (5379) | 94.1 | 92.2 | 16.5 | 65.9 |
| Bendix | .2 | 2272 | (7452) | 90.8 | 85.2 | 21.4 | 67.8 |
| Boeing Closed Loop | .2 | 2245 | (7366) | 91.9 | 83.4 | 18.5 | 71.2 |
| Hydro-Aire Mk III | .2 | 2169 | (7120) | 95.5 | 94.3 | 21.2 | 63.8 |
| Performance-Adaptability Studies Test 1 7.5 Hz | | | | | | | |
| Bendix | .1 | 3498 | (11474) | 93.8 | 88.9 | 31.2 | 66.7 |
| Boeing Closed Loop | .1 | 3620 | (11876) | 90.6 | 80.5 | 27.8 | 69.9 |
| Hydro-Aire Mk III | .1 | 3434 | (11139) | 95.7 | 96.2 | 33.5 | 60.5 |
| Bendix | .075 | 4121 | (13520) | 94.8 | 89.1 | 38.4 | 65.7 |
| Boeing Closed Loop | .075 | 4339 | (14235) | 90.1 | 78.8 | 33.1 | 68.5 |
| Hydro-Aire Mk III | .075 | 4080 | (13239) | 96.8 | 95.7 | 39.6 | 60.4 |

TABLE V. SPACE SHUTTLE SCREENING DATA (Continued)

| VENDOR | MU | STOPPING DISTANCE | | STOPPING EFFICIENCY | MU EFFICIENCY | SKID INDEX | CORNERING INDEX |
|--|---------|-------------------|---------|---------------------|---------------|------------|-----------------|
| | | METERS | (FEET) | | | | |
| Performance-Adaptability Studies Test 2 7.5 Hz | | | | | | | |
| Bendix | .5 | 1187 | (3894) | 91.3 | 86.7 | 16.8 | 68.7 |
| Boeing Closed Loop | .5 | 1318 | (4325) | 82.2 | 72.7 | 13.7 | 73.0 |
| Hydro-Aire Mk III | .5 | 1182 | (3867) | 93.4 | 88.9 | 17.4 | 63.9 |
| Performance-Adaptability Studies Test 3 7.5 Hz | | | | | | | |
| Bendix | | 1350 | (4429) | 76.5 | 67.1 | 13.6 | 75.7 |
| Boeing Closed Loop | | 1489 | (4884) | 70.0 | 59.2 | 13.5 | 77.5 |
| Hydro-Aire Mk III | | 1255 | (4007) | 88.9 | 79.0 | 13.1 | 71.6 |
| Operational Studies Test 1 7.5 Hz | | | | | | | |
| Bendix | Curve 1 | 2428 | (7966) | 92.3 | 87.8 | 22.2 | 69.0 |
| Boeing Closed Loop | Curve 1 | 2417 | (7929) | 92.7 | 84.6 | 21.1 | 68.7 |
| Hydro-Aire Mk III | Curve 1 | 2328 | (7667) | 96.0 | 93.5 | 24.7 | 62.2 |
| Bendix | Curve 2 | 3016 | (9893) | 95.2 | 88.1 | 28.8 | 67.6 |
| Boeing Closed Loop | Curve 2 | 3060 | (10039) | 93.8 | 84.2 | 23.3 | 71.0 |
| Hydro-Aire Mk III | Curve 2 | 2847 | (9832) | 92.0 | 93.3 | 31.8 | 60.1 |

TABLE V. SPACE SHUTTLE SCREENING DATA (Continued)

| VENDOR | MU | STOPPING DISTANCE | | MU EFFICIENCY | SKID INDEX | CORNERING INDEX |
|---------------------|---------|---------------------------|--------|------------------|---------------|--------------------|
| | | METERS | (FEET) | | | |
| Operational Studies | Test 2 | 81,820 kg. (180,000 lbs) | | | | |
| Bendix | .5 | 996 | (3268) | 89.4 | 10.7 | 70.9 |
| Boeing Closed Loop | .5 | 1025 | (3363) | 81.1 | 10.8 | 69.4 |
| Hydro-Aire Mk III | .5 | 1011 | (3231) | 90.2 | 11.1 | 67.0 |
| Bendix | .2 | 2003 | (6570) | 86.8 | 17.9 | 68.5 |
| Boeing Closed Loop | .2 | 2007 | (6583) | 83.1 | 16.2 | 71.0 |
| Hydro-Aire Mk III | .2 | 1942 | (6275) | 93.3 | 18.5 | 62.8 |
| Bendix | Curve 1 | 2110 | (6924) | 86.7 | 19.8 | 68.8 |
| Boeing Closed Loop | Curve 1 | 2105 | (6906) | 84.4 | 17.5 | 70.0 |
| Hydro-Aire Mk III | Curve 1 | 2031 | (6729) | 93.2 | 20.2 | 63.3 |
| Operational Studies | Test 2 | 100,000 kg. (220,000 lbs) | | | | |
| Bendix | .5 | 1256 | (4122) | 87.2 | 14.8 | 72.6 |
| Boeing Closed Loop | .5 | 1296 | (4251) | 80.6 | 14.1 | 72.1 |
| Hydro-Aire Mk III | .5 | 1248 | (4046) | 89.3 | 12.6 | 66.7 |
| Bendix | .2 | 2409 | (7903) | 90.1 | 24.1 | 68.0 |
| Boeing Closed Loop | .2 | 2509 | (8232) | 83.6 | 20.2 | 71.1 |
| Hydro-Aire Mk III | .2 | 2430 | (7864) | 92.2 | 23.6 | 64.2 |
| Bendix | Curve 1 | 2745 | (9004) | 88.3 | 23.7 | 69.5 |
| Boeing Closed Loop | Curve 1 | 2773 | (9097) | 85.3 | 23.5 | 70.1 |
| Hydro-Aire Mk III | Curve 1 | 2680 | (8744) | 91.3 | 26.8 | 63.9 |

TABLE V. SPACE SHUTTLE SCREENING DATA (Continued)

| VENDOR | MU | STOPPING DISTANCE | | STOPPING EFFICIENCY (12 ft-lb-sec ²) | Wheel Inertia | SKID INDEX | CORNERING INDEX |
|--|---------|-------------------|--------|---|---------------|------------|-----------------|
| | | METERS | (FEET) | | | | |
| Operational Studies Test 3 8.85 n-m-sec ² (20 ft-lb-sec ²) Wheel Inertia | | | | | | | |
| Bendix | .5 | 1141 | (3743) | 91.4 | 86.1 | 13.1 | 70.5 |
| Closed Loop | .5 | 1169 | (3837) | 89.1 | 79.4 | 12.8 | 72.7 |
| Mark III | .5 | 1135 | (3718) | 92.5 | 86.8 | 12.8 | 69.3 |
| Bendix | .2 | 2243 | (7359) | 92.0 | 87.6 | 19.6 | 69.0 |
| Closed Loop | .2 | 2278 | (7475) | 90.5 | 81.2 | 19.3 | 70.4 |
| Mark III | .2 | 2175 | (7148) | 95.1 | 93.8 | 20.1 | 64.7 |
| Bendix | Curve 1 | 2434 | (7986) | 92.0 | 86.6 | 21.5 | 68.8 |
| Closed Loop | Curve 1 | 2455 | (8053) | 91.3 | 82.9 | 20.1 | 70.1 |
| Mark III | Curve 1 | 2335 | (7671) | 95.9 | 93.5 | 23.2 | 64.2 |
| Operational Studies Test 3 14.75 n-m-sec ² (20 ft-lb-sec ²) Wheel Inertia | | | | | | | |
| Bendix | .5 | 1112 | (3648) | 93.8 | 90.1 | 12.4 | 69.0 |
| Closed Loop | .5 | 1141 | (3744) | 91.4 | 82.9 | 13.0 | 69.4 |
| Mark III | .5 | 1125 | (3650) | 94.2 | 91.0 | 12.9 | 66.9 |
| Bendix | .2 | 2234 | (7330) | 92.3 | 85.6 | 22.8 | 63.3 |
| Closed Loop | .2 | 2232 | (7322) | 92.4 | 85.0 | 19.2 | 69.7 |
| Mark III | .2 | 2160 | (7028) | 96.8 | 95.6 | 21.6 | 62.6 |
| Bendix | Curve 1 | 2403 | (7882) | 93.2 | 87.9 | 25.3 | 64.9 |
| Closed Loop | Curve 1 | 2403 | (7883) | 93.2 | 87.0 | 20.1 | 68.6 |
| Mark III | Curve 1 | 2326 | (7585) | 97.0 | 96.0 | 23.2 | 63.1 |

TABLE V. SPACE SHUTTLE SCREENING DATA (Continued)

APPENDIX III

| VENDOR | MU | STOPPING DISTANCE | | STOPPING EFFICIENCY | MU EFFICIENCY | SKID INDEX | CORNERING INDEX |
|----------------------------|---------|-------------------|--------|---------------------|---------------|------------|-----------------|
| | | METERS | (FEET) | | | | |
| Operational Studies Test 4 | | | | | | | |
| Bendix | .5 | 1137 | (3730) | 91.7 | 86.5 | 13.0 | 70.2 |
| Closed Loop | .5 | 1158 | (3799) | 90.0 | 79.4 | 12.6 | 73.1 |
| Mark III | .5 | 1144 | (3675) | 93.6 | 89.5 | 10.0 | 67.5 |
| Bendix | .2 | 2254 | (7393) | 91.5 | 85.3 | 20.7 | 67.7 |
| Closed Loop | .2 | 2260 | (7413) | 91.3 | 81.6 | 20.0 | 71.1 |
| Mark III | .2 | 2176 | (7144) | 95.2 | 93.3 | 20.3 | 64.1 |
| Bendix | Curve 1 | 2421 | (7942) | 92.5 | 87.2 | 22.8 | 68.2 |
| Closed Loop | Curve 1 | 2424 | (7953) | 92.4 | 84.2 | 20.5 | 71.5 |
| Mark III | Curve 1 | 2336 | (7667) | 96.0 | 93.2 | 23.4 | 64.1 |
| Operational Studies Test 5 | | | | | | | |
| Bendix | .5 | 1141 | (3745) | 91.3 | 86.0 | 13.1 | 71.3 |
| Closed Loop | .5 | 1199 | (3935) | 86.9 | 75.2 | 13.2 | 71.3 |
| Mark III | .5 | 1152 | (3754) | 91.6 | 87.4 | 13.1 | 68.2 |
| Bendix | .2 | 2254 | (7395) | 91.5 | 86.0 | 20.2 | 67.7 |
| Closed Loop | .2 | 2267 | (7436) | 91.0 | 82.1 | 19.4 | 72.5 |
| Mark III | .2 | 2190 | (7185) | 94.6 | 93.0 | 21.0 | 64.3 |
| Bendix | Curve 1 | 2430 | (7973) | 92.2 | 86.6 | 21.9 | 68.1 |
| Closed Loop | Curve 1 | 2437 | (7994) | 91.9 | 83.9 | 19.8 | 72.4 |
| Mark III | Curve 1 | 2350 | (7713) | 95.4 | 92.4 | 23.4 | 64.1 |

TABLE V. SPACE SHUTTLE SCREENING DATA (Continued)

APPENDIX III

| VENDOR | MU | STOPPING DISTANCE | | STOPPING EFFICIENCY | MU EFFICIENCY | SKID INDEX | CORNERING INDEX |
|----------------------------|---------|-------------------|--------|---------------------|---------------|------------|-----------------|
| | | METERS | (FEET) | | | | |
| Operational Studies Test 6 | | | | | | | |
| Bendix | .5 | 947 | (3109) | 93.1 | 87.2 | 10.8 | 69.7 |
| Closed Loop | .5 | 977 | (3207) | 90.2 | 79.0 | 10.6 | 72.3 |
| Mark III | .5 | 940 | (3085) | 94.5 | 89.9 | 13.2 | 67.5 |
| Bendix | .2 | 1679 | (5510) | 92.9 | 85.3 | 14.3 | 68.3 |
| Closed Loop | .2 | 1686 | (5533) | 92.5 | 82.3 | 14.2 | 72.9 |
| Mark III | .2 | 1645 | (5413) | 95.3 | 91.7 | 15.3 | 64.7 |
| Bendix | Curve 1 | 1686 | (5531) | 92.9 | 85.1 | 14.9 | 68.6 |
| Closed Loop | Curve 1 | 1690 | (5544) | 92.7 | 84.2 | 14.1 | 72.7 |
| Mark III | Curve 1 | 1640 | (5371) | 96.6 | 92.7 | 16.4 | 64.2 |
| Operational Studies Test 7 | | | | | | | |
| Bendix | .5 | 1178 | (3866) | 92.4 | 87.9 | 13.1 | 70.8 |
| Closed Loop | .5 | 1211 | (3974) | 89.9 | 80.5 | 13.6 | 72.5 |
| Mark III | .5 | 1186 | (3837) | 93.4 | 90.4 | 13.6 | 67.3 |
| Bendix | .2 | 2465 | (8086) | 91.6 | 87.1 | 22.9 | 67.3 |
| Closed Loop | .2 | 2497 | (8190) | 90.4 | 82.4 | 21.3 | 72.9 |
| Mark III | .2 | 2386 | (7814) | 95.2 | 94.6 | 23.4 | 63.7 |
| Bendix | Curve 1 | 2681 | (8796) | 91.4 | 87.9 | 25.0 | 67.8 |
| Closed Loop | Curve 1 | 2690 | (8825) | 91.1 | 85.0 | 21.9 | 72.1 |
| Mark III | Curve 1 | 2588 | (8473) | 95.3 | 94.2 | 26.7 | 62.8 |